

SYNTHESIS AND ANTIDIABETIC ACTIVITY OF FUROFURAN LIGNANS CONTAINING MULTIPLE
PHENOLIC GROUPS



A Thesis Submitted in Partial Fulfillment of the Requirements
for the Degree of Master of Science in Chemistry
Department of Chemistry
Faculty of Science
Chulalongkorn University
Academic Year 2018
Copyright of Chulalongkorn University

การสังเคราะห์และฤทธิ์ต้านเบาหวานของฟิวโรฟิวแรนลิกันแนนที่มีฟีนอลิกหลายหมู่



วิทยานิพนธ์นี้เป็นส่วนหนึ่งของการศึกษาตามหลักสูตรปริญญาวิทยาศาสตรมหาบัณฑิต

สาขาวิชาเคมี ภาควิชาเคมี

คณะวิทยาศาสตร์ จุฬาลงกรณ์มหาวิทยาลัย

ปีการศึกษา 2561

ลิขสิทธิ์ของจุฬาลงกรณ์มหาวิทยาลัย

ฐิติฤทัย ดวงวิจิตรกุล : การสังเคราะห์และฤทธิ์ต้านเบาหวานของฟิวโรฟิวแรนลิกแนนที่มี
ฟีนอลิกหลายหมู่. (

SYNTHESIS AND ANTIDIABETIC ACTIVITY OF FUROFURAN LIGNANS CONTAINING
MULTIPHENOLIC GROUPS) อ.ที่ปรึกษาหลัก : รศ. ดร.ปรีชา ภูวไพริศรศาสตร์

การสังเคราะห์ฟิวโรฟิวแรนลิกแนนที่มีหมู่ฟีนอลิกหลายหมู่ (6-12) โดยใช้สารตั้งต้นเป็นซามิน (5) ที่ได้จากการทำปฏิกิริยาไฮโดรไลซิสด้วยกรดกับเซซาโมลินที่แยกได้จากน้ำมันงา เพื่อสังเคราะห์ลิกแนนเป้าหมายด้วยการทำปฏิกิริยากันของซามินกับฟีนอลิกชนิดต่าง ๆ ด้วยปฏิกิริยา Friedel-Crafts ได้ผลิตภัณฑ์ที่ต้องการ (6) หลังจากนั้นนำลิกแนนที่สังเคราะห์ได้มาทำปฏิกิริยาออกซิเดชันด้วยเลด (IV) เตตระอะซีเตต เพื่อเพิ่มจำนวนไฮดรอกซี โดยการดิงหมู่เมทิลีนไดออกซีออกจากฟิวโรฟิวแรนลิกแนน เกิดผลิตภัณฑ์ที่ไม่คาดคิด คือ ฟิวโรฟิวแรนลิกแนนที่มี พารา-ควิโนน และ ออโท-ไดไฮดรอกซี (8-9) ดังนั้นเพื่อหลีกเลี่ยงการเกิดออกซิเดชันของหมู่ไฮดรอกซี จึงมีการใช้ปฏิกิริยาการปกป้อง (protection) ก่อนการทำปฏิกิริยาออกซิเดชัน เพื่อให้ได้ผลิตภัณฑ์ที่ต้องการ ซึ่งในการทดลองนี้ได้ใช้ tetra-n-butylammonium fluoride (TBAF) ในปฏิกิริยาสามารถดิงหมู่ปกป้องและหมู่เมทิลีนไดออกซีได้ในขั้นตอนเดียว ได้ฟิวโรฟิวแรนลิกแนนที่ต้องการ (11-12) จากนั้นนำฟิวโรฟิวแรนลิกแนนที่สังเคราะห์ไปทดสอบฤทธิ์ในการต้านเบาหวาน ผลปรากฏว่าปัจจัยหลักของการยับยั้งแอลฟา-กลูโคซิเดส คือ จำนวนไฮดรอกซีบนฟิวโรฟิวแรนลิกแนน โดยฟิวโรฟิวแรนลิกแนนที่มีฤทธิ์สูงสุดในการทดลองนี้ คือ บีตา-ฟิวโรฟิวแรนลิกแนน 12 ที่มีหมู่อะเซตทอกซีและหมู่ไฮดรอกซี 4 หมู่ (IC_{50} 25.7, 12.9 and 5.3 μ M สำหรับมอลเทส, ซูเครส และยีสต์ ตามลำดับ) นอกจากนี้ยังมีปัจจัยอื่น ๆ ที่สามารถส่งผลต่อการยับยั้งแอลฟา-กลูโคซิเดส ได้แก่ คอนฟอร์เมชันที่คาร์บอนตำแหน่งที่ 2 ของวงฟิวโรฟิวแรนลิกแนนหลัก ซึ่งผลิตภัณฑ์แบบเบตามีผลต่อการยับยั้งที่ดีกว่าผลิตภัณฑ์แบบแอลฟา อีกทั้งตำแหน่งของไดไฮดรอกซี ที่เรียงแบบออโท-ไดไฮดรอกซี แสดงบทบาทสำคัญในการยับยั้งแอลฟา-กลูโคซิเดสด้วยเช่นกัน จากนั้นจึงนำฟิวโรฟิวแรนลิกแนนมาศึกษาทางด้านกลไกการยับยั้งเอนไซม์แอลฟา-กลูโคซิเดส พบว่ากลุ่มฟิวโรฟิวแรนลิกแนนสามารถยับยั้งเอนไซม์แบบ non-competitive และ mixed ซึ่งในกรณีการยับยั้งแบบ mixed ฟิวโรฟิวแรนลิกแนนแสดงยับยั้งเอนไซม์โดยการสร้างสารประกอบกับเอนไซม์เพื่อไม่ให้เอนไซม์ทำปฏิกิริยากับสารตั้งต้นและผลิตภัณฑ์

สาขาวิชา เคมี
ปีการศึกษา 2561

ลายมือชื่อนิสิต
ลายมือชื่อ อ.ที่ปรึกษาหลัก

5971946623 : MAJOR CHEMISTRY

KEYWORD: Furofuran lignans, alpha-glucosidase

Titiruetai

Doungwichitrkul

:

SYNTHESIS AND ANTIDIABETIC ACTIVITY OF FUROFURAN LIGNANS CONTAINING MULTIPHENOLIC GROUPS. Advisor: Assoc. Prof. Preecha Phuwapraisirisan, Ph.D.

Synthesis of furofuran lignans containing multiphenolic groups (6-12) was carried out. The starting material samini (5) was obtained by acid hydrolysis of sesamin (2), which was isolated from sesame seed oil. A series of target lignans were synthesized from samini (5) and a variety of phenolics through Friedel-Crafts reaction, yielding desired products (6). To increase number of hydroxy moieties on the synthesized lignans, oxidative reaction using lead (IV) tetraacetate was performed. Removal of methylenedioxy of furofuran lignans containing a phenolic moiety produced unexpected products which contains *para*-quinone together with *ortho*-dihydroxy moieties on furofuran core structures (8-9). Consequently, to avoid oxidation of hydroxy groups, protection reaction was operated before oxidative cleavage was applied. Specially, tetra-*n*-butylammonium fluoride (TBAF) was successfully applied to remove protecting groups and methylenedioxy moiety in one step to obtain the desired products (11-12). The synthesized furofuran lignans (6-12) were further evaluated for antidiabetic activity through α -glucosidase inhibition. This experiment indicated that the number of free phenolic groups plays important role in α -glucosidase inhibition. The most potent inhibitor is beta-12 (IC_{50} 25.7, 12.9 and 5.3 μ M for maltase, sucrase and baker's yeast, respectively) which contains acetoxy and four hydroxy units on a furofuran lignan. Moreover, conformation at C-2 of furofuran core also has effect on α -glucosidase inhibition, in which b-products enhanced inhibition higher than a-products. Furthermore, *ortho*-dihydroxy also play important role to increase α -glucosidase inhibition. For kinetic study represented that furofuran lignans inhibited the enzymes by non-competitive and mixed inhibition. As mixed inhibition, furofuran lignans were predominantly inhibited by pathway of enzyme-inhibitor (EI) complex.

Field of Study: Chemistry

Student's Signature

Academic Year: 2018

Advisor's Signature

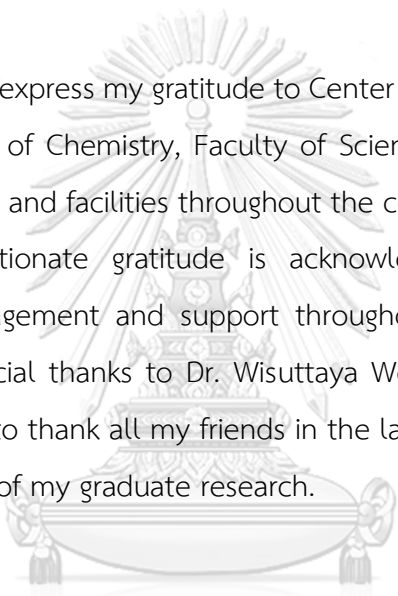
ACKNOWLEDGEMENTS

I wish to express my deep gratitude to my advisor, Associate Professor Dr. Preecha Phuwapraisirisan for his generous assistance, kind guidance and encouragement throughout the course of this research.

I would like to gratefully acknowledge the committees, Associate Professor Dr. Vudhichai Parasuk, Dr. Tanatorn Khotavivattana and Assistant Professor Dr. Vachiraporn Ajavakom for their comments, guidance and extending cooperation over my presentation.

I would like to express my gratitude to Center of Excellence in Natural Products Chemistry, Department of Chemistry, Faculty of Science, Chulalongkorn University for providing the chemicals and facilities throughout the course of study.

A deep affectionate gratitude is acknowledged to my family for their understanding, encouragement and support throughout the education course and I would like to give special thanks to Dr. Wisuttaya Worawalai for technical assistance. Moreover, I would like to thank all my friends in the laboratory for their friendships and help during the course of my graduate research.



จุฬาลงกรณ์มหาวิทยาลัย
CHULALONGKORN UNIVERSITY

Titiruetai Doungwichitrkul

TABLE OF CONTENTS

	Page
ABSTRACT (THAI).....	iii
ABSTRACT (ENGLISH).....	iv
ACKNOWLEDGEMENTS	v
TABLE OF CONTENTS	vi
LIST OF TABLES	ix
LIST OF FIGURES	x
LIST OF SCHEMES	xii
LIST OF ABBREVIATIONS	xiv
Chapter I Introduction	1
1.1 Lignans	1
1.2 Furofuran lignans	2
1.3 Bioactive lignans from sesame (<i>Sesamum indicum</i>).....	3
1.3.1 Anticancer activity.....	3
1.3.2 Antioxidative activity.....	4
1.3.3 Antidiabetic activity.....	5
1.4 Synthesis of furofuran lignans	7
1.5 Aims and scope of the present study.....	10
Chapter II Isolation and Preparation of the Starting Lignans	11
2.1 Isolation of starting lignans (1 and 2) and synthesis of samin (5).....	11
2.2 Experimental section	12
2.2.1 General experiment procedures	12

2.2.2 Chemical.....	12
2.2.3 Isolation of sesamin (1) and sesamolin (2).....	12
2.2.4 Synthesis of samin.....	13
Chapter III Synthesis of Furofuran Lignans <i>via</i> Friedel-Crafts Reaction	15
3.1 General procedure for the Friedel-Crafts reaction of lignans.....	15
3.1.1 Structural characterization of synthesized lignans	17
3.2 Experimental section	19
3.2.1 General experiment procedures	19
3.2.2 Chemical.....	20
3.2.3 General procedure for the Friedel-Crafts reaction of lignans	20
Chapter IV Synthesis of Furofuran Lignans <i>via</i> Methylendioxy Cleavage	30
4.1 General procedure for oxidative cleavage of methylendioxy.....	30
4.2 Methylendioxy cleavage of Silylated lignans.....	32
4.3 Experimental section	34
4.3.1 General experiment procedures	34
4.3.2 General procedure for the methylendioxy cleavage of lignans.....	34
4.3.3 Methylendioxy cleavage of protected lignans.....	39
Chapter V Antidiabetic Activity Evaluation	48
5.1 Antidiabetic activity evaluation of synthesized lignans	48
5.2 Experimental section	54
5.2.1 General experiment procedures	54
5.2.2 Chemical.....	54
5.2.3 Antidiabetic activity evaluation of synthesized lignans.....	54
5.2.3.1 Rat intestinal α -Glucosidase inhibition assay	54

5.2.3.2 Baker's yeast α -glucosidase inhibitory activity	55
Chapter VI Kinetic study and a possible mechanism.....	57
6.1 Kinetic Study.....	57
6.2 Experimental section	61
6.2.2 General experiment procedures	61
6.2.3 Chemical.....	61
6.2.4 Antidiabetic activity evaluation of synthesized lignans.....	61
6.2.5 Kinetic study.....	61
Chapter VII Conclusion	63
REFERENCES	65
APPENDIX.....	70
VITA.....	133

LIST OF TABLES

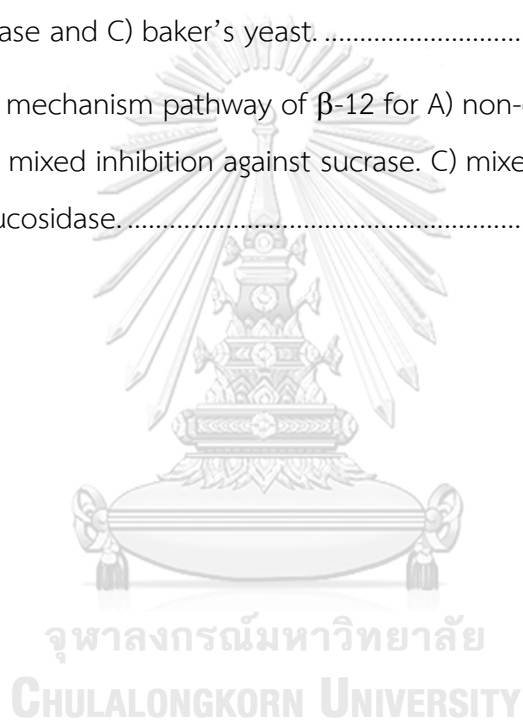
	Page
Table 3.1 Synthesis of furofuran lignans having multiphenolic groups (ArOH).....	16
Table 5.1 α -Glucosidase inhibitory effect of synthesized compounds (1-2, 5 and 6).	48
Table 5.1 (Cont.) α -Glucosidase inhibitory effect of synthesized compounds (6-7)....	49
Table 5.2 α -Glucosidase inhibitory effect of synthesized compounds (3-4, 8-12).....	50
Table 6.1 Inhibition types and kinetic parameters of β -12, α -12, 4 and β -8d on α -glucosidases.....	60



LIST OF FIGURES

	Page
Figure 1.1 The C6–C3 unit and subtypes of classical lignans (Ar = aryl).....	1
Figure 1.2 Stereoemer arrangement of 2,6-diaryl substituent on furofuran core structure relation to bridgehead hydrogen. Hydrogen atoms in the right hand structures are omitted for clarity.	2
Figure 1.3 Structures of sesamin (1) and sesamol (2).	3
Figure 1.4 Conformations of 1 and 2.	3
Figure 1.5 Types of diabetic mellitus (https://stemcellthailand.org/therapies/diabetes-mellitus-type-1-2).	5
Figure 1.6 α -Glucosidase hydrolyzed starch to produce α -glucose.	6
Figure 1.7 Inhibition of α -glucosidase by inhibitor restrains carbohydrate metabolism resulting in decrease in blood glucose. ²¹	6
Figure 1.8 Structure of pinoreosinol.	7
Figure 1.9 Proposed metabolic pathway of sesamin (1) to catechol derivatives (3 and 4) and enterolactone.	7
Figure 1.10 Particular phenolic compounds (ArOH) used in Worawalai's project. Arrow indicates the linkage between phenolic and samin moiety.	9
Figure 3.1 Electron density on phenolics ring indicated by arrows.	17
Figure 3.2 HMBC correlations of α -6c.	18
Figure 3.3 HMBC correlations of furofuran lignans containing dihydroxy moieties (6g, 6h and 6h'). A) The desired products. B) The desired products with less steric effect.	18
Figure 3.4 ¹ H NMR spectra of α -6h and β -6h.	19
Figure 3.5 Cyclic conformations of α - and β -products. The Newman projections demonstrate dihedral angles of H-4 and H-5.	19

Figure 4.1 HMBC correlations of α -10.....	32
Figure 5.1 α -glucosidase inhibition of the synthesized lignans containing free hydroxy groups (3-4, 6-7, 11-12).....	51
Figure 5.2 Sucrase inhibition of the synthesized lignans containing dihydroxy moiety.	52
Figure 5.3 Sucrase inhibition of the synthesized lignans (3-4, 8 and 12).....	53
Figure 6.1 Lineweaver-Burk and secondary plots for inhibitory activity of β -12 against A) maltase, B) sucrase and C) baker's yeast.	58
Figure 6.2 Putative mechanism pathway of β -12 for A) non-competitive inhibition against maltase. B) mixed inhibition against sucrase. C) mixed inhibition against baker's yeast α -glucosidase.....	60



LIST OF SCHEMES

	Page
Scheme 1.1 Antioxdative metabolites of sesamin (1).....	5
Scheme 1.2 The methodology of furofuran lignans synthesis. A) Using small molecules as starting materials. B) Using 5 as an intermediate. C) Using natural sesamolin (2) as starting materials to synthesize 5.	8
Scheme 1.3 Synthesis of furofuran lignans.	9
Scheme 1.4 Formation of furofuran lignans containing a phenolic moiety.	9
Scheme 1.5 Methylendioxy cleavage of 1.	9
Scheme 1.6 Synthesis of new furofuran lignans containing catechol moiety	10
Scheme 2.1 Separation of sesamin (1) and sesamolin (2).	11
Scheme 2.2 Preparation of samin (5).	11
Scheme 2.3 Formation of samin (5).....	12
Scheme 3.1 Synthesis of furofuran lignans having free phenolic group(s) (ArOH). Arrow indicates the linkage between phenolic and samin moiety while drash arrow indicates another possible regioselective site.	15
Scheme 3.2 Synthesis of α -sesaminol (α -7) and β -sesaminol (β -7).	17
Scheme 4.1 Synthesis of 3 and 4.....	30
Scheme 4.2 Synthesis of lignans containing para-quinone (8 and 9).	31
Scheme 4.3 Synthesis of α -10.	31
Scheme 4.4 Synthesis of new furofuran lignan via protection and deprotection reaction.....	33
Scheme 4.5 Synthesis of 12.	34
Scheme 4.6 Proposed formation of acetoxy group in 12.	34
Scheme 5.1 Colorimetric technique for the determination of glucose.	55

Scheme 5.2 Hydrolysis by yeast α -glucosidase. 56



LIST OF ABBREVIATIONS

acetone- d_6	deuterated acetone
brd	broad doublet (NMR)
brs	broad singlet (NMR)
calcd	calculated
^{13}C NMR	carbon-13 nuclear magnetic resonance
CDCl_3	deuterated chloroform
CD_3OD	deuterated methanol
COSY	correlated spectroscopy
CoMFA	comparative molecular field analysis
CoMSIA	comparative molecular similarity indices analysis
D_2O	deuterium oxide
DMF	<i>N,N</i> -dimethylformamide
DMAP	4-(dimethylamino)pyridine
DM	diabetes mellitus
ddd	doublet of doublet of doublet (NMR)
dt	doublet of triplet (NMR)
d	doublet (NMR)
dd	doublet of doublet (NMR)
2D NMR	two dimensional nuclear magnetic resonance
1D NMR	one dimensional nuclear magnetic resonance
ESIMS	electrospray ionization mass spectrometry
equiv	equivalent (s)
GLUT-4	glucose transporter 4

g	gram (s)
^1H NMR	proton nuclear magnetic resonance
Hz	Hertz
HRESIMS	high resolution electrospray ionization mass spectrum
HIV	human immunodeficiency virus
h	hour (s)
IC ₅₀	concentration that required for 50% inhibition <i>in vitro</i>
IDDM	insulin-dependent diabetes mellitus
J	coupling constant
mg	milligram (s)
mL	milliliter (s)
mmol	millimole (s)
m/z	mass per charge
m	multiplet (NMR)
MsCl	mesyl chloride
M.W.	molecular weight
M	molar
NIDDM	non-insulin-dependent diabetes mellitus
PNP-G	<i>p</i> -nitrophenyl- α -D-glucopyranoside
PLS	partial least squares
rt	room temperature
s	singlet (NMR)
TFA	trifluoroacetic acid
THF	tetrahydrofuran

TMS	tetramethylsilane
TsOH	<i>p</i> -toluenesulfonic acid
TLC	thin layer chromatography
U	unit
UV	ultraviolet
δ	chemical shift
δ_{C}	chemical shift of carbon
δ_{H}	chemical shift of proton
$^{\circ}\text{C}$	degree Celsius
U_{max}	maximum wave number
μL	microliter (s)
μM	micromolar (s)
% yield	percentage yield
$[\alpha]_{\text{D}}$	specific optical rotation

Chapter I

Introduction

1.1 Lignans

Natural products, a driving force for the discovery of new chemical reactivity, have been extracted to be a main source of medicines. Lignans, one of the largest families, have interesting biological and pharmacological activities.¹ In general, lignans are presented in a wide variety of plant-based foods, including fruits, vegetables and high concentration in seeds² which are derived from the shikimic acid biosynthetic pathway. The structure of lignan contains two C₆-C₃ unit (phenylpropanoids) linked by a bond between phenyl group (C₆) or propyl residue of each unit. A survey on the molecular structure of lignans obtained from different plant families could be classified into eight groups based on their structural patterns, carbon skeletons and oxygen which is incorporated into the skeletons. These are aryl-naphthalene, aryl-tetralin, dibenzocyclooctadiene, dibenzylbutane, dibenzylbutyrolactol, dibenzylbutyrolactone, furofuran, and furan (Figure 1.1).³

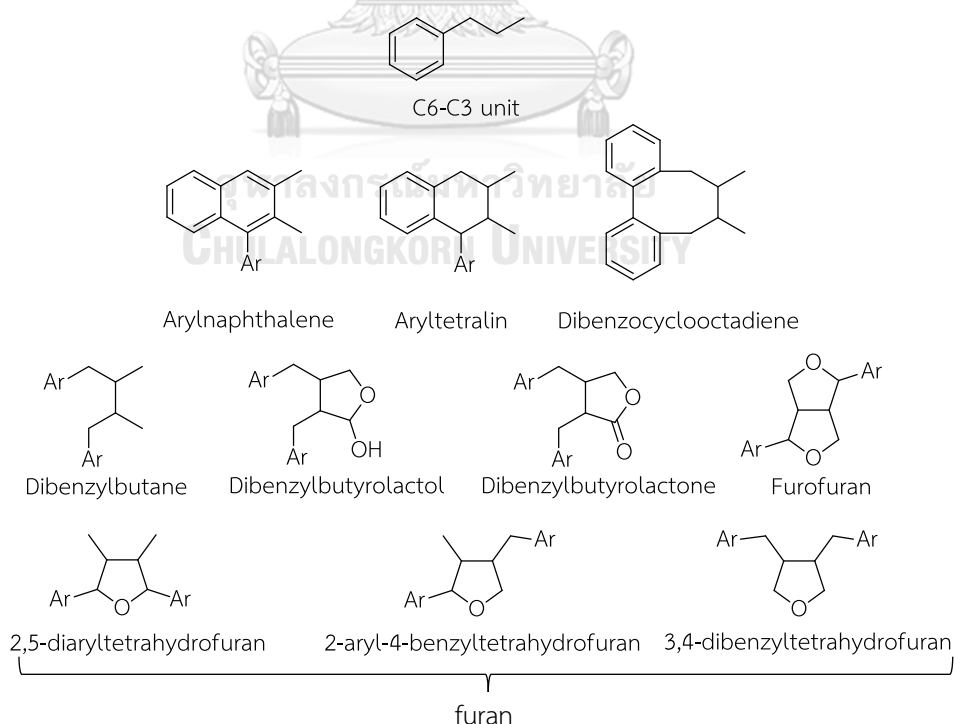


Figure 1.1 The C₆-C₃ unit and subtypes of classical lignans (Ar = aryl).

1.2 Furofuran lignans

Furofuran type lignans are widely distributed in edible plants, seeds, cereal products, and *Brassica* vegetables. Furofuran lignans (2,6-diaryl-3,7-dioxabicyclo [3.3.0] octane lignan) are a large group of lignans which are biosynthesized from oxidative coupling of two phenylpropanoids ($2 \times C_6-C_3$) to form two fused tetrahydrofuran rings as a central core. There are three different main types of furofuran lignans found in natural products (Figure 1.2), depending on configurations at 2,6-diaryl groups on the face the bicyclic core. The majority of furofuran lignans have been exo-exo aryl substitution, although many compounds with endo-exo aryl substitution and a few compounds with endo-endo substitution have been reported.

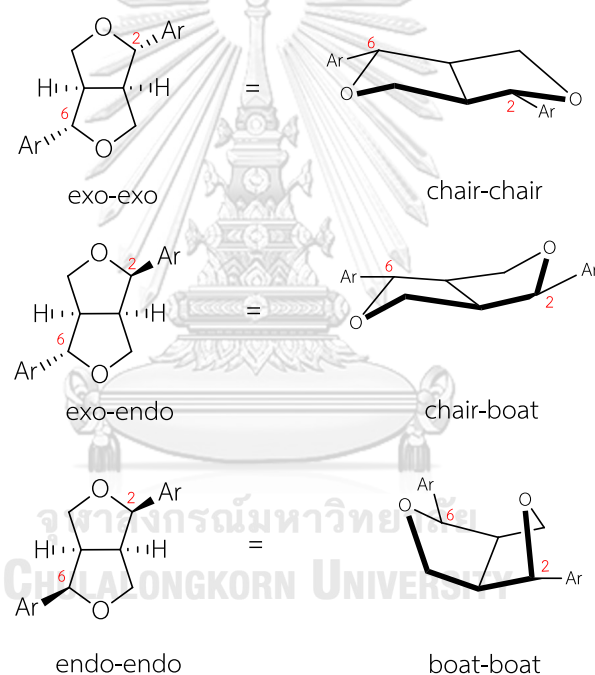


Figure 1.2 Stereomer arrangement of 2,6-diaryl substituent on furofuran core structure relation to bridgehead hydrogen. Hydrogen atoms in the right hand structures are omitted for clarity.

Sesame (*Sesamum indicum*) has been a traditional healthy food in Asian countries for centuries. It is found in Asia, Africa, and South America that is grown for the oil in its seed. Of furofuran lignans reported so far, sesamin (**1**) and sesamol (**2**), major lignans in sesame seed oil, have been most widely investigated. Sesamin (**1**) and

sesamol (1) and sesamin (2) are closely related analogues differing only in one additional oxygen atom in sesamin (2) structure (Figure 1.3).

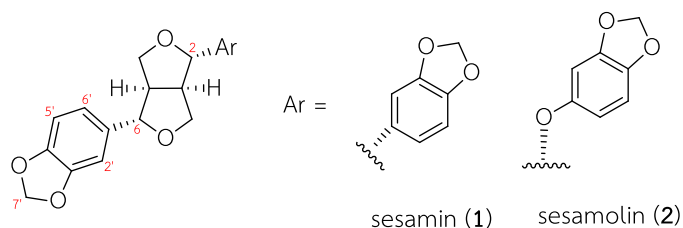


Figure 1.3 Structures of sesamin (1) and sesaminol (2).

Although the structures of sesamin (1) and sesaminol (2) are closely related, the cyclic acetal of 2 favors a pseudo-axial position for the aryloxy substituent. Hence, the chair-boat conformation of 2 is preferred while the chair-chair conformation of 1 is dominant (Figure 1.4).⁴

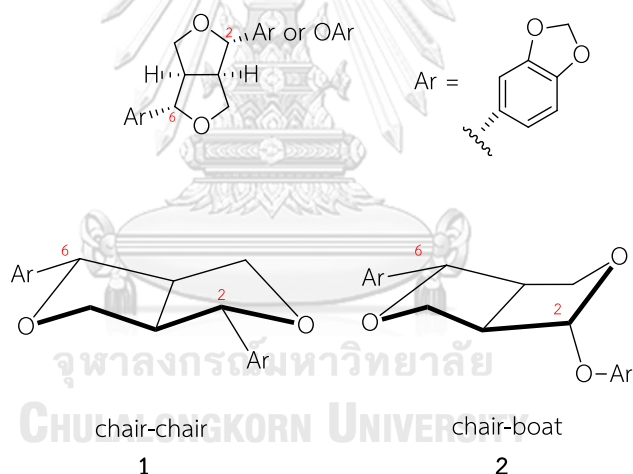


Figure 1.4 Conformations of 1 and 2.

1.3 Bioactive lignans from sesame (*Sesamum indicum*)

Interestingly, sesamin (1) and sesaminol (2) revealed several bioactivities that are beneficial to human health such as anticancer, antioxidative and antidiabetic activities.

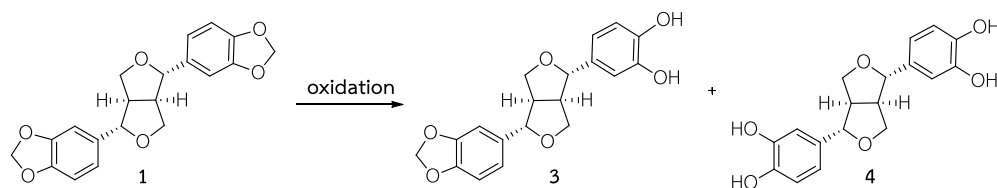
1.3.1 Anticancer activity

The anticancer activity of furofuran lignans from sesame has so far been developed as drugs.⁵⁻¹⁰ In 1992, Hirose and co-workers reported that the dietary

supplementation of **1** suppressed against 7,12-dimethylbenz[a]anthracene which induced mammary carcinogenesis. The dietary supplementation of **1** significantly reduced the cumulative number of palpable mammary cancers by 36% compared with animals on a control diet in 12 weeks.⁶ In 2001, **2** was reported by Miyahara and co-workers to induce apoptosis in the human lymphoid leukemia Molt 4B cells⁷, while Ryu and co-workers found that **2** inhibited the growth of human leukemia HL-60 cells in cultures.⁸ Both of **1** and **2** were tested for their ability to protect BV-2 microglia from hypoxia-induced cell death. Their results indicated that the mechanism of sesame antioxidants involved inhibition against mitogen-activated protein kinases pathways and apoptosis through scavenging of reactive oxygen species in hypoxia-stressed BV-2 cells.⁹ Moreover, **1** and **2** were also proved on Raji cells by Kim and colleagues. They observed that only **2** improved the cytotoxic activity of NK cells to enhance antitumor activity on Raji cells.¹⁰

1.3.2 Antioxidative activity

To develop antioxidant activity, Kang and co-workers determined the ability of **2** to act as an antioxidant *in vivo* in 1998. Rats were fed with a diet containing **2**, and its metabolism and effects on oxidative stress were studied. After 2 weeks, **2** was not detected in urine while 2-thiobarbituric acid reactive substances was significantly lower in the kidneys and liver. These results suggested that **2** and its metabolites may contribute to the antioxidative properties.¹¹ However, **1** was not actually active against oxidative stress *in vitro* experiments. It is suggested that **1** is a prodrug, in which its methylenedioxyphenyl moiety was transformed into dihydrophenyl (catechol) moieties found in structures of **3** and **4** (Scheme 1.1).¹² In the same way, Hou and co-workers studied that **1** and **2** prevented hypoxia on BV-2 and PC12 cells. In all experiments, **1** and **2** were carried out in the presence of sesame antioxidants which treated with cells. Moreover, sesame antioxidants suppressed p38 mitogen-activated protein kinases and reactive oxygen species generation using nitrite.¹³⁻¹⁴ Specially, antioxidative activity was reported to involve prevention of cardiovascular disease¹⁵ and possession of neuroprotection¹⁶.



Scheme 1.1 Antioxidative metabolites of sesamin (1).

1.3.3 Antidiabetic activity

Diabetes mellitus (DM) is a chronic disease, in which blood sugar level is raised or so called hyperglycaemia. DM occurs either when insulin is not produced or cannot effectively work in the body. Insulin is a hormone, which is produced by the pancreas and regulates blood sugar level. There are two main types of diabetes: type 1 and type 2 (Figure 1.5). Type 1 DM is body's cells cannot take glucose from the blood because of deficient insulin production. On the other hand, type 2 DM is resulted from insufficient insulin.¹⁷⁻¹⁹

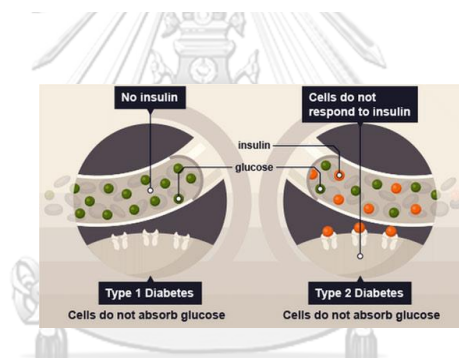


Figure 1.5 Types of diabetic mellitus (<https://stemcellthailand.org/therapies/diabetes-mellitus-type-1-2>).

There are many types of enzymes which hydrolyze starch to glucose (Figure 1.6). α -Glucosidase, such as maltase, sucrase and isomaltase, is a group of enzymes that hydrolyze starch at α -glucosidic linkage to produce α -glucose. α -Glucosidase inhibitors restrain α -glucosidase to decrease glucose level in blood vessel (Figure 1.7). Nowadays, Acarbose[®] is common drug used to treat type 2 DM. However, gastrointestinal adverse effects are common in patients treated with acarbose, and it may decrease efficacy of diabetes therapy.²⁰

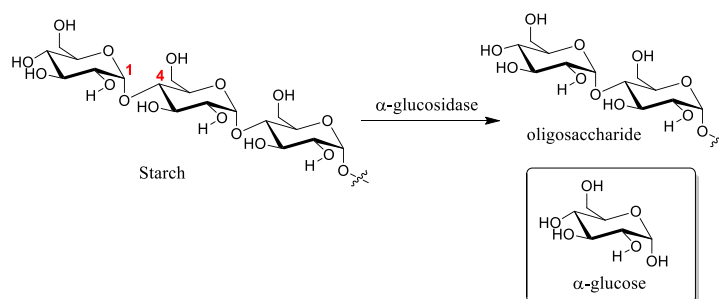


Figure 1.6 α -Glucosidase hydrolyzed starch to produce α -glucose.

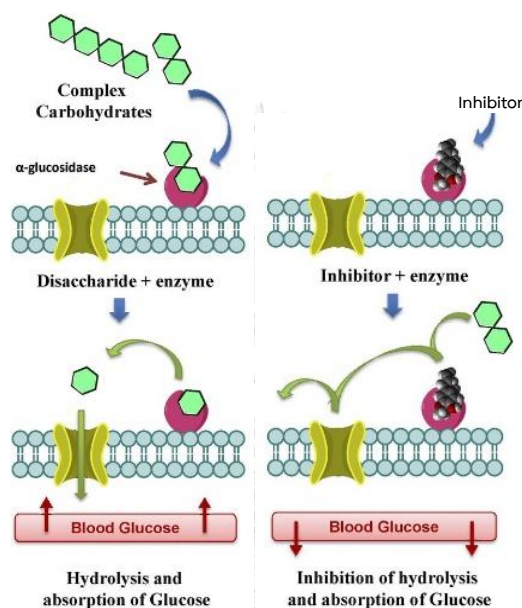


Figure 1.7 Inhibition of α -glucosidase by inhibitor restrains carbohydrate metabolism resulting in decrease in blood glucose.²¹

A few works were reported about antidiabetic activity. In 2011 Dehkordi and Roghani found that **2** prevented abnormal changes in diabetic rats and attenuated oxidative stress in aortic tissue.²² In addition, Hong and colleagues showed that **1** was able to ameliorate insulin resistance in type 2 diabetes mice.²³ Apart from **1** and **2**, pinorelinol was also isolated from sesame seeds. Only pinorelinol (Figure 1.8) showed inhibitory activity against rat intestinal maltase with an IC_{50} value of $34.3 \mu\text{M}$.²⁴ Active compounds for antidiabetic activity were observed by Worawalai and co-workers.²⁵ Of products examined, the synthesized lignans having at least one free phenolic motif showed enhanced inhibition over those bearing no free phenolic motif.

This observation supported the postulation that free phenolic motif plays a critical role in exerting inhibitory effect against α -glucosidase and free radical.

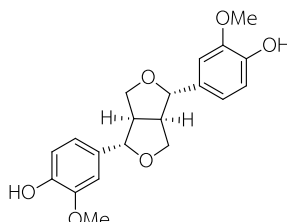


Figure 1.8 Structure of pinoresinol.

As evidences, **1** and **2** induced inhibition against cancer while antioxidant and antidiabetic activities were noted when they were metabolized. Further, Peñalvo²⁶ and Liu²⁷ demonstrated that enterolactone as a final product was the major metabolite of **1** both *in vivo* and *in vitro*. These observations imply that the presence of free phenolic motifs would be associated with enhancing bioactivity (Figure 1.9).²⁴

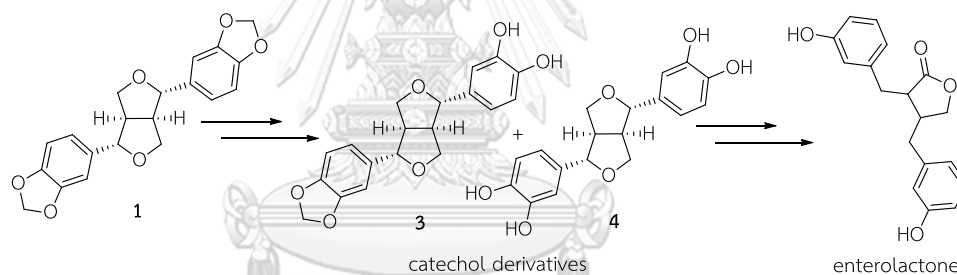
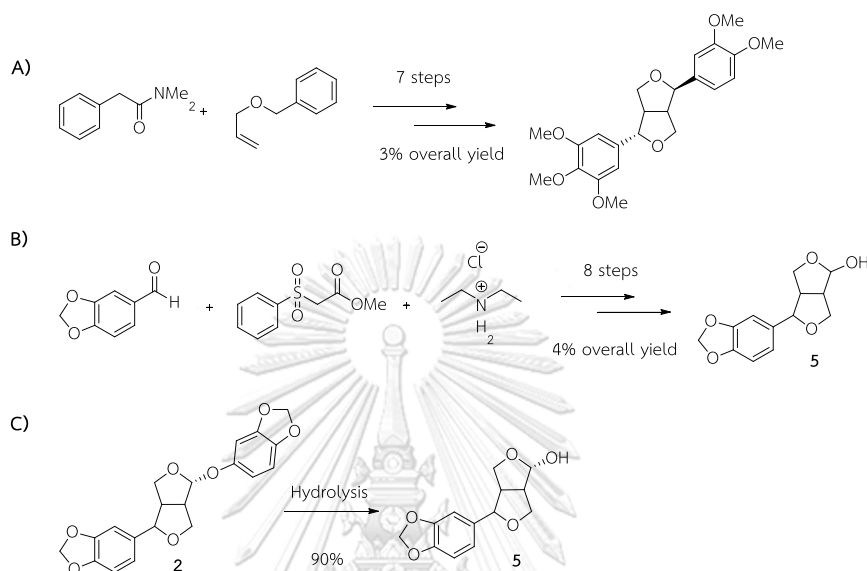


Figure 1.9 Proposed metabolic pathway of sesamin (**1**) to catechol derivatives (**3** and **4**) and enterolactone

1.4 Synthesis of furofuran lignans

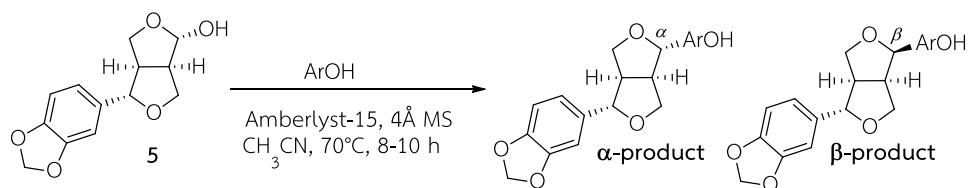
Due to the interesting biological activities of **1** and **2**, including related lignans, several attempts have been made to synthesize the desired products. To synthesize furofuran lignan, total synthesis using small molecules as starting materials afforded the desired furofuran lignans with limit of phenolic moieties and low overall yield (Scheme 1.2A).²⁸⁻²⁹ To synthesize a wide variety of furofuran lignans, an alternative synthesis approach using samini (**5**) as starting material was introduced. Samini (**5**) is considered as a reactive lignan because it contains hemiacetal unit which can be coupled with a wide variety of phenolic compounds to produce the desired furofuran

lignans. Samin (**5**) can be obtained from total synthesis using small molecules (Scheme 1.2B);³⁰ however, this method produced **5** in low overall yields, in 8 steps. To address this problem, **5** can be obtained in high yield from sesamol (**2**), a major lignan found in sesame seed oil, by one-step hydrolysis (Scheme 1.2C).^{25, 31}



Scheme 1.2 The methodology of furofuran lignans synthesis. A) Using small molecules as starting materials. B) Using **5** as an intermediate. C) Using natural sesamol (**2**) as starting materials to synthesize **5**.

In 2016, Worawalai and coworkers²⁵ synthesized series of furofuran lignans containing a phenolic moiety using **5** as a starting material (Scheme 1.3). Under acidic condition, **5** was dehydrated to afford oxocarbenium ion, which was attacked by phenolic compounds (ArOH, Figure 1.10) as a nucleophile *via* S_EAr mechanism, thus yielding the desired lignans as a mixture of two epimers, α - and β -products (Scheme 1.4). The regioselectivity of desired products were generated from C-2 of furan moiety and phenolic at *ortho*-position to hydroxy or methoxy groups through the carbon-carbon bond, as indicated by the arrows in Figure 1.10.



Scheme 1.3 Synthesis of furofuran lignans.

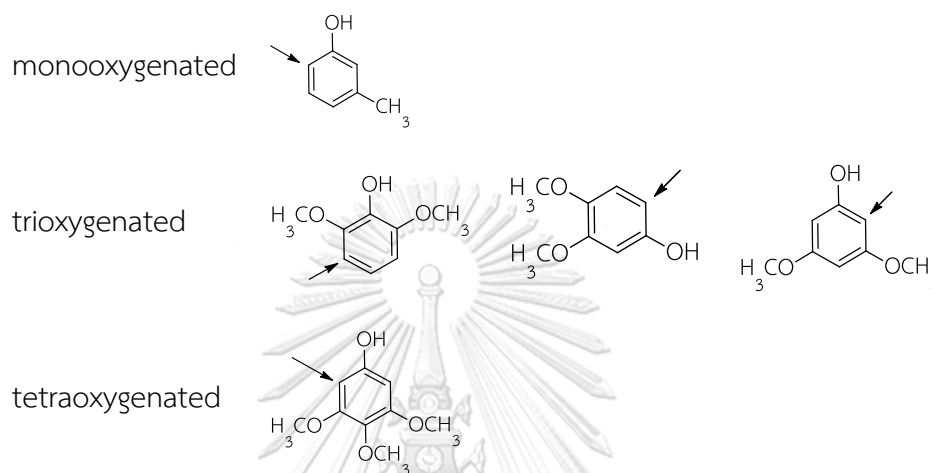
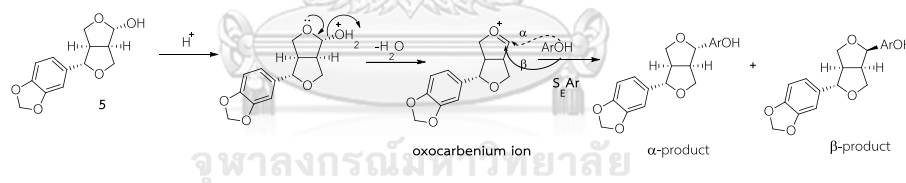
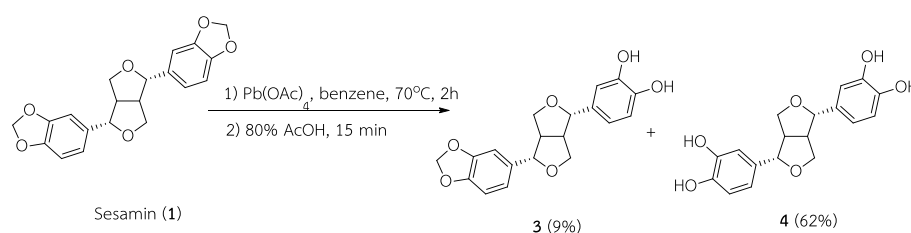


Figure 1.10 Particular phenolic compounds (ArOH) used in Worawalai's project. Arrow indicates the linkage between phenolic and samini moiety.



Scheme 1.4 Formation of furofuran lignans containing a phenolic moiety.

In 2008, Urata oxidized sesamin (**1**) using Pb(OAc)₄ to remove methylenedioxy (-OCH₂O-) moieties (Scheme 1.5), affording the products bearing one (**3**) and two catechol moieties (**4**).³² In addition, the methylenedioxy moieties in sesamin (**1**) were also oxidized by BBr₃ to yield **3** and **4**, together with their epimers.³³

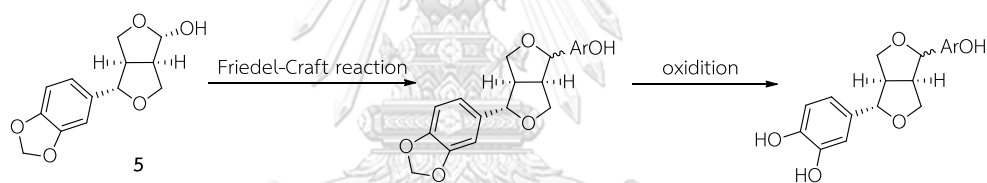


Scheme 1.5 Methylenedioxy cleavage of **1**.

1.5 Aims and scope of the present study

Regarding metabolized furofuran lignans, the hydroxy moiety was reported to enhance bioactivity and are crucial to antidiabetic activity.²⁵ This is the first study of the relation between number of hydroxy units and antidiabetic activity. The methylenedioxy cleavage could increase number of hydroxy units in good yield using $\text{Pb}(\text{OAc})_4$.

In this project, furofuran lignans having multiple phenolics are synthesized using Worawalai's method. The products obtained from the first step are further oxidized by $\text{Pb}(\text{OAc})_4$ to eliminate methylenedioxy ($-\text{OCH}_2\text{O}-$) moiety, thus affording the catechol analogues (Scheme 1.6). Furthermore, the synthesized lignans will be evaluated for their antidiabetic activity as well as the mechanism underlying the inhibitory effect. This project is expected to obtain the potent antidiabetic agents and provide the insight into the critical role of multiphenolic groups in exerting antidiabetic activity.



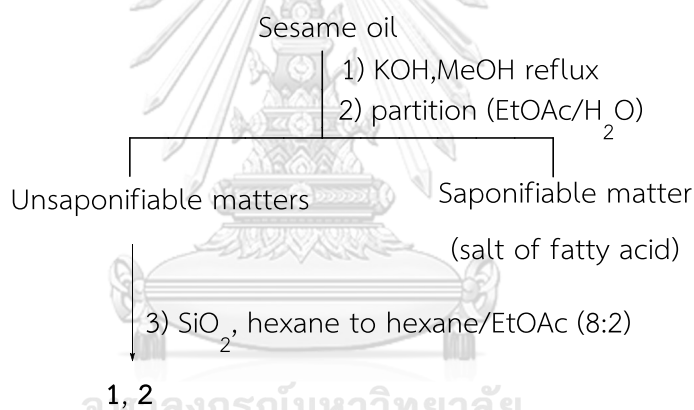
Scheme 1.6 Synthesis of new furofuran lignans containing catechol moiety

Chapter II

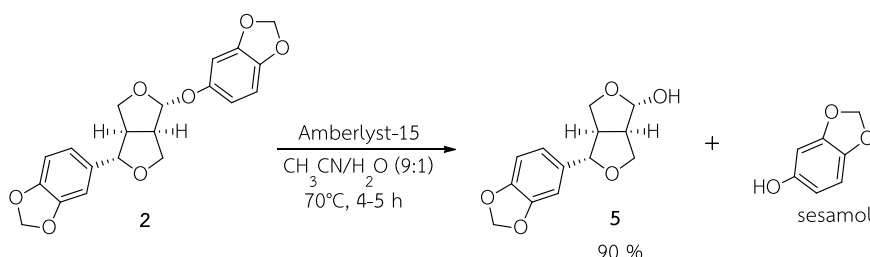
Isolation and Preparation of the Starting Lignans

2.1 Isolation of starting lignans (1 and 2) and synthesis of samin (5)

Commercially available sesame seed oil was used as a source of sesamin (1) and sesamol (2). However, the oil comprises 1-2% of sesamin and sesamol while the major components are fatty acid. To facilitate the isolation of target lignans, sesame seed oil was first saponified by KOH/MeOH to remove fatty acid (saponifiable matter), yielding unsaponifiable matter as a mixture of sesamin (1) and sesamol (2) (Scheme 2.1). Finally, sesamin (1) and sesamol (2) could be purified by silica gel column chromatography. Samin (5, 90%) was obtained by acid-catalyzed hydrolysis of sesamol (2) (Scheme 2.2).²⁵



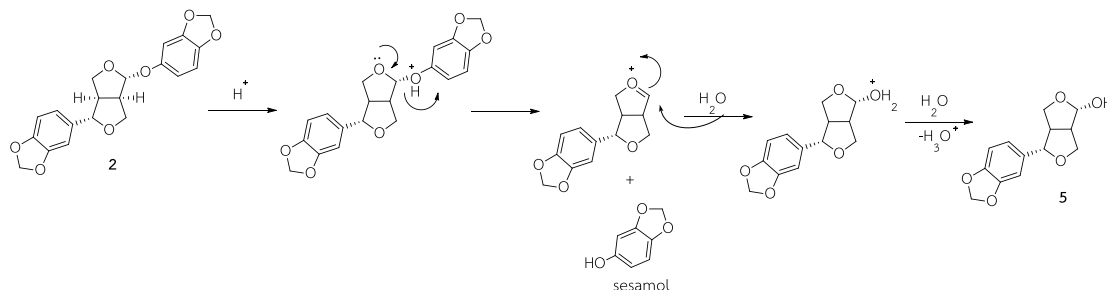
Scheme 2.1 Separation of sesamin (1) and sesamol (2).



Scheme 2.2 Preparation of samin (5).

Amberlyst-15, acidic resin, was used to protonate hydroxy group of sesamol (2). Subsequently, the carbon-oxygen bond broke to obtain oxocarbenium ion which was attacked by a water molecule as a nucleophile to obtain samin (5). Although water

could attack on each face of the planar carbocation, **5** is dominated by α -product due to anomeric effect (Scheme 2.3).



Scheme 2.3 Formation of samin (**5**).

2.2 Experimental section

2.2.1 General experiment procedures

All experiments were carried out under a nitrogen atmosphere. The ^1H spectra were recorded on a 400 MHz Bruker AVANCE spectrometer and on a Varian Mercury⁺ 400 NMR spectrometer (CDCl_3 as a solvent). Analytical thin layer chromatography (TLC) was performed on pre-coated Merck silica gel 60 F_{254} plates (0.25 mm thick layer). Column chromatography was performed on Merck silica gel 60 (70–230 mesh).

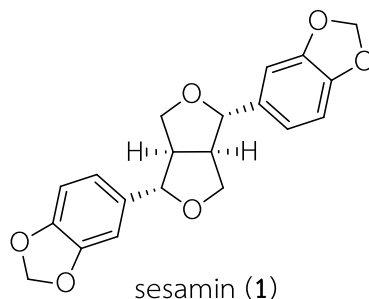
2.2.2 Chemical

Sesame seed oils was purchased from Soumpa-na (Samutsakorn, Thailand) in 2017. Saponification number of purchased oil is approximately 156.6 mgKOH/oil. All reagents were obtained from Sigma-Aldrich and used without further purification.

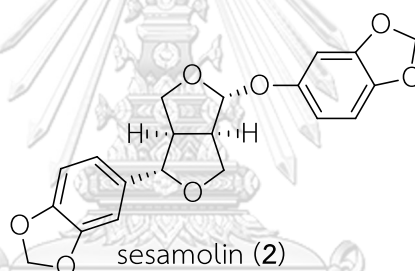
2.2.3 Isolation of sesamin (**1**) and sesamol (**2**)

Sesame seed oil (150 g) was added by KOH (25 g) in MeOH (150 mL) and heated at 70°C for 5 h, yielding unsaponifiable matter as a mixture of sesamin (**1**) and sesamol (**2**). After cooling, the reaction mixture was evaporated to dryness and extracted by ethyl acetate/ H_2O (1:1, 3 times). The combined organic layers were dried over anhydrous Na_2SO_4 and concentrated under reduced pressure. A portion of the organic layer was subjected to silica gel column chromatography eluted with hexane and the mixture of hexane and ethyl acetate. Fractions eluted with 85:15 hexane/ethyl

acetate yielded sesamin (**1**, 2.9762 g, 2%) whereas fractions eluted with 8:2 hexane/ethyl acetate afforded sesamolol (**2**, 1.5029 g, 1%).³⁴



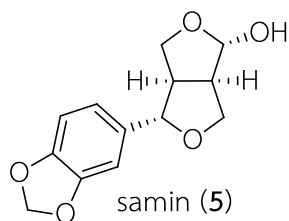
Sesamin (**1**); white solid; ¹H NMR (400 MHz, CDCl₃) δ 6.85 (s, 2H), 6.79 (d, *J* = 2.2 Hz, 4H), 5.95 (s, 4H), 4.71 (d, *J* = 3.7 Hz, 2H), 4.23 (dd, *J* = 8.6, 6.5 Hz, 2H), 3.87 (dd, *J* = 9.1, 2.8 Hz, 2H), 3.07-3.03 (m, 2H). The data were consistent with previous report.³⁵



Sesamolol (**2**); white solid; $[\alpha]_D^{25} = +198$ (c 0.1, CHCl₃); ¹H NMR (CDCl₃, 400 MHz) δ 6.88 (s, 1H), 6.84-6.77 (m, 2H), 6.71 (d, *J* = 8.5 Hz, 1H), 6.62 (d, *J* = 2.3 Hz, 1H), 6.50 (dd, *J* = 8.4, 2.4 Hz, 1H), 5.96 (s, 2H), 5.92 (s, 2H), 5.50 (s, 1H), 4.47-4.39 (m, 2H), 4.13 (dd, *J* = 9.2, 6.1 Hz, 1H), 3.96 (d, *J* = 9.2 Hz, 1H), 3.64 (dd, *J* = 9.0, 7.6 Hz, 1H), 3.31 (dd, *J* = 16.7, 8.7 Hz, 1H), 2.95 (dd, *J* = 15.4, 6.6 Hz, 1H). The data were consistent with previous report.²⁵

2.2.4 Synthesis of samin

Sesamolol (**2**, 0.27 mmol) was hydrolyzed by Amberlyst-15 (1 mg/0.005 mmol of **2**) in 9:1 acetonitrile/H₂O (10 mL) at 70°C for 8 h. Samin (**5**, 60 mg, 90%) was obtained as a brown oil after evaporation to dryness and purification by silica gel column chromatography (1:1 hexane/ethyl acetate).



Samin (5); Yield 90%; brown oil; ^1H NMR (400 MHz, CDCl_3) δ 6.86 (s, 1H), 6.80-6.75 (m, 2H), 5.95 (s, 2H), 5.39 (s, 1H), 4.37 (dd, $J = 19.8, 8.2$ Hz, 2H), 4.17 (dd, $J = 9.3, 6.1$ Hz, 1H), 3.91 (d, $J = 8.8$ Hz, 1H), 3.56 (dd, $J = 9.1, 7.5$ Hz, 1H), 3.08 (dd, $J = 16.8, 9.1$ Hz, 1H), 2.86 (dd, $J = 16.0, 6.6$ Hz, 1H). The data were consistent with previous report.²⁵



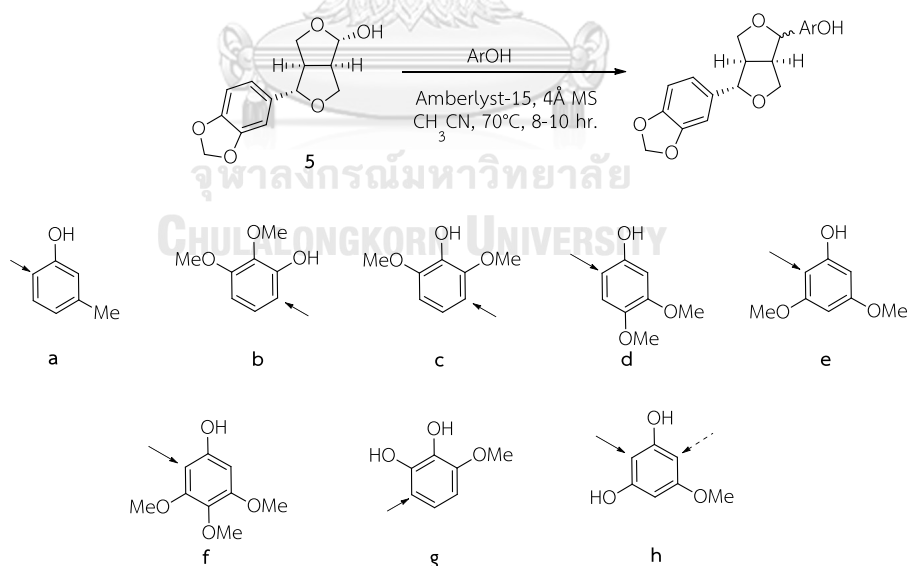
Chapter III

Synthesis of Furofuran Lignans *via* Friedel-Crafts Reaction

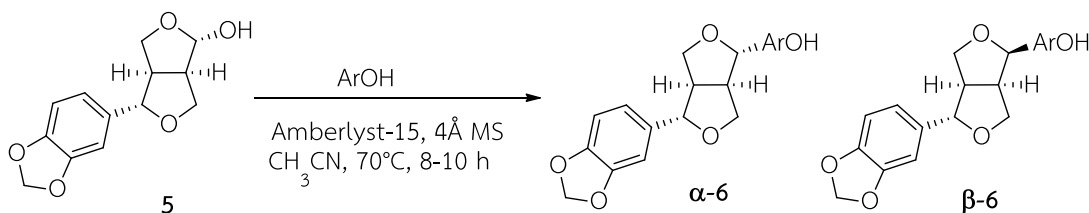
3.1 General procedure for the Friedel-Crafts reaction of lignans

Following the previous' method,²⁵ furofuran lignans containing free phenolic groups were synthesized by replacing the hydroxy group of samin (**5**) with a variety of phenolic moieties (ArOH, **a-h**) under acidic condition using Amberlyst-15 and purified by Sephadex LH-20. Then Prep-TLC was used to separate relative configurations (Table 3.1). Interestingly, molecular sieves 4Å were used to trap water molecules, driving a forward direction to obtain desired products in high yields.

The coupling reaction between samin (**5**) and phenolic moieties proceeded though Friedel-Crafts reaction. As expected, the α - and β -products were observed under acidic condition. Oxocarbenium ion as an intermediate was generated by protonation and cleavage of the carbon-oxygen bond of **5**. Subsequently, phenolic groups (**a-h**) as nucleophiles could attack at regioselective site as shown in Scheme 3.1.



Scheme 3.1 Synthesis of furofuran lignans having free phenolic group(s) (ArOH). Arrow indicates the linkage between phenolic and samin moiety while dashed arrow indicates another possible regioselective site.

Table 3.1 Synthesis of furofuran lignans having multiphenolic groups (ArOH)

Entry	ArOH	Isolated yield (%)	
		α -6	β -6
1	a	α -6a (30%)	β -6a (15%)
2	b	α -6b (78%)	- ^c
3	c	α -6c (27%)	β -6c (31%)
4	d	α -6d (68%)	β -6d (17%)
5	e	α -6e (47%)	β -6f (51%)
6	f	α -6f (30%)	β -6g (40%)
7	g	α -6g (41%)	β -6g (21%)
8 ^a	h	α -6h (5%)	β -6h (13%)
9 ^b	h'	α -6h' (2%)	β -6h' (11%)

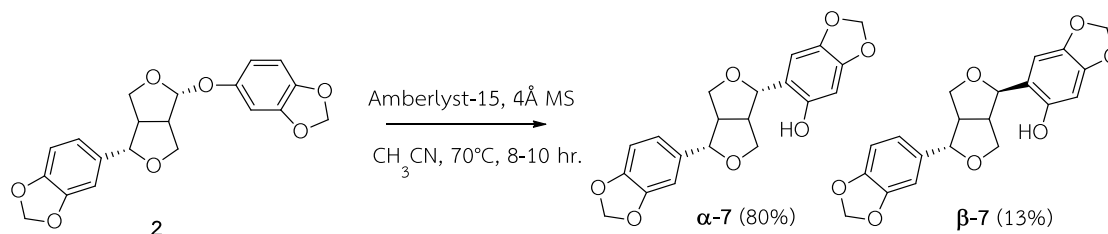
^a The connectivity between furan moiety and 5-methoxyresorcinal (**h**) in product **6h** is indicated by an arrow (Scheme 3.1).

^b The connectivity between furan moiety and 5-methoxyresorcinal (**h**) in product **6h'** is indicated by a dash arrow (Scheme 3.1).

^c The desired product was decomposed after purification.

Moreover, α -sesaminol (α -7) and β -sesaminol (β -7) were obtained from the reaction of sesamol (**2**) under acidic condition without water because water molecule can work as a nucleophile and produce samin (**5**, Scheme 2.3). Sesamol (**2**) was first protonated at sesamol moiety. The leaving of protonated sesamol generated oxocarbenium ion through the E₂ mechanism. Consequently, leaving sesamol reattacked oxocarbenium ion via S_EAr mechanism to obtain α -7 and β -7 (Scheme 3.2).

α -7 and β -7 were further purified by Sephadex LH-20 and Prep-TLC to give 80% and 13% yield, respectively.



Scheme 3.2 Synthesis of α -sesaminol (α -7) and β -sesaminol (β -7).

Orientation of the substituents on phenolic ring was another key factor to denominate the regioselective site and enhance reactivity. As for regioselectivity, it could be generalized that the highest electron density on phenolic group was critical to connect with furofuran lignan core structure. Moreover, the regioselective site was insignificantly predominated by steric effect (Figure 3.1).

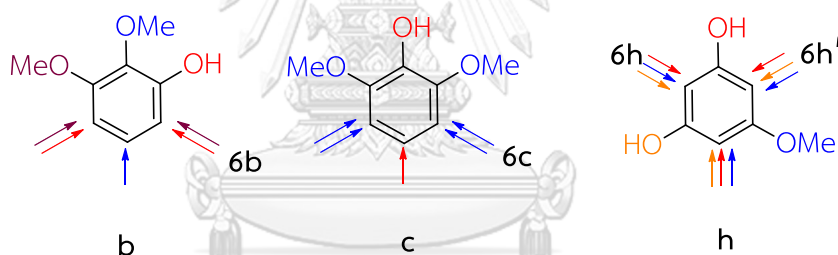


Figure 3.1 Electron density on phenolics ring indicated by arrows.

3.1.1 Structural characterization of synthesized lignans

In general, all synthesized lignans were characterized using ^1H NMR and ^{13}C NMR data. In case of unclear connectivity between samini (**5**) and phenolic moieties were found, 2D NMR such as COSY, HSQC and HMBC were applied to address the problem. In addition, the structures of all new products were also proved by 2D NMR together with HRMS. Herein, an example of unambiguous structural characterization of α -6b is shown in Figure 3.2. The HMBC correlation from H-2 ($\delta_{\text{H}} = 5.00$, d, $J = 5.1$ Hz, 1H) to C-1'' ($\delta_{\text{C}} = 120.5$), C-2'' ($\delta_{\text{C}} = 147.3$) and C-6'' ($\delta_{\text{C}} = 120.8$) suggested that furofuran moiety connected with **c** through C2/C1'' bond formation near hydroxy moiety. In addition, a methoxy unit at C-4'' could be significantly observed and the regioselective

site can be affirmed from the correlation between -OMe ($\delta_{\text{H}} = 3.85$, s, 1H) to C-4'' ($\delta_{\text{C}} = 152.1$) and H-5'' ($\delta_{\text{H}} = 6.45$, d, $J = 8.7$ Hz, 1H) to C-4'' ($\delta_{\text{C}} = 152.1$). In addition, other products having unclear connectivity between samini (**5**) and phenolic moieties were also proved by HMBC correlations shown in Figure 3.3.

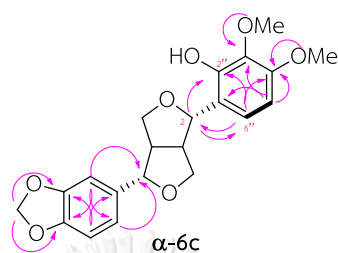


Figure 3.2 HMBC correlations of α -6c

A)



B)

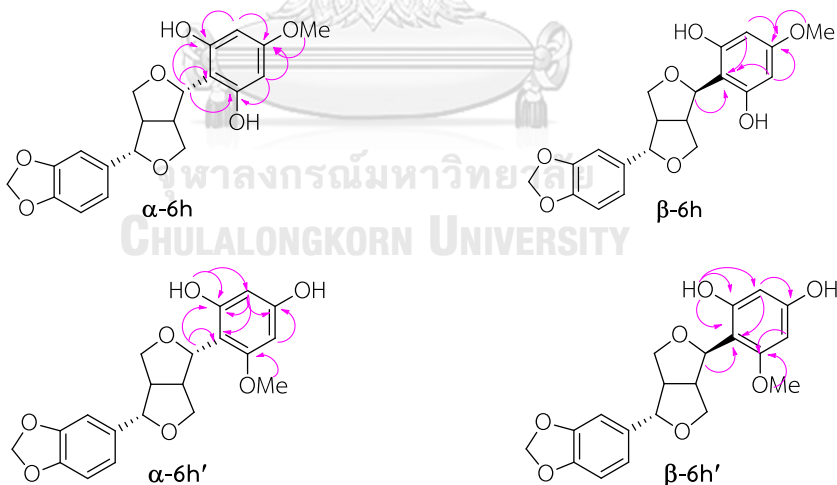


Figure 3.3 HMBC correlations of furofuran lignans containing dihydroxy moieties (**6g**, **6h** and **6h'**). A) The desired products. B) The desired products with less steric effect.

Among various approaches for assigning relative configuration, $^1\text{H-NMR}$ spectroscopy has attracted considerable attention to instantly confirm relative

configuration.²⁵ Worawalai's group demonstrated that α - and β -products could be distinguished by spin-spin splitting pattern of H-4_{eq}. Theoretically, H-4_{eq} and H-4_{ax} are enantiomeric protons and each would show doublet of doublet caused by geminal and vicinal coupling. In the experiment, H-4_{eq} of α -products showed doublet of doublet while H-4_{eq} revealed unexpected doublet pattern (Figure 3.4). The unexpected splitting of H-4_{eq} in β -products could be explained by a 90° dihedral angle of H-4_{eq} and H-5, thus yielding $J_{\text{H-4eq/5}} = 0$ Hz (Figure 3.5).

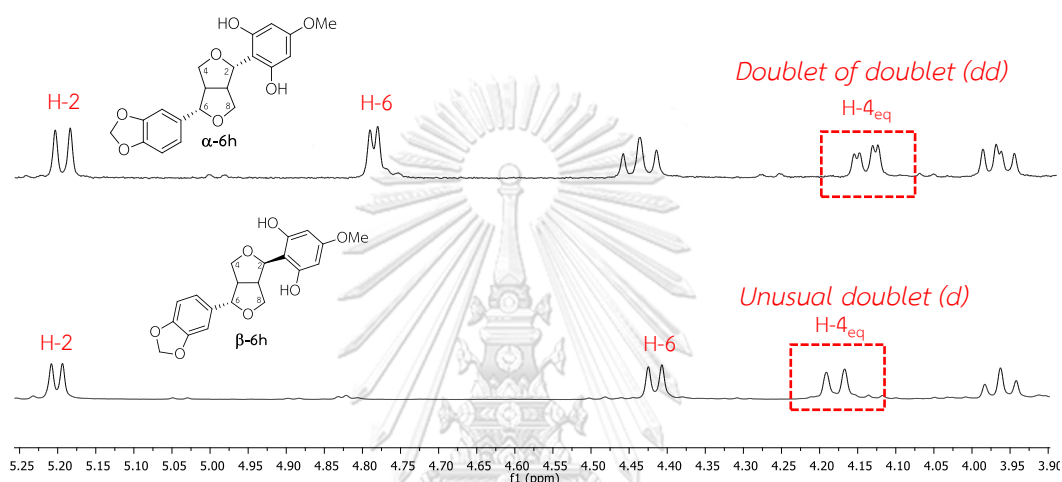


Figure 3.4 ¹H NMR spectra of α -6h and β -6h.

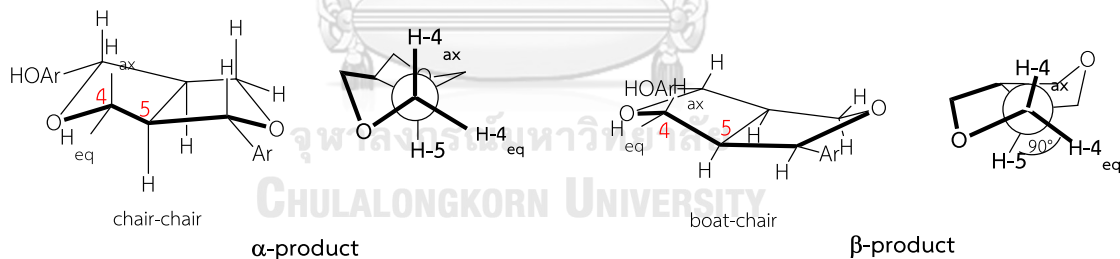


Figure 3.5 Cyclic conformations of α - and β -products. The Newman projections demonstrate dihedral angles of H-4 and H-5.

3.2 Experimental section

3.2.1 General experiment procedures

All experiments were carried out under a nitrogen atmosphere. The ¹H and ¹³C NMR spectra were recorded on a 400 MHz Bruker AVANCE spectrometer and on a Varian Mercury⁺ 400 NMR spectrometer (CDCl₃ as a solvent). Analytical thin layer chromatography (TLC) was performed on pre-coated Merck silica gel 60 F₂₅₄ plates (0.25

mm thick layer). Column chromatography was performed on Merck silica gel 60 (70–230 mesh) and Sephadex LH-20. Preparative thin-layer chromatography (Prep-TLC) separations were carried out on 0.50 or 0.75 mm Merck silica gel 60 PF₂₅₄ containing gypsum.

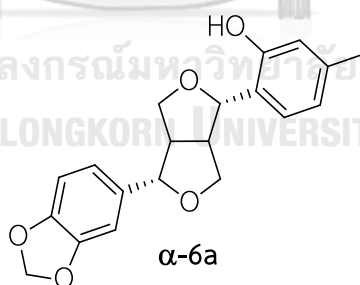
3.2.2 Chemical

All reagents were obtained from Sigma-Aldrich (St. Louis, MO, USA) and used without further purification.

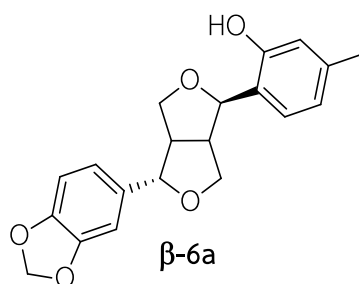
3.2.3 General procedure for the Friedel-Crafts reaction of lignans

A mixture of samin (**5**, 1 equiv) and acetonitrile (1.0 mL/0.1 mmol of **5**) was treated with phenolic compounds (**a-h**, 1.5–2 equiv), Amberlyst-15 (1 mg/0.005 mmol of **5**) and a 4 Å molecular sieve at 70°C for 8–10 h. The reaction mixture was evaporated to dryness, separated by Sephadex LH-20 using 1:1 dichloromethane/methanol as eluent and purified by Prep-TLC to separate α - and β -products.

Following general procedure, reaction of **5** (64.5 mg, 0.26 mmol) and **a** (40 μ L, 0.39 mmol) in acetonitrile (2 mL). After separation using Sephadex LH-20, Prep-TLC was developed in dichloromethane/ethyl acetate (95:5) to yield **α -6a** (27 mg, 30%) and **β -6a** (13 mg, 15%) both as a white powder.

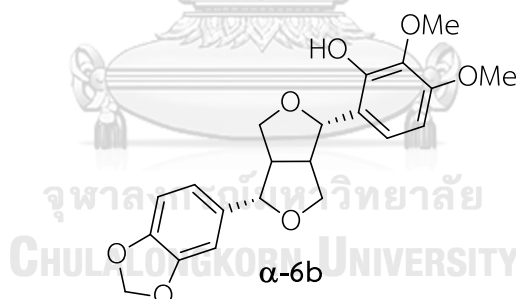


α -6a; ¹H NMR (CDCl₃, 400 MHz) δ 7.89 (brs, 1H), 6.92 (d, J = 7.6 Hz, 1H), 6.83 – 6.78 (m, 3H), 6.71 (s, 1H), 6.67 (d, J = 7.6 Hz, 1H), 5.95 (s, 2H), 4.87 (d, J = 4.0 Hz, 1H), 4.78 (d, J = 4.0 Hz, 1H), 4.34 (dd, J = 9.2, 7.6 Hz, 1H), 4.15 (dd, J = 9.2, 6.8 Hz, 1H), 3.92 – 3.85 (m, 2H), 3.22 – 3.18 (m, 1H), 3.17 – 3.11 (m, 1H), 2.29 (s, 3H); ¹³C NMR (CDCl₃, 100 MHz) δ 155.5, 148.2, 147.4, 139.8, 134.8, 126.8, 120.9, 120.9, 119.5, 117.9, 108.4, 106.7, 101.3, 86.7, 85.6, 72.5, 70.9, 53.6, 53.1, 21.2. The data were consistent with previous report.²⁵



β -6a; ^1H NMR (CDCl_3 , 400 MHz) δ 7.85 (brs, 1H), 6.92 (d, J = 7.6 Hz, 1H), 6.86 – 6.80 (m, 3H), 6.71 (s, 1H), 6.67 (d, J = 7.6 Hz, 1H), 5.97 (s, 2H), 4.85 (d, J = 5.6 Hz, 1H), 4.55 (d, J = 8.0 Hz, 1H), 4.11 (d, J = 9.6 Hz, 1H), 3.90 (dd, J = 8.4, 7.6 Hz, 1H), 3.82 (dd, J = 9.6, 6.0 Hz, 1H), 3.38 – 3.28 (m, 2H), 3.07 – 3.01 (m, 1H), 2.29 (s, 3H); ^{13}C NMR (CDCl_3 , 100 MHz) δ 155.5, 147.9, 146.9, 139.8, 132.0, 126.9, 121.2, 120.8, 118.8, 118.0, 108.4, 106.5, 101.2, 88.6, 82.0, 70.7, 70.2, 53.4, 49.9, 21.3. The data were consistent with previous report.²⁵

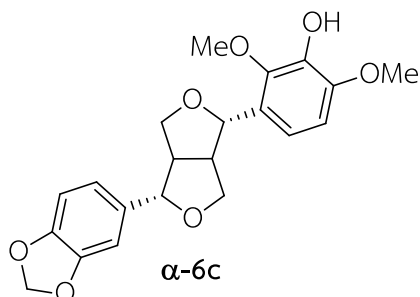
Following general procedure, reaction of **5** (235.8 mg, 0.94 mmol) and **b** (184 μL , 1.41 mmol) in acetonitrile (9 mL). After separation using Sephadex LH-20, Prep-TLC was developed in hexane/ethyl acetate (8:2, 3 times) to yield **α -6b** (284.0 mg, 78%) as a pale-yellow oil and mixture of **β -products** (215.6 mg) as yellow oil.



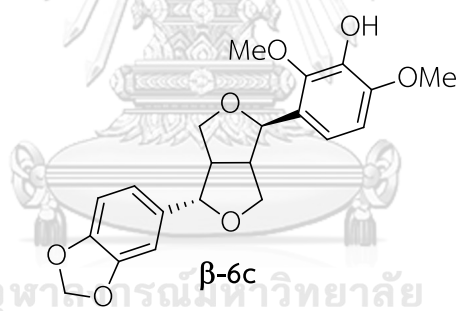
α -6b; ^1H NMR (400 MHz, CDCl_3) δ 6.95 (d, J = 8.7 Hz, 1H, H-6''), 6.86 (s, 1H, H-6'), 6.80 (s, 1H, H-2'), 6.78 (s, 1H, H-5'), 6.45 (d, J = 8.7 Hz, 1H, H-5''), 5.94 (s, 2H, H-7'), 5.00 (d, J = 5.1 Hz, 1H, H-2), 4.69 (d, J = 5.6 Hz, 1H, H-6), 4.29 – 4.22 (m, 2H, H-4 and H-8), 3.98 (dd, J = 9.1, 4.6 Hz, 1H, H-8), 3.92 (d, J = 4.6 Hz, 1H, H-4), 3.89 (s, 3H, -OMe), 3.85 (s, 3H, -OMe), 3.21 – 3.12 (m, 1H, H-1), 3.02 – 2.97 (m, 1H, H-5); ^{13}C NMR (100 MHz, CDCl_3) δ 152.1, 148.1, 147.3, 147.2, 136.1, 135.4, 120.8, 120.5, 119.6, 108.3, 106.7, 103.5, 101.2, 85.7, 83.1, 72.7, 71.7, 61.0, 56.0, 54.5, 53.3.

Following general procedure, reaction of **5** (36.0 mg, 0.14 mmol) and **c** (43 mg, 0.28 mmol) in acetonitrile (2 mL). After separation using Sephadex LH-20, Prep-TLC was

developed in dichloromethane/ethyl acetate (95:5) to yield **α -6c** (15 mg, 27%) as a yellow oil and **β -6c** (20 mg, 37%) as a yellow oil.

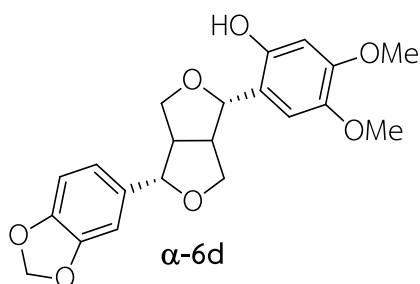


α -6c; ^1H NMR (CDCl_3 , 400 MHz) δ 6.89 – 6.73 (m, 4H), 6.62 (d, J = 8.6 Hz, 1H), 5.94 (s, 2H), 5.05 (d, J = 4.0 Hz, 1H), 4.68 (d, J = 4.0 Hz, 1H), 4.31 (dd, J = 9.1, 7.3 Hz, 1H), 4.22 (dd, J = 9.1, 6.6 Hz, 1H), 4.01 (dd, J = 9.2, 4.7 Hz, 1H), 3.92 (d, J = 4.3 Hz, 4H), 3.89 (d, J = 7.1 Hz, 4H), 3.10 – 3.02 (m, 1H), 3.01 – 2.93 (m, 1H); ^{13}C NMR (CDCl_3 , 100 MHz) δ 148.1, 147.4, 144.6, 138.7, 135.4, 128.3, 119.6, 115.9, 108.3, 106.7, 105.9, 101.2, 85.6, 82.4, 73.1, 71.6, 60.6, 56.4, 54.8, 54.2. The data were consistent with previous report.²⁵

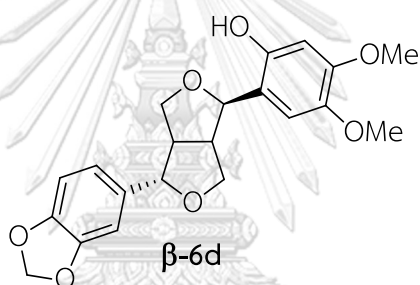


β -6c; ^1H NMR (CDCl_3 , 400 MHz) δ 7.02 (d, J = 8.5 Hz, 1H), 6.89 – 6.73 (m, 3H), 6.65 (d, J = 8.4 Hz, 1H), 5.95 (s, 2H), 4.95 (d, J = 5.9 Hz, 1H), 4.36 (d, J = 8.0 Hz, 1H), 4.09 (d, J = 9.4 Hz, 1H), 3.97 – 3.84 (m, 7H), 3.86 – 3.74 (m, 2H), 3.51 – 3.40 (m, 1H), 3.24 (t, J = 8.6 Hz, 1H), 2.86 (dd, J = 15.4, 7.2 Hz, 1H); ^{13}C NMR (CDCl_3 , 100 MHz) δ 148.1, 147.3, 147.2, 138.2, 135.5, 129.9, 124.6, 119.7, 116.8, 108.3, 106.8, 105.8, 101.2, 87.7, 78.7, 70.6, 69.9, 60.3, 56.4, 54.9, 49.2. The data were consistent with previous report.²⁵

Following general procedure, reaction of **5** (46.8 mg, 0.19 mmol) and **d** (58.0 mg, 0.37 mmol) in acetonitrile (2 mL). After separation using Sephadex LH-20, Prep-TLC was developed in dichloromethane/ethyl acetate (95:5) to yield **α -6d** (49 mg, 68%) as a white powder and **β -6d** (15 mg, 17%) as a white powder.

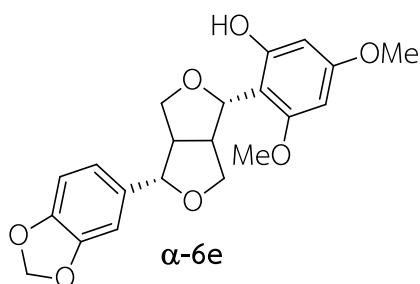


α -6d; $^1\text{H NMR}$ (CDCl_3 , 400 MHz) δ 7.71 (brs, 1H), 6.84 – 6.79 (m, 3H), 6.54 (s, 1H), 6.49 (s, 1H), 5.96 (s, 2H), 4.82 (d, $J = 8.0$ Hz, 1H), 4.78 (d, $J = 8.0$ Hz, 1H), 4.36 (dd, $J = 8.8, 7.2$ Hz, 1H), 4.16 (dd, $J = 9.6, 6.4$ Hz, 1H), 3.92 – 3.86 (m, 2H), 3.84 (s, 3H), 3.82 (s, 3H), 3.21 – 3.14 (m, 2H); $^{13}\text{C NMR}$ (CDCl_3 , 100 MHz) δ 150.3, 150.1, 148.2, 147.4, 142.6, 134.8, 125.2, 119.5, 111.2, 108.4, 106.7, 102.1, 101.3, 86.7, 85.6, 72.6, 70.8, 57.2, 56.1, 53.6, 53.2. The data were consistent with previous report.²⁵

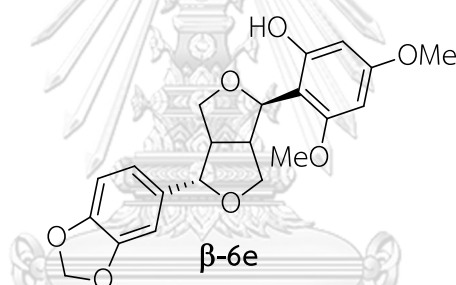


β -6d; $^1\text{H NMR}$ (CDCl_3 , 400 MHz) δ 8.05 (brs, 1H), 6.87 – 6.77 (m, 3H), 6.46 (s, 1H), 6.42 (s, 1H), 5.95 (s, 2H), 5.01 (d, $J = 8.0$ Hz, 1H), 4.44 (d, $J = 6.8$ Hz, 1H), 4.19 (d, $J = 9.6$ Hz, 1H), 3.98 (t, $J = 8.8$ Hz, 1H), 3.88 – 3.80 (m, 1H), 3.85 (s, 3H), 3.80 (s, 3H), 3.49 (dd, $J = 8.4, 9.2$ Hz, 1H), 3.51 – 3.40 (m, 1H), 2.94 – 2.88 (m, 1H); $^{13}\text{C NMR}$ (CDCl_3 , 100 MHz) δ 150.1, 149.8, 148.2, 147.5, 142.7, 134.8, 125.2, 119.8, 110.5, 108.4, 106.7, 101.9, 101.2, 87.7, 84.6, 71.9, 70.1, 57.0, 56.0, 53.7, 50.8. The data were consistent with previous report.²⁵

Following general procedure, reaction of **5** (56.5 mg, 0.22 mmol) and **e** (52.0 mg, 0.34 mmol) in acetonitrile (2 mL). After separation using Sephadex LH-20, Prep-TLC was developed in hexane/ethyl acetate (8:2, 3 times) to yield **α -6e** (41 mg, 47%) as a yellow oil and **β -6e** (44 mg, 51%) as a yellow oil.

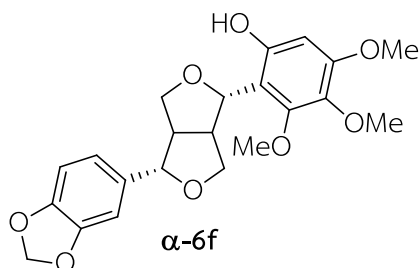


α -6e; ^1H NMR (CDCl_3 , 400 MHz) δ 8.96 (brs, 1H), 6.82 – 6.77 (m, 3H), 6.06 (d, J = 2.4 Hz, 1H), 6.01 (d, J = 2.4 Hz, 1H), 5.95 (s, 2H), 5.21 (d, J = 4.8 Hz, 1H), 4.81 (d, J = 4.0 Hz, 1H), 4.47 (dd, J = 9.2, 8.4 Hz, 1H), 4.13 (dd, J = 9.2, 2.8 Hz, 1H), 4.03 (dd, J = 9.2, 6.8 Hz, 1H), 3.79 – 3.78 (m, 1H), 3.76 (s, 6H), 3.19 – 3.17 (m, 1H), 3.02 – 2.99 (m, 1H); ^{13}C NMR (CDCl_3 , 100 MHz) δ 161.0, 158.0, 157.6, 148.2, 147.3, 134.9, 119.5, 108.3, 106.7, 105.0, 101.2, 94.6, 91.0, 84.2, 84.2, 72.7, 71.0, 55.5, 55.5, 54.8, 53.7. The data were consistent with previous report.²⁵

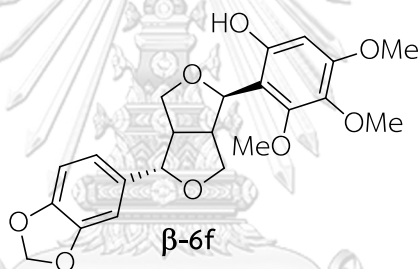


β -6e; ^1H NMR (CDCl_3 , 400 MHz) δ 9.15 (brs, 1H), 6.87 – 6.77 (m, 3H), 6.07 (d, J = 2.0 Hz, 1H), 6.00 (d, J = 2.4 Hz, 1H), 5.95 (s, 2H), 5.17 (d, J = 8.0 Hz, 1H), 4.40 (d, J = 6.8 Hz, 1H), 4.17 (d, J = 10.0 Hz, 1H), 3.91 (dd, J = 8.0, 8.0 Hz, 1H), 3.81 (dd, J = 9.6, 6.4 Hz, 1H), 3.77 (s, 3H), 3.76 (s, 3H), 3.51 – 3.42 (m, 2H), 2.90 – 2.85 (m, 1H); ^{13}C NMR (CDCl_3 , 100 MHz) δ 160.9, 158.1, 157.4, 148.2, 147.5, 134.9, 119.8, 108.3, 106.8, 101.7, 101.2, 94.3, 90.8, 87.5, 81.9, 71.4, 70.3, 55.7, 55.4, 53.7, 49.6. The data were consistent with previous report.²⁵

Following general procedure, reaction of **5** (151.0 mg, 0.60 mmol) and **f** (167 mg, 0.91 mmol) in acetonitrile (6 mL). After separation using Sephadex LH-20, Prep-TLC was developed in dichloromethane/ethyl acetate (95:5) to yield **α -6f** (75 mg, 30%) as a colorless oil and **β -6f** (100 mg, 40%) as a colorless oil.

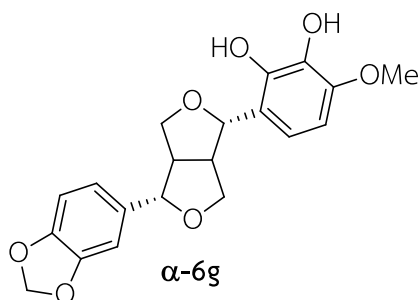


α -6f; ^1H NMR (CDCl_3 , 400 MHz) δ 8.58 (brs, 1H), 6.82 – 6.77 (m, 3H), 6.22 (s, 1H), 5.95 (s, 2H), 5.12 (d, $J = 8.0$ Hz, 1H), 4.83 (d, $J = 8.0$ Hz, 1H), 4.49 (dd, $J = 8.4, 8.4$ Hz, 1H), 4.13 (dd, $J = 9.6, 2.8$ Hz, 1H), 4.04 (dd, $J = 9.2, 6.8$ Hz, 1H), 3.90 (s, 3H), 3.81 (s, 3H), 3.81 – 2.79 (m, 1H), 3.79 (s, 3H), 3.26 – 3.21 (m, 1H), 3.07 – 3.01 (m, 1H); ^{13}C NMR (CDCl_3 , 100 MHz) δ 153.9, 152.1, 150.9, 148.2, 147.3, 135.2, 134.7, 119.5, 109.1, 108.4, 106.8, 101.2, 97.0, 84.4, 84.2, 72.9, 70.8, 61.1, 60.9, 56.0, 54.7, 53.7. The data were consistent with previous report.²⁵

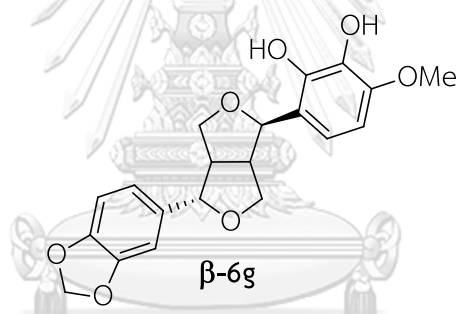


β -6f; ^1H NMR (CDCl_3 , 400 MHz) δ 8.87 (brs, 1H), 6.87 (s, 1H), 6.83 – 6.77 (m, 2H), 6.21 (s, 1H), 5.95 (s, 2H), 5.15 (d, $J = 8.0$ Hz, 1H), 4.40 (d, $J = 4.0$ Hz, 1H), 4.18 (d, $J = 10.0$ Hz, 1H), 3.94 – 3.92 (m, 1H), 3.90 (s, 3H), 3.82 (s, 3H), 3.81 – 3.78 (m, 1H), 3.78 (s, 3H), 3.48 – 3.43 (m, 2H), 2.93 – 2.87 (m, 1H); ^{13}C NMR (CDCl_3 , 100 MHz) δ 153.8, 152.6, 150.2, 148.2, 147.5, 135.0, 134.8, 119.8, 108.3, 106.7, 105.7, 101.2, 96.8, 87.5, 82.0, 71.4, 70.3, 61.1, 60.9, 55.9, 53.8, 50.2. The data were consistent with previous report.²⁵

Following general procedure, reaction of **5** (108.9 mg, 0.46 mmol) and **g** (91.5, 0.65 mmol) in acetonitrile (5 mL). After separation using Sephadex LH-20, Prep-TLC was developed in dichloromethane/ethyl acetate (9:1) to yield **α -6g** (70.1 mg, 41%) as a brown oil and **β -6g** (36.4 mg, 21%) as a brown oil.



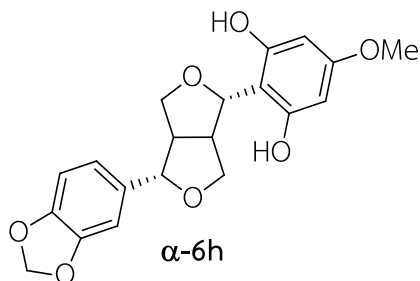
α -6g; ^1H NMR (400 MHz, CDCl_3) δ 6.84 (s, 1H, H-6'), 6.78 – 6.68 (m, 2H, H-2' and H-5'), 6.67 (d, $J = 8.4$ Hz, 1H, H-6''), 6.43 (d, $J = 8.5$ Hz, 1H, H-5''), 5.94 (s, 2H, H-7'), 4.97 (d, $J = 5.4$ Hz, 1H, H-2), 4.71 (d, $J = 4.9$ Hz, 1H, H-6), 4.25 (dt, $J = 12.6, 8.4$ Hz, 2H, H-4 and H-8), 3.94 (dd, $J = 9.0, 3.8$ Hz, 1H, H-8), 3.90 – 3.84 (m, 1H, H-4), 3.85 (s, 3H, -OMe), 3.19 – 3.17 (m, 1H, H-1), 3.07 – 3.01 (m, 1H, H-5); ^{13}C NMR (100 MHz, CDCl_3) δ 148.1, 147.2, 147.1, 142.5, 135.1, 133.6, 119.6, 119.5, 116.6, 108.3, 106.7, 103.0, 101.2, 85.6, 84.4, 72.0, 56.3, 54.1, 53.0.



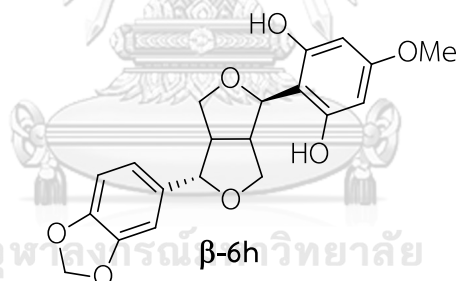
β -6g; ^1H NMR (400 MHz, CDCl_3) δ 6.86 (s, 1H, H-6'), 6.82 – 6.72 (m, 3H, H-2', H-5' and H-6''), 6.45 (d, $J = 8.3$ Hz, 1H, H-5''), 5.93 (s, 2H, H-7'), 5.00 (d, $J = 5.8$ Hz, 1H, H-2), 4.39 (d, $J = 7.0$ Hz, 1H, H-6), 4.12 (dd, $J = 8.3, 5.4$ Hz, 1H, H-4), 3.90 – 3.81 (m, 1H, H-8), 3.85 (s, 3H, -OMe), 3.81 (s, 1H, H-4), 3.48 – 3.44 (m, 1H, H-1), 3.38 – 3.33 (m, 1H, H-8), 2.87 (dd, $J = 15.3, 6.9$ Hz, 1H, H-5); ^{13}C NMR (100 MHz, CDCl_3) δ 148.0, 147.3, 146.6, 142.0, 135.1, 133.1, 119.7, 118.9, 116.9, 108.2, 106.7, 103.1, 101.1, 87.6, 81.3, 71.2, 70.0, 56.2, 54.2, 49.5; HRMS m/z 395.1110 $[\text{M}+\text{Na}]^+$ (calcd for $\text{C}_{20}\text{H}_{20}\text{NaO}_7$, 395.1107).

Following general procedure, reaction of **5** (128.1 mg, 0.51 mmol) and **h** (107.6 mg, 0.77 mmol) in acetonitrile (5 mL). After separation using Sephadex LH-20, Prep-TLC was used in 9:1 dichloromethane/ethyl acetate to yield **α -6h** (9.2mg, 5%) as a brown oil, **β -6h** (24.3 mg, 13%) as a brown oil and mixture of **α -6h'** and **β -6h'** that

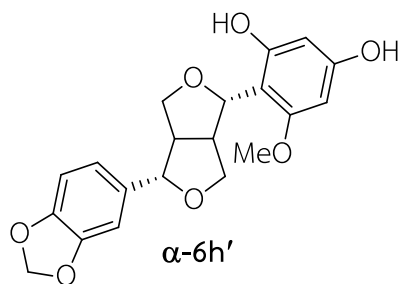
was separated using Prep-TLC (hexane/dichloromethane/ethyl acetate, 40:45:15) to obtain α -6h' (3.6 mg, 2%) as a yellow oil and β -6h' (21 mg, 11%) as a yellow oil.



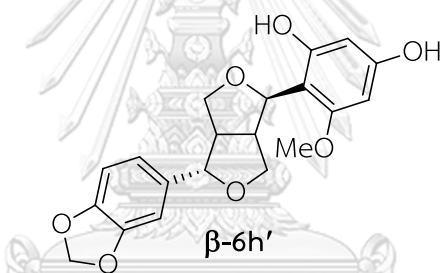
α -6h; $^1\text{H NMR}$ (400 MHz, CDCl_3) δ 6.98 (brs, 2H), 6.82 (s, 1H, H-6'), 6.77 (s, 2H, H-2' and H-4'), 5.95 (d, $J = 3.1$ Hz, 2H, H-7'), 5.23 (d, $J = 7.7$ Hz, 1H, H-2), 4.83 (d, $J = 3.9$ Hz, 1H, H-6), 4.52 – 4.46 (m, 1H, H-4), 4.20 (dd, $J = 9.4, 2.7$ Hz, 1H, H-8), 4.03 (dd, $J = 9.3, 6.7$ Hz, 1H, H-8), 3.83 – 3.77 (m, 1H, H-4), 3.72 (s, 3H, -OMe), 3.25 – 3.17 (m, 1H, H-5), 3.10 – 3.02 (m, 1H, H-1); $^{13}\text{C NMR}$ (100 MHz, CDCl_3) δ 160.7, 156.0, 148.2, 147.3, 134.9, 119.5, 108.4, 106.8, 104.1, 101.2, 94.8, 84.4, 83.7, 72.9, 70.7, 55.4, 54.6, 53.7.



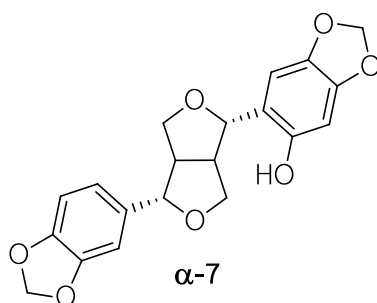
β -6h; $^1\text{H NMR}$ (400 MHz, CDCl_3) δ 6.88 – 6.78 (m, 3H, H-2', H-5' and H-6'), 5.95 (s, 4H, H-7', H-3'' and H-5''), 5.20 (d, $J = 5.8$ Hz, 1H, H-2), 4.42 (d, $J = 7.1$ Hz, 1H, H-6), 4.18 (d, $J = 9.7$ Hz, 1H, H-4), 3.96 (t, $J = 8.3$ Hz, 1H, H-8), 3.82 (dd, $J = 9.7, 6.3$ Hz, 1H, H-4), 3.73 (s, 3H, -OMe), 3.54 – 3.50 (m, 1H, H-1), 3.48 – 3.46 (m, 1H, H-8), 2.92 – 2.86 (m, 1H, H-5); $^{13}\text{C NMR}$ (100 MHz, CDCl_3) δ 160.7, 156.0, 148.2, 147.5, 134.8, 119.9, 108.3, 106.8, 101.2, 101.0, 94.5, 87.6, 81.7, 71.5, 70.3, 55.4, 53.6, 49.6; HRMS m/z 395.1111 [$\text{M}+\text{Na}$] $^+$ (calcd for $\text{C}_{20}\text{H}_{20}\text{NaO}_7$, 395.1107).



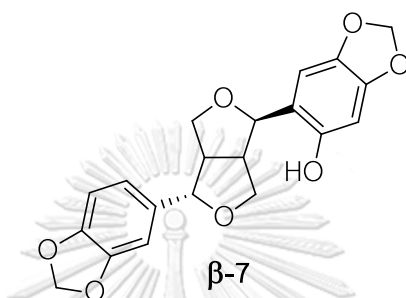
α -6h'; ^1H NMR (400 MHz, CDCl_3) δ 8.94 (s, 1H, -OH), 6.82 (s, 1H, H-6'), 6.77 (s, 2H, H-2' and H-5'), 5.97 (s, 2H, H-3'' and H-5''), 5.95 (s, 2H, H-7'), 5.20 (d, $J = 7.6$ Hz, 1H, H-2), 4.81 (d, $J = 3.8$ Hz, 1H, H-6), 4.47 (t, $J = 8.5$ Hz, 1H, H-4), 4.13 (dd, $J = 9.3, 2.8$ Hz, 1H, H-8), 4.05 – 4.01 (m, 1H, H-8), 3.79 (d, $J = 7.5$ Hz, 1H, H-4), 3.75 (s, 3H, -OMe), 3.19 – 3.17 (m, 1H, H-5), 3.02 – 3.00 (m, 1H, H-1); ^{13}C NMR (100 MHz, CDCl_3) δ 158.2, 157.6, 156.9, 148.2, 147.3, 134.8, 119.5, 108.4, 106.7, 105.0, 101.2, 97.1, 91.1, 84.2, 84.1, 72.8, 71.0, 55.6, 54.7, 53.7; HRMS m/z 395.1108 $[\text{M}+\text{Na}]^+$ (calcd for $\text{C}_{20}\text{H}_{20}\text{NaO}_7$, 395.1107).



β -6h'; ^1H NMR (400 MHz, CDCl_3) δ 9.14 (s, 1H, -OH), 6.87 (s, 1H, H-6'), 6.82 – 6.77 (m, 2H, H-2' and H-5'), 5.98 (s, 1H, H-3''), 5.96 (s, 1H, H-5''), 5.95 (s, 2H, H-7'), 5.16 (d, $J = 5.6$ Hz, 1H, H-2), 4.40 (d, $J = 7.1$ Hz, 1H, H-6), 4.17 (d, $J = 9.8$ Hz, 1H, H-4), 3.91 (t, $J = 7.8$ Hz, 1H, H-8), 3.80 (dd, $J = 9.5, 6.4$ Hz, 1H, H-4), 3.75 (s, 3H, -OMe), 3.46 – 3.44 (m, 2H, H-1 and H-8), 2.88 – 2.85 (m, 1H, H-5); ^{13}C NMR (100 MHz, CDCl_3) δ 158.1, 157.6, 156.9, 148.2, 147.5, 134.9, 119.8, 108.3, 106.8, 101.8, 101.2, 96.9, 91.0, 87.5, 81.9, 71.4, 70.2, 55.7, 53.6, 49.5; HRMS m/z 395.1104 $[\text{M}+\text{Na}]^+$ (calcd for $\text{C}_{20}\text{H}_{20}\text{NaO}_7$, 395.1107).



α -7; ^1H NMR (CDCl_3 , 400 MHz) δ 7.76 (brs, 1H, -OH), 6.83 – 6.78 (m, 3H), 6.51 (s, 1H), 6.45 (s, 1H), 5.96 (s, 2H), 5.89 (s, 2H), 4.77 (d, J = 4.0 Hz, 2H), 4.35 (dd, J = 8.8, 7.6 Hz, 1H), 4.14 (dd, J = 9.2, 6.0 Hz, 1H), 3.89 – 3.83 (m, 2H), 3.18 – 3.11 (m, 2H); ^{13}C NMR (CDCl_3 , 100 MHz) δ 150.9, 148.3, 148.2, 147.4, 141.1, 134.7, 125.2, 119.5, 115.2, 108.4, 106.7, 106.3, 101.3, 99.6, 86.7, 85.5, 72.6, 70.7, 53.5, 53.1. The data were consistent with previous report.²⁵



β -7; ^1H NMR (CDCl_3 , 400 MHz) δ 8.17 (brs, 1H, -OH), 6.87 – 6.77 (m, 3H), 6.42 (s, 1H), 6.40 (s, 1H), 5.96 (s, 2H), 5.90 (s, 2H), 4.97 (d, J = 5.9 Hz, 1H), 4.41 (d, J = 7.0 Hz, 1H), 4.17 (d, J = 10.0 Hz, 1H), 4.00 (dd, J = 9.2, 8.8 Hz, 1H), 3.84 (dd, J = 9.6, 6.4 Hz, 1H), 3.49 (dd, J = 9.2, 8.4 Hz, 1H), 3.39 – 3.35 (m, 1H), 2.89 (m, 1H); ^{13}C NMR (CDCl_3 , 100 MHz) δ 150.8, 148.2, 147.9, 147.5, 141.2, 134.7, 119.8, 112.1, 108.3, 106.7, 105.8, 101.3, 101.2, 99.4, 87.7, 84.5, 71.9, 70.1, 53.6, 50.7. The data were consistent with previous report.²⁵

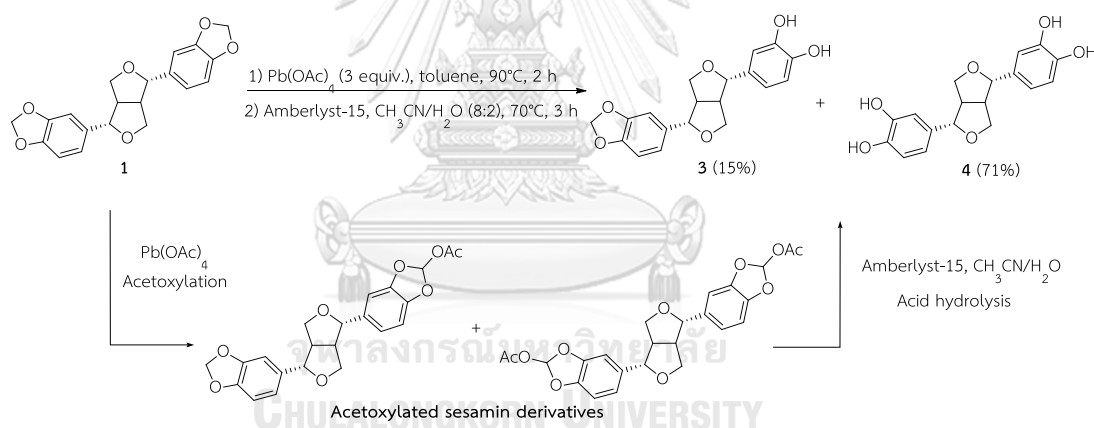
Chapter IV

Synthesis of Furofuran Lignans *via* Methylenedioxy Cleavage

This chapter describes removal of methylenedioxy unit by oxidative cleavage using Urata protocol.³²

4.1 General procedure for oxidative cleavage of methylenedioxy

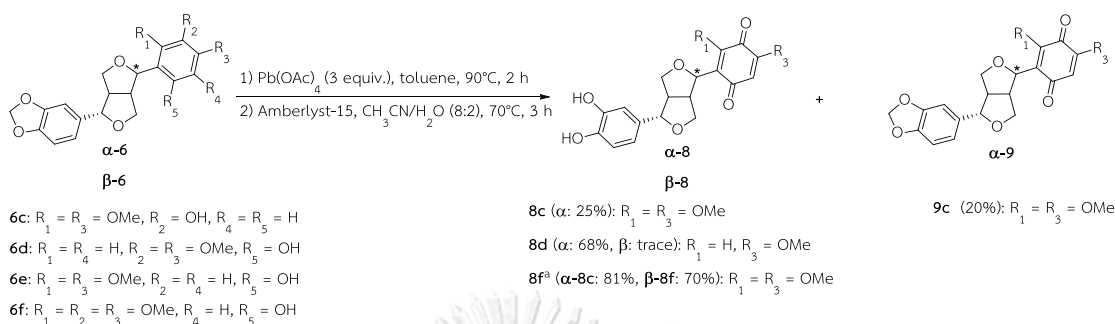
To test the viability of Urata protocol,³² sesamin (**1**) was used as a model substrate. **1** was initially oxidized by $\text{Pb}(\text{OAc})_4$ to produce the acetoxylation methylenedioxy units, which was later hydrolyzed to afford catechol moiety. In hydrolysis step, Amberlyst-15 was used in place of acetic acid to improve product yield, and the Amberlyst residue could be easily removed by filtration. Thus, the products **3** (15%) and **4** (71%) were obtained in a better yield compared with previous' method³² (Scheme 4.1).



Scheme 4.1 Synthesis of **3** and **4**.

With the success of removing methylenedioxy by $\text{Pb}(\text{OAc})_4$ in hand, this condition was applied to other furofuran lignans containing a hydroxy moiety (**6c-6f**). Unexpectedly, the phenolic moiety containing free hydroxy was more vulnerable to be oxidized than methylenedioxy, thus yielding *para*-quinone residue (Scheme 4.2).³⁶ Although *para*-quinone moiety, unexpected product, was obtained on furofuran lignan (**8c**, **8d** and **8f**), synthesis of catechol moiety was successful to increase the number of hydroxy unit. These observations were noted in all lignans having free hydroxy group in the structure, except for **6e** whose structure containing one free hydroxy group

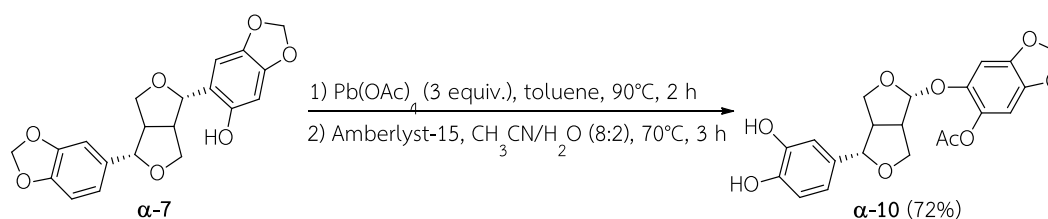
located at *meta*-position to the remaining two methoxy groups. It has been recognized that 1,3-benzenediol or resorcinol unit cannot be oxidized under such mild condition but can be converted to trace amount of quinone under strong oxidizing power.³⁷



^a α -8f was obtained as the same product α -8c

Scheme 4.2 Synthesis of lignans containing *para*-quinone (**8** and **9**).

However, α -7 underwent oxidation but yielded unexpected product α -10 (72%), which was obtained as a brown oil (Scheme 4.3). The structure of α -10 was fully proved by 2D NMR and HRMS. The HRESIMS (m/z 439.1001 $[\text{M}+\text{Na}]^+$, calcd for 439.1005) of α -10 showed that it had the molecular formula of $\text{C}_{21}\text{H}_{20}\text{O}_9$. The NMR spectra of α -10 showed the presence of acetal moiety at δ_{C} 103.1 and δ_{H} 5.27 and one additional oxygenated benzene at δ_{C} 132.9, indicating one additional oxygen atom linked between furan moiety and phenolic residue at C-2. However, the presence of δ_{H} 5.86 (s, 2H, H-7'') revealed that only one methylenedioxy unit was removed. Furthermore, HMBC correlations of α -10 showed that catechol moiety was located at C-3' and C-4' while C-2'' was connected to acetoxy moiety (Figure 4.1).



Scheme 4.3 Synthesis of α -10.

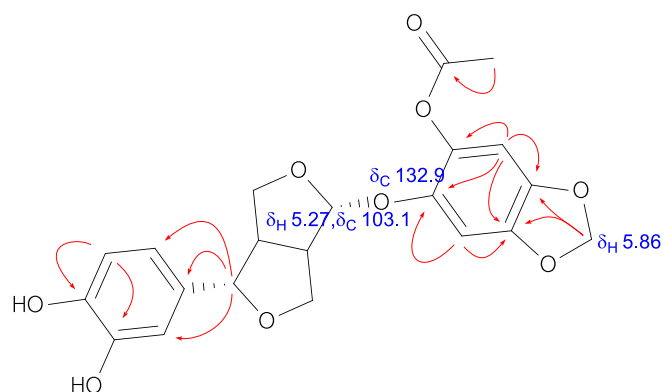


Figure 4.1 HMBC correlations of **α -10**

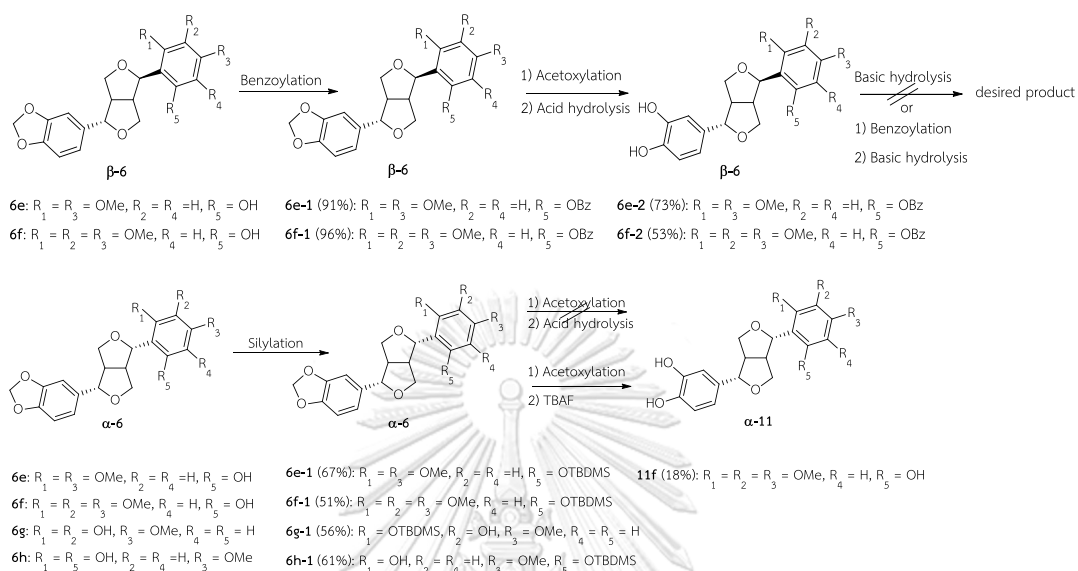
Although removal of methylenedioxy unit was successfully carried out, the free hydroxy group was more susceptible to oxidation by $\text{Pb}(\text{OAc})_4$; thus yielding *para*-quinone moiety. This observation was not detected in case of free hydroxy and methoxy groups being *meta*-position.

In general, methylenedioxy moiety could be removed by oxidation using $\text{Pb}(\text{OAc})_4$. The structures were characterized comfortably by ^1H NMR spectra, which displayed no methylenedioxy singlet signal at δ 5.90 ppm.

4.2 Methylenedioxy cleavage of Silylated lignans

Due to the susceptibility of free hydroxy group toward oxidation using $\text{Pb}(\text{OAc})_4$, protection of hydroxy group is required to avoid quinone formation. It is essential to use a protecting group that remains stable throughout methylenedioxy cleavage. In a preliminary experiment (synthesis of **6e-1** and **6f-1**), benzylation reaction using benzoyl chloride (BzCl) as a reagent was initially performed. Methylenedioxy cleavage proceeded smoothly until the desired catechol unit was obtained (**6e-2** and **6f-2**). However, deprotection of benzoyl group under basic condition (K_2CO_3) failed to afford the desired product because there was no ^1H NMR signals of furofuran lignan core structure around 4.00-5.30 ppm. Subsequently, silylation reaction using *tert*-butyldimethylsilyl chloride (TBDMSCl) as a reagent was also performed to protect hydroxy unit. However, deprotection of silyl group under acidic condition using Amberlyst-15 failed to afford the desired products because there was no ^1H NMR signals of furofuran lignan core structure around 4.00-5.30 ppm. In the last step, deprotection using tetra-*n*-butylammonium fluoride (TBAF) was successful to remove

both methylenedioxy and silyl unit in one step, providing the desired product (**11f**). It should be noted that acetoxyated methylenedioxy unit formed after acetoxylation was simultaneously removed together with silyl group using TBAF (Scheme 4.4).



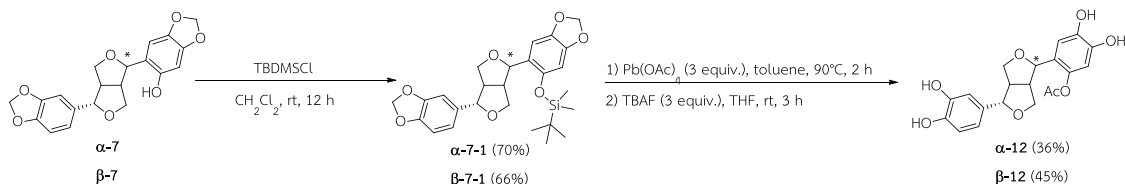
Scheme 4.4 Synthesis of new furofuran lignan *via* protection and deprotection reaction.

Noticeably, the silylation reaction of dihydroxy units (**6g** and **6h**) provided partially silylated products. Then **6g** and **6h** were applied in step of methylenedioxy cleavage. The desired products were not obtained. An attempt to prove undesired products were not identified.

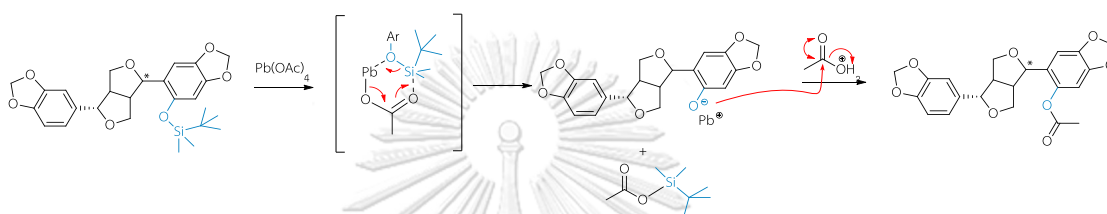
In this experiment, only **α-11f** was displayed as the representative of three hydroxy units.

With the success of silylation prior to methylenedioxy cleavage, this approach was applied to **7** (Scheme 4.5). Although all methylenedioxy moieties were fully removed, the silyl group was also replaced by acetate unit (-Ac). According to Wang,³⁸ the silyl group was likely to be substituted *via* a six-membered cyclic transition state to obtain the product having acetoxy group (Scheme 4.6). $\text{Pb}(\text{OAc})_4$ acted as an effective Lewis acid-Lewis base bifunctional catalyst to remove the silyl group from silylated furofuran lignans (**7-1**). Substitution of silyl group by acetate moiety was expected to proceed before oxidative cleavage of methylenedioxy; however, acetate

group could not be removed under TBAF condition. An attempt to remove acetate group using stronger basic condition was performed but several unexpected products were observed.



Scheme 4.5 Synthesis of **12**.



Scheme 4.6 Proposed formation of acetoxy group in **12**.

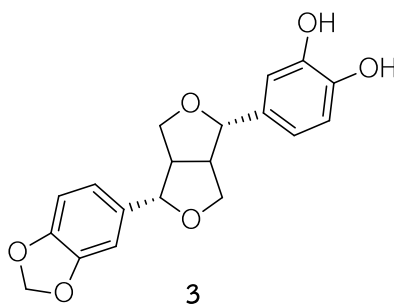
4.3 Experimental section

4.3.1 General experiment procedures

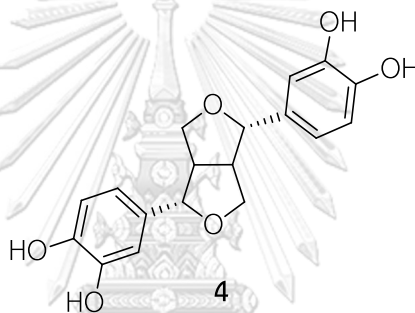
General experiments performed in this Chapter were similar to those described in Chapter 3

4.3.2 General procedure for the methylenedioxy cleavage of lignans

A mixture of sesamin (**1**, 0.16 mmol) and lead (IV) tetraacetate (213 mg, 0.48 mmol) in toluene (2 mL) was treated at 90°C for 2 h under atmospheric N₂. After cooling, the reaction mixture was diluted with toluene and filtered through a celite pad. The filtrate was evaporated to dryness and extracted by ethyl acetate/H₂O (1:1, 3 times). The organic layers were dried over anhydrous Na₂SO₄ and concentrated under reduced pressure. The resulting residue was treated with acidic resin Amberlyst-15 (1 mg/0.005 mmol of **1**) in 8:2 acetonitrile/H₂O (2 mL) at 70°C for 3 h. The reaction mixture was evaporated to dryness and purified by silica gel column chromatography (1:1 hexane/ethyl acetate to 3:7 hexane/ethyl acetate) to give **3** (8 mg, 15%) as a brown oil and **4** (37 mg, 71%) as a dark brown oil.



3; $^1\text{H NMR}$ (400 MHz, CD_3OD) δ 7.23 – 7.12 (m, 6H), 7.08 (dd, $J = 8.1, 1.7$ Hz, 1H), 6.31 (s, 2H), 5.25 (brs, 2H), 5.07 (d, $J = 4.7$ Hz, 1H), 5.03 (d, $J = 4.6$ Hz, 1H), 4.59 (dd, $J = 6.4, 2.6$ Hz, 1H), 4.23 – 4.18 (m, 2H), 3.72 – 3.70 (m, 1H), 3.46 (t, $J = 11.0$ Hz, 2H). The data were consistent with previous report.³²

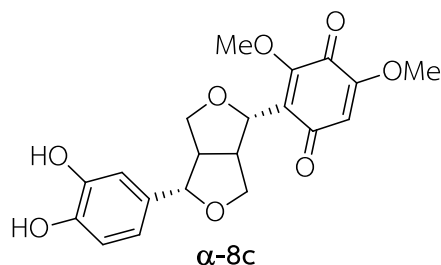


4; $^1\text{H NMR}$ (CD_3OD , 400 MHz) δ 6.82 - 6.68 (m, 6H), 4.63 (d, $J = 4.3$, 2H), 4.21 (dd, $J = 9.0, 7.1$ Hz, 2H), 3.80 (dd, $J = 9.0, 3.5$ Hz, 2H), 3.10 – 3.05 (m, 2H). The data were consistent with previous report.³²

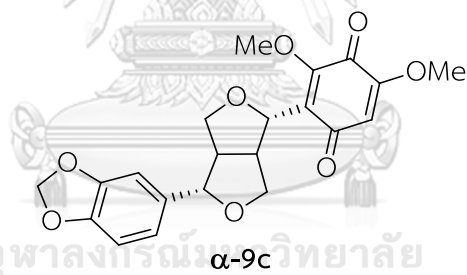
Following the general procedure for the methylenedioxy cleavage of **1**, reaction of **α -6c** (127.3 mg, 0.33 mmol) and lead (IV) tetraacetate (438.2 mg, 0.99 mmol) was carried out in toluene (3 mL). After extraction and evaporation, the resulting residue was heated in 8:2 acetonitrile/ H_2O (3 mL) at 70°C for 3 h and purified by silica gel column chromatography (1:1 hexane/ethyl acetate) to yield **α -8c** (32.5 mg, 25%) as an orange oil, **α -9c** (26.8 mg, 20%) as a yellow oil.

Following the general procedure for the methylenedioxy cleavage of **1**, reaction of **α -6f** (46 mg, 0.11 mmol) and lead (IV) tetraacetate (147 mg, 0.33 mmol) in toluene (1.1 mL) was carried out. After extraction and evaporation, the resulting residue was heated in 8:2 acetonitrile/ H_2O (2 mL) at 70°C for 3 h and purified by silica gel

column chromatography (1:1 hexane/ethyl acetate) to yield **α -8c** (35.4 mg, 81%) as a yellow oil.



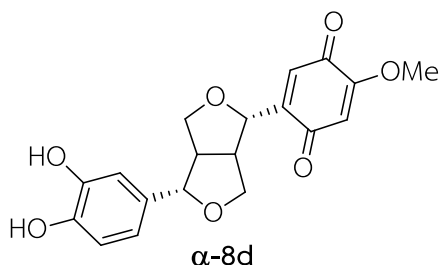
α -8c; $^1\text{H NMR}$ (CDCl_3 , 400 MHz) δ 6.81 – 6.73 (m, 3H, H-2', H-5', and H-6'), 5.82 (s, 1H, H-3''), 5.15 (d, $J = 5.6$ Hz, 1H, H-2), 4.61 (d, $J = 6.4$ Hz, 1H, H-6), 4.26 – 4.17 (m, 2H, H-4 and H-8), 4.01 (s, 3H, H-8''), 3.89 – 3.83 (m, 2H, H-4 and H-8), 3.79 (s, 3H, H-7''), 3.25 – 3.20 (m, 1H, H-1), 3.15 – 3.09 (m, 1H, H-5); $^{13}\text{C NMR}$ (CDCl_3 , 100 MHz) δ 187.0, 178.6, 157.4, 155.4, 144.1, 143.9, 133.6, 130.3, 118.8, 115.5, 113.6, 107.6, 85.5, 78.3, 72.8, 72.7, 61.9, 56.6, 55.5, 52.0; HRESIMS m/z 411.1067 $[\text{M}+\text{Na}]^+$ (calcd for $\text{C}_{20}\text{H}_{20}\text{NaO}_8$, 411.1056).



α -9c; $^1\text{H NMR}$ (400 MHz, CDCl_3) δ 6.84 (d, $J = 0.8$ Hz, 1H, H-6'), 6.79 – 6.75 (m, 2H, H-2' and H-5'), 5.93 (s, 2H, H-7'), 5.82 (s, 1H, H-5''), 5.13 (d, $J = 5.5$ Hz, 1H, H-2), 4.62 (d, $J = 6.6$ Hz, 1H, H-6), 4.21 (m, 2H, H-4 and H-8), 4.00 (s, 3H, -OMe), 3.87 – 3.82 (m, 2H, H-4 and H-8), 3.78 (s, 3H, -OMe), 3.24 – 3.19 (m, 1H, H-1), 3.10 – 3.05 (m, 1H, H-5); $^{13}\text{C NMR}$ (100 MHz, CDCl_3) δ 186.8, 178.6, 157.3, 155.3, 148.1, 147.3, 135.3, 130.6, 119.6, 108.3, 107.6, 107.5, 106.6, 101.2, 85.5, 78.2, 72.9, 72.6, 61.8, 56.6, 55.9, 52.1; HRMS m/z 423.1057 $[\text{M}+\text{Na}]^+$ (calcd for $\text{C}_{21}\text{H}_{20}\text{NaO}_8$, 423.1056).

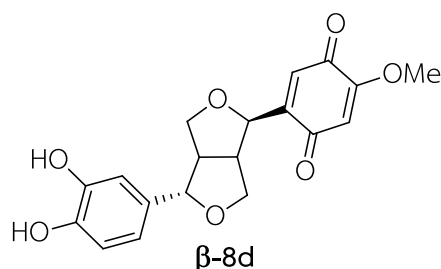
Following the general procedure for the methylenedioxy cleavage of **1**, reaction of **α -6d** (169 mg, 0.44 mmol) and lead (IV) tetraacetate (582 mg, 1.31 mmol) in toluene (5 mL) was achieved. After extraction and evaporation, the resulting residue

was heated in acetonitrile/H₂O (8:2, 5 mL) at 70°C for 3 h and purified by silica gel column chromatography (1:1 hexane/ethyl acetate) to yield **α -8d** (107 mg, 68%) as a yellow oil.



α -8d; ¹H NMR (CD₃OD, 400 MHz) δ 6.79 (d, *J* = 2.0 Hz, 1H, H-2'), 6.73 (d, *J* = 8.1 Hz, 1H, H-5'), 6.67 (dd, *J* = 8.1, 2.0 Hz, 1H, H-6'), 6.63 (s, 1H, H-6''), 6.02 (s, 1H, H-3''), 4.77 (d, *J* = 2.8 Hz, 1H, H-2), 4.56 (d, *J* = 5.4 Hz, 1H, H-6), 4.29 (dd, *J* = 9.3, 6.7 Hz, 1H, H-8), 4.14 (dd, *J* = 9.1, 5.8 Hz, 1H, H-4), 4.05 (dd, *J* = 9.3, 4.0 Hz, 1H, H-8), 3.89 (dd, *J* = 9.1, 3.2 Hz, 1H, H-4), 3.82 (s, 3H, H-7''), 2.98 – 2.95 (m, 2H, H-1 and H-5); ¹³C NMR (CD₃OD, 100 MHz) δ 189.0, 183.5, 160.5, 150.6, 146.5, 146.1, 133.6, 128.6, 118.9, 116.3, 114.5, 108.7, 86.7, 82.6, 74.2, 72.6, 57.0, 55.2, 54.3; HRESIMS *m/z* 381.0949 [M+Na]⁺ (calcd for C₁₉H₁₈NaO₇, 381.0950).

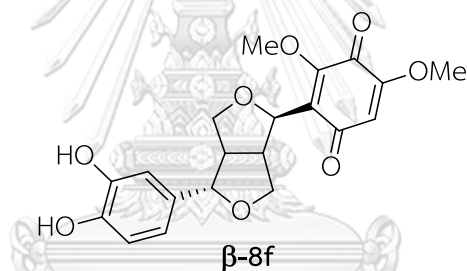
Following the general procedure for the methylenedioxy cleavage of **1**, reaction of **β -6d** (50 mg, 0.13 mmol) and lead (IV) tetraacetate (173 mg, 0.39 mmol) in toluene (1.3 mL) was performed. After extraction and evaporation, the resulting residue was heated in acetonitrile/H₂O (8:2, 2 mL) at 70°C for 3 h and purified by silica gel column chromatography (1:1 hexane/ethyl acetate) to yield **β -8d** (30 mg, 64%) as a yellow oil.



β -8d; ¹H NMR (CD₃OD, 400 MHz) δ 6.83 – 6.78 (m, 2H, H-6' and H-6''), 6.75 (d, *J* = 8.1 Hz, 1H, H-5'), 6.70 (d, *J* = 8.2 Hz, 1H, H-2'), 6.05 (s, 1H, H-3''), 4.72 (d, *J* = 6.6 Hz, 1H, H-

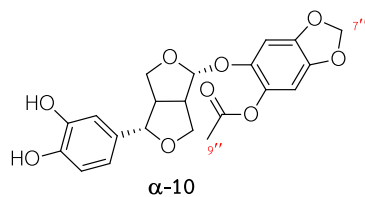
2), 4.27 (d, $J = 7.3$ Hz, 1H, H-6), 4.05 (d, $J = 9.3$ Hz, 1H, H-4), 3.90 (d, $J = 8.8$ Hz, 1H, H-8), 3.85 (d, $J = 5.7$ Hz, 3H), 3.84 – 3.79 (m, 1H, H-4), 3.50 (dd, $J = 15.6, 8.5$ Hz, 1H, H-1), 3.28 (d, $J = 8.5$ Hz, 1H, H-8), 2.93 (m, 1H, H-5); ^{13}C NMR (101 MHz, CD_3OD) δ 188.2, 183.0, 160.6, 148.0, 146.5, 146.3, 133.5, 131.1, 119.0, 116.2, 114.5, 108.4, 89.0, 78.6, 71.5, 70.3, 57.0, 55.8, 50.3.

Following the general procedure for the methylenedioxy cleavage of **1**, reaction of **β -6f** (66 mg, 0.16 mmol) and lead (IV) tetraacetate (210 mg, 0.47 mmol) in toluene (2 mL) was performed. After extraction and evaporation, the resulting residue was heated in 8:2 acetonitrile/ H_2O (2 mL) at 70°C for 3 h and purified by silica gel column chromatography (1:1 hexane/ethyl acetate) to yield **β -8f** (40 mg, 70%) as a yellow oil.



β -8f; ^1H NMR (CDCl_3 , 400 MHz) δ 6.79 – 6.73 (m, 3H), 5.83 (s, 1H), 4.90 (d, $J = 6.6$ Hz, 1H), 4.40 (d, $J = 7.4$ Hz, 1H), 4.03 – 4.01 (m, 2H), 3.99 (s, 3H), 3.80 (s, 3H), 3.70 (dd, $J = 9.4, 6.0$ Hz, 1H), 3.53 (dd, $J = 8.3, 8.3$ Hz, 1H), 3.40 – 3.31 (m, 1H), 2.87 – 2.81 (m, 1H); ^{13}C NMR (CDCl_3 , 100 MHz) δ 187.2, 178.4, 157.6, 155.7, 144.1, 144.1, 133.1, 128.7, 119.0, 115.5, 113.7, 107.4, 86.7, 77.9, 70.8, 70.0, 62.2, 56.7, 54.3, 49.9; HRESIMS m/z 411.1067 $[\text{M}+\text{Na}]^+$ (calcd for $\text{C}_{20}\text{H}_{20}\text{NaO}_8$, 411.1056).

Following the general procedure for the methylenedioxy cleavage of **1**, reaction of **α -7** (119 mg, 0.25 mmol) and lead (IV) tetraacetate (337mg, 0.76 mmol) in toluene (3 mL) was achieved. After extraction and evaporation, the resulting residue was heated in acetonitrile/ H_2O (8:2, 3 mL) at 70°C for 3 h and purified by silica gel column chromatography (1:1 hexane/ethyl acetate) to yield **α -10** (76 mg, 72%) as a brown oil.



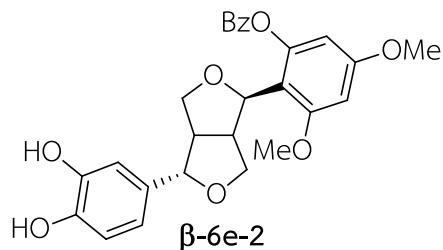
α -10; ^1H NMR (CD_3OD , 400 MHz) δ 6.80 (s, 1H, H-2'), 6.74 (d, J = 8.0 Hz, 1H, H-5'), 6.67 (d, J = 8.1, 1H, H-6'), 6.53 (s, 1H, H-3''), 6.47 (s, 1H, H-6''), 5.86 (s, 2H, H-7''), 5.27 (s, 1H, H-2), 4.33 – 4.27 (m, 2H, H-4 and H-6), 4.11 (dd, J = 9.0, 6.1 Hz, 1H, H-8), 3.84 (brd, J = 9.4 Hz, 1H, H-8), 3.50 (dd, J = 9.2, 7.1 Hz, 1H, H-4), 2.98 (dd, J = 8.4, 8.4 Hz, 1H, H-1), 2.86 (dd, J = 7.1, 7.1 Hz, 1H, H-5), 2.24 (s, 3H, H-9''); ^{13}C NMR (CD_3OD , 100 MHz) δ 171.5, 146.9, 146.4, 146.1, 144.4, 141.5, 133.6, 132.9, 119.0, 116.2, 114.4, 104.7, 103.1, 102.6, 99.4, 88.6, 72.3, 70.1, 55.0, 53.6, 20.6; HRESIMS m/z 439.1001 [$\text{M}+\text{Na}$] $^+$ (calcd for $\text{C}_{21}\text{H}_{20}\text{NaO}_9$, 439.1005).

4.3.3 Methylenedioxy cleavage of protected lignans

To a solution of **β -6e** (54.5 mg, 0.14 mmol), triethylamine (49 μL , 0.42 mmol) in dichloromethane (2 mL) was added benzoyl chloride (49 μL , 0.42 mmol) and 4-dimethylaminopyridine (catalytic amount). The mixture was stirred at room temperature for 3 h. The reaction mixture was washed with water and extracted with dichloromethane (2 mL, 3 times). The organic layer was washed with saturated aqueous NaCl, followed by dried over Na_2SO_4 . After filtration and removal of the solvent under reduced pressure, the crude product was purified by silica gel column (8:2 hexane/ethyl acetate) to obtain **β -6e-1** (63 mg, 91%) as a pale yellow oil.

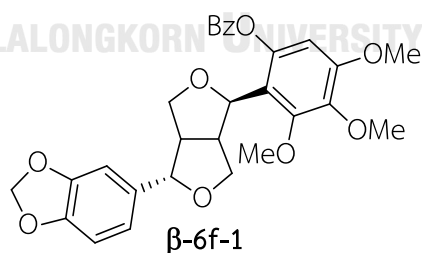
A mixture of **β -6e-1** (63 mg, 0.13 mmol) and lead tetraacetate (170 mg, 0.39 mmol) in toluene (1.5 mL) was stirred at 90°C for 2 h. After being cooled to room temperature, the reaction mixture was diluted with toluene and filtered through a celite pad. The filtrate was evaporated until dryness, washed with water and extracted with ethyl acetate (2 mL, 3 times). The organic layer was dried with anhydrous Na_2SO_4 , and concentrated under reduced pressure to give a mixture of crude reaction. This mixture was then treated with amberlyst-15 (1mg/0.005 mmol of starting material) in a mixture of acetonitrile/ H_2O (8:2, 2 mL). After stirring at 70°C for 3 h, the resulting

mixture was evaporated to dryness and purified by sephadex LH-20 column (1:1 dichloromethane/methanol) to give **β -6e-2** (44 mg, 73%) as a yellow oil.



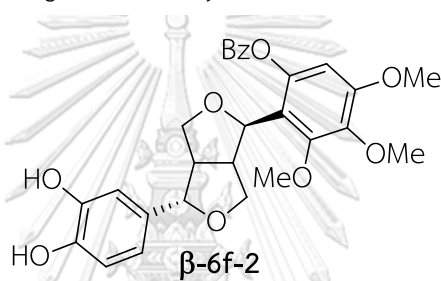
β -6e-2; $^1\text{H NMR}$ (CDCl_3 , 400 MHz) δ 8.22 (d, $J = 7.2$ Hz, 1H), 7.62 (m, 1H), 7.53 – 7.47 (m, 2H), 6.68 – 6.65 (m, 2H), 6.47 (d, $J = 7.7$ Hz, 1H), 6.42 – 6.37 (m, 1H), 6.33 – 6.28 (m, 1H), 5.02 (d, $J = 6.0$ Hz, 1H), 4.18 – 4.11 (m, 2H), 3.94 – 3.91 (m, 1H), 3.80 (s, 3H), 3.79 (s, 3H), 3.74 – 3.70 (m, 1H), 3.46 – 3.36 (m, 3H), 2.67 (brs, 1H).

To a solution of **β -6f** (47 mg, 0.11 mmol), triethylamine (47 μL , 0.33 mmol) in dichloromethane (1.5 mL) was added benzoyl chloride (40 μL , 0.33 mmol) and 4-dimethylaminopyridine (catalytic amount). The mixture was stirred at room temperature for 3 h. The reaction mixture was washed with water and extracted with dichloromethane (2 mL, 3 times). The organic layer was washed with saturated aqueous NaCl, followed by dried over Na_2SO_4 . After filtration and removal of the solvent under reduced pressure, the crude product was purified by silica gel column (8:2 hexane/ethyl acetate) to obtain **β -6f-1** (58 mg, 96%) as a pale yellow oil.



β -6f-1; $^1\text{H NMR}$ (CDCl_3 , 400 MHz) δ 8.23 (d, $J = 7.4$ Hz, 2H), 7.70 – 7.64 (m, 1H), 7.55 – 7.52 (m, 2H), 6.71 – 6.69 (m, 2H), 6.55 (d, $J = 7.7$ Hz, 1H), 6.48 (s, 1H), 5.91 (s, 2H), 5.03 (d, $J = 6.3$ Hz, 1H), 4.18 (d, $J = 7.4$ Hz, 1H), 4.11 (d, $J = 7.1$ Hz, 1H), 3.93 (s, 3H), 3.87 (s, 3H), 3.85 (s, 3H), 3.75 – 3.71 (m, 1H), 3.51 (brs, 2H), 3.32 – 3.30 (m, 1H), 2.68 – 2.66 (m, 1H).

A mixture of **β -6f-1** (58 mg, 0.11 mmol) and lead tetraacetate (148 mg, 0.33 mmol) in toluene (1.5 mL) was stirred at 90°C for 2 h. After being cooled to room temperature, the reaction mixture was diluted with toluene and filtered through a celite pad. The filtrate was evaporated until dryness, washed with water and extracted with ethyl acetate (2 mL, 3 times). The organic layer was dried with anhydrous Na₂SO₄, and concentrated under reduced pressure to give a mixture of crude reaction. This mixture was then treated with amberlyst-15 (1mg/0.005 mmol of starting material) in a mixture of acetonitrile/H₂O (8:2, 2 mL). After stirring at 70°C for 3 h, the resulting mixture was evaporated to dryness and purified by silica gel column (1:1 hexane/ethyl acetate) to give **β -6f-2** (30 mg, 53%) as a yellow oil.

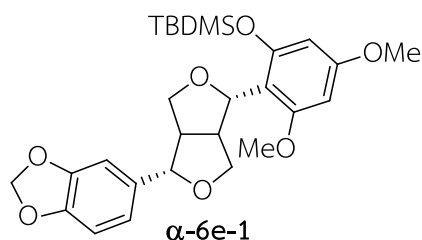


β -6f-2; ¹H NMR (CDCl₃, 400 MHz) δ 8.22 (d, *J* = 6.9 Hz, 2H), 7.67 – 7.66 (m, 1H), 7.52 (t, *J* = 7.6 Hz, 2H), 6.68 (dd, *J* = 5.0, 3.1 Hz, 2H), 6.48 (s, 1H), 6.46 – 6.44 (m, 1H), 5.02 (d, *J* = 6.4 Hz, 1H), 4.20 (d, *J* = 7.7 Hz, 1H), 3.99 – 3.97 (m, 1H), 3.93 (s, 3H), 3.87 (s, 3H), 3.85 (s, 3H), 3.74 (t, *J* = 8.5 Hz, 1H), 3.52 – 3.46 (m, 2H), 3.36 – 3.34 (m, 1H), 2.70 – 2.67 (m, 1H).

A mixture of synthesized lignan (1 equiv), *tert*-butyldimethylsilyl chloride (5 equiv) and imidazole (5 equiv) in dichloromethane (1.0 mL/0.1 mmol of synthesized lignans) at room temperature for 12 h. The reaction mixture was washed with water and extracted with dichloromethane (5 mL, 3 times). The organic layer was washed with saturated aqueous NaCl, followed by dried over Na₂SO₄. After filtration and removal of the solvent under reduced pressure, the crude product was purified by silica gel column chromatography (9:1 hexane/ethyl acetate) to obtain silylated product.

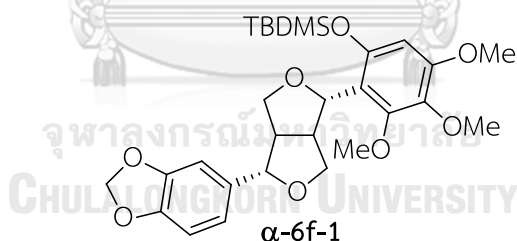
Following the general procedure, reaction of **α -6e** (38 mg, 0.10 mmol), *tert*-butyldimethylsilyl chloride (74 mg, 0.50 mmol) and imidazole (33 mg, 0.50 mmol) in

dichloromethane (1.5 mL). After purification, the silylated product (**α -6e-1**, 33 mg, 67%) was obtained as a pale-yellow oil.



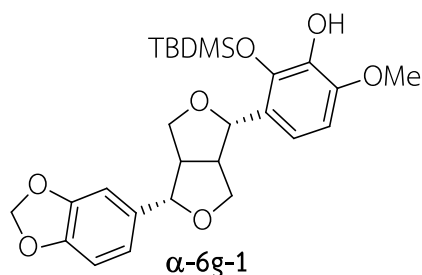
α -6e-1; $^1\text{H NMR}$ (CDCl_3 , 400 MHz) δ 6.88 (s, 1H), 6.83 (dd, $J = 7.9, 1.7$ Hz, 1H), 6.78 (d, $J = 7.7$ Hz, 1H), 6.13 (d, $J = 2.3$ Hz, 1H), 6.02 (d, $J = 2.4$ Hz, 1H), 5.95 (s, 2H), 5.31 (d, $J = 6.5$ Hz, 1H), 4.73 (d, $J = 5.5$ Hz, 1H), 4.31 (dd, $J = 8.6, 6.9$ Hz, 1H), 4.10 (dd, $J = 9.0, 6.9$ Hz, 1H), 3.84 – 3.79 (m, 2H), 3.78 (s, 3H), 3.76 (s, 3H), 3.43 – 3.40 (m, 1H), 3.10 – 3.09 (m, 1H), 1.02 (s, 9H), 0.26 (s, 6H).

Following the general procedure, reaction of **α -6f** (144 mg, 0.35 mmol), *tert*-butyldimethylsilyl chloride (104 mg, 0.69 mmol) in dichloromethane (4 mL). After purification, the silylated product (**α -6f-1**, 92.4, 51%) was obtained as a pale-yellow oil.



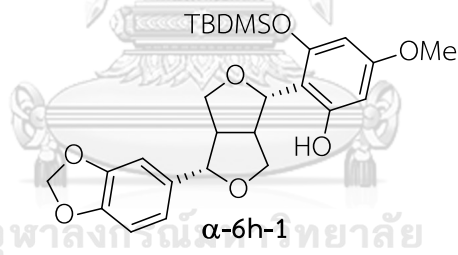
α -6f-1; $^1\text{H NMR}$ (CDCl_3 , 400 MHz) δ 6.86 – 6.77 (m, 3H), 6.16 (s, 1H), 5.95 (s, 2H), 5.18 (d, $J = 7.0$ Hz, 1H), 4.78 (d, $J = 4.8$ Hz, 1H), 4.35 (dd, $J = 8.0, 8.0$ Hz, 1H), 4.10 – 4.06 (m, 1H), 3.90 (s, 3H), 3.87 – 3.84 (m, 2H), 3.80 (s, 6H), 3.38 – 3.35 (m, 1H), 3.18 – 3.14 (m, 1H), 1.02 (s, 9H), 0.25 (s, 6H).

Following the general procedure, reaction of **α -6g** (40.5 mg, 0.11 mmol), *tert*-butyldimethylsilyl chloride (82.0 mg, 0.54 mmol) and imidazole (37.0 mg, 0.54 mmol) in dichloromethane (2 mL). After purification, the silylated product (**α -6g-1**, 52.9 mg, 56%) was obtained as a pale-yellow oil.



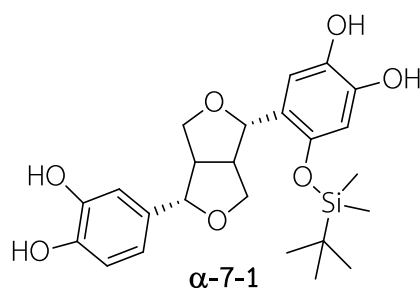
α -6g-1; $^1\text{H NMR}$ (400 MHz, CDCl_3) δ 6.86 (s, 1H), 6.81 (t, $J = 9.4$ Hz, 3H), 6.42 (d, $J = 8.6$ Hz, 1H), 5.94 (s, 2H), 5.00 (d, $J = 5.1$ Hz, 1H), 4.69 (d, $J = 5.7$ Hz, 1H), 4.26 (dd, $J = 10.9, 4.6$ Hz, 2H), 3.98 (dd, $J = 9.2, 4.7$ Hz, 1H), 3.90 (dd, $J = 9.1, 4.1$ Hz, 1H), 3.79 (d, $J = 5.5$ Hz, 3H), 3.21 – 3.13 (m, 1H), 3.01 (dd, $J = 9.8, 4.1$ Hz, 1H), 1.02 (s, 9H), 0.21 (d, $J = 5.0$ Hz, 6H).

Following the general procedure, reaction of **α -6h** (21.8 mg, 0.06 mmol), *tert*-butyldimethylsilyl chloride (52.9 mg, 0.29 mmol) and imidazole (19.9 mg, 0.29 mmol) in dichloromethane (1 mL). After purification, the silylated product (**α -6h-1**, 17.4, 61%) was obtained as a pale-yellow oil.



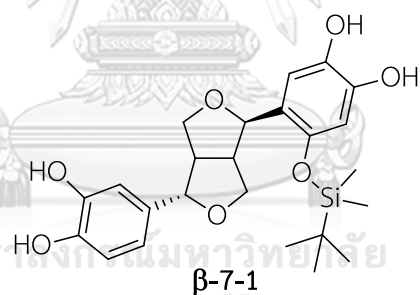
α -6h-1; $^1\text{H NMR}$ (400 MHz, CDCl_3) δ 6.81 (s, 1H), 6.77 (s, 2H), 6.11 (d, $J = 2.2$ Hz, 1H), 5.97 (d, $J = 2.4$ Hz, 1H), 5.95 (s, 2H), 5.16 (d, $J = 8.2$ Hz, 1H), 4.85 (d, $J = 3.4$ Hz, 1H), 4.56 – 4.50 (m, 1H), 4.11 (dd, $J = 9.4, 2.3$ Hz, 1H), 3.94 – 3.89 (m, 1H), 3.77 (d, $J = 7.6$ Hz, 1H), 3.73 (s, 3H), 3.26 (m, 1H), 3.04 (m, 1H), 1.01 (s, 9H), 0.27 (d, $J = 8.6$ Hz, 6H).

Following the general procedure, reaction of **α -7** (192 mg, 0.52 mmol), *tert*-butyldimethylsilyl chloride (390 mg, 2.60 mmol) and imidazole (176 mg, 2.60 mmol) in dichloromethane (3 mL) to obtain silylated product (**α -7-1**, 176 mg, 70%) as a colorless oil.



α -7-1; $^1\text{H NMR}$ (CDCl_3 , 400 MHz) δ 6.84 – 6.78 (m, 4H), 6.38 (s, 1H), 5.94 (s, 2H), 5.89 (d, $J = 2.6$ Hz, 2H), 5.06 (d, $J = 3.6$ Hz, 1H), 4.69 (d, $J = 3.9$ Hz, 1H), 4.29 – 4.23 (m, 2H), 3.93 (dd, $J = 9.2, 3.8$ Hz, 1H), 3.87 (dd, $J = 9.2, 3.4$ Hz, 1H), 3.02 – 2.97 (m, 2H), 1.01 (s, 9H), 0.24 (s, 3H), 0.24 (s, 3H).

Following the general procedure, reaction of **β -7** (96 mg, 0.26 mmol), *tert*-butyldimethylsilyl chloride (195 mg, 1.30 mmol) and imidazole (88 mg, 1.30 mmol) in dichloromethane (3 mL). After extraction and evaporation, the resulting residue was purified by silica gel column chromatography (8:2 hexane/ethyl acetate) to obtain silylated product (**β -7-1**, 83 mg, 66%) as a colorless oil.

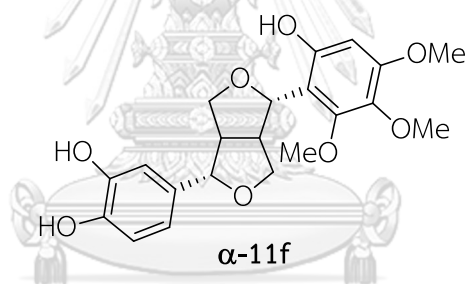


β -7-1; $^1\text{H NMR}$ (CDCl_3 , 400 MHz) δ 7.05 (s, 1H), 6.88 (s, 1H), 6.84 – 6.76 (m, 2H), 6.37 (s, 1H), 5.94 (s, 2H), 5.91 (s, 2H), 4.88 (d, $J = 6.2$ Hz, 1H), 4.34 (d, $J = 7.4$ Hz, 1H), 4.08 (d, $J = 9.4$ Hz, 1H), 3.82 – 3.76 (m, 2H), 3.45 – 3.40 (m, 1H), 3.30 – 3.25 (m, 1H), 2.87 – 2.80 (m, 1H), 1.00 (s, 9H), 0.27 (s, 3H), 0.22 (s, 3H).

A solution of silylated product (1 equiv) and lead (IV) tetraacetate (3 equiv) in toluene (1.0 mL/0.1 mmol of protected lignan) was stirred at 90°C for 2 h under atmospheric N_2 . After cooling, the reaction mixture was diluted with toluene and filtered through a celite pad. The filtrate was evaporated to dryness and extracted by ethyl acetate/ H_2O (1:1, 3 times). The organic layers were dried over anhydrous Na_2SO_4 and concentrated under reduced pressure. The resulting residue was treated with

tetra-*n*-butylammonium fluoride (3-5 equiv of silylated lignans) in tetrahydrofuran (0.1 mmol of silylated lignans) at room temperature. After being quenched with water, the resulting mixture was extracted with ethyl acetate (5 mL, 3 times). The extracts were washed with saturated aqueous NaCl, followed by dried over anhydrous Na₂SO₄. After filtration and removal of the solvent under reduced pressure, the crude product was purified by Sephadex LH-20 column using methanol to afford desired product.

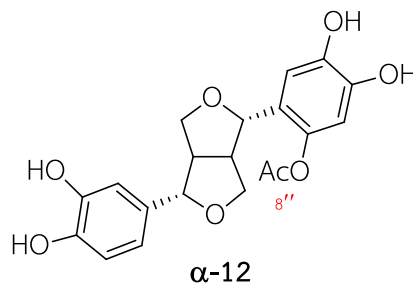
Following the general procedure, silylated product **α -6f-1** (79.9 mg, 0.15 mmol) and lead (IV) tetraacetate (200.1 mg, 0.45 mmol) were added in toluene (2 mL). After extraction and evaporation, the resulting residue was treated with tetra-*n*-butylammonium fluoride (131 μ L) in tetrahydrofuran (2 mL) at room temperature for 3 h. After purified by Sephadex LH-20 column, silica gel column chromatography was performed to yield **α -11f** (12.4 mg, 70%) as a brown oil and starting lignan (**α -6f**, 11.3 mg, 18%).



α -11f; ¹H NMR (400 MHz, CDCl₃) δ 8.60 (s, 1H, -OH), 6.87 – 6.81 (m, 2H, H-5' and H-6'), 6.73 (s, 1H, H-2'), 6.22 (s, 1H, H-3''), 5.60 (brs, 1H, -OH), 5.46 (brs, 1H, -OH), 5.11 (d, *J* = 7.4 Hz, 1H, H-2), 4.82 (d, *J* = 3.3 Hz, 1H, H-6), 4.49 (t, *J* = 8.5 Hz, 1H, H-4), 4.12 (d, *J* = 7.5 Hz, 1H, H-8), 4.03 – 4.01 (m, 1H, H-8), 3.90 (s, 3H, -OMe), 3.81 (s, 3H, -OMe), 3.80 – 3.77 (m, 1H, H-4), 3.78 (s, 3H, -OMe), 3.24 – 3.21 (m, 1H, H-5), 3.14 – 3.00 (m, 1H, H-1); ¹³C NMR (100 MHz, CDCl₃) δ 153.9, 152.1, 143.9, 143.3, 135.4, 133.8, 125.2, 118.9, 115.5, 113.5, 109.2, 97.0, 84.4, 83.9, 73.0, 70.7, 61.1, 61.0, 56.0, 54.7, 53.4.

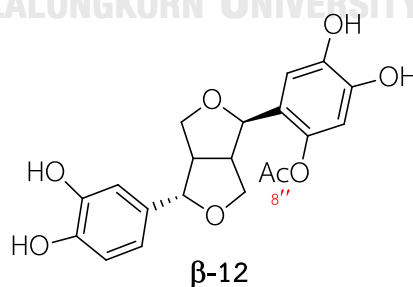
Following the general procedure, silylated product **α -7-1** (134.7 mg, 0.28) and lead (IV) tetraacetate (616.2 mg, 1.39 mmol) were added in toluene (3 mL). After extraction and evaporation, the resulting residue was treated with

tetra-*n*-butylammonium fluoride (291 μ L) in tetrahydrofuran (3 mL) at room temperature for 3 h to yield **α -12** (29.7 mg, 36%) as a dark brown oil.



α -12; ^1H NMR (400 MHz, CD_3OD) δ 6.85 (s, 1H, H-6''), 6.80 (s, 1H, H-6'), 6.75 (d, J = 8.1 Hz, 1H, H-5'), 6.68 (d, J = 7.6 Hz, 1H, H-2'), 6.52 (s, 1H, H-3''), 4.75 (d, J = 4.3 Hz, 1H, H-2), 4.61 (d, J = 4.3 Hz, 1H, H-6), 4.20 (dd, J = 16.1, 9.4 Hz, 2H, H-4 and H-8), 3.81 (dd, J = 8.8, 3.2 Hz, 2H, H-4 and H-8), 3.05 (s, 2H, H-1 and H-5), 2.27 (s, 3H, H-8''); ^{13}C NMR (100 MHz, CD_3OD) δ 171.59, 146.42, 146.22, 146.07, 144.49, 141.90, 133.77, 125.36, 118.90, 116.28, 114.48, 113.75, 111.03, 87.07, 82.89, 73.08, 72.79, 55.36, 55.03, 54.77, 20.83; HRMS m/z 411.1058 $[\text{M}+\text{Na}]^+$ (calcd for $\text{C}_{20}\text{H}_{20}\text{NaO}_8$, 411.1056)

Following the general procedure, silylated product **β -7-1** (85 mg, 0.18 mmol) lead (IV) tetraacetate (389 mg, 0.88 mmol) was added in toluene (2 mL). After extraction and evaporation, the resulting residue was treated with tetra-*n*-butylammonium fluoride (300 μ L, 0.88 mmol) in tetrahydrofuran (2 mL) at room temperature for 3 h to yield **β -12** (31 mg, 45%) as a yellow oil.



β -12; ^1H NMR (CD_3OD , 400 MHz) δ 7.02 (s, 1H, H-6''), 6.80 (s, 1H, H-2'), 6.74 (d, J = 8.3 Hz, 1H, H-5'), 6.69 (d, J = 7.9 Hz, 1H, H-6'), 6.50 (s, 1H, H-3''), 4.75 (d, J = 5.3 Hz, 1H, H-2), 4.30 (d, J = 7.3 Hz, 1H, H-6), 4.03 (d, J = 9.3 Hz, 1H, H-4), 3.78-3.74 (m, 2H, H-4 and H-8), 3.25-3.23 (m, 2H, H-1 and H-8), 2.88 (m, 1H, H-5), 2.28 (s, 3H, H-8''); ^{13}C NMR (CD_3OD , 100 MHz) δ 171.6, 146.4, 146.1, 145.8, 144.1, 140.9, 133.7, 122.6, 119.0, 116.3,

114.5, 114.4, 110.7, 89.1, 79.2, 71.4, 70.3, 55.6, 50.2, 20.8; HRESIMS m/z 411.1053
[M+Na]⁺ (calcd for C₂₀H₂₀NaO₈, 411.1056).



Chapter V

Antidiabetic Activity Evaluation

5.1 Antidiabetic activity evaluation of synthesized lignans

All synthesized lignans including starting lignans (**1-2, 5**) were evaluated for α -glucosidase inhibition from two different sources; (1) rat intestine (maltase & sucrase) and (2) baker's yeast. Starting lignans (**1-2, 5**) showed no inhibition (IC_{50} more than 50,000 μ M for rat intestine and more than 50,000 μ M for baker's yeast) while synthesized lignans (**α -6** and **β -6**) containing a phenolic moiety revealed low inhibition (IC_{50} 685.4-14,670 μ M) and moderate inhibition (IC_{50} 25.4-400.0 μ M), respectively, for synthesized lignans containing dihydroxy moieties (Table 5.1). It is likely that α -glucosidase inhibitory potency increases according to the number of free phenolic hydroxy group. Therefore, removal of methylenedioxy moiety to afford *ortho*-dihydroxy analogues would express improved antidiabetic activity as well as antioxidant property.

Table 5.1 α -Glucosidase inhibitory effect of synthesized compounds (**1-2, 5** and **6**)

Entry	Compounds	IC_{50} (μ M)		
		Maltase	Sucrase	Baker's yeast
1	1	>50,000	>50,000	>10,000
2	2	>50,000	>50,000	>10,000
3	5	>50,000	>50,000	>10,000
4	α-6a	8,239.6 \pm 14.8	14,670.2 \pm 18.2	1,146.2 \pm 6.4
5	β-6a	7,010.0 \pm 8.4	8,520.7 \pm 10.0	1,028.4 \pm 7.4
6	α-6b	2,483.2 \pm 6.5	4,800.5 \pm 10.0	937.0 \pm 5.6
7	α-6c	2,149.7 \pm 8.9	3,831.2 \pm 5.6	700.4 \pm 4.0
8	β-6c	1,516.3 \pm 9.1	3,133.2 \pm 11.4	698.1 \pm 3.8
9	α-6d	5,587.0 \pm 12.2	8,210.2 \pm 16.0	729.3 \pm 5.2

Table 5.1 (Cont.) α -Glucosidase inhibitory effect of synthesized compounds (**6-7**)

Entry	Compounds	IC ₅₀ (μ M)		
		Maltase	Sucrase	Baker's yeast
10	β-6d	2,440.2 \pm 10.4	3,300.2 \pm 9.6	715.7 \pm 3.7
11	α-6e	4,668.3 \pm 9.8	18,890.4 \pm 17.2	964.0 \pm 4.4
12	β-6e	2,987.1 \pm 7.3	11,100.3 \pm 16.3	883.7 \pm 6.9
13	α-6f	3,358.9 \pm 9.9	3,590.8 \pm 14.8	691.6 \pm 2.4
14	β-6f	1,308.3 \pm 9.1	3,841.2 \pm 11.0	685.4 \pm 2.1
15	α-6g	150.7 \pm 0.9	180.1 \pm 1.1	32.2 \pm 1.5
16	β-6g	110.0 \pm 1.1	170.5 \pm 1.7	25.4 \pm 1.4
17	α-6h	380.3 \pm 3.5	340.4 \pm 1.9	56.4 \pm 1.0
18	β-6h	260.0 \pm 1.6	230.6 \pm 2.4	42.9 \pm 1.7
19	α-6h'	350.0 \pm 5.5	400.0 \pm 5.0	53.0 \pm 2.4
20	β-6h'	210.0 \pm 2.5	200.0 \pm 3.4	40.3 \pm 1.1
21	α-7	3,439.9 \pm 10.1	6,903.2 \pm 13.6	210.3 \pm 1.2
22	β-7	1,140 \pm 8.7	4,012.3 \pm 12.7	205.8 \pm 1.1

After methylenedioxy cleavage, all synthesized lignans (**3-4**, **8-12**) were evaluated against α -glucosidase inhibition (Table 5.2). To clearly demonstrate the effect of number of free hydroxy on α -glucosidase inhibition, the IC₅₀ values of synthesized lignans in Chapters III and IV are compared in Figure 5.1.

Table 5.2 α -Glucosidase inhibitory effect of synthesized compounds (**3-4, 8-12**)

Entry	Compounds	IC ₅₀ (μ M)		
		Maltase	Sucrase	Baker's yeast
1	3	170.2 \pm 1.9	190.8 \pm 3.7	21.6 \pm 1.4
2	4	42.6 \pm 1.1	29.2 \pm 1.2	10.0 \pm 1.0
3	α-8d	97.0 \pm 1.2	46.6 \pm 1.3	15.9 \pm 1.0
4	β-8d	47.0 \pm 1.1	33.0 \pm 0.2	14.6 \pm 0.7
5	α-8f	96.5 \pm 1.4	110.2 \pm 1.0	23.4 \pm 1.2
6	β-8f	63.3 \pm 1.6	61.1 \pm 1.8	19.8 \pm 1.9
7	α-9c	>50,000	>50,000	>10,000
8	α-10	200 \pm 7.5	165.7 \pm 5.3	30.5 \pm 3.3
9	α-11f	173.6 \pm 3.7	136.4 \pm 3.2	17.8 \pm 1.8
10	α-12	38.8 \pm 1.0	18.7 \pm 0.3	7.7 \pm 0.6
11	β-12	25.7 \pm 1.0	12.9 \pm 0.4	5.3 \pm 0.6
12	Acarbose [®]	1.4 \pm 0.2	3.2 \pm 0.4	147.2 \pm 0.5

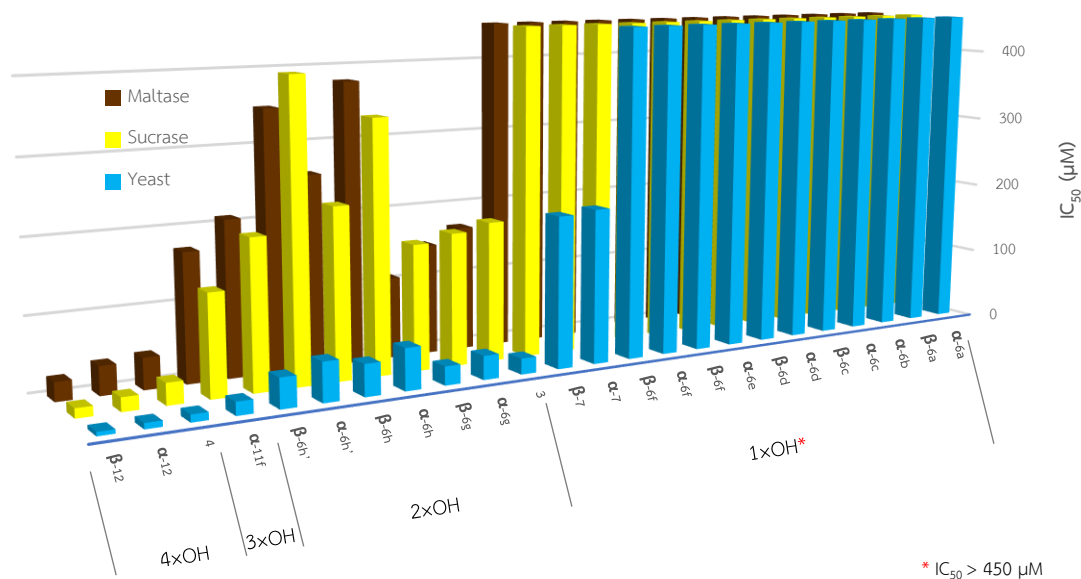


Figure 5.1 α -glucosidase inhibition of the synthesized lignans containing free hydroxy groups (3-4, 6-7, 11-12).

Generally, α -glucosidase inhibitory potency largely depended on the number of hydroxy groups (n) in the lignan structure. The maximum inhibitions against α -glucosidase were observed where n was 4 (**4** and **12**, IC₅₀ 12.9-42.6 μ M for rat intestine and IC₅₀ 5.3-10.0 μ M for baker's yeast). The inhibitory effect dropped significantly when n was 2 and 3 (**3**, **6g**, **6h**, **6h'** and **11**, IC₅₀ 110-400 μ M for rat intestine and IC₅₀ 17.8-56.4 μ M for baker's yeast). The low potency or no inhibition was observed where n was 1 (**6a-6f**, IC₅₀ 1,140-14,670 μ M for rat intestine and IC₅₀ 685.4-1,146.0 μ M for baker's yeast).

To get more insight into structure-activity relationship, key functional groups and chemical moieties affecting α -glucosidase inhibition were analyzed and discussed in Figure 5.2 and Figure 5.3. Although the structure-activity relationship (SAR) of synthesized compounds against three different α -glucosidases showed similar tendency, herein the discussion on SAR of synthesized compounds against sucrase is exemplified.

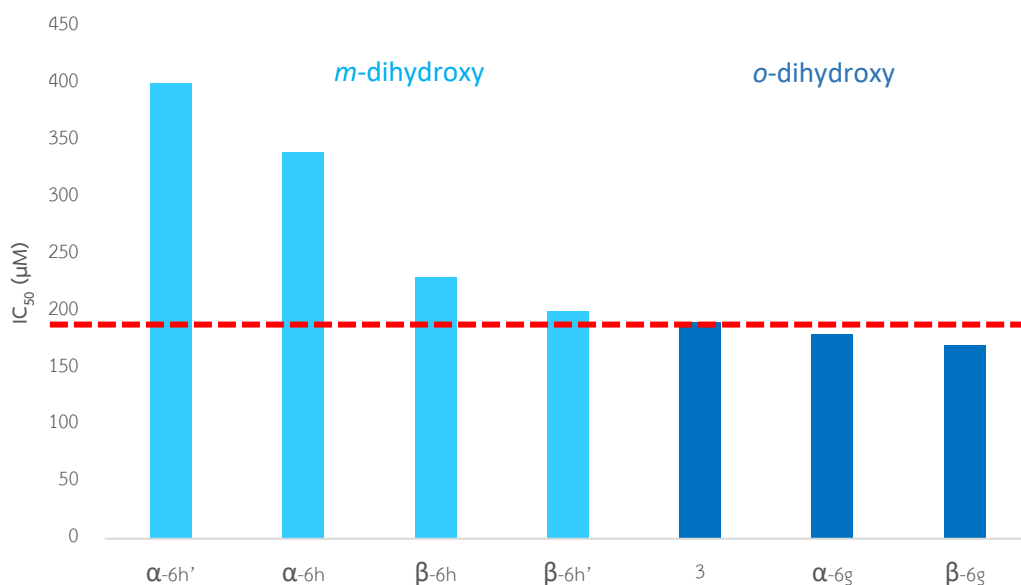


Figure 5.2 Sucrase inhibition of the synthesized lignans containing dihydroxy moiety.

The presence of dihydroxy moieties could generally be classified into two different types; *ortho*-dihydroxy and *meta*-dihydroxy moieties. Lignans containing *ortho*-dihydroxy moiety (**3** and **6g**, IC₅₀ 170.0-190.0 µM) apparently exerted stronger inhibition than *meta*-dihydroxy moiety (**6h-6h'**, IC₅₀ 200.0-400.0 µM). Accordingly, a catechol analogue led to improved inhibition against α-glucosidase, possibly through chelating between the catechol moiety and enzymes.³⁹ The H-bonding interactions of the hydroxy of the catechol group and the carbonyl group of the amino acid were predicted to be the predominant interactions. Moreover, the nitrogen of the amino acid residues might form hydrogen bonds with the hydroxyl group. Herein, catechol analogues displayed the highest potency in this experiment (IC₅₀ 12.9-136.0 µM). Interestingly, a relationship between conformation was further observed. The results indicated that the β-product was likely to be more potent than its epimer, the α-product.

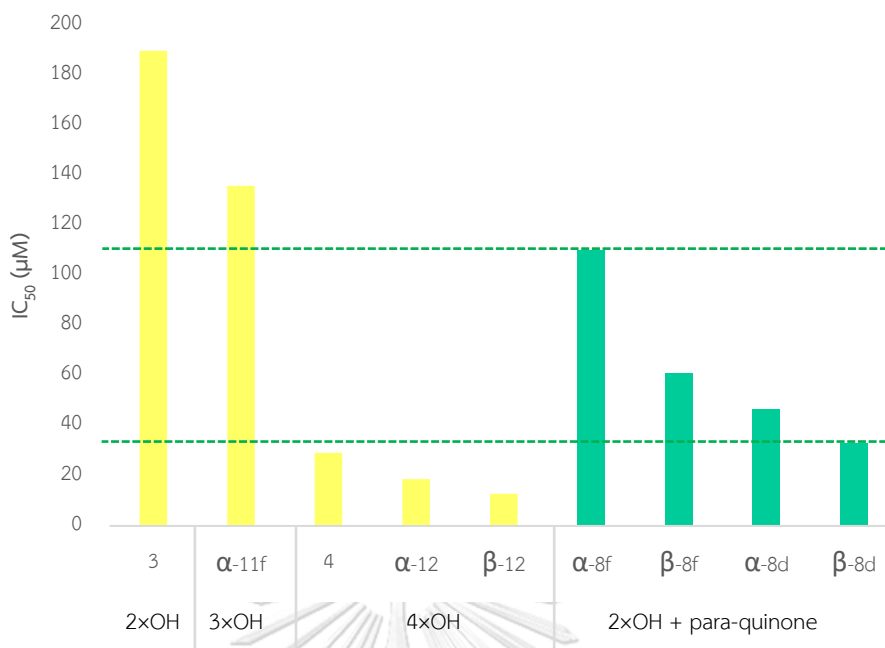


Figure 5.3 Sucrase inhibition of the synthesized lignans (**3-4**, **8** and **12**)

The IC₅₀ values of furofuran lignans containing catechol moiety against sucrase are displayed in Figure 5.3. Unexpectedly, furofuran lignans containing *para*-quinone moieties (**8**) were observed significantly high potency (IC₅₀ 33.0-110.0 µM), however, only *para*-quinone moiety on (**α-9c**) showed no inhibition (IC₅₀ more than 10,000 µM). Hence, a hydroxy unit is indispensable group of the inhibition. Moreover, **8** which contains two hydroxy groups presented higher potency than three hydroxy groups of **α-11f** (IC₅₀ 136.0 µM). This observation suggested *para*-quinone enhanced inhibition against α -glucosidase. Besides, **8f** (IC₅₀ 61.0-110.0 µM) slightly decreased inhibition compared with **8d** (IC₅₀ 33.0-46.6 µM) owing to different number of a methoxy moiety.

In addition, the presence of acetoxy unit of **12** remarkably represented enhancing inhibition comparing with **4** (1-2 times). Therefore, the acetoxy unit plays an important role to improve the activity.

For another type, baker's yeast α -glucosidase, the inhibition effects were similar to rat intestine α -glucosidase. First, the inhibition depends on the number of hydroxy units and bearing catechol analogue revealed crucial role. Moreover, *para*-quinone moiety worked synergistically (**8**, IC₅₀ 14.6-23.4 µM). Furthermore, β -products displayed higher inhibition than its epimers, α -products. Finally, acetoxy unit demonstrated

enhancing baker's yeast α -glucosidase according to **12** that revealed the highest inhibition (IC_{50} 5.3-7.7 μ M). Especially, β -12 (IC_{50} 5.3 μ M) was the most potent inhibitor that was 28 times more active than the standard drug acarbose (IC_{50} 147.2 μ M).

5.2 Experimental section

5.2.1 General experiment procedures

α -Glucosidase inhibition was measured on a BioRed microplate reader model 3550 UV.

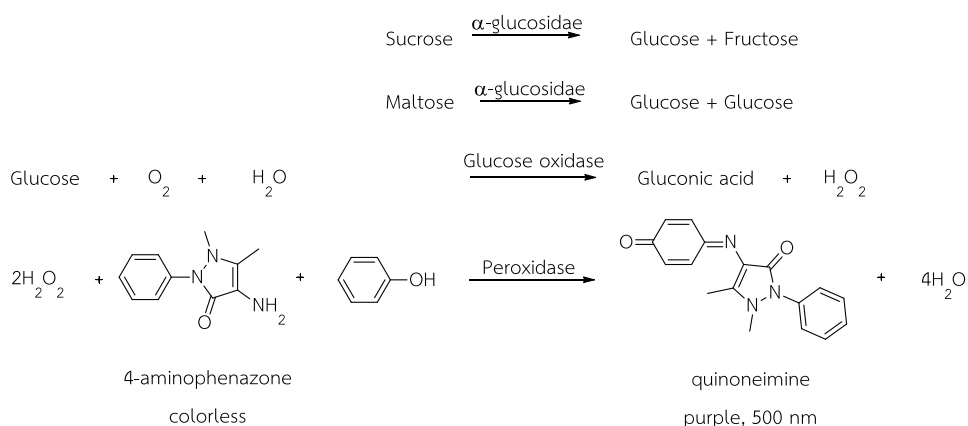
5.2.2 Chemical

Sucrose, maltose, baker's yeast α -glucosidase, rat intestinal acetone powder, and *p*-nitrophenyl- α -D-glucopyranoside were obtained from Sigma-Aldrich (St.Louis, MO, USA). Glucose assay kit was obtained from Human Gesellschaft für Biochemica und Diagnostica mbH (Germany). Acarbose[®] was obtained from Bayer (Germany).

5.2.3 Antidiabetic activity evaluation of synthesized lignans

5.2.3.1 Rat intestinal α -Glucosidase inhibition assay

The antidiabetic activity was evaluated using rat intestinal α -glucosidase inhibition assay because oligosaccharides and disaccharides such as sucrose and maltose in nature are digested by rat intestinal α -glucosidase to yield glucose. The determination the amount of the resulting glucose can be conducted using colorimetric technique. Briefly, hydrogen peroxide (H_2O_2) produced after oxidation of glucose by glucose oxidase oxidizes phenol to *p*-quinone, which is immediately coupled to 4-aminophenazone, in the presence of peroxidase, to form purple solution of quinoneimine (Scheme 5.1).⁴⁰ Thus, the inhibitory effect of the synthesized compounds against rat α -glucosidase was quantified by measuring the absorbance of quinoneimine formed (503 nm). Acarbose[®] was used as the standard control.



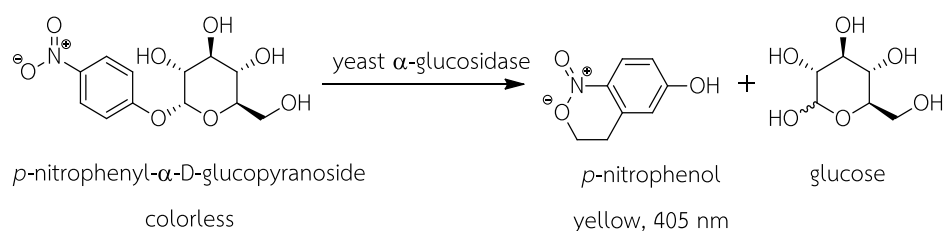
Scheme 5.1 Colorimetric technique for the determination of glucose.

α -Glucosidase (rat intestinal maltase and sucrase) inhibitory activity was determined according to our previous report.⁴⁰ The synthesized lignans (1 mg/mL in DMSO, 10 μ L) were added to 0.1 M phosphate buffer (pH 6.9, 30 μ L), the substrate solution (maltose: 10 mM, 20 μ L; sucrose: 100 mM, 20 μ L) in 0.1 M phosphate, glucose assay kit (80 μ L) and crude enzyme solution (20 μ L). Then, the reaction mixture was incubated at 37°C for 10 min (maltose) and 40 min (sucrose). The absorbance of quinoneimine was measured at 503 nm. The assay was performed in triplicate, and Acarbose[®] was used as a positive control. The inhibition percentage was calculated according to $[(A_0 - A_1)/A_0] \times 100$, whereas A is the absorbance without the sample (A_0) and with the sample (A_1). The IC_{50} value was estimated from a plot of percentage inhibition and sample concentration.

5.2.3.2 Baker's yeast α -glucosidase inhibitory activity

To approve α -glucosidase inhibitory activity, baker's yeast α -glucosidase inhibition assay was performed using colorimetric technique to determine the amount of the resulting glucose. Briefly, yeast α -glucosidase hydrolyzed the substrate *p*-nitrophenyl- α -D-glucopyranoside, colorless solution, to produce *p*-nitrophenol and glucose.

p-Nitrophenol was observed as yellow solution (Scheme 5.2). Thus, the inhibitory effect of the synthesized compounds against yeast α -glucosidase was quantified by measuring the absorbance of *p*-nitrophenol formed (405 nm). Acarbose[®] was used as the standard control.



Scheme 5.2 Hydrolysis by yeast α -glucosidase.

The baker's yeast α -glucosidase inhibitory activity was determined according to Wacharasindhu's method.⁴¹ The synthesized lignans (1 mg/mL in DMSO, 10 μ L) were added to α -glucosidase solution (0.1 U/mL, 40 μ L) in 0.1 M phosphate buffer (pH 6.9, 50 μ L). Then, the reaction mixture was incubated at 37°C for 10 min. The substrate solution (1 mM *p*-nitrophenyl- α -D-glucopyranoside, 50 μ L) in 0.1 M phosphate was added to the reaction mixture and incubated at 37°C for further 20 min. The reaction mixture was terminated by adding 1 M Na₂CO₃ (100 μ L). The absorbance of *p*-nitrophenol was measured at 405 nm. The assay was performed in triplicate, and Acarbose[®] was used as a positive control. The inhibition percentage was calculated according to $[(A_0 - A_1)/A_0] \times 100$, whereas A is the absorbance without the sample (A_0) and with the sample (A_1). The IC₅₀ value was estimated from a plot of percentage inhibition and sample concentration.

Chapter VI

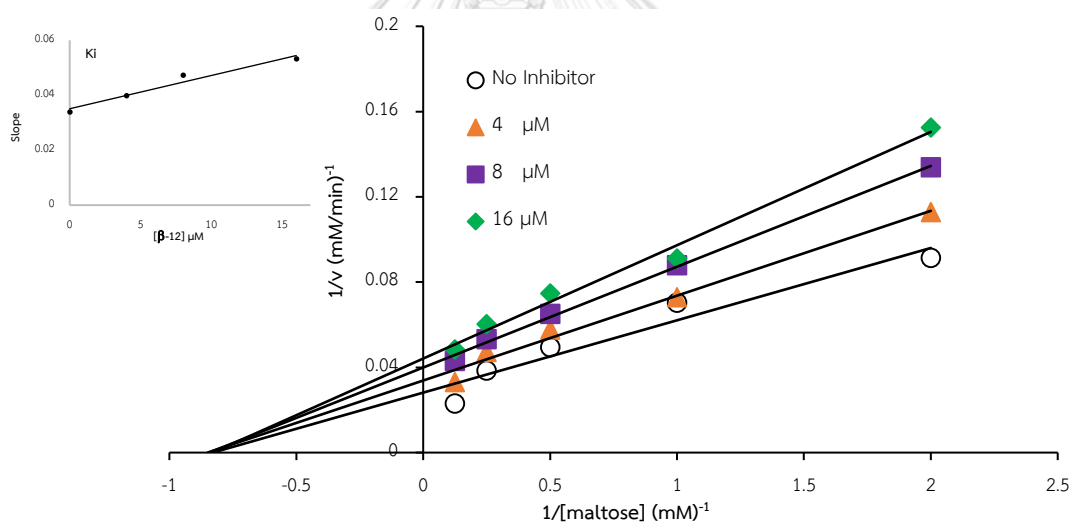
Kinetic study and a possible mechanism

6.1 Kinetic Study

To provide some insights into the mechanism of inhibition, efforts were made to analyze kinetic study by constructing Lineweaver–Burk plot.⁴² The kinetic parameters were determined by varying the concentration of the substrates of rat intestinal (maltose and sucrose) and yeast (*p*NPG) α -glucosidase in the absence and presence of glucose.

Of synthesized lignans, **β -12**, **α -12**, **4** and **α -8d** represented the most potent inhibitor of each group (Figure S116-118).

A)



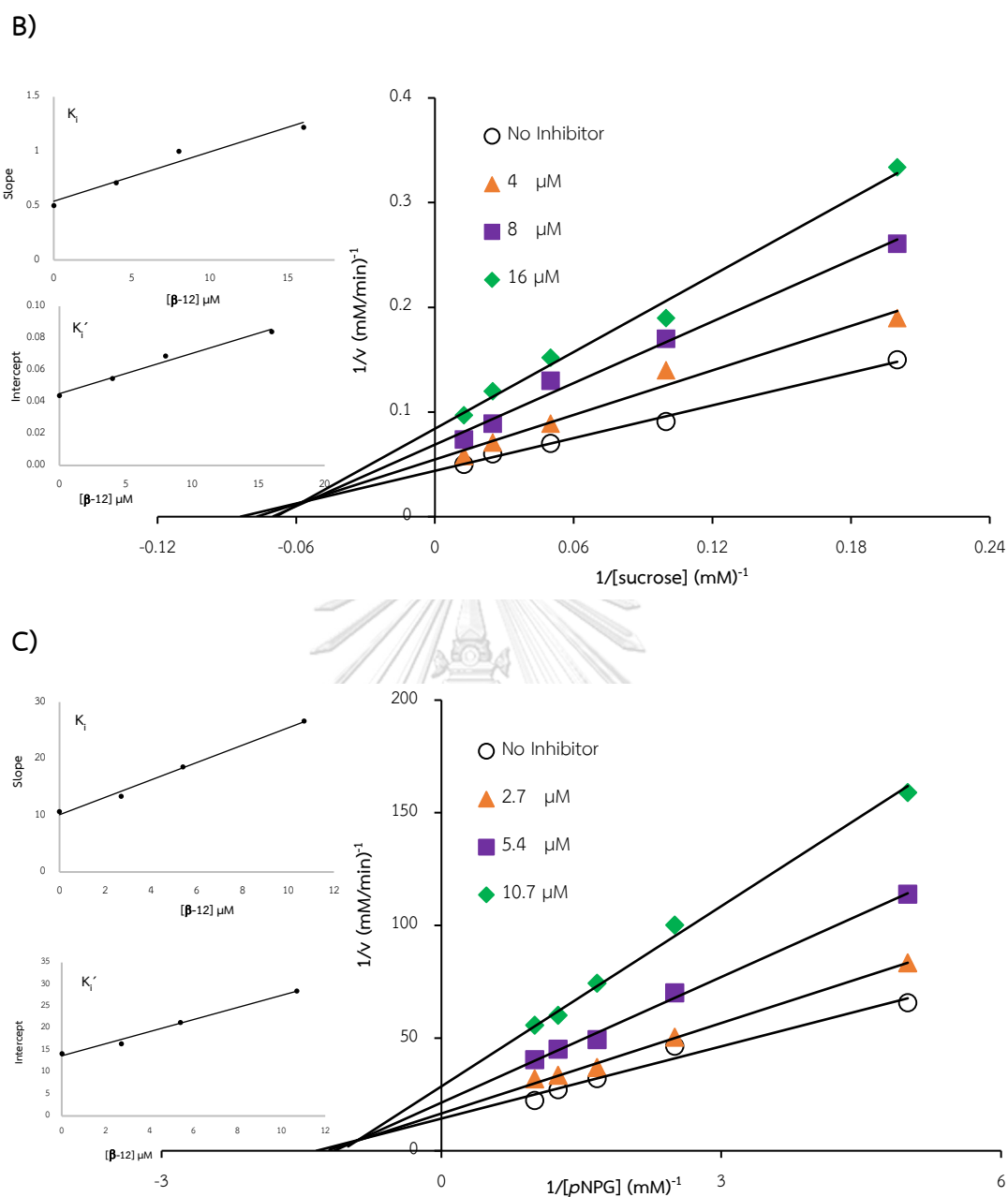


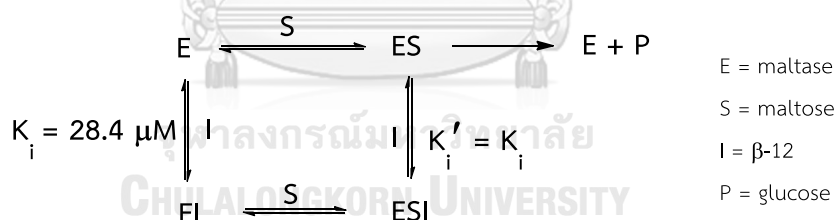
Figure 6.1 Lineweaver-Burk and secondary plots for inhibitory activity of β -12 against A) maltase, B) sucrose and C) baker's yeast.

Although β -12 was the most potent against all α -glucosidases, its results revealed different types of inhibition. In Figure 6.1A, the intersection on the X-axis was observed allowing the identification of a non-competitive against maltase. Meanwhile the intersection on the second quadrant was obtained in Figure 6.1B and Figure 6.1C. The inhibitory type against sucrose and baker's yeast of allowing mixed inhibitory type

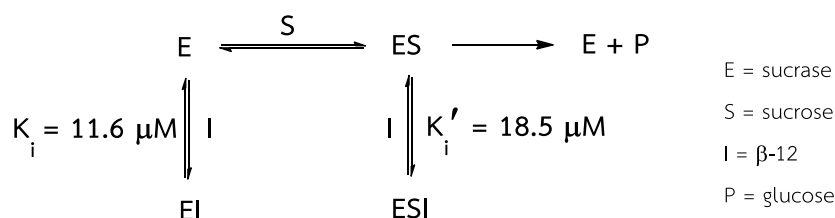
against maltase, sucrase and baker's yeast, respectively. The results indicated that β -12 could work in different types depended on enzymes.

Kinetic experiments were conducted to validate the simulation results and to obtain data regarding the functions underlying the binding of inhibitors (I) to α -glucosidase (E, enzyme) and substrates (S). In this experiment, the behavior of inhibitors could be indicated through two different pathways; forming enzyme-inhibitor (EI) complex and interrupting enzyme-substrate (ES) complex by forming enzyme-substrate-inhibitor (ESI) complex. The value of the dissociation constant for the EI complex (K_i) of maltase- β -12 was 28.4 μ M, presumably $K_i = K_i'$ due to non-competitive inhibition (Figure 6.2A). Meanwhile, mixed inhibition revealed K_i of sucrase- β -12 was 11.6 μ M and K_i' of sucrase-sucrose- β -12 (ESI) complex was 18.5 μ M (Figure 6.2B). The smaller value of K_i indicated that sucrase was predominantly inhibited by pathway of the EI complex over the ESI complex. Similarly, baker's yeast α -glucosidase was also predominantly inhibited by pathway of EI complex (Figure 6.2C).

A)



B)



C)

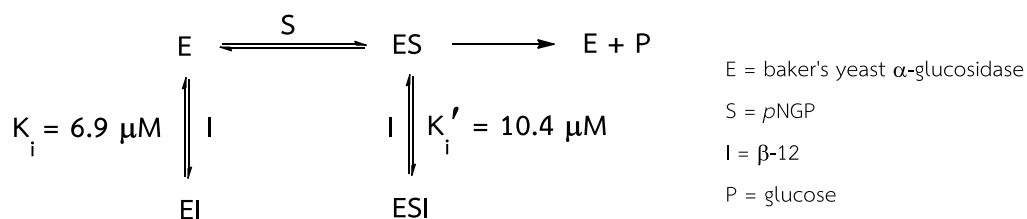


Figure 6.2 Putative mechanism pathway of β -12 for A) non-competitive inhibition against maltase. B) mixed inhibition against sucrase. C) mixed inhibition against baker's yeast α -glucosidase.

The inhibition types, K_i and K_i' of furofuran lignans (β -12, α -12, 4 and α -8d) against rat intestinal and baker's yeast α -glucosidases are summarized in Table 6.1.

Table 6.1 Inhibition types and kinetic parameters of β -12, α -12, 4 and β -8d on α -glucosidases

		Compounds			
		β -12	α -12	4	α -8d
Maltase	Inhibition types	Non-competitive	Non-competitive	Mixed	Mixed
	K_i (μM)	28.4 \pm 0.95	31.6 \pm 1.10	19.9 \pm 0.82	67.8 \pm 1.68
	K_i' (μM)	-	-	40.1 \pm 1.48	93.7 \pm 1.12
Sucrase	Inhibition types	Mixed	Non-competitive	Mixed	Mixed
	K_i (μM)	11.6 \pm 0.80	18.6 \pm 0.66	15.1 \pm 0.75	34.2 \pm 0.95
	K_i' (μM)	18.5 \pm 1.03	-	39.9 \pm 1.06	62.7 \pm 1.04
Baker's yeast	Inhibition types	Mixed	Mixed	Mixed	Mixed
	K_i (μM)	6.9 \pm 0.76	10.1 \pm 1.27	9.1 \pm 0.57	15.6 \pm 0.50
	K_i' (μM)	10.4 \pm 0.51	19.6 \pm 1.31	16.5 \pm 0.60	59.7 \pm 1.25

Although some inhibitors presented the different types of inhibition, all inhibitors bound to enzyme at the binding site. While, the inhibitory type of Acarbose[®] was reported to be a competitive which bound to enzyme at the active site.⁴³

For biological activity results, the hydroxy moiety on phenolic group, specially, catechol analogues played an important role to enhance antidiabetic activity. Furthermore, stereochemistry at C-2 and acetoxy unit revealed slightly effecting to inhibition against α -glucosidases. Another inhibitor, *para*-quinone, might work together with catechol moiety to improve the activity. Although all furofuran lignans containing phenolic moieties were able to inhibit α -glucosidases, the mechanism of each inhibitor could be different pathway.

6.2 Experimental section

6.2.2 General experiment procedures

α -Glucosidase inhibition was measured on a BioRed microplate reader model 3550 UV.

6.2.3 Chemical

Sucrose, maltose, baker's yeast α -glucosidase, rat intestinal acetone powder, and *p*-nitrophenyl- α -D-glucopyranoside were obtained from Sigma-Aldrich (St.Louis, MO, USA). Glucose assay kit was obtained from Human Gesellschaft für Biochemica und Diagnostica mbH (Germany). Acarbose[®] was obtained from Bayer (Germany).

6.2.4 Antidiabetic activity evaluation of synthesized lignans

Antidiabetic activity evaluation were performed using the methodology described in section 3.3.4

6.2.5 Kinetic study

The kinetic parameters, maximum reaction rate (V_{max}) and Michaelis constant (K_m), were calculated by Lineweaver-Burk linearization by varying the concentration of the substrate (maltose, sucrose and *p*NPG) in the absence and presence of glucose. The value of the dissociation constant for the enzyme-inhibitor complex (K_i) and the dissociation constant for the enzyme-substrate-inhibitor complex (K_i') for glucose were calculated from the secondary plots.

The Lineweaver-Burk equation in double reciprocal form can be written as:

$$\frac{1}{v_0} = \frac{K_m}{V_{max}} \frac{1}{[S]} + \frac{1}{V_{max}}$$

Secondary plots can be constructed from

$$\text{Slope} = \frac{K_m}{V_{\max}} + \frac{K_m[I]}{V_{\max}K_i}$$

$$Y - \text{intercept} = \frac{1}{V_{\max}} + \frac{[I]}{\alpha K_i V_{\max}}$$

α -Glucosidase (**rat intestinal maltase and sucrase**) inhibitory activity was determined according to our previous report³⁰. The synthesized lignans (1 mg/mL in DMSO, 10 μ L) were added to 0.1 M phosphate buffer (pH 6.9, 30 μ L) with increasing concentrations of the substrate solution (maltose: 0.5-8 mM, 20 μ L; sucrose: 5-80 mM, 20 μ L) in 0.1 M phosphate, glucose assay kit (80 μ L) and crude enzyme solution (20 μ L). Then, the reaction mixture was incubated at 37°C for 10 min (maltose) and 40 min (sucrose). α -Glucosidase activity was measured at 503 nm. The assay was performed in triplicate, and Acarbose[®] was used as a positive control.

The baker's yeast α -glucosidase inhibitory activity was determined according to Wacharasindhu's method³¹. Briefly, the synthesized lignans (1 mg/mL in DMSO, 10 μ L) were added to α -glucosidase solution (0.1 U/mL, 40 μ L) in 0.1 M phosphate buffer (pH 6.9, 50 μ L). Then, the reaction mixture was incubated at 37°C for 10 min. The increasing concentrations of the substrate solution (0.2-1 mM *p*-nitrophenyl- α -D-glucopyranoside, 50 μ L) in 0.1 M phosphate was added to the reaction mixture and incubated at 37°C for 20 min. Terminating the reaction mixture by adding 1 M Na₂CO₃ (100 μ L). α -Glucosidase activity was measured at 405 nm. The assay was performed in triplicate, and Acarbose[®] was used as a positive control

Chapter VII

Conclusion

This research represents the first synthesis, a series of furofuran lignans containing multiple phenolics (**6-12**). The starting materials named sesamin (**1**) and sesamol (**2**) were obtained from sesame seed oil through saponification followed by chromatographic separation. Sesamol (**2**) was subsequently converted to more reactive lignan named samidin (**5**), which is a versatile building block in synthesis of desired lignans. A series of furofuran lignans having different substituents at C-2 of the furofuran core structure (**6-7**) were synthesized through Friedel-Crafts reaction by coupling of **5** and phenolic compounds under acidic conditions. The desired products were afforded in the form of α - and β -products due to the planar nature of the oxocarbenium ion. This methodology offers an alternative route for the synthesis of furofuran lignans containing multiple phenolic moieties in good yields compared with the previous synthesis. Moreover, this work also introduced a method that could instantly distinguish the α - and β -products using ^1H NMR data. After series **6** and **7** were evaluated for antidiabetic activity using α -glucosidases, it is likely that α -glucosidase inhibitory potency increases according to the number of free phenolic hydroxyl groups.

A key inhibition was observed in furofuran lignans having *ortho*-dihydroxy unit or catechol moiety, which was generated by removal of the methylenedioxy unit through oxidative reaction using lead (IV) tetraacetate. Unexpectedly, some furofuran lignans containing free hydroxyl groups produced *para*-quinone moieties under oxidative conditions. Therefore, protection of free hydroxyl groups by silylation reaction using *tert*-butyldimethylsilyl chloride was introduced to maintain the hydroxyl moiety and afford the desired catechol moiety. All synthesized lignans were subsequently evaluated for α -glucosidase inhibition. In this experiment, furofuran lignans containing tetraphenolics (**4** and **12**) showed the most potent inhibition against α -glucosidases (IC_{50} 5.3-42.6 μM). The observation suggested critical scientific clues that having more phenolic groups, especially the catechol unit, is required for more potent inhibition against α -glucosidase. Meanwhile, an acetoxy group could slightly improve activity. Moreover, β -products generally showed more potent inhibition than the α -anomers.

Although the presence of *para*-quinone unit alone in furofuran lignan structure revealed no inhibition, the presence *para*-quinone and hydroxy moieties together could significantly enhance inhibition. Hence, *para*-quinone moiety worked synergistically in new α -glucosidase inhibitors.

Our findings also provided an insight into the mechanism of α -glucosidase inhibition by particularly active compounds using kinetic studies. The observation suggested that they inhibited the enzymes by non-competitive and mixed inhibition. It could be implied that the all structures of active compounds fit well into the binding site of enzyme while Acarbose[®] interacted enzyme at the active site. As the results, the synthesized furofuran lignans could represent a new class of promising compounds that have the potential for diabetes therapy applied together with Acarbose[®].



REFERENCES

1. Fazary, A. E.; Alfaifi, M. Y.; Saleh, K. A.; Alshehri, M. A.; Elbehairi, S. E. I., Bioactive lignans: A survey report on their chemical structures. *Natural Products Chemistry & Research* **2016**, *4*, 226-241.
2. Landete, J. M., Plant and mammalian lignans: A review of source, intake, metabolism, intestinal bacteria and health. *Food Research International* **2012**, *46*, 410-424.
3. Teponno, R. B.; Kusari, S.; Spiteller, M., Recent advances in research on lignans and neolignans. *Natural Product Reports* **2016**, *33*, 1044-1092.
4. Ward, S. R., Lignans, neolignans and related compounds. *Natural Product Reports* **1999**, *16*, 75-96.
5. Dar, A.; Arumugam, N., Lignans of sesame: Purification methods, biological activities and biosynthesis. *Bioorganic Chemistry* **2013**, *50*, 1-10.
6. Hirose, N.; Doi, F.; Ueki, T.; Akazawa, K.; Chijiwa, K.; Sugano, M.; Akimoto, K.; Shimizu, S.; Yamada, H., Suppressive effect of sesamin against 7,12-dimethylbenz[a]-anthracene induced rat mammary carcinogenesis. *Anticancer Research* **1992**, *12*, 1259-1265.
7. Miyahara, Y.; Hibasami, H.; Katsuzaki, H.; Imai, K.; Komiya, T., Sesamolin from sesame seed inhibits proliferation by inducing apoptosis in human lymphoid leukemia Molt 4B cells. *International Journal of Molecular Medicine* **2001**, *7*, 369-371.
8. Ryu, S.; Kim, K.; Kang, S., Growth inhibitory effects of sesamolin from sesame seeds on human leukemia HL-60 cells. *Korean Journal of Pharmacognasy* **2003**, *34*, 237-241.
9. Hou, R. C. W.; Wu, C. C.; Yang, C. H.; Jeng, K. C. G., Protective effects of sesamin and sesamolin on murine BV-2 microglia cell line under hypoxia. *Neuroscience Letters* **2004**, *367*, 10-13.
10. Kim, J. H.; Lee, J. K., Sesamolin enhances NK cell lysis activity by increasing the expression of NKG2D ligands on Burkitt's lymphoma cells. *International Immunopharmacol* **2015**, *28*, 977-984.
11. Kang, M. H.; Naito, M.; Tsujihara, N.; Osawa, T., Sesamolin inhibits lipid peroxidation in rat liver and kidney. *The Journal of Nutrition* **1998**, *128*, 1018-1022.

12. Nakai, M.; Harada, M.; Nakahara, K.; Akimoto, K.; Shibata, H.; Miki, W.; Kiso, Y., Novel antioxidative metabolites in rat liver with ingested sesamin. *Journal of Agricultural and Food Chemistry* **2003**, *51*, 1666-1670.
13. Hou, R. C. W.; Huang, H. M.; Tzen, J. T.; Jeng, K. C. G., Protective effects of sesamin and sesamol on hypoxic neuronal and PC12 cells. *Journal of Neuroscience Research* **2003**, *74*, 123-133.
14. Hou, R. C. W.; Wu, C. C.; Huang, J. R.; Chen, Y. S.; Jeng, K. C. G., Oxidative toxicity in BV-2 microglia cells: Sesamol neuroprotection of H₂O₂ injury involving activation of p38 mitogen-activated protein kinase. *Annals of the New York Academy of Sciences* **2005**, *1042*, 279-285.
15. Wichitsranoi, J.; Weerapreeyakul, N.; Boonsiri, P.; Settasatian, C.; Settasatian, N.; Komanasin, N.; Sirijaichingkul, S.; Teerajetgul, Y.; Rangkadilok, N.; Leelayuwat, N., Antihypertensive and antioxidant effects of dietary black sesame meal in pre-hypertensive humans. *Nutrition Journal* **2011**, *10*, 82.
16. Hung, C.-T.; Chen, L.-D.; Hou, C.-W., Neuroprotection of a sesamin derivative, 1, 2-bis[(3-methoxyphenyl)methyl]ethane-1,2-dicarboxylic acid (MMEDA) against ischemic and hypoxic neuronal injury. *Iranian Journal of Basic Medical Sciences* **2017**, *20*, 1324.
17. Emerging Risk Factors, C.; Sarwar, N.; Gao, P.; Seshasai, S. R. K.; Gobin, R.; Kaptoge, S.; Di Angelantonio, E.; Ingelsson, E.; Lawlor, D. A.; Selvin, E.; Stampfer, M.; Stehouwer, C. D. A.; Lewington, S.; Pennells, L.; Thompson, A.; Sattar, N.; White, I. R.; Ray, K. K.; Danesh, J., Diabetes mellitus, fasting blood glucose concentration, and risk of vascular disease: a collaborative meta-analysis of 102 prospective studies. *Lancet (London, England)* **2010**, *375*, 2215-2222.
18. Bourne, R. R.; Stevens, G. A.; White, R. A.; Smith, J. L.; Flaxman, S. R.; Price, H.; Jonas, J. B.; Keeffe, J.; Leasher, J.; Naidoo, K., Causes of vision loss worldwide, 1990–2010: a systematic analysis. *The Lancet Global Health* **2013**, *1*, 339-349.
19. Saran, R.; Robinson, B.; Abbott, K. C.; Agodoa, L. Y.; Albertus, P.; Ayanian, J.; Balkrishnan, R.; Bragg-Gresham, J.; Cao, J.; Chen, J. L., US renal data system 2016 annual data report: epidemiology of kidney disease in the United States. *American Journal of Kidney Diseases* **2017**, *69*, 7-8.

20. Yee, H. S.; Fong, N. T., A review of the safety and efficacy of acarbose in diabetes mellitus. *Pharmacotherapy* **1996**, *16*, 792-805.
21. Singh, P.; J, R.; B. Agawane, S.; Garikapati, V.; Korwar, A.; Anand, A.; S. Dhayude, V.; L. Shaikh, M.; Joshi, R.; Boppana, R.; Kulkarni, M.; Thulasiram, H. V.; Giri, A., Potential Dual Role of Eugenol in Inhibiting Advanced Glycation End Products in Diabetes: Proteomic and Mechanistic Insights. *Scientific Reports* **2016**, *6*, 18798.
22. Roghani, D. F.; Roghani, M., Mechanisms underlying sesamol-induced attenuation of vascular dysfunction in rats with streptozotocin-induced diabetes. *International Journal of Endocrinology and Metabolism* **2011**, *9*, 311-316.
23. Hong, L.; Yi, W.; Liangliang, C.; Juncheng, H.; Qin, W.; Xiaoxiang, Z., Hypoglycaemic and hypolipidaemic activities of sesamin from sesame meal and its ability to ameliorate insulin resistance in KK-Ay mice. *Journal of the Science of Food and Agriculture* **2013**, *93*, 1833-1838.
24. Wikul, A.; Damsud, T.; Kataoka, K.; Phuwapraisirisan, P., (+)-Pinoresinol is a putative hypoglycemic agent in defatted sesame (*Sesamum indicum*) seeds though inhibiting α -glucosidase. *Bioorganic & Medicinal Chemistry Letters* **2012**, *22*, 5215-5217.
25. Worawalai, W.; Khongchai, P.; Surachaitanawat, N.; Phuwapraisirisan, P., Synthesis of furofuran lignans as antidiabetic agents simultaneously achieved by inhibiting α -glucosidase and free radical. *Archives of Pharmacal Research* **2016**, *39*, 1370-1381.
26. Peñalvo, J. L.; Heinonen, S. M.; Aura, A. M.; Adlercreutz, H., Dietary sesamin is converted to enterolactone in humans. *Journal of Nutrition* **2005**, *135*, 1056-1062.
27. Liu, Z.; Saarinen, N. M.; Thompson, L. U., Sesamin is one of the major precursors of mammalian lignans in sesame seed (*Sesamum indicum*) as observed *in vitro* and in rats. *Journal of Nutrition* **2006**, *136*, 906-912.
28. Brown, R. C. D.; Bataille, C. J.; Hinks, J. D., Total synthesis of (\pm)-epimagnolin A. *Tetrahedron Letters* **2001**, *42*, 473-475.
29. Pohmakotr, M.; Pinsa, A.; Mophuang, T.; Tuchinda, P.; Prabpai, S.; Kongsaree, P.; Reutrakul, V., General strategy for stereoselective synthesis of 1-substituted exo,endo-2,6-diaryl-3,7-dioxabicyclo[3.3.0]octanes: Total synthesis of (\pm)-gmelinol. *Journal of Organic Chemistry* **2006**, *71*, 386-389.

30. Hull, H. M.; Knight, D. W., Diastereospecific approach to (\pm)-samin and 2,6-diaryl-3,7-dioxabicyclo[3.3.0]octane (furofuran lignans) using the Ireland–Claisen rearrangement of unsaturated oxamacrolides. *Journal of the Chemical Society, Perkin Transactions 1* **1997**, *0*, 857-864.
31. Warra, A.; Suraj, L.; Jega, S., Production of soap from Northern Nigerian sesame (*Sesamum indicum*, L.) seed oil. *Bayero Journal of Pure and Applied Science* **2011**, *4*, 180-183.
32. Urata, H.; Nishioka, Y.; Tobashi, T.; Matsumura, Y.; Tomimori, N.; Ono, Y.; Kiso, Y.; Wada, S.-i., First chemical synthesis of antioxidative metabolites of sesamin. *Chemical and Pharmaceutical Bulletin* **2008**, *56*, 1611-1612.
33. Horikawa, M., One-pot preparation of catechol group-introduced dioxabicyclo[3.3.0]octanes. JP2009143884, 2009.
34. Hemalatha, S., Lignans and tocopherols in Indian sesame cultivars. *Journal of the American Oil Chemists' Society* **2004**, *81*, 467-470.
35. Zhang, F.; Chu, C. H.; Xu, Q.; Fu, S. P.; Hu, J. H.; Xiao, H. B.; Liang, X. M., A new amide from *Asarum forbesii* Maxim. *Journal of Asian Natural Products Research* **2005**, *7*, 1-5.
36. Quiroz, M. A.; Reyna, S.; Martínez-Huitle, C. A.; Ferro, S.; De Battisti, A., Electrocatalytic oxidation of p-nitrophenol from aqueous solutions at Pb/PbO₂ anodes. *Applied Catalysis B: Environmental* **2005**, *59*, 259-266.
37. Bensalah, N.; Abdellatif, G.; Cañizares, P.; Saez, C.; Lobato, J.; Rodrigo, M., Electrochemical oxidation of hydroquinone, resorcinol, and catechol on boron-doped diamond anodes. *Environmental Science & Technology* **2005**, *39*, 7234-7239.
38. Wang, B.; Sun, H.-X.; Sun, Z.-H., LiOAc-catalyzed chemoselective deprotection of aryl silyl ethers under mild conditions. *The Journal of Organic Chemistry* **2009**, *74*, 1781-1784.
39. Zhang, B. W.; Li, X.; Sun, W. L.; Xing, Y.; Xiu, Z. L.; Zhuang, C. L.; Dong, Y. S., Dietary flavonoids and acarbose synergistically inhibit α -glucosidase and lower postprandial blood glucose. *Journal of Agricultural and Food Chemistry* **2017**, *65*, 8319-8330.
40. Barham, D.; Trinder, P., An improved colour reagent for the determination of blood glucose by the oxidase system. *Analyst* **1972**, *97*, 142-145.

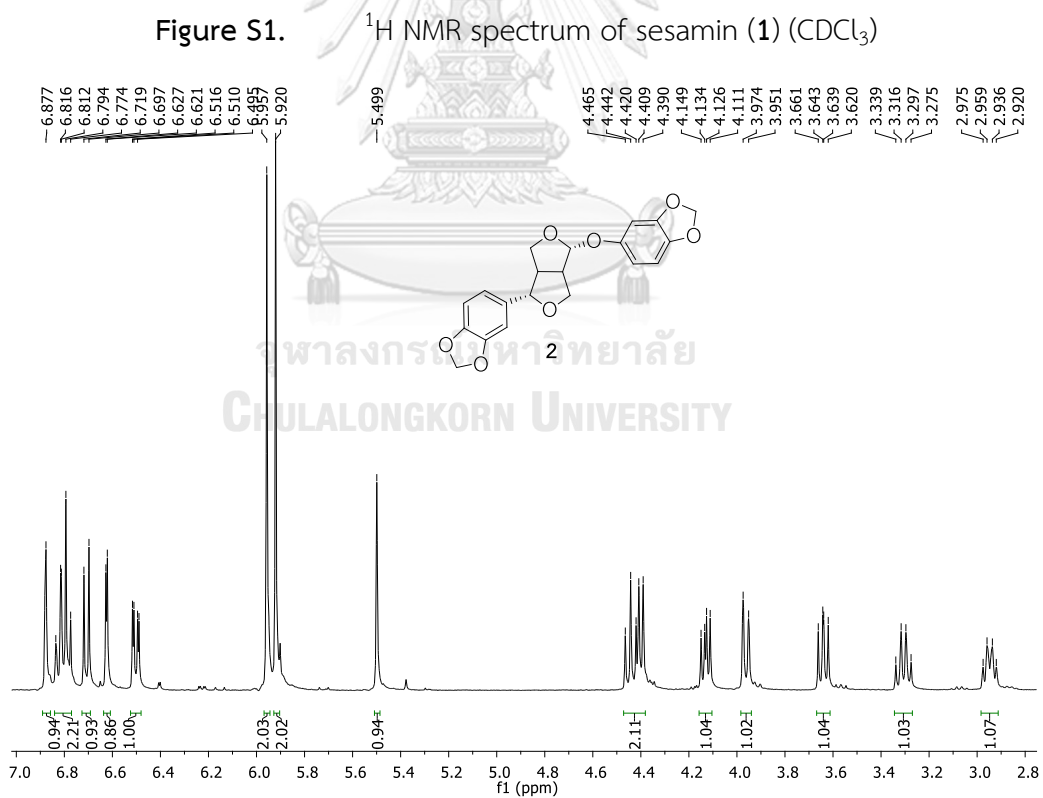
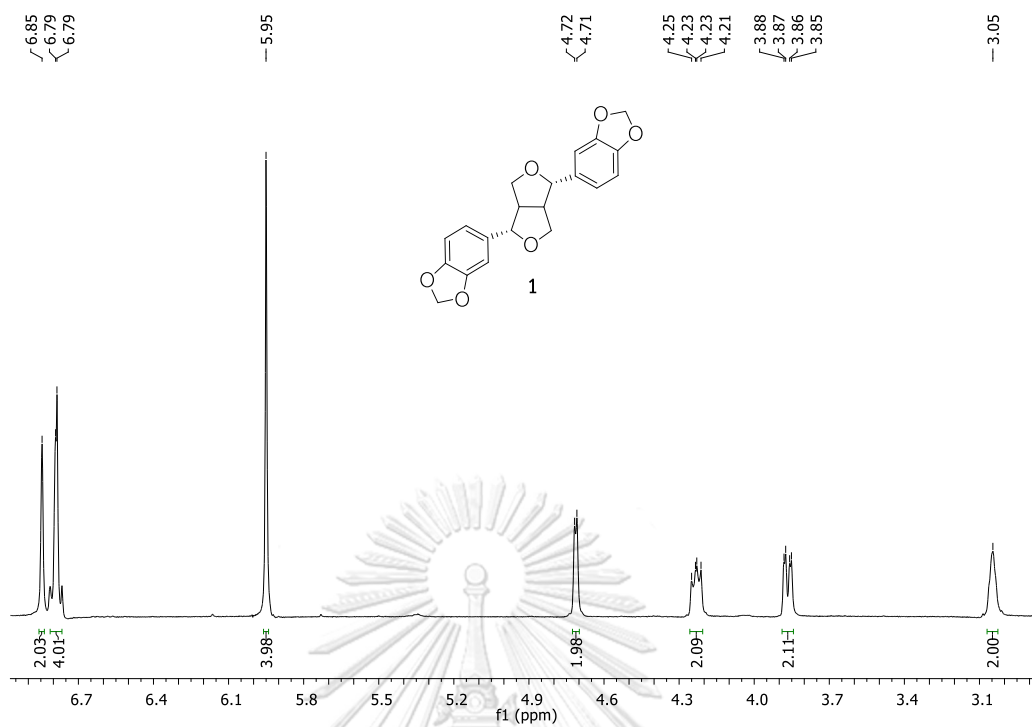
41. Wacharasindhu, S.; Worawalai, W.; Rungprom, W.; Phuwapraisirisan, P., (+)-proto-Quercitol, a natural versatile chiral building block for the synthesis of the α -glucosidase inhibitors, 5-amino-1,2,3,4-cyclohexanetetrols. *Tetrahedron Letters* **2009**, *50*, 2189-2192.
42. Rattanangkool, E.; Kittikhunnatham, P.; Damsud, T.; Wacharasindhu, S.; Phuwapraisirisan, P., Quercitylcinnamates, a new series of antidiabetic bioconjugates possessing α -glucosidase inhibition and antioxidant. *European Journal of Medicinal Chemistry* **2013**, *66*, 296-304.
43. Escandón-Rivera, S.; González-Andrade, M.; Bye, R.; Linares, E.; Navarrete, A.; Mata, R., α -Glucosidase inhibitors from *Brickellia cavanillesii*. *Journal of Natural Products* **2012**, *75*, 968-974.





APPENDIX

จุฬาลงกรณ์มหาวิทยาลัย
CHULALONGKORN UNIVERSITY



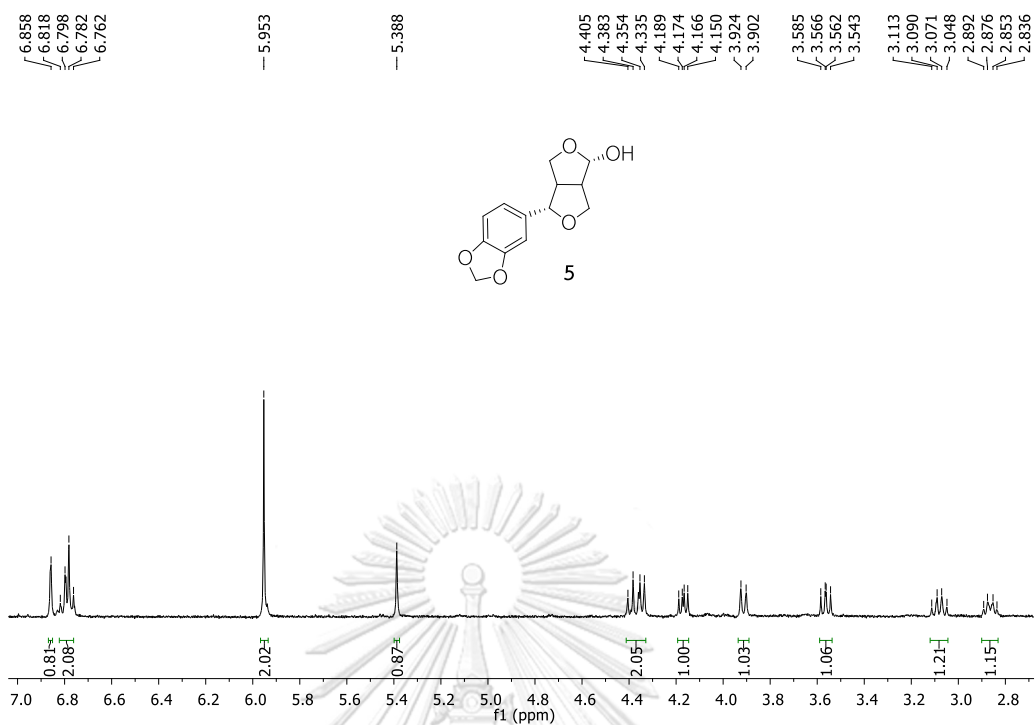


Figure S3. ^1H NMR spectrum of samin (5) (CDCl_3)

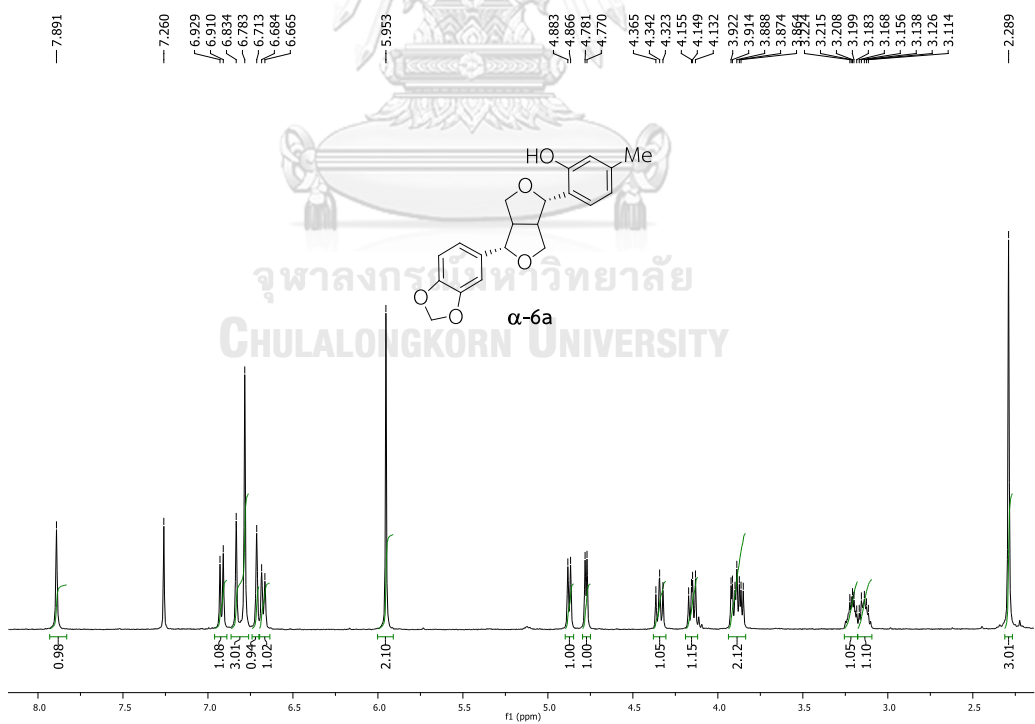


Figure S4. ^1H NMR spectrum of α -6a (CDCl_3)

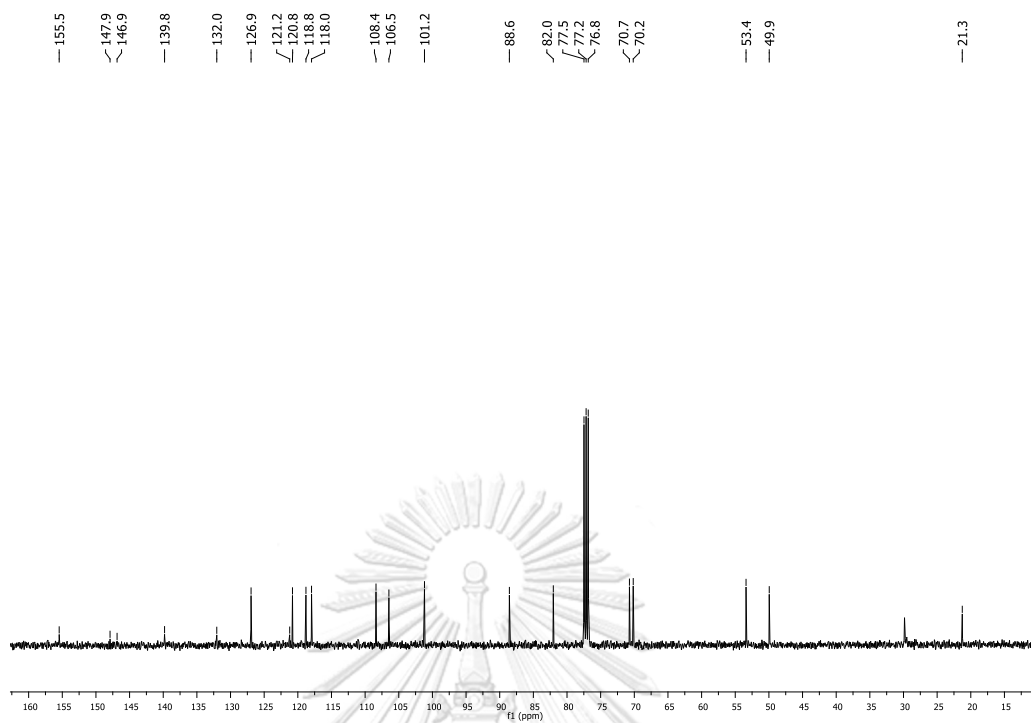


Figure S7. ^{13}C NMR spectrum of $\beta\text{-6a}$ (CDCl_3)

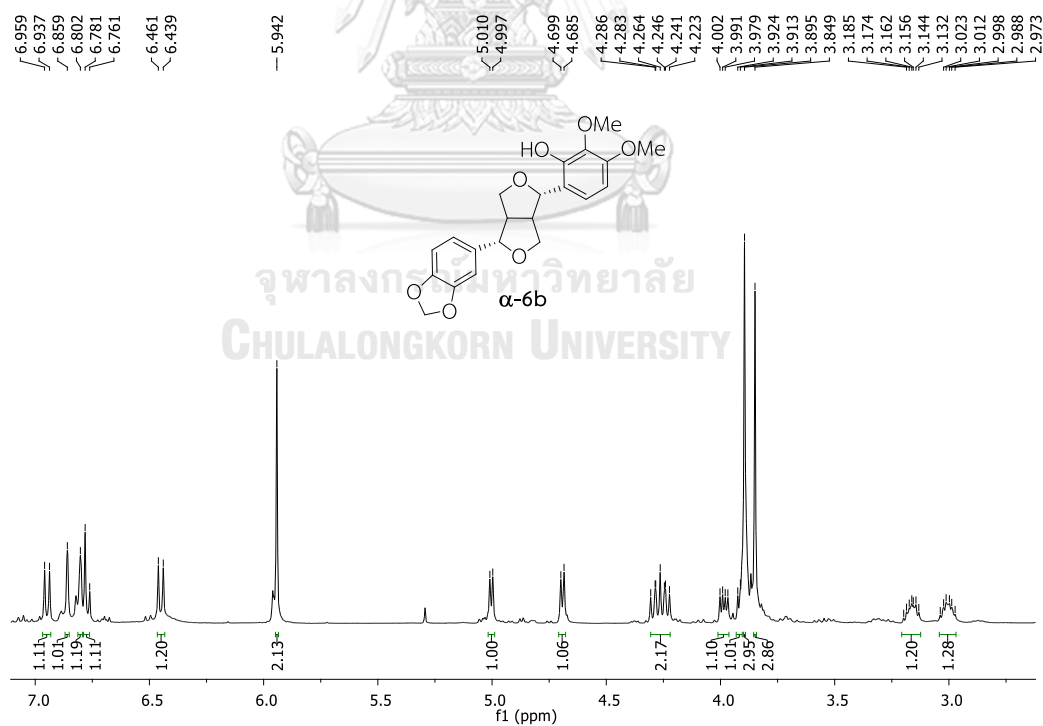


Figure S8. ^1H NMR spectrum of $\alpha\text{-6b}$ (CDCl_3)

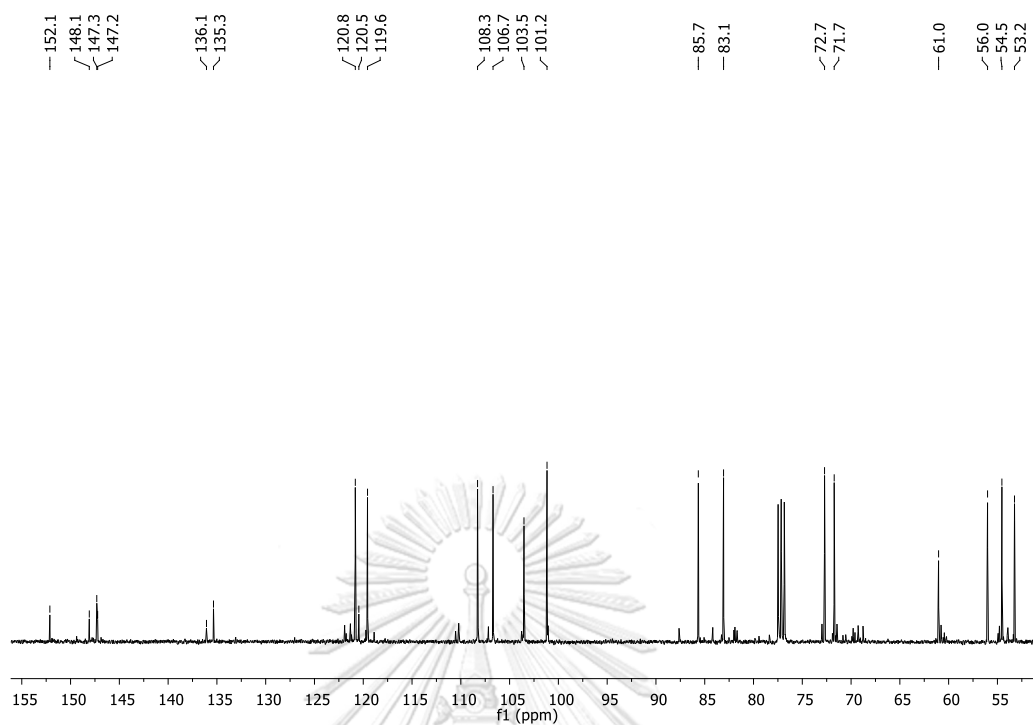


Figure S9. ^{13}C NMR spectrum of $\alpha\text{-6b}$ (CDCl_3)

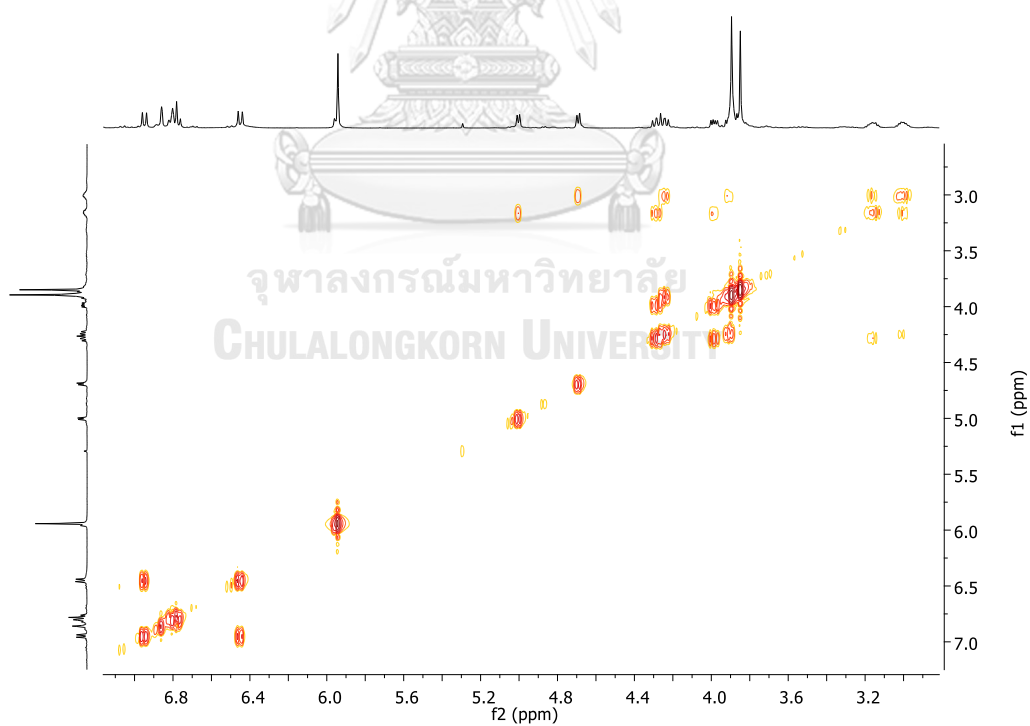


Figure S10. COSY spectrum of $\alpha\text{-6b}$ (CDCl_3)

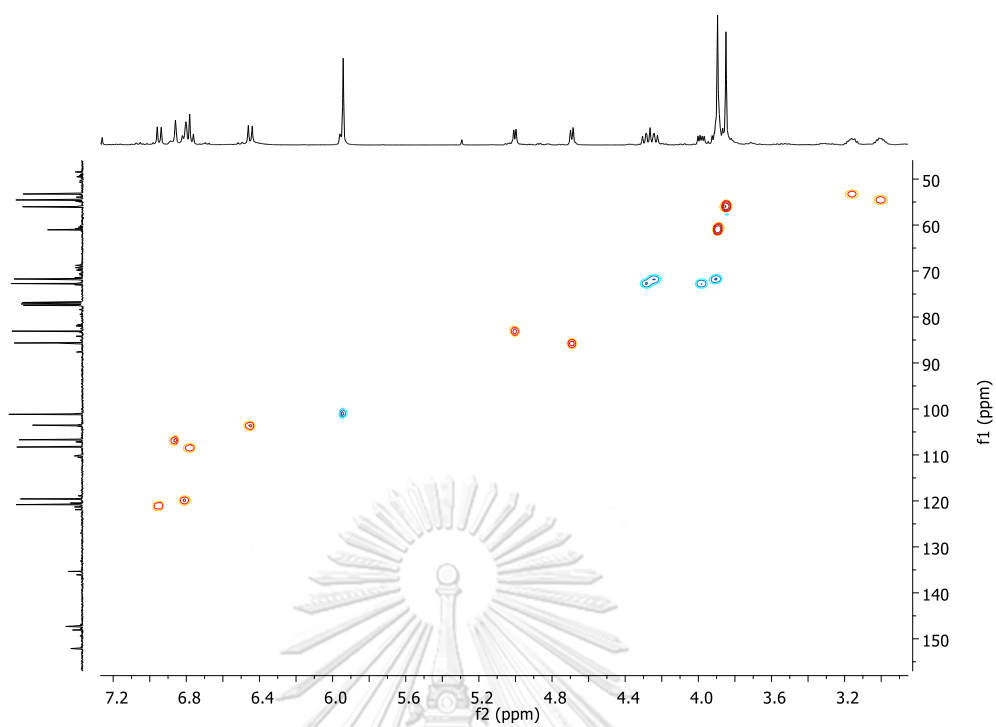


Figure S11. HSQC spectrum of α -6b (CDCl₃)

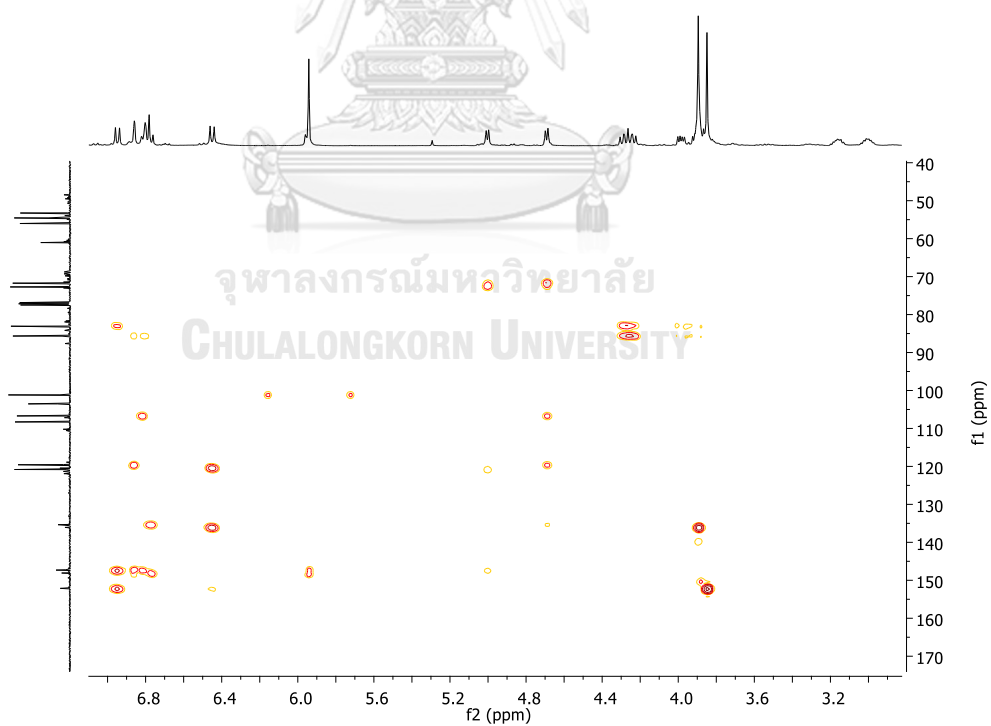


Figure S12. HMBC spectrum of α -6b (CDCl₃)

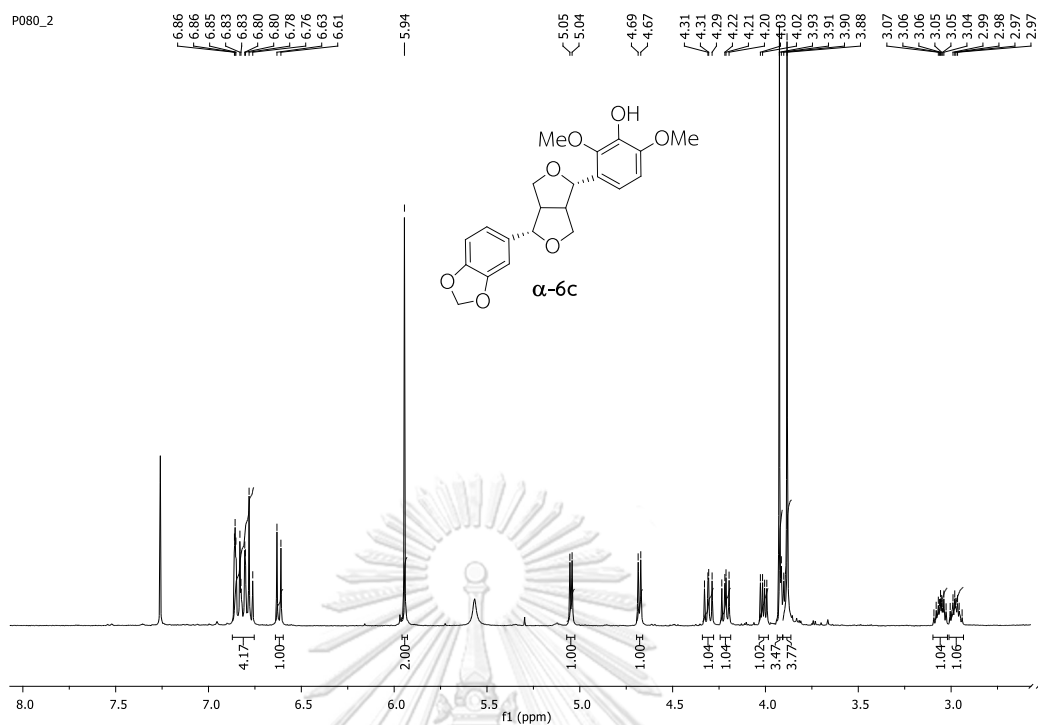


Figure S13. ^1H NMR spectrum of α -6c (CDCl_3)

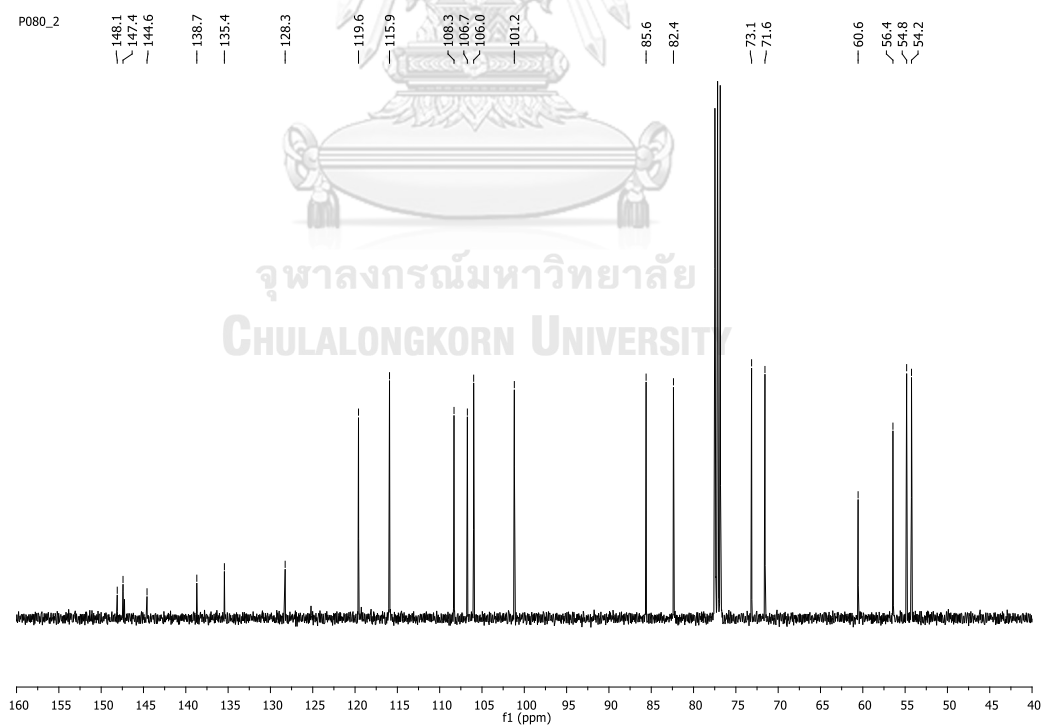


Figure S14. ^{13}C NMR spectrum of α -6c (CDCl_3)

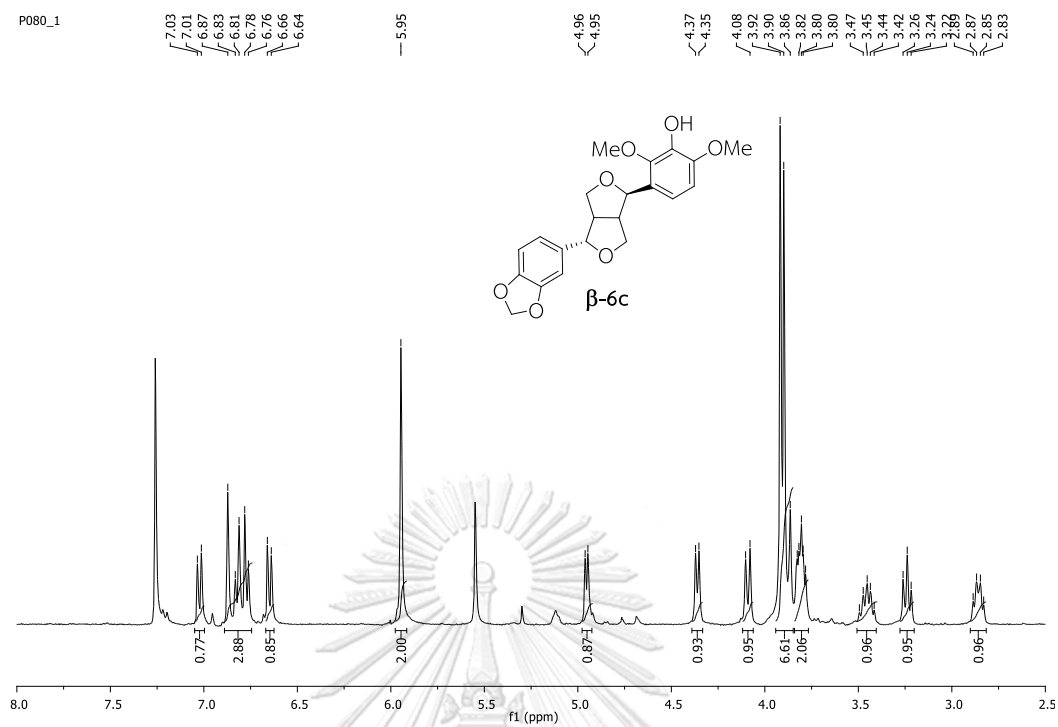


Figure S15. ^1H NMR spectrum of β -6c (CDCl_3)

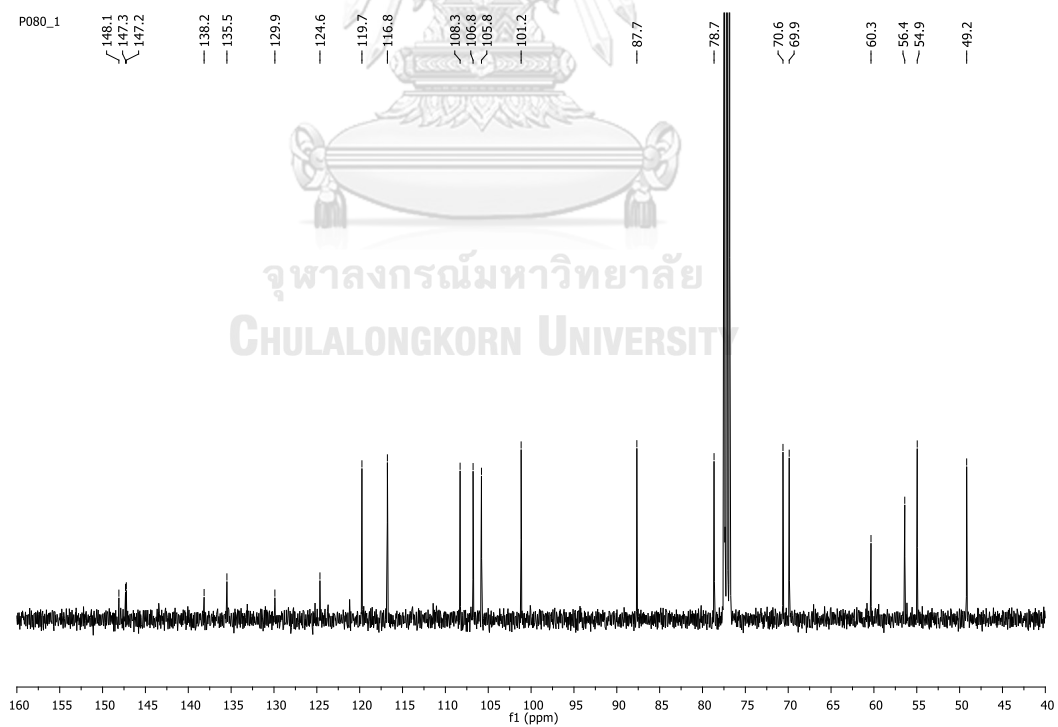


Figure S16. ^{13}C NMR spectrum of β -6c (CDCl_3)

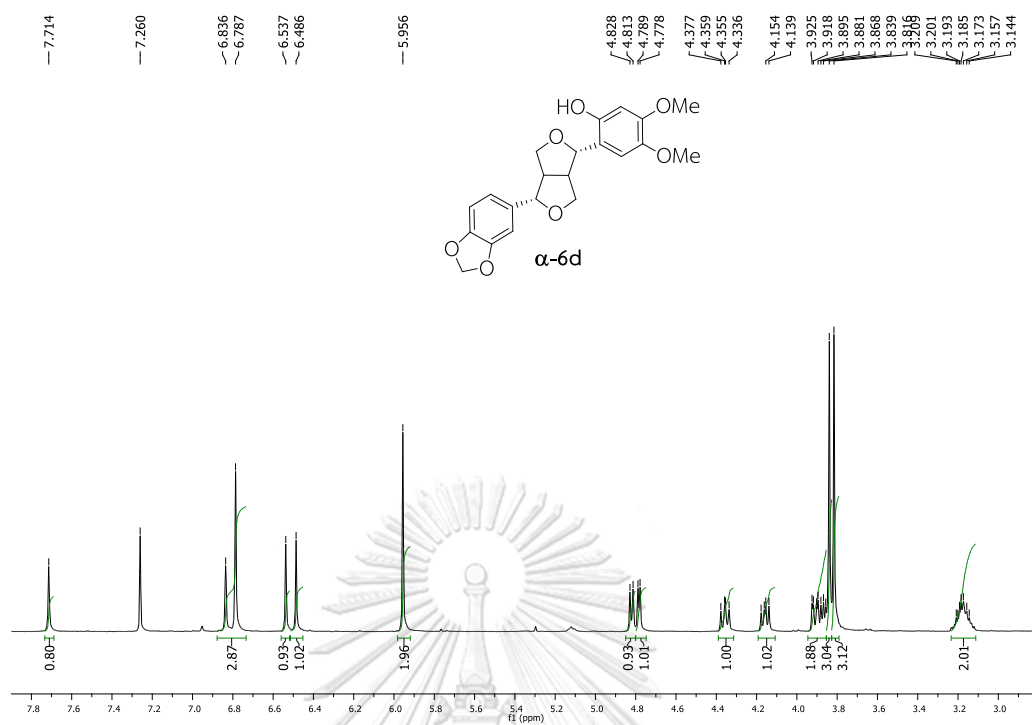


Figure S17. ^1H NMR spectrum of α -6d (CDCl_3)

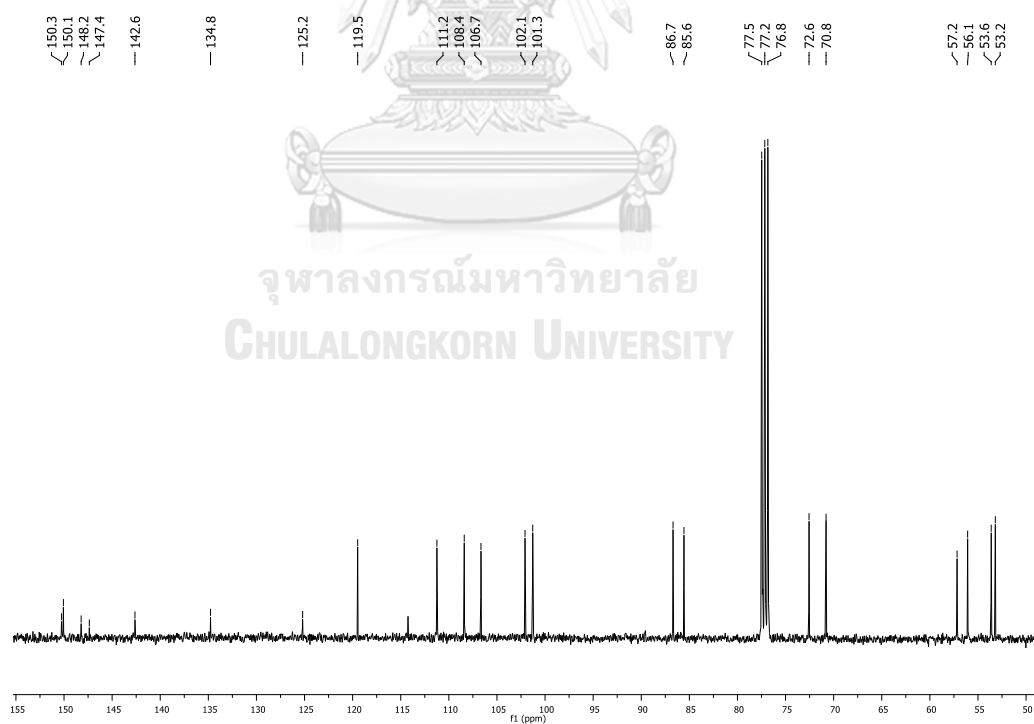


Figure S18. ^{13}C NMR spectrum of α -6d (CDCl_3)

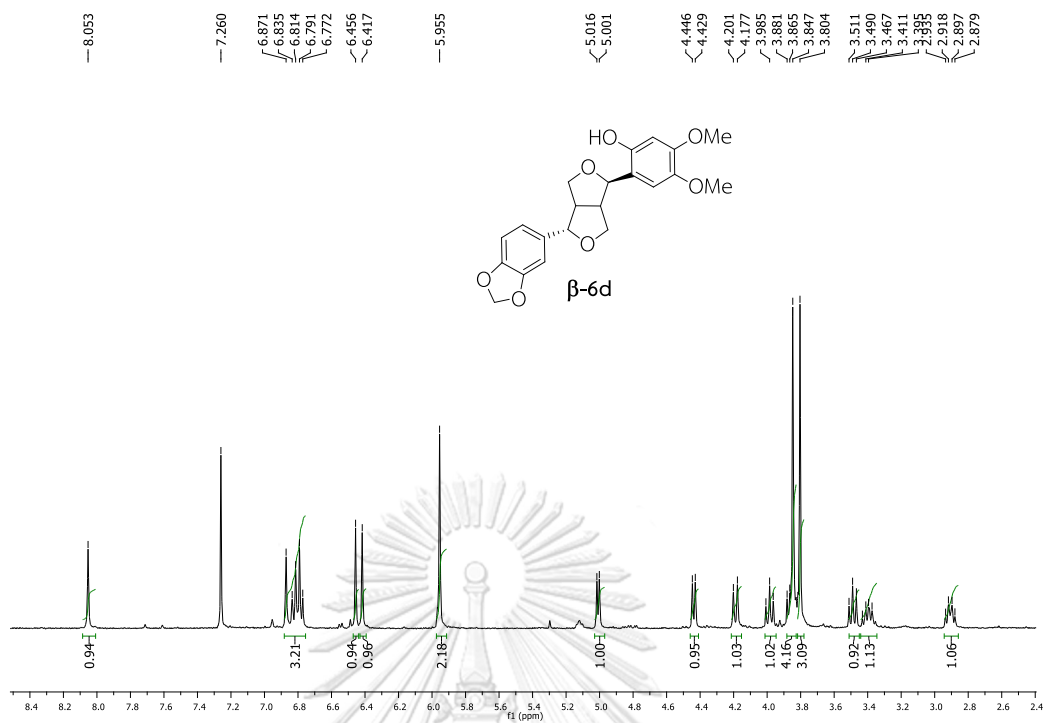


Figure S19. ^1H NMR spectrum of β -6d (CDCl_3)

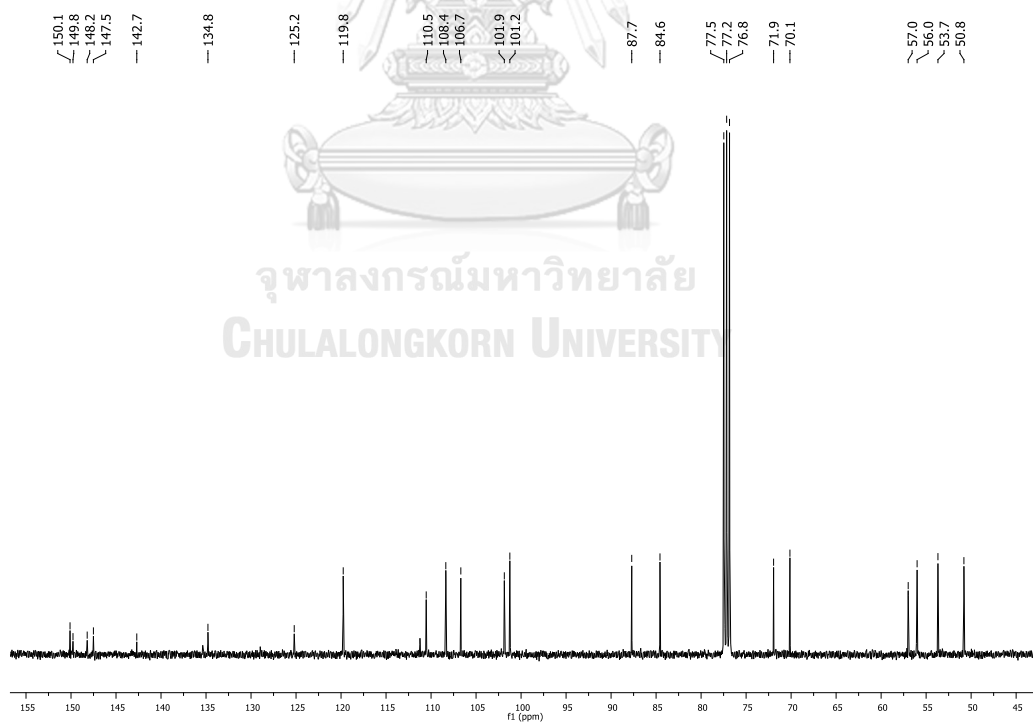


Figure S20. ^{13}C NMR spectrum of β -6d (CDCl_3)

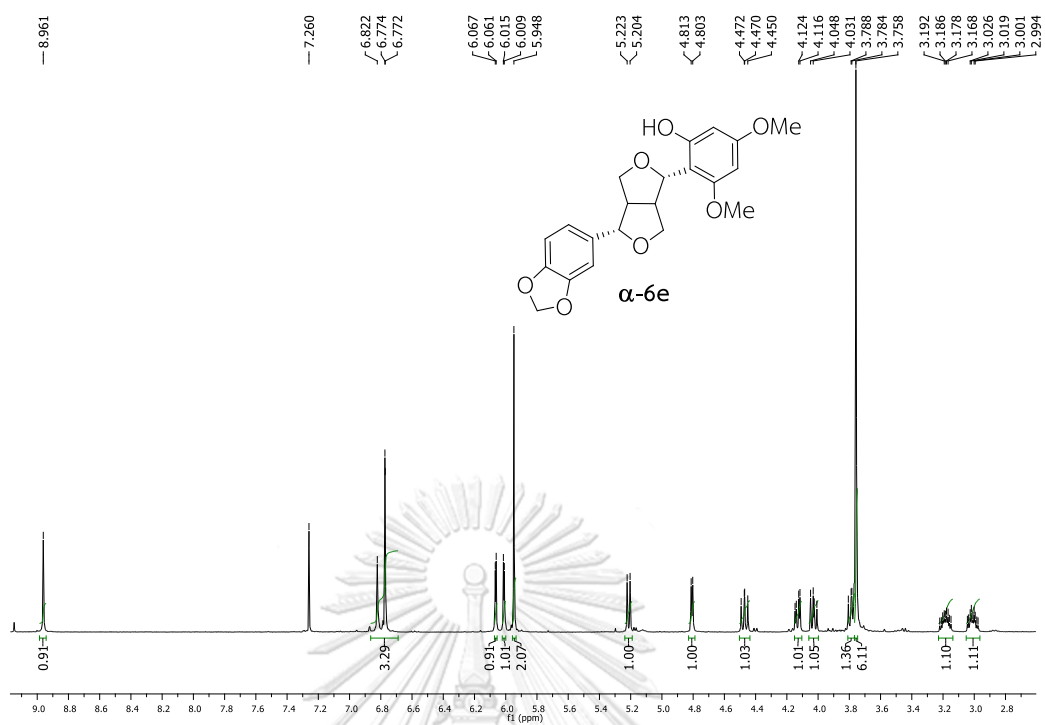


Figure S21. ^1H NMR spectrum of α -6e (CDCl_3)

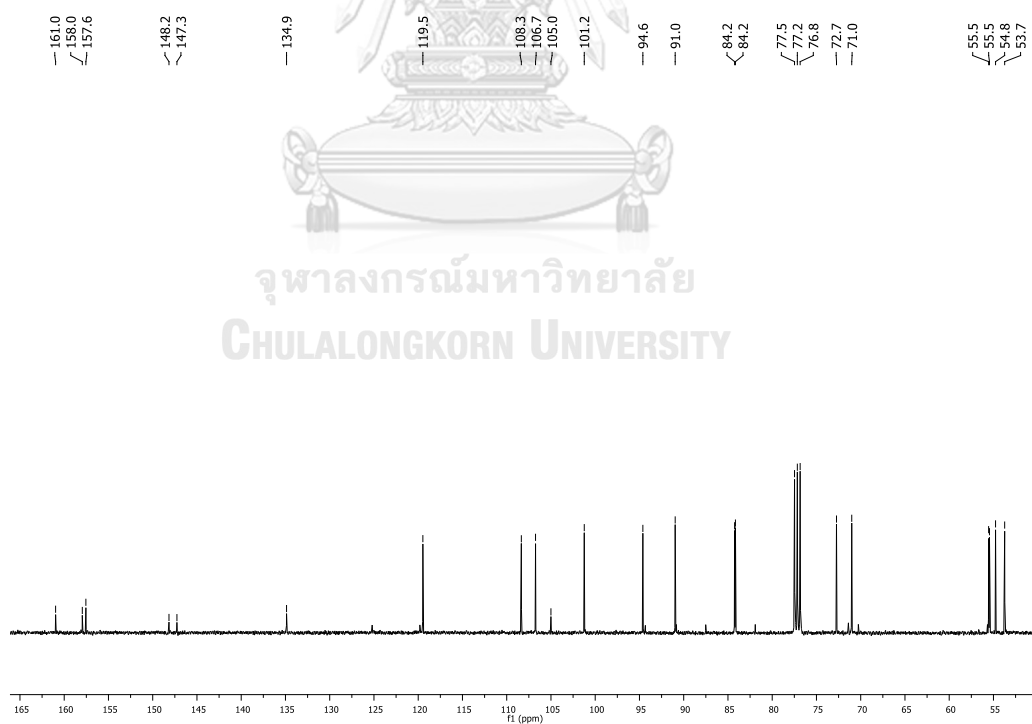


Figure S22. ^{13}C NMR spectrum of α -6e (CDCl_3)

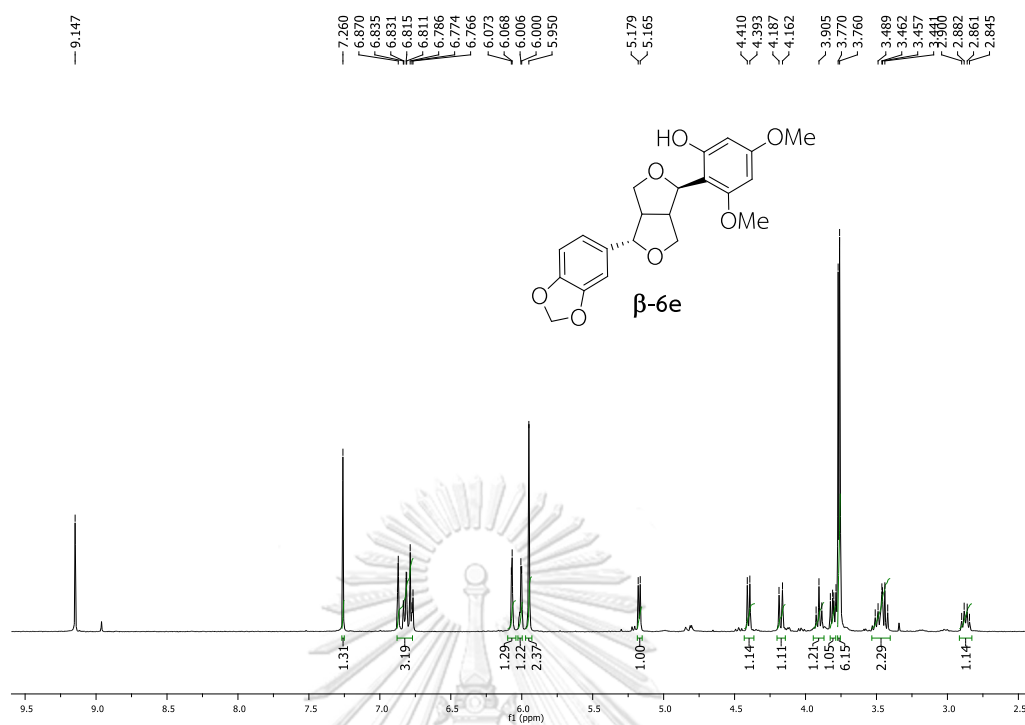


Figure S23. ^1H NMR spectrum of β -6e (CDCl_3)

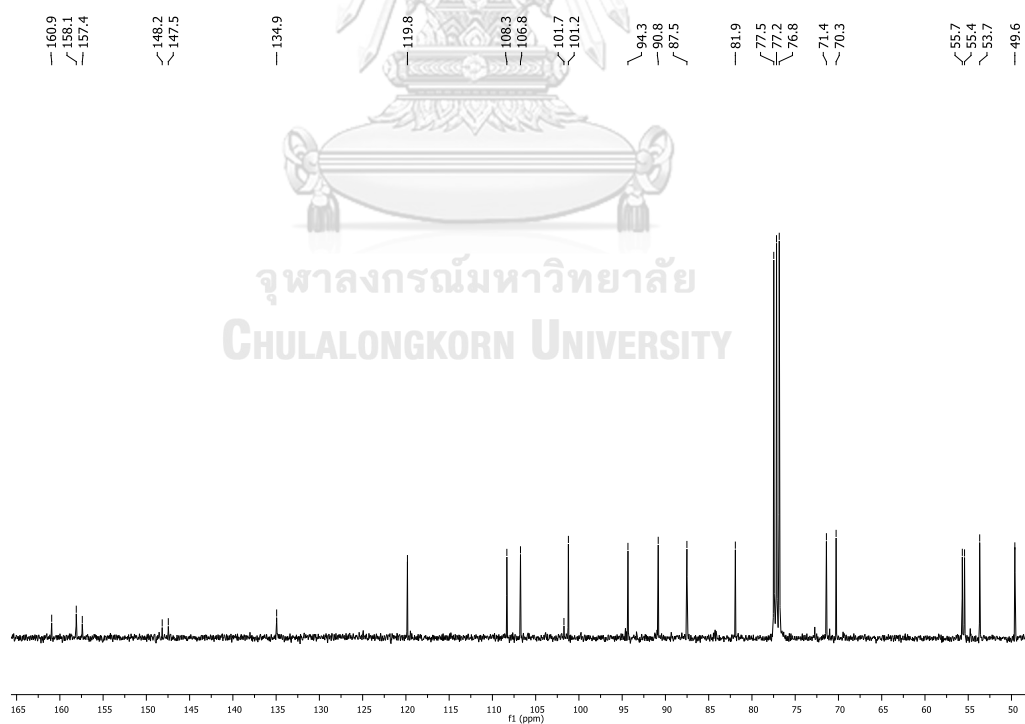


Figure S24. ^{13}C NMR spectrum of β -6e (CDCl_3)

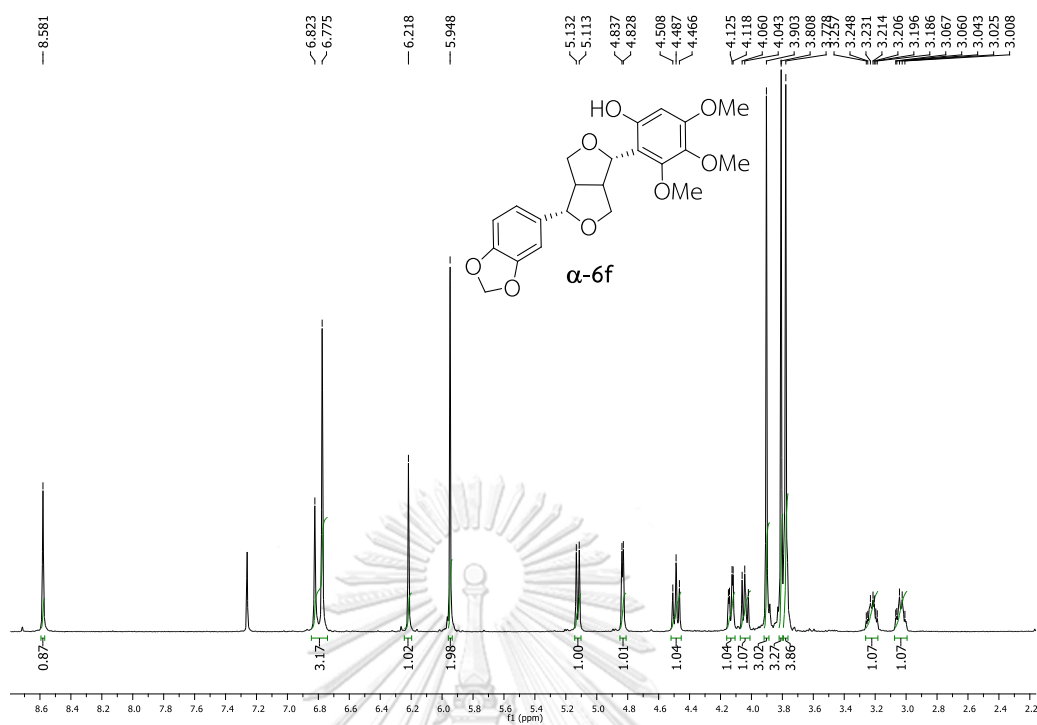


Figure S25. ^1H NMR spectrum of α -6f (CDCl_3)

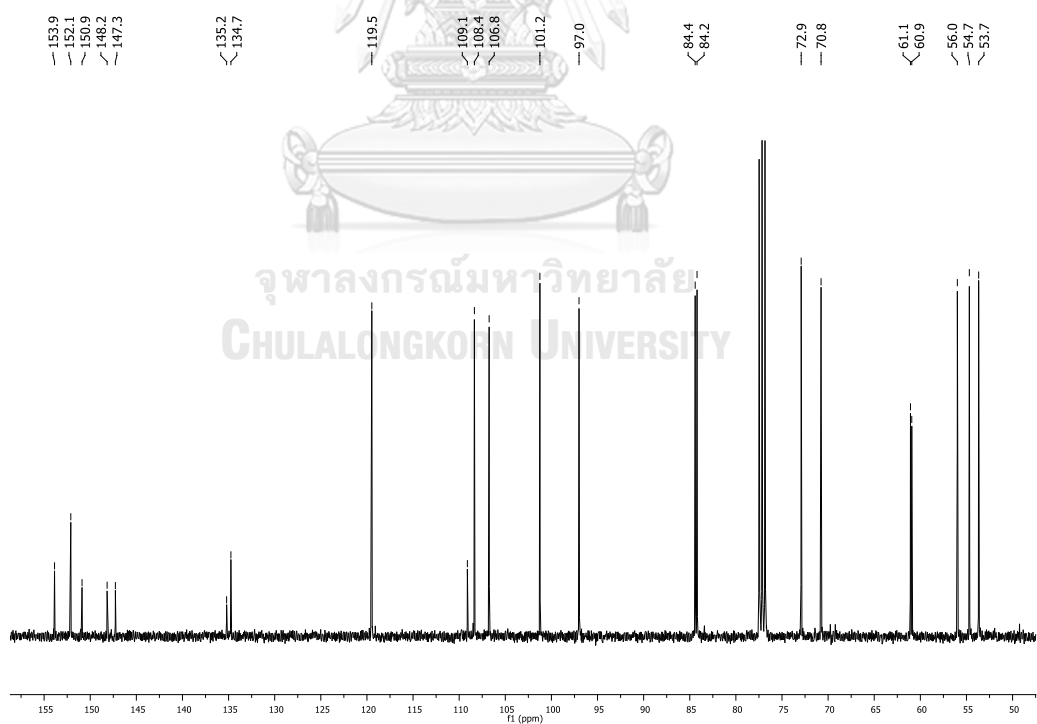


Figure S26. ^{13}C NMR spectrum of α -6f (CDCl_3)

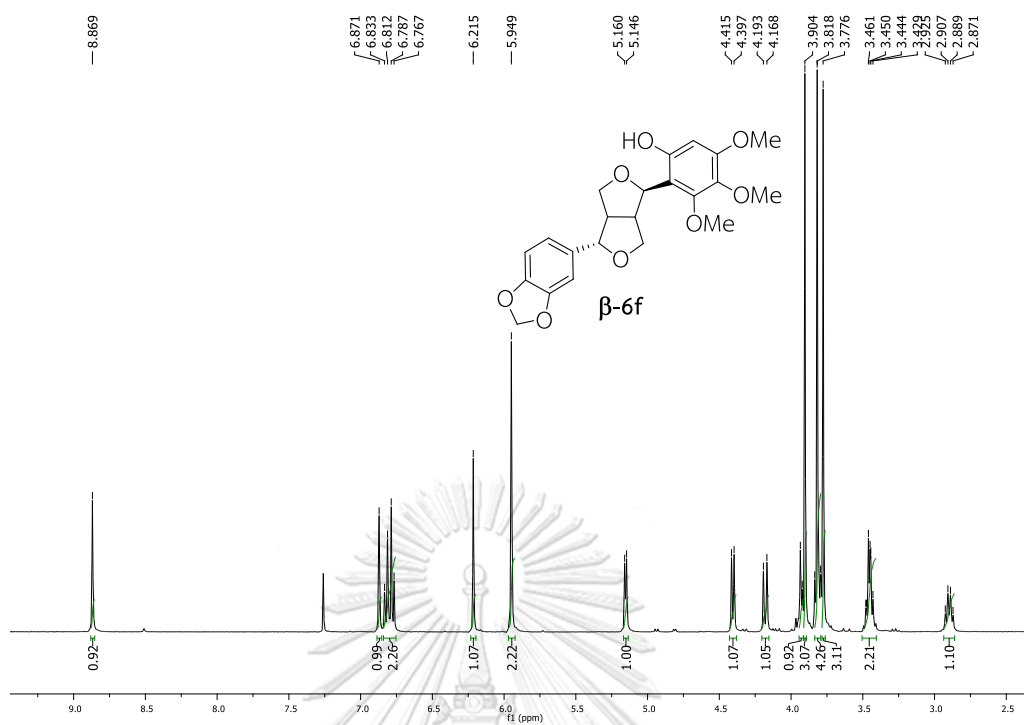


Figure S27. ^1H NMR spectrum of β -6f (CDCl_3)

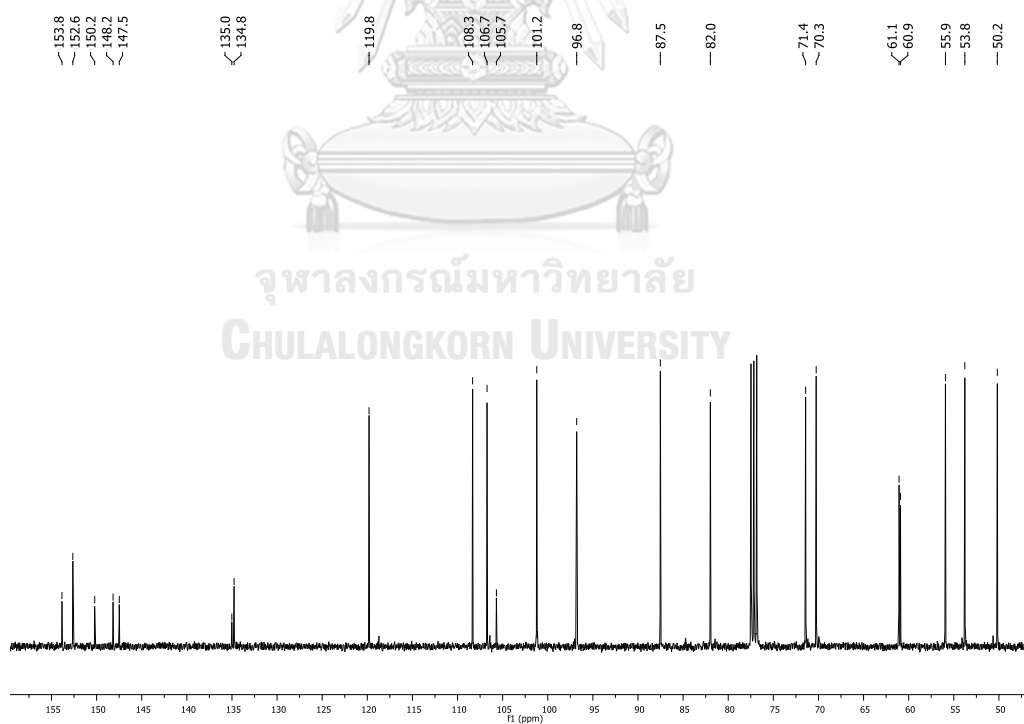


Figure S28. ^{13}C NMR spectrum of β -6f (CDCl_3)

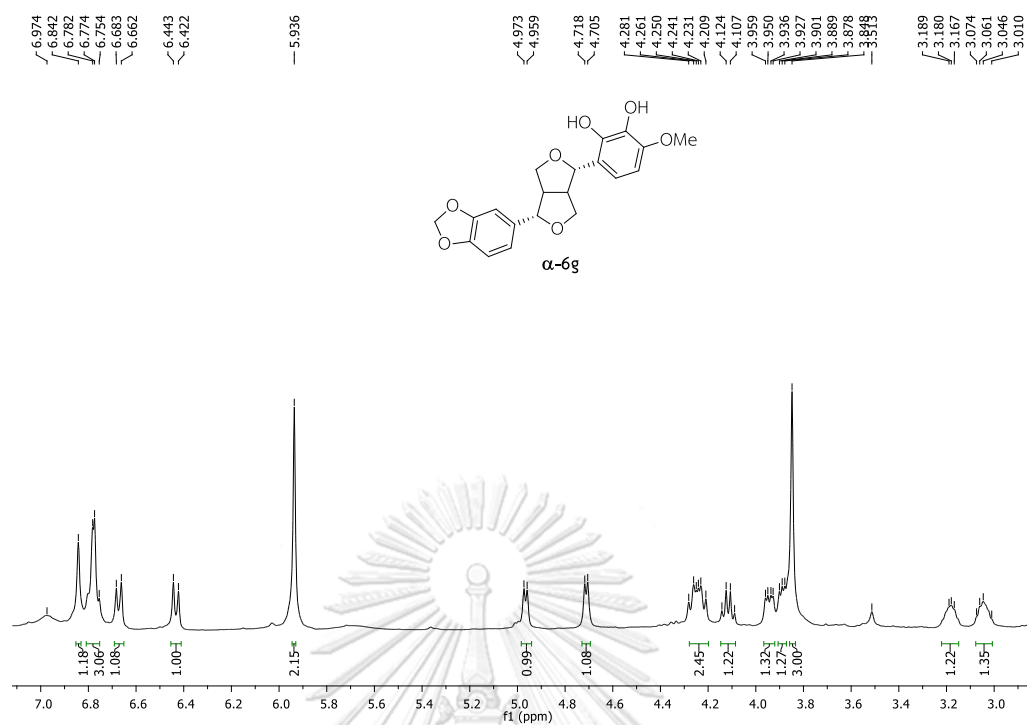


Figure S29. ^1H NMR spectrum of α -6g (CDCl_3)

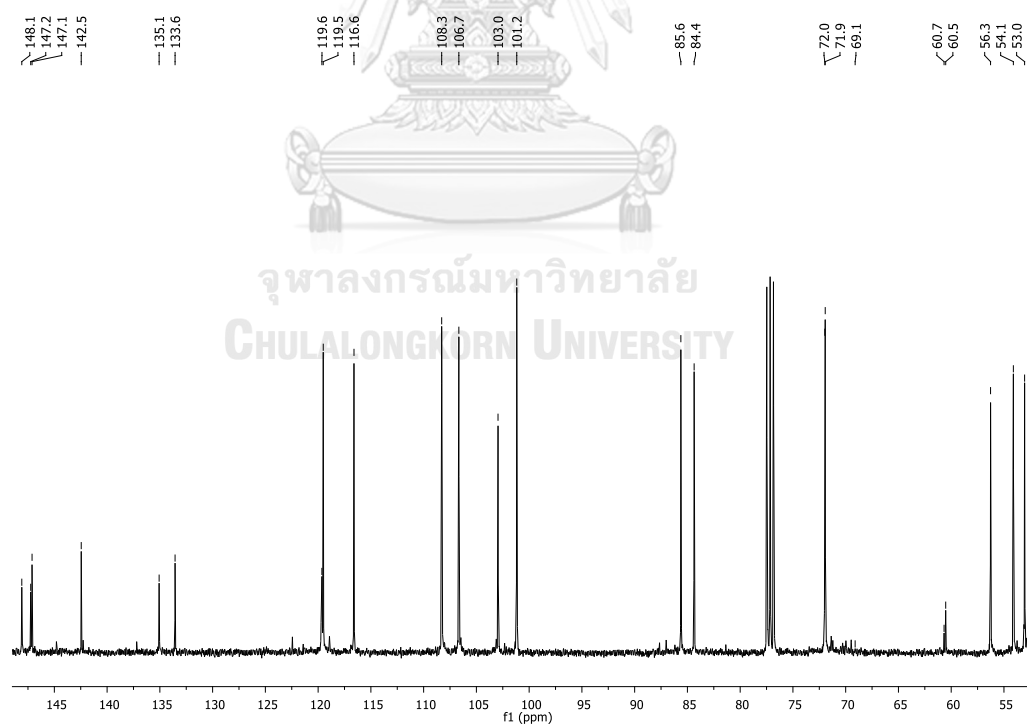


Figure S30. ^{13}C NMR spectrum of α -6g (CDCl_3)

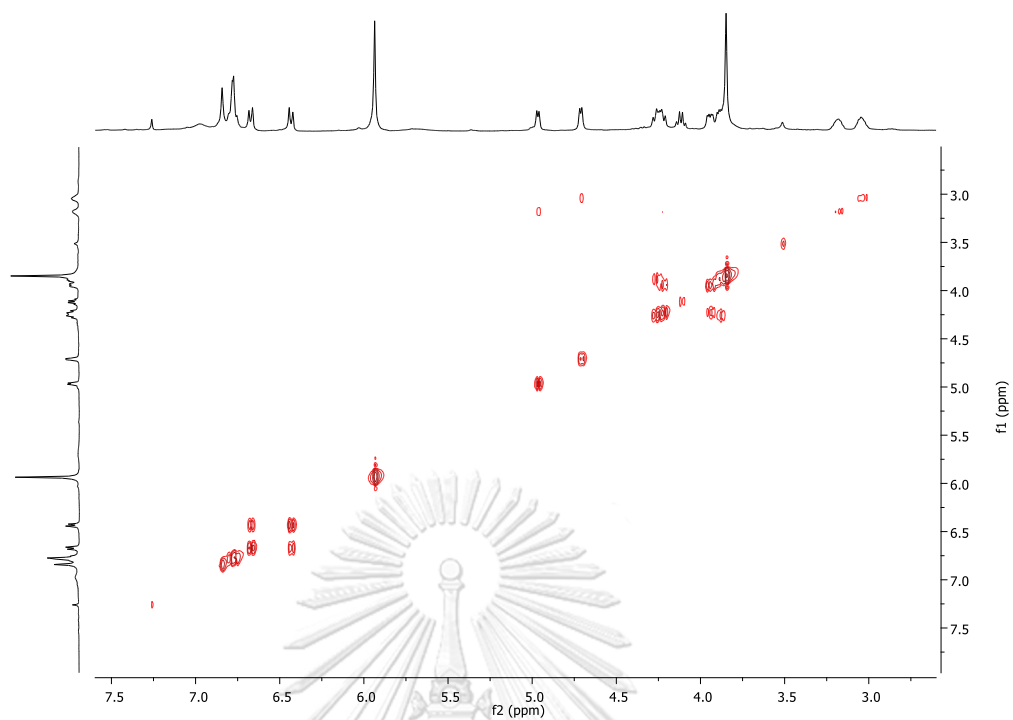


Figure S31. COSY spectrum of α -6g (CDCl_3)

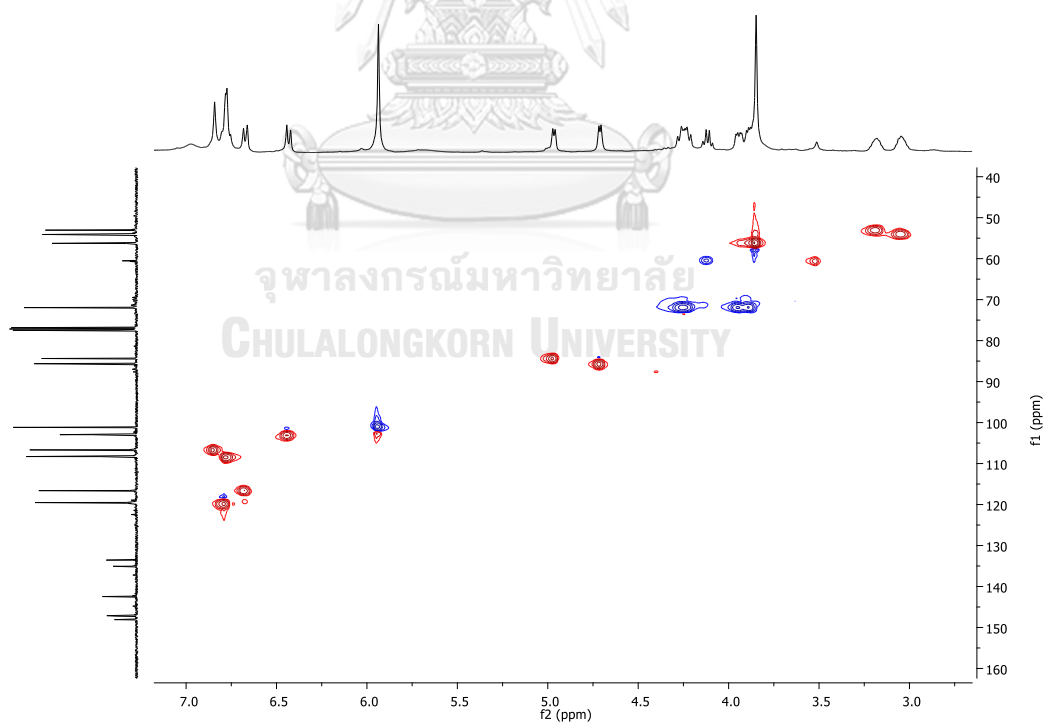


Figure S32. HSQC spectrum of α -6g (CDCl_3)

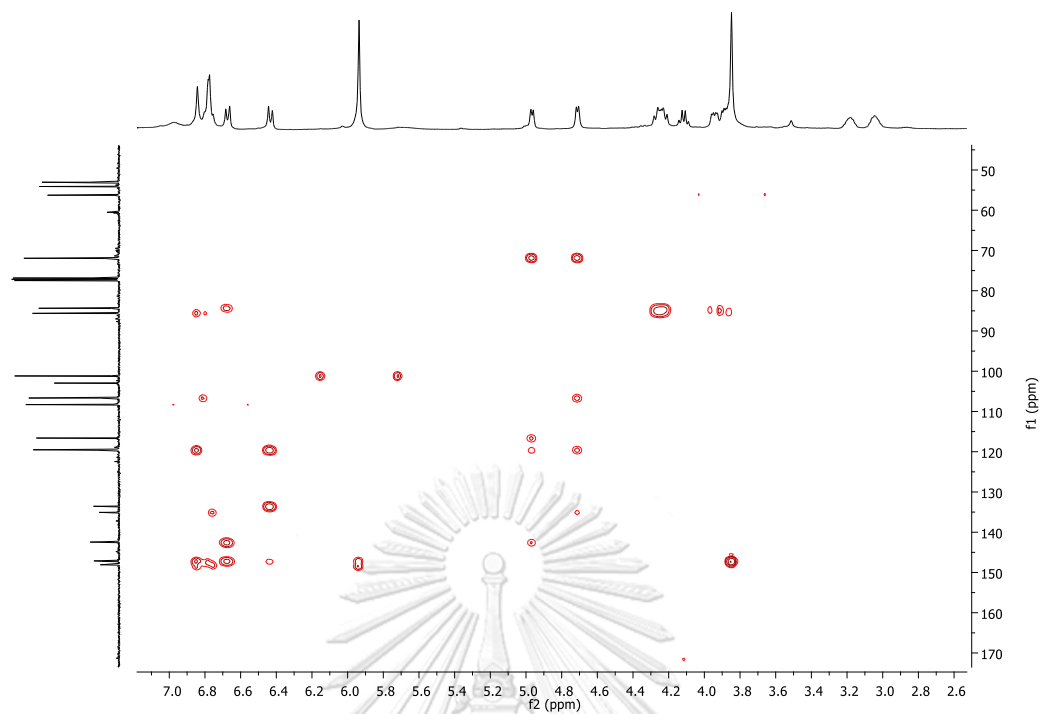


Figure S33. HMBC spectrum of α -6g (CDCl_3)

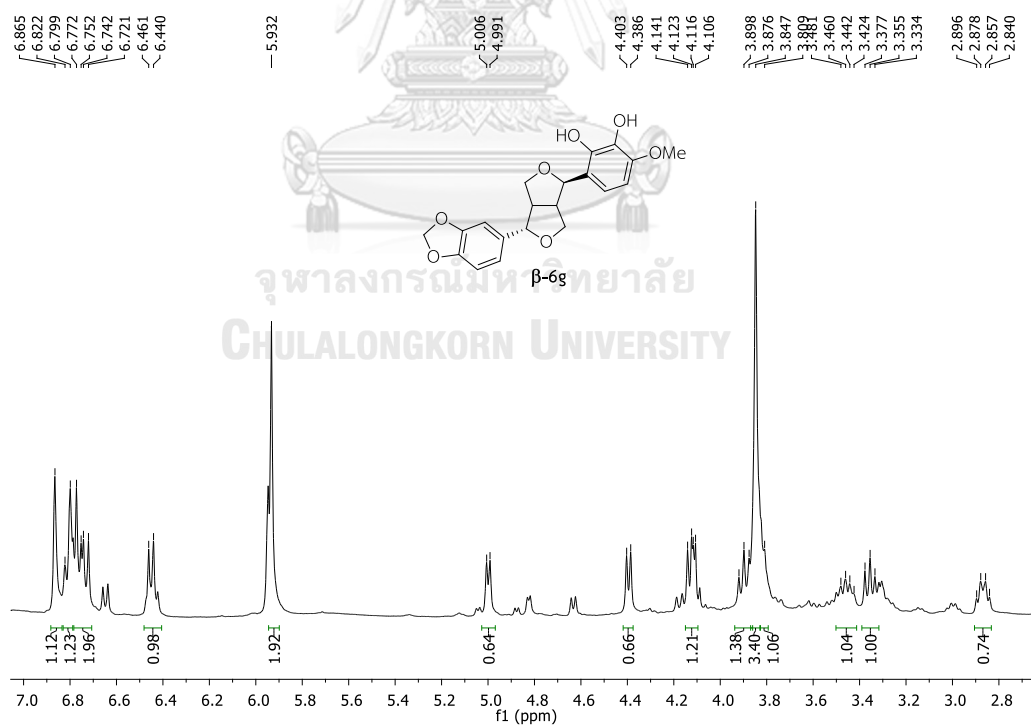


Figure S34. ^1H NMR spectrum of β -6g (CDCl_3)

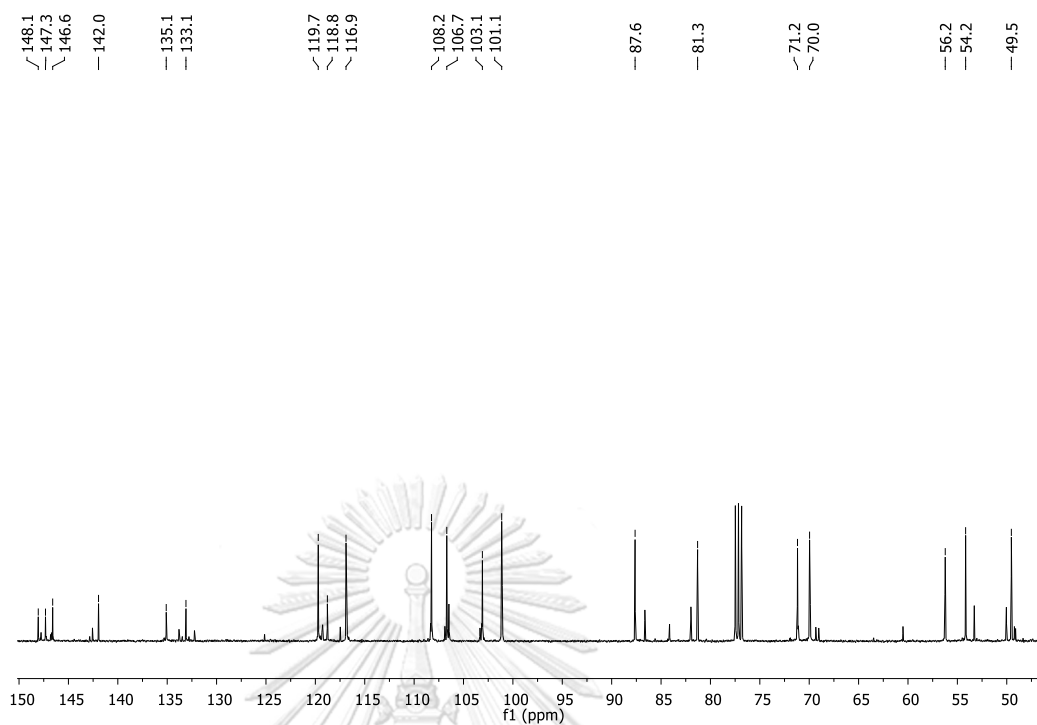


Figure S35. ^{13}C NMR spectrum of β -6g (CDCl_3)

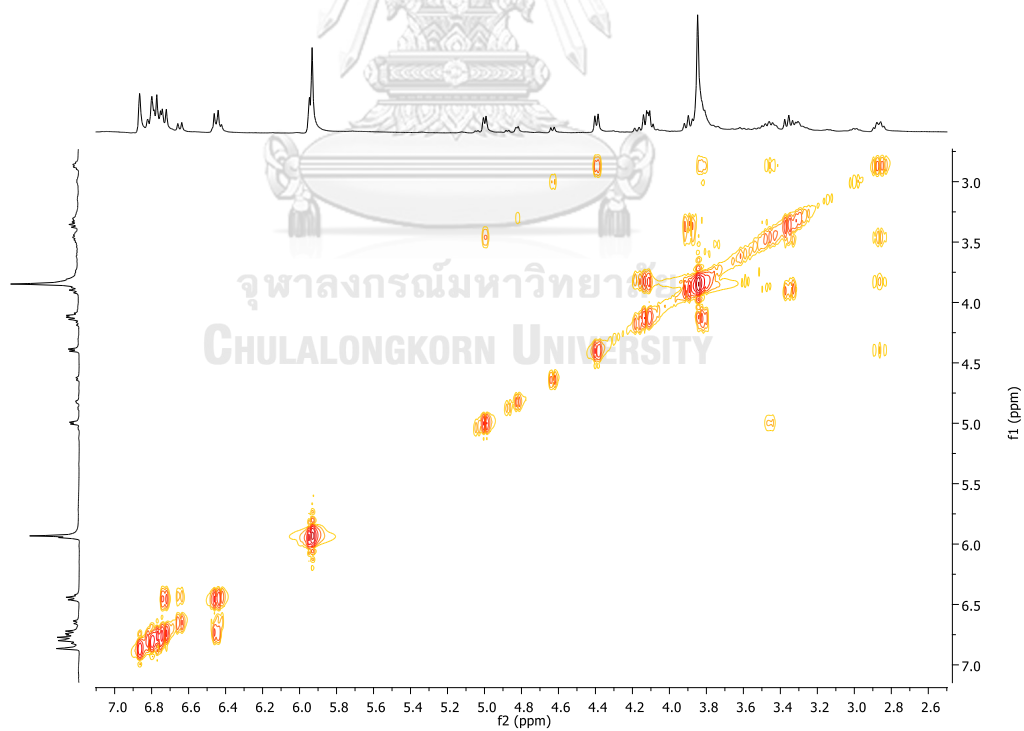


Figure S36. COSY spectrum of β -6g (CDCl_3)

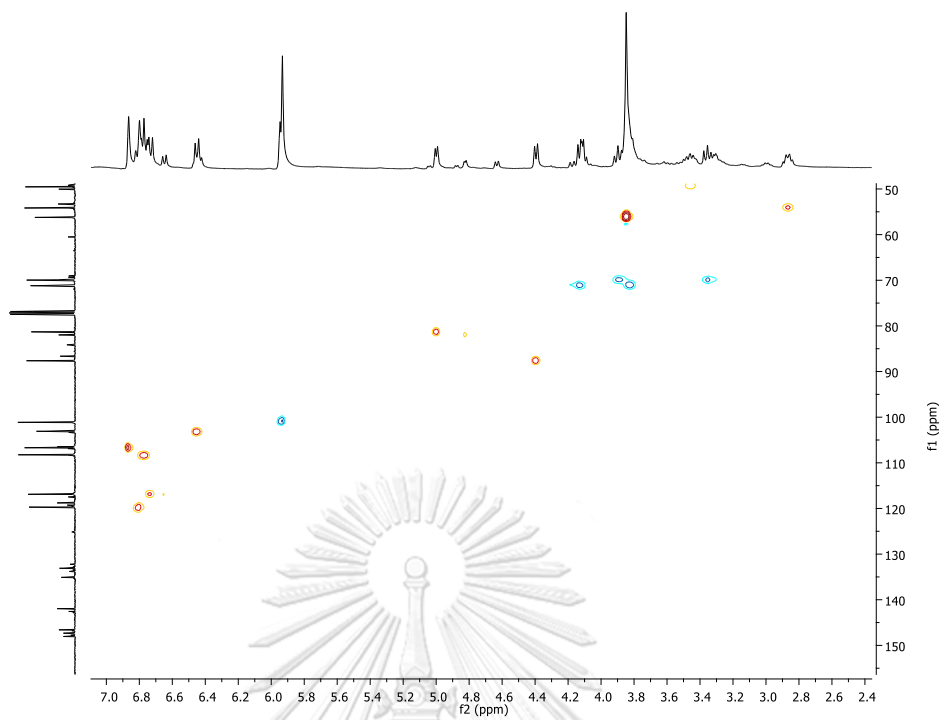


Figure S37. HSQC spectrum of β -6g (CDCl_3)

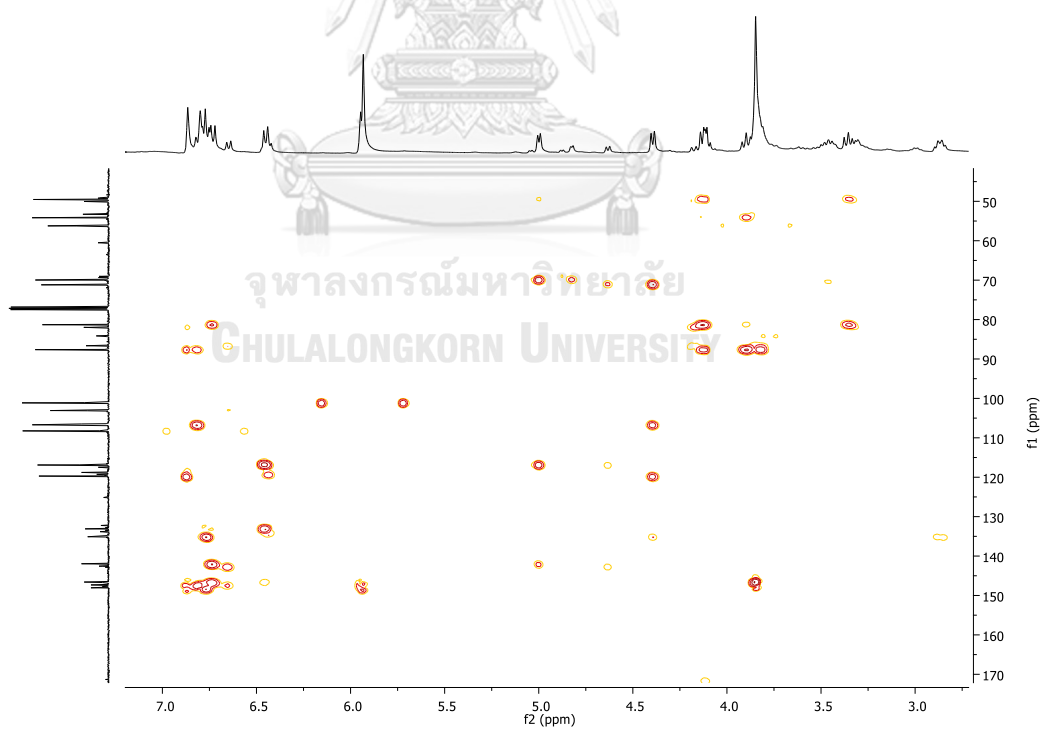
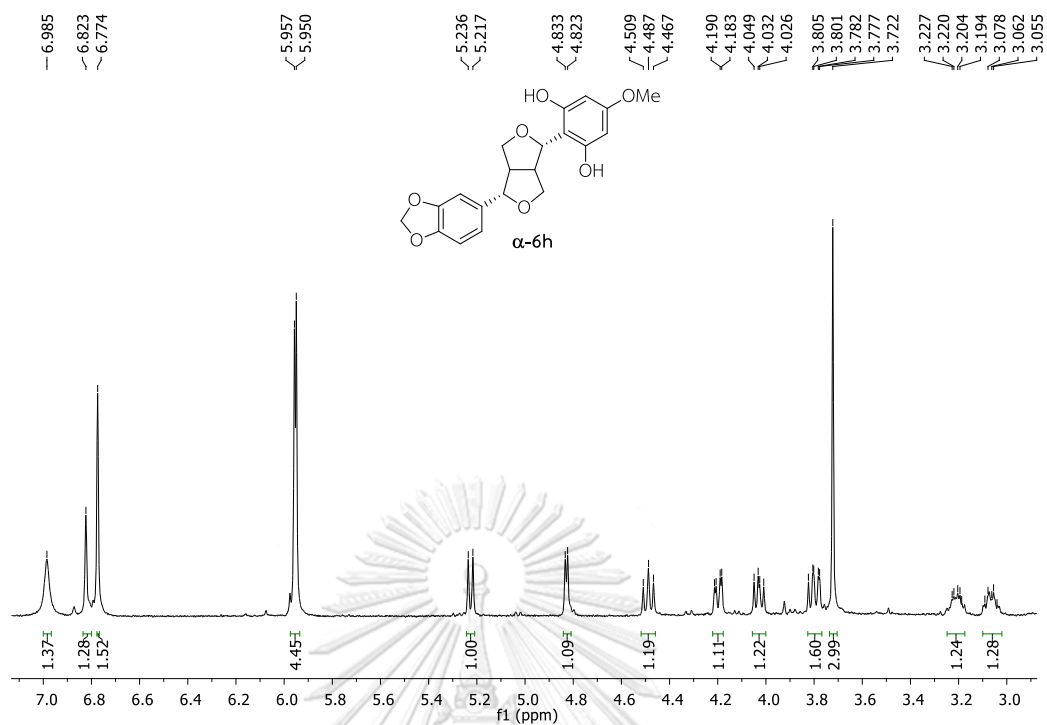
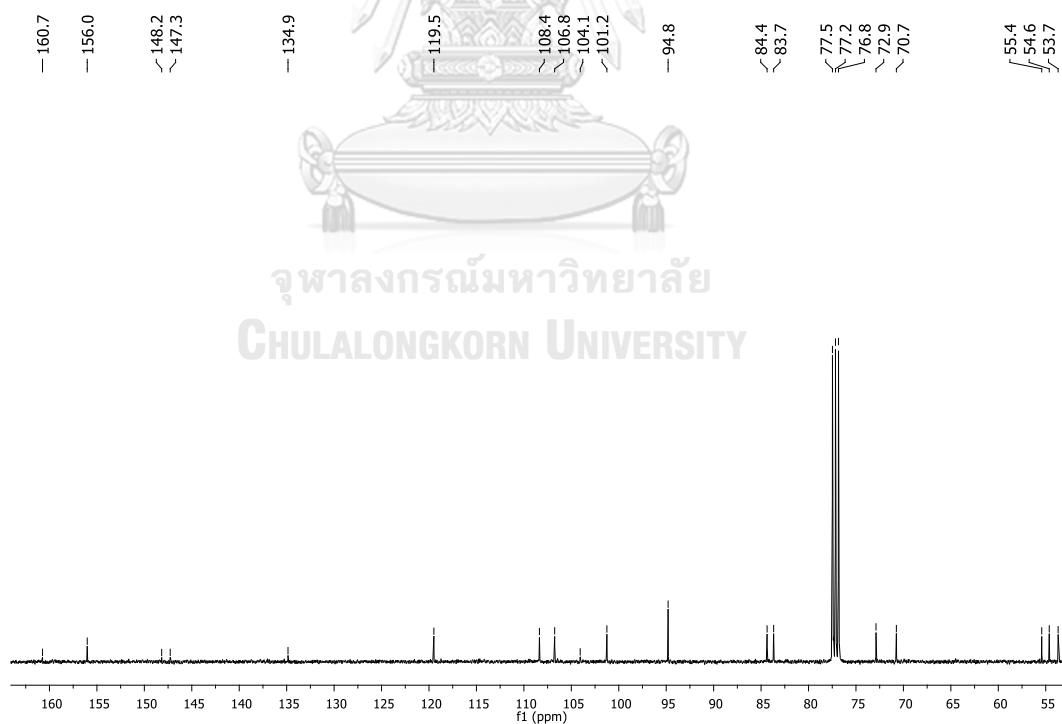


Figure S38. HMBC spectrum of β -6g (CDCl_3)

Figure S39. ^1H NMR spectrum of α -6h (CDCl_3)Figure S40. ^{13}C NMR spectrum of α -6h (CDCl_3)

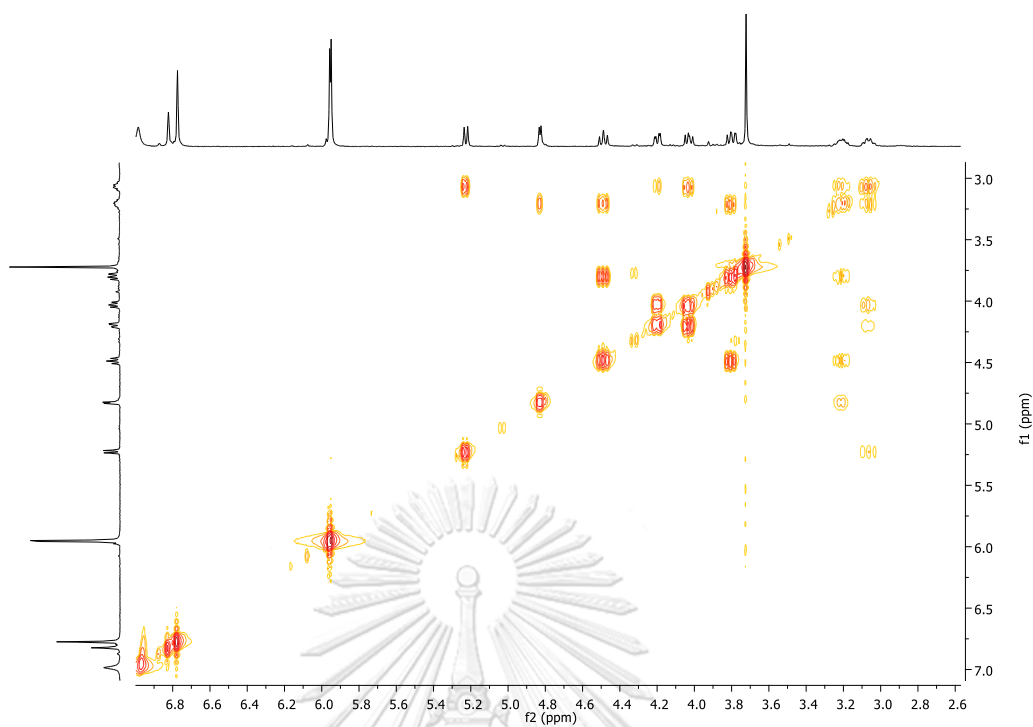


Figure S41. COSY spectrum of α -6h (CDCl_3)

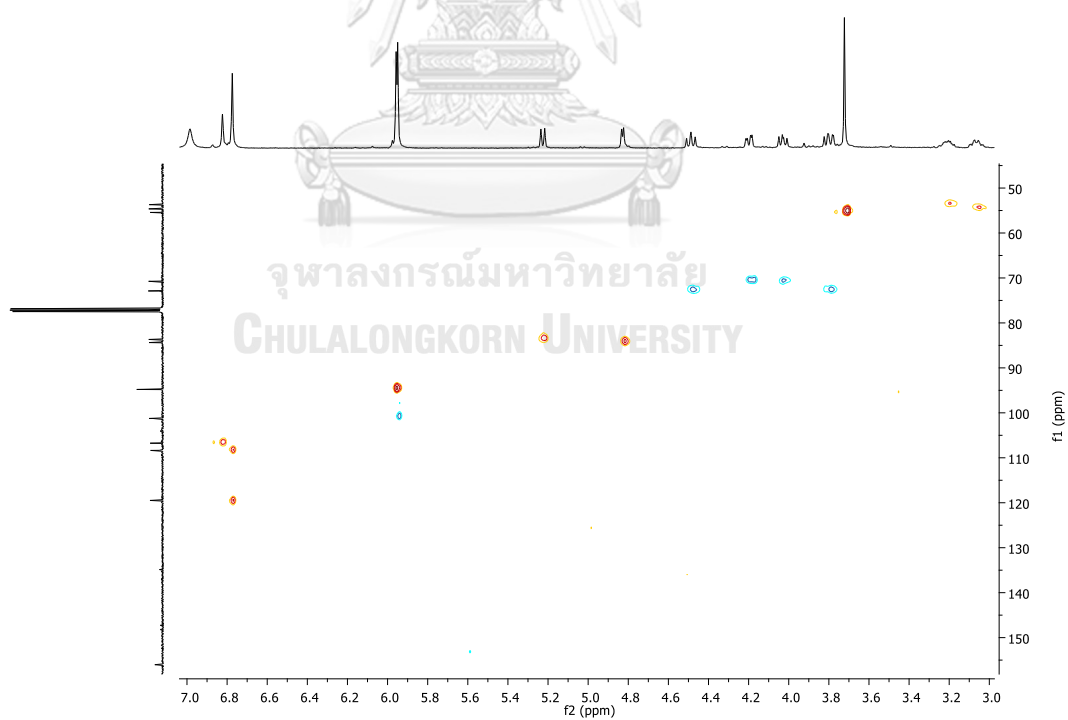


Figure S42. HSQC spectrum of α -6h (CDCl_3)

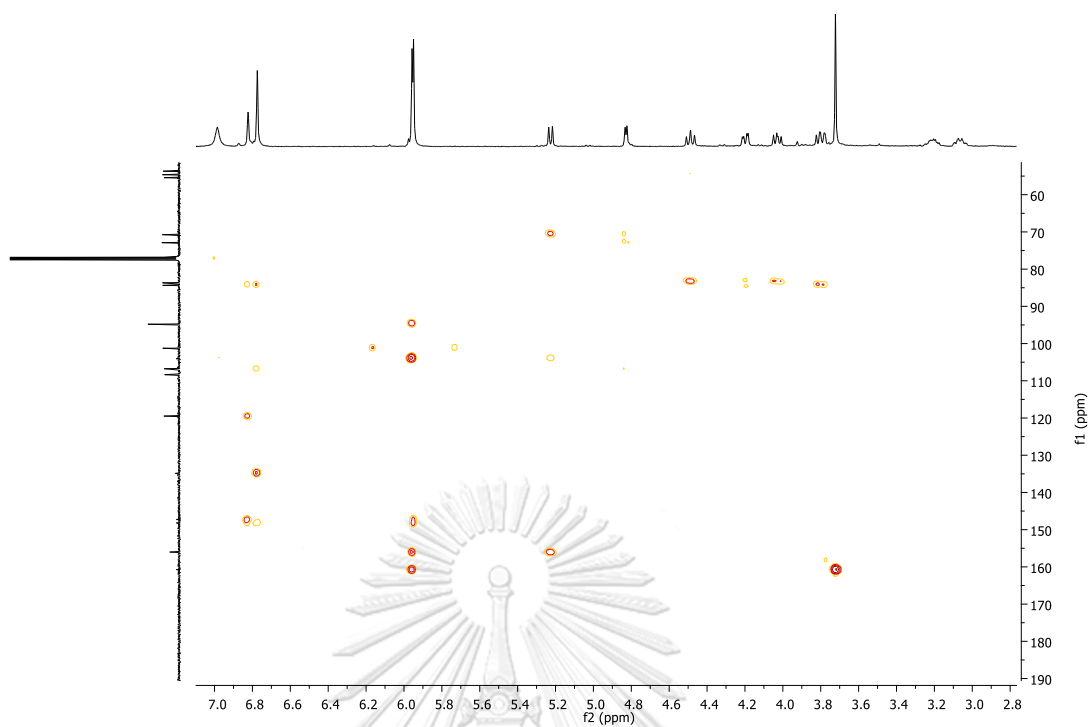


Figure S43. HMBC spectrum of α -6h (CDCl_3)

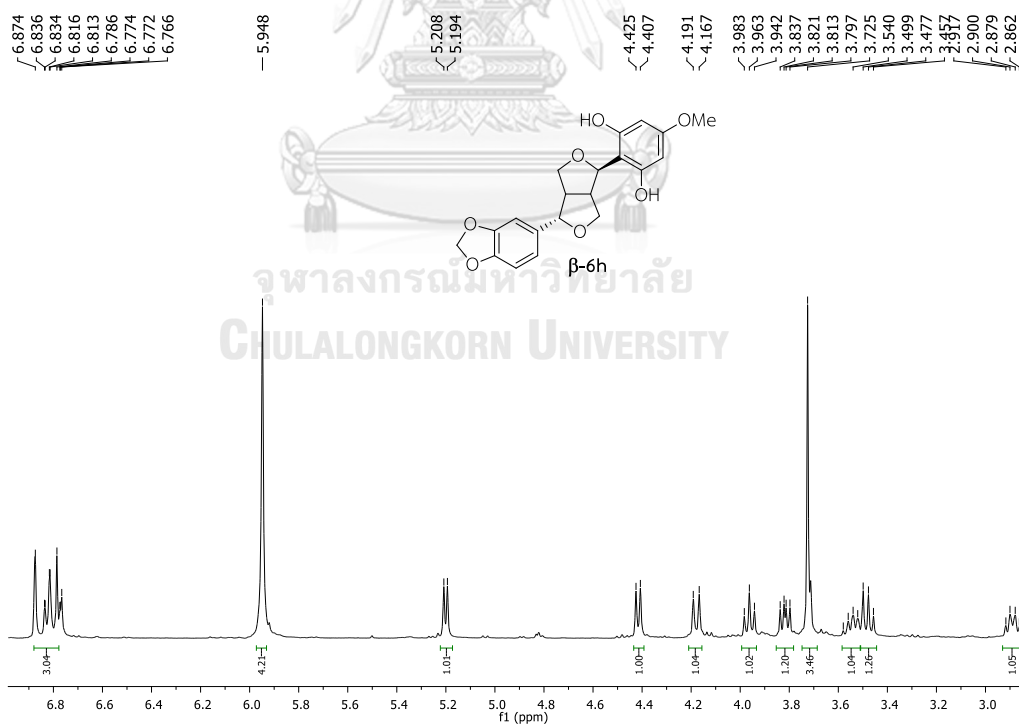


Figure S44. ^1H NMR spectrum of β -6h (CDCl_3)

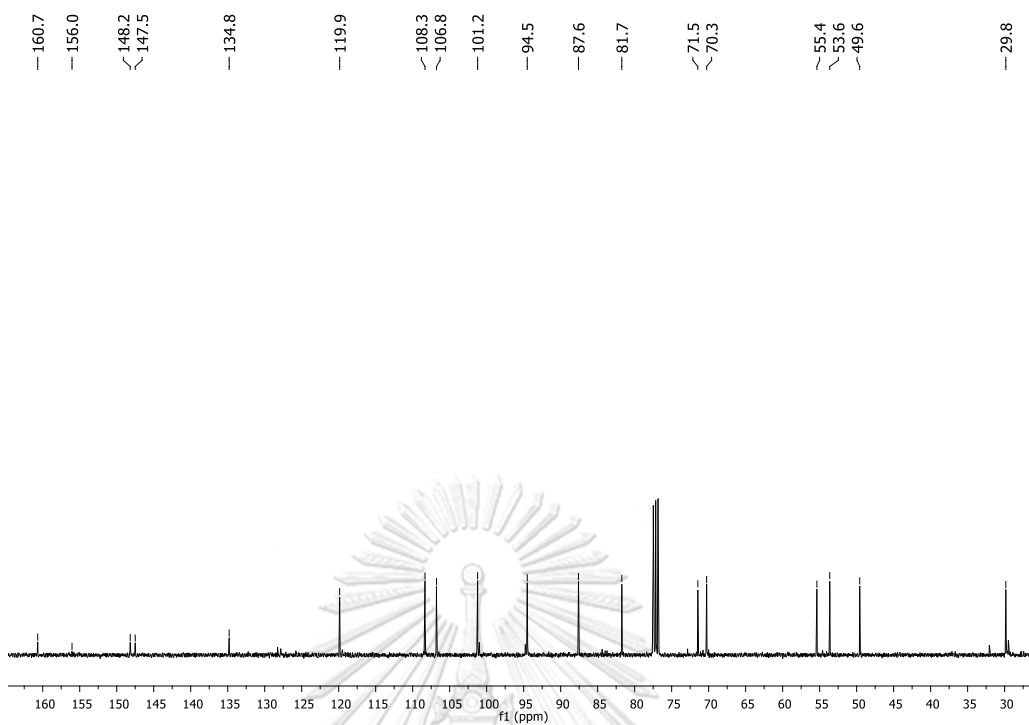


Figure S45. ^{13}C NMR spectrum of $\beta\text{-6h}$ (CDCl_3)

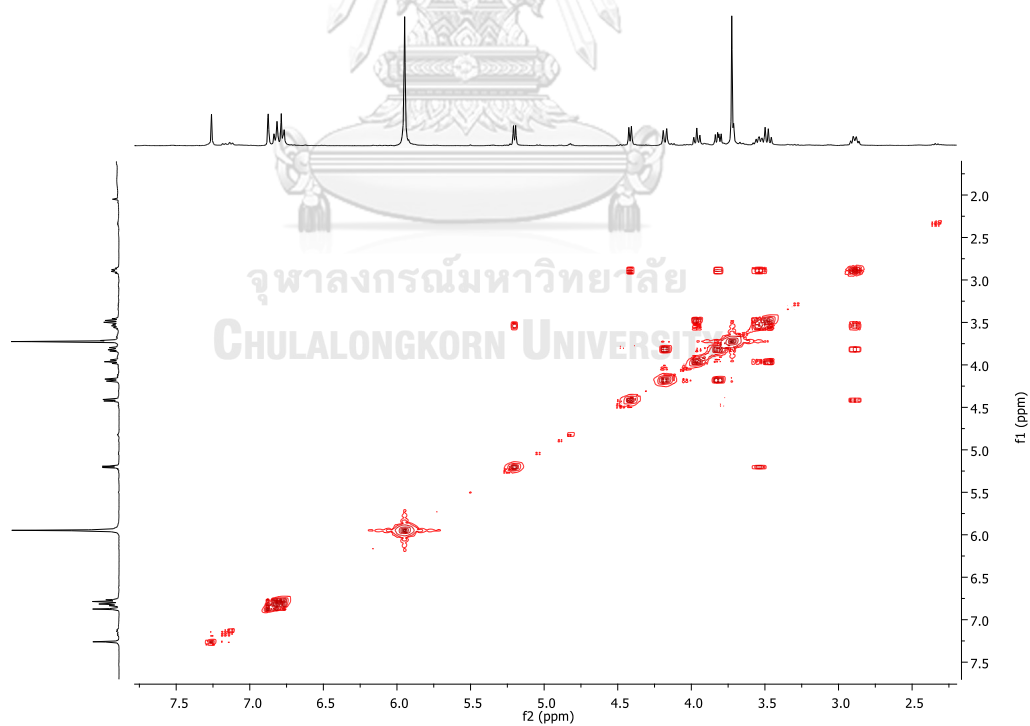


Figure S46. COSY spectrum of $\beta\text{-6h}$ (CDCl_3)

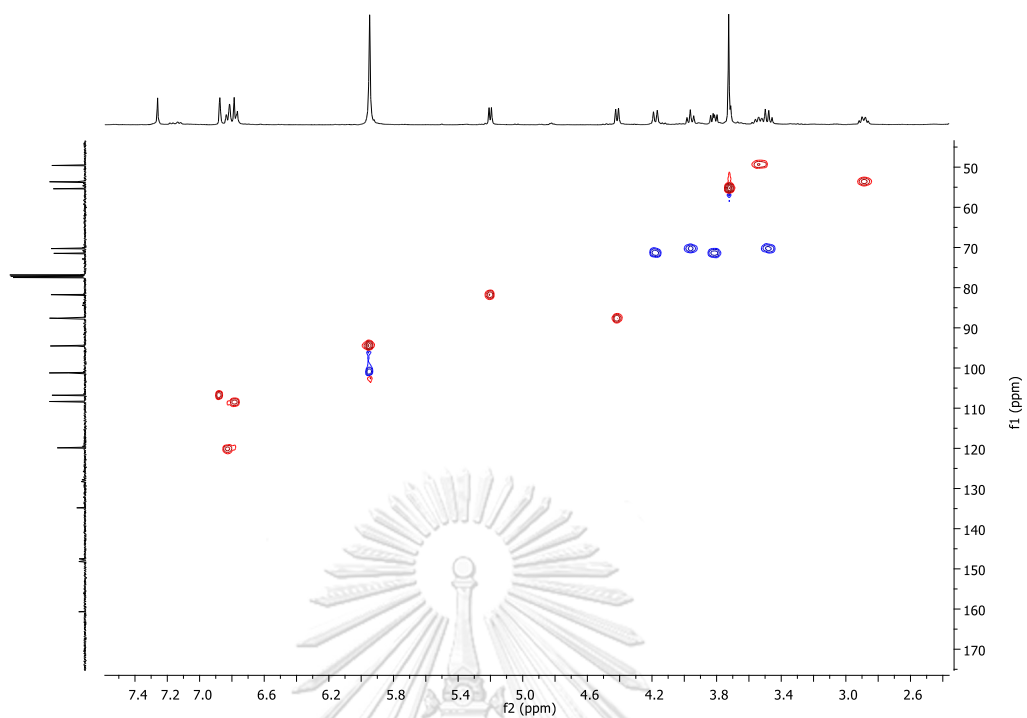


Figure S47. HSQC spectrum of β -6h (CDCl_3)

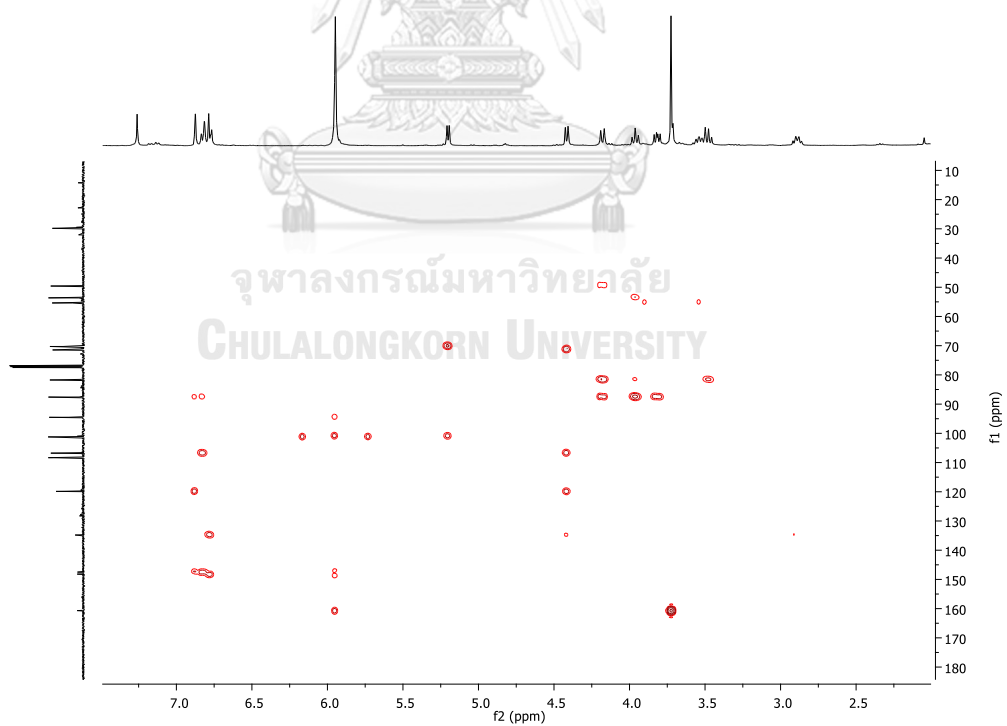


Figure S48. HMBC spectrum of β -6h (CDCl_3)

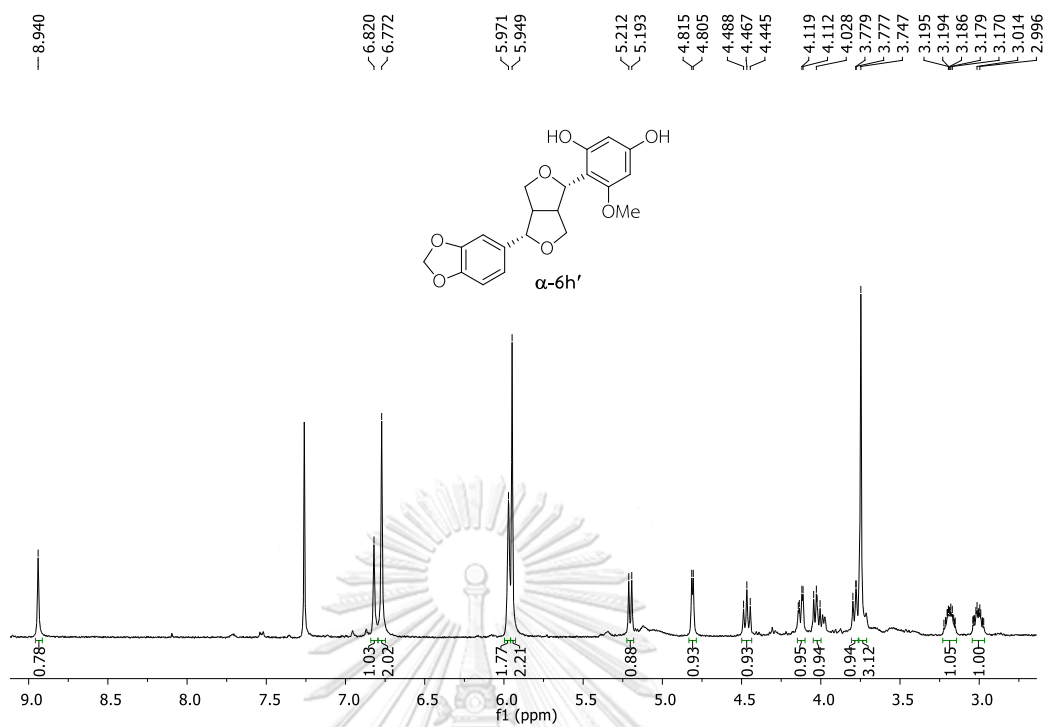


Figure S49. ^1H NMR spectrum of α -6h' (CDCl_3)

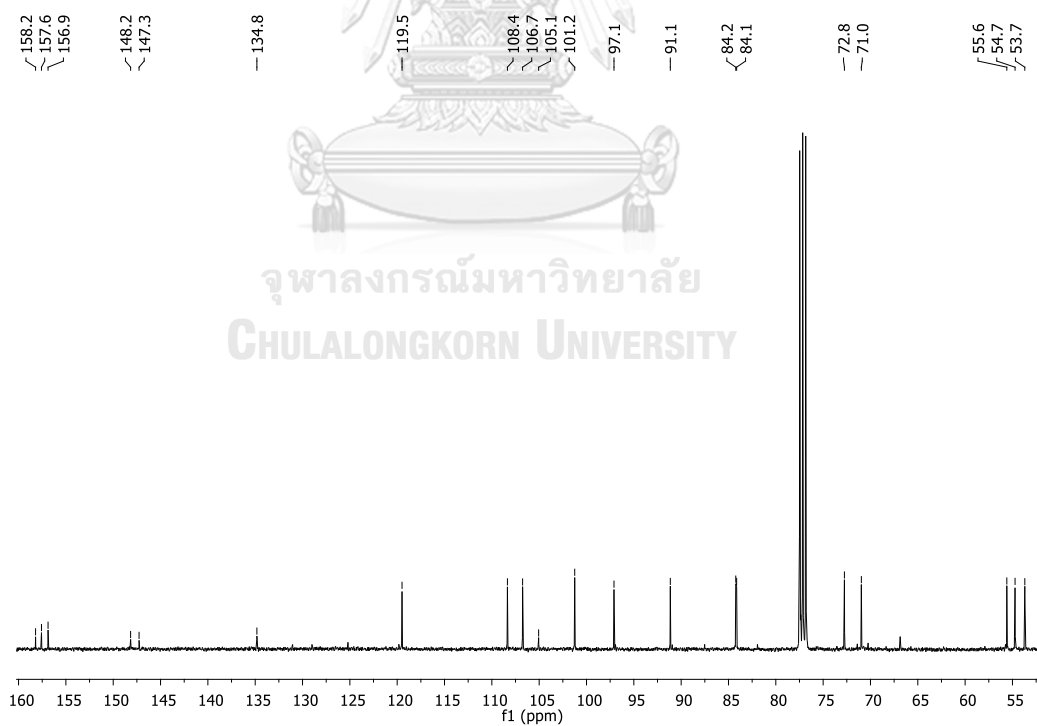


Figure S50. ^{13}C NMR spectrum of α -6h' (CDCl_3)

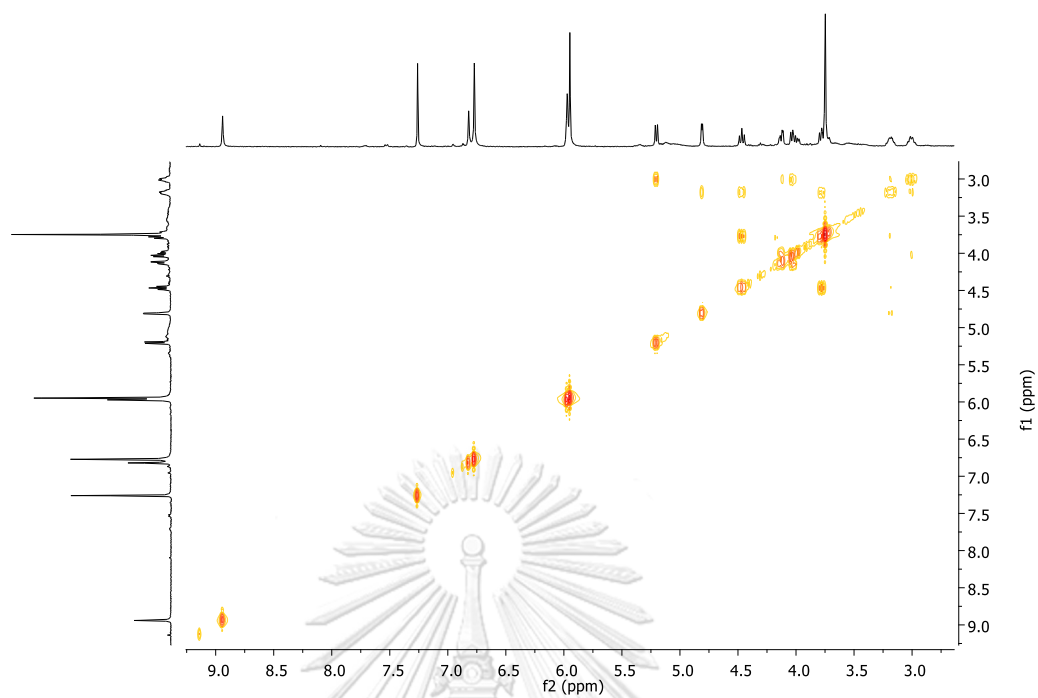


Figure S51. COSY spectrum of α -6h' (CDCl_3)

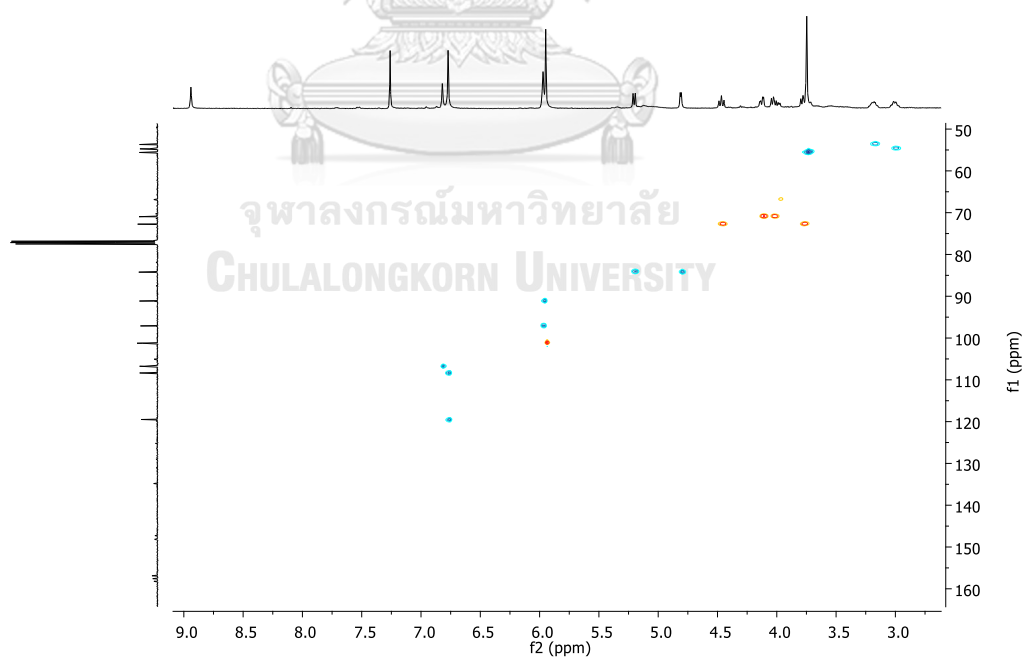


Figure S52. HSQC spectrum of α -6h' (CDCl_3)

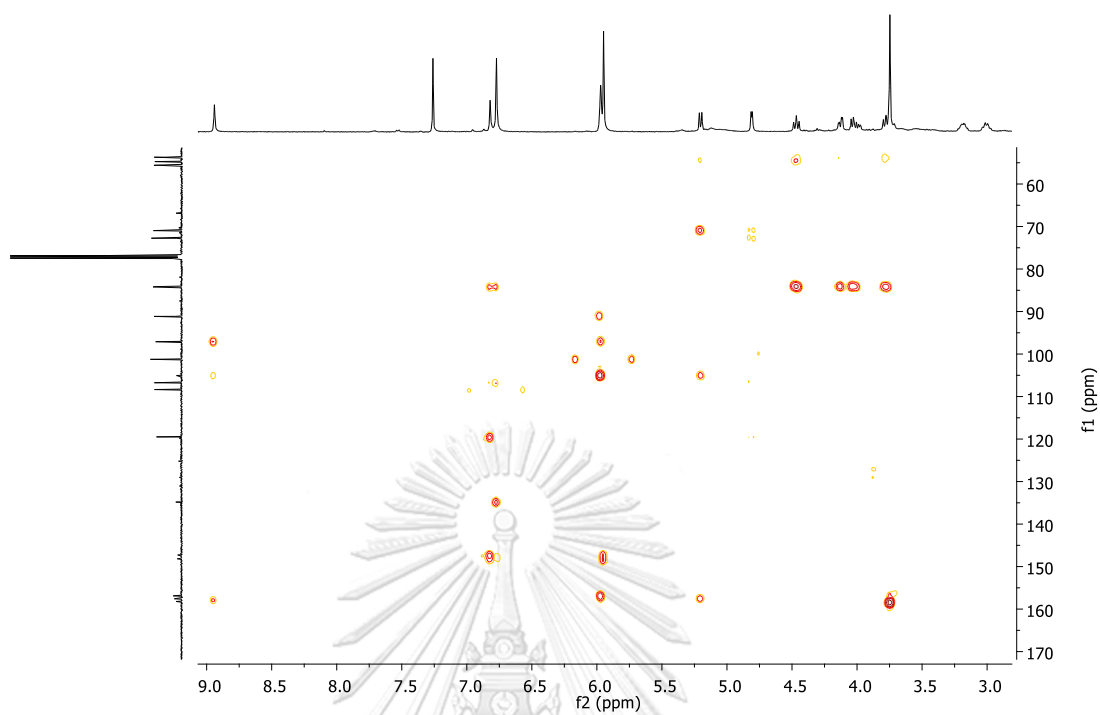


Figure S53. HMBC spectrum of α -6h' (CDCl₃)

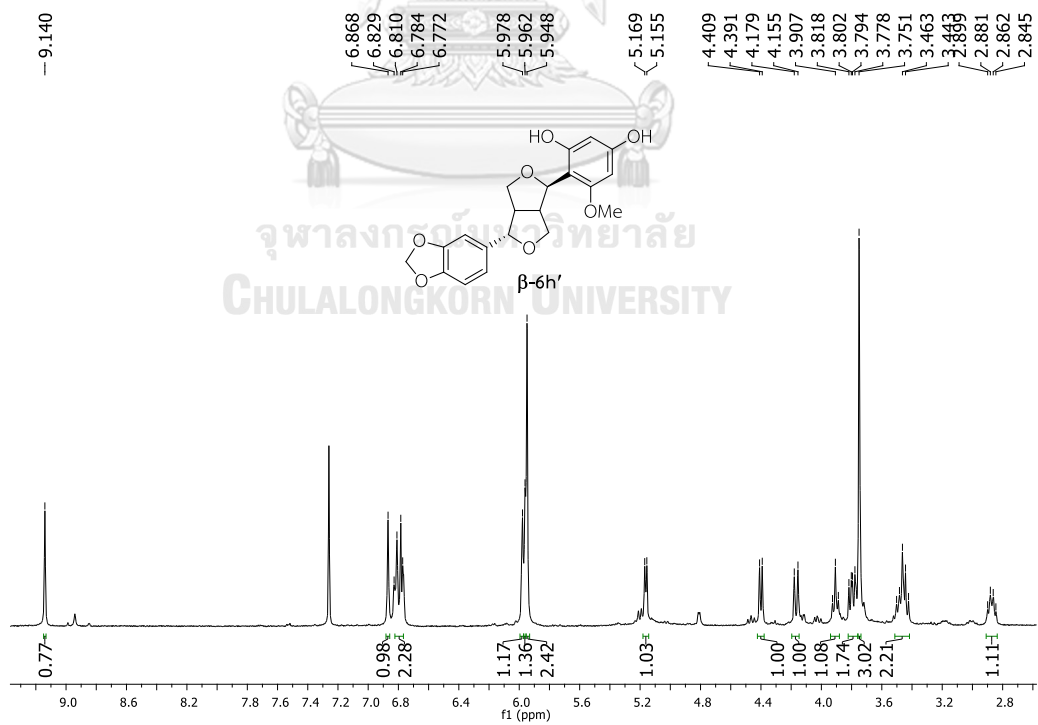


Figure S54. ¹H NMR spectrum of β -6h' (CDCl₃)

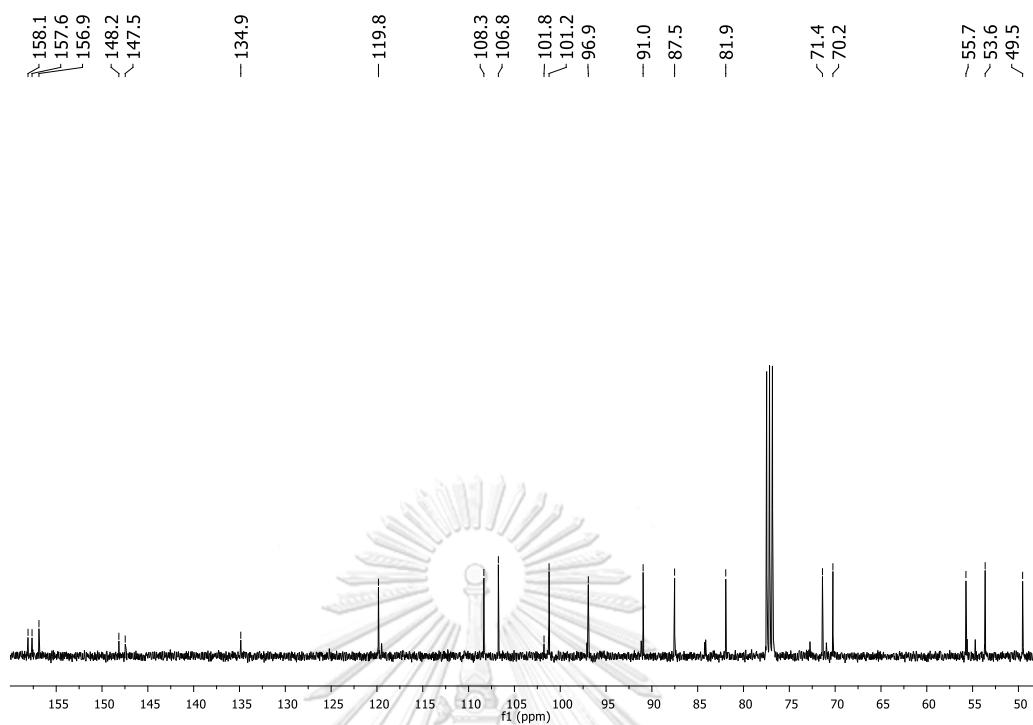


Figure S55. ^{13}C NMR spectrum of $\beta\text{-6h}'$ (CDCl_3)

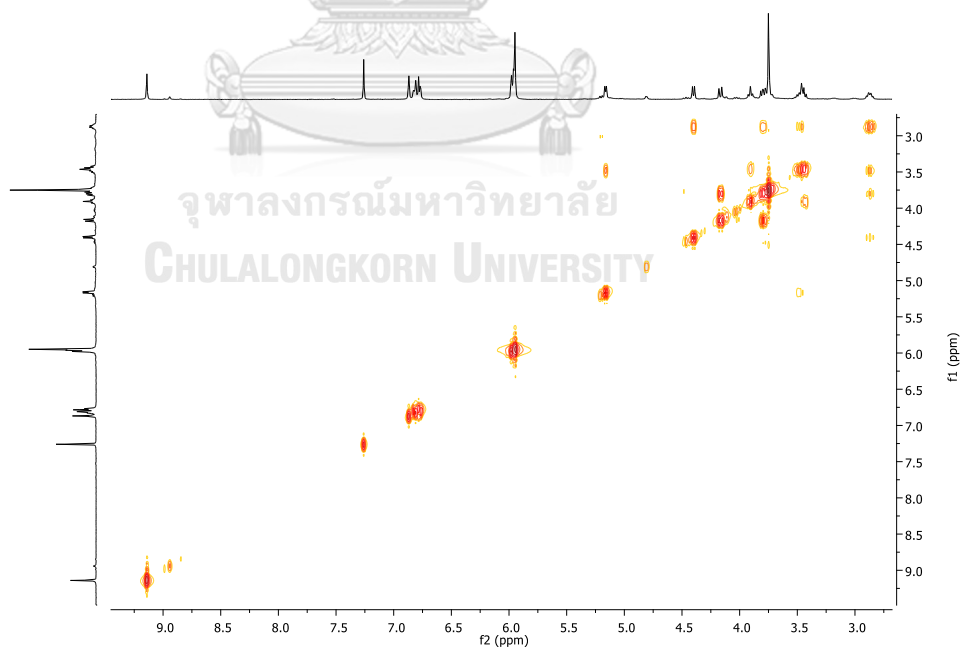


Figure S56. COSY spectrum of $\beta\text{-6h}'$ (CDCl_3)

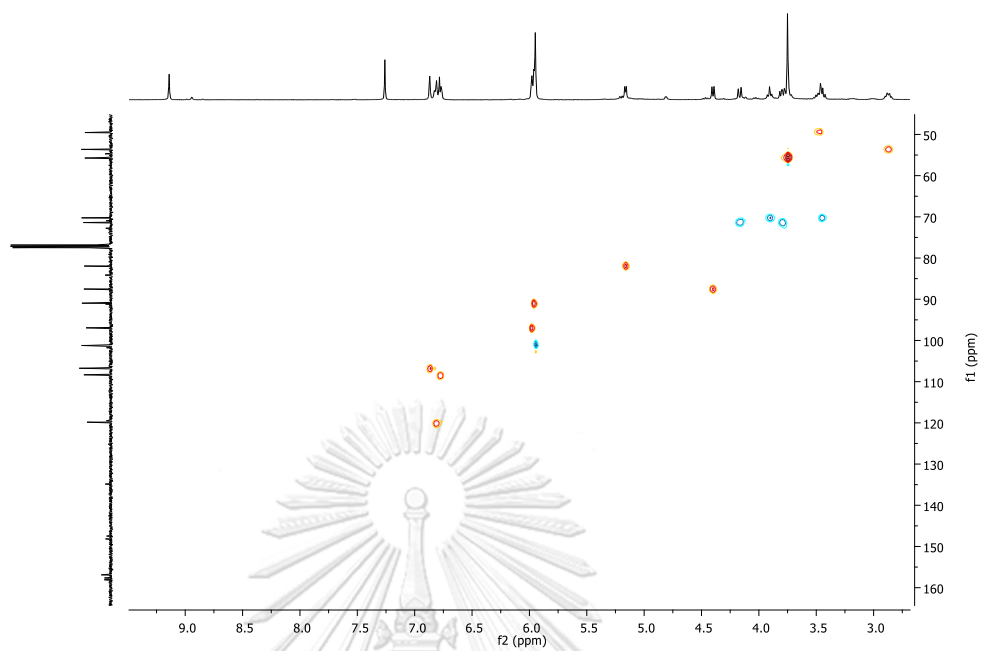


Figure S57. HSQC spectrum of β -6h' (CDCl_3)

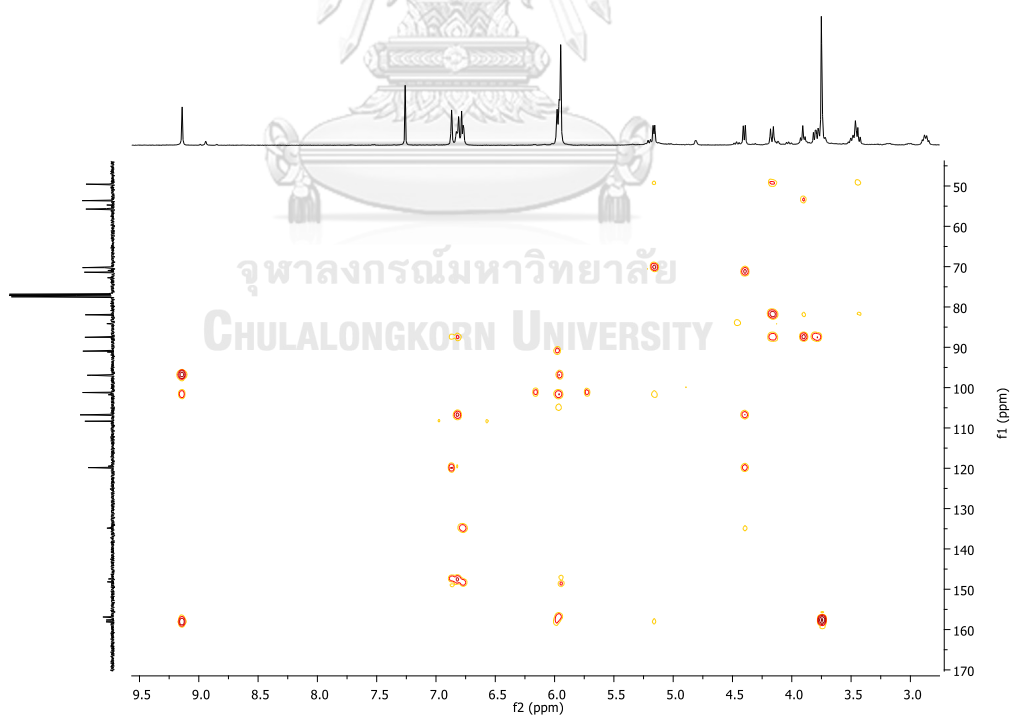


Figure S58. HMBC spectrum of β -6h' (CDCl_3)

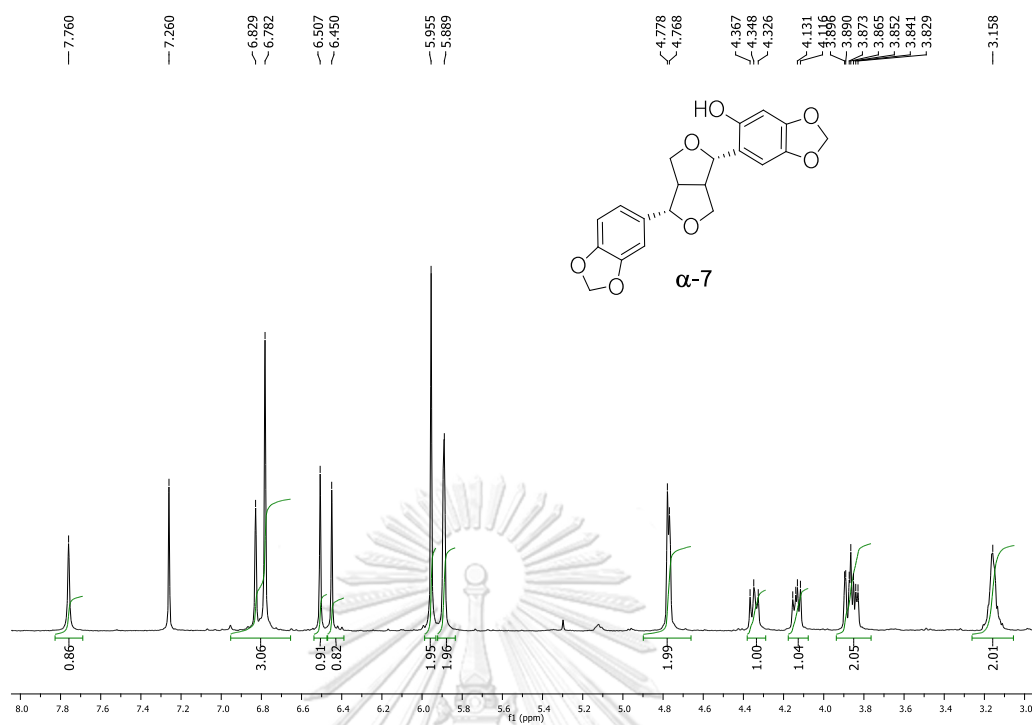


Figure S59. ^1H NMR spectrum of α -sesaminol (α -7) (CDCl_3)

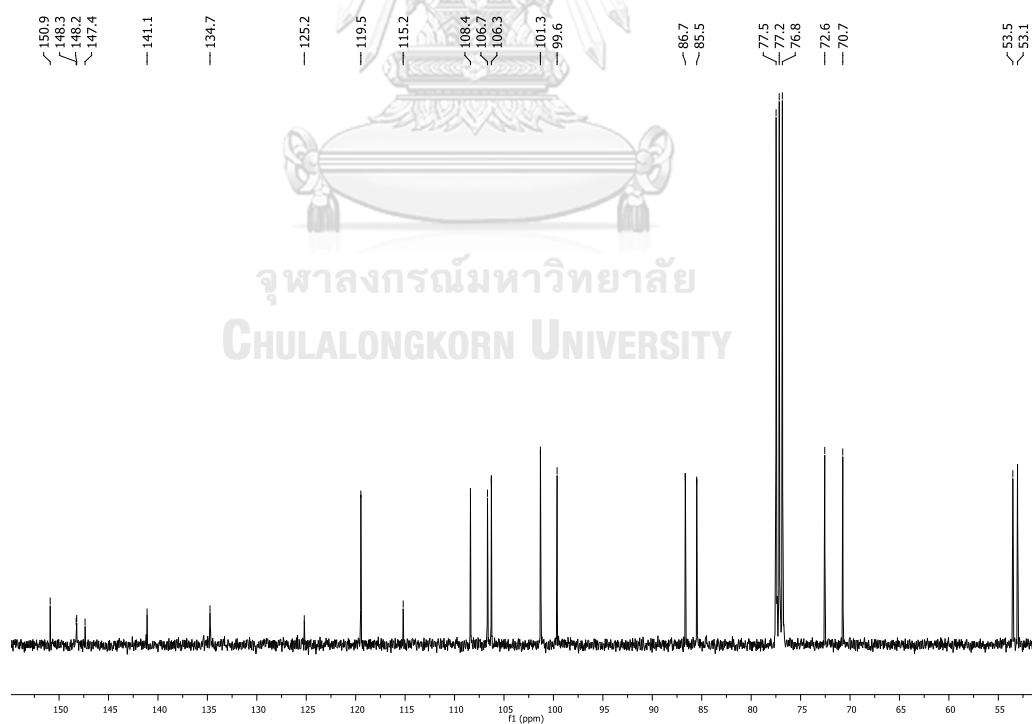


Figure S60. ^{13}C NMR spectrum of α -sesaminol (α -7) (CDCl_3)

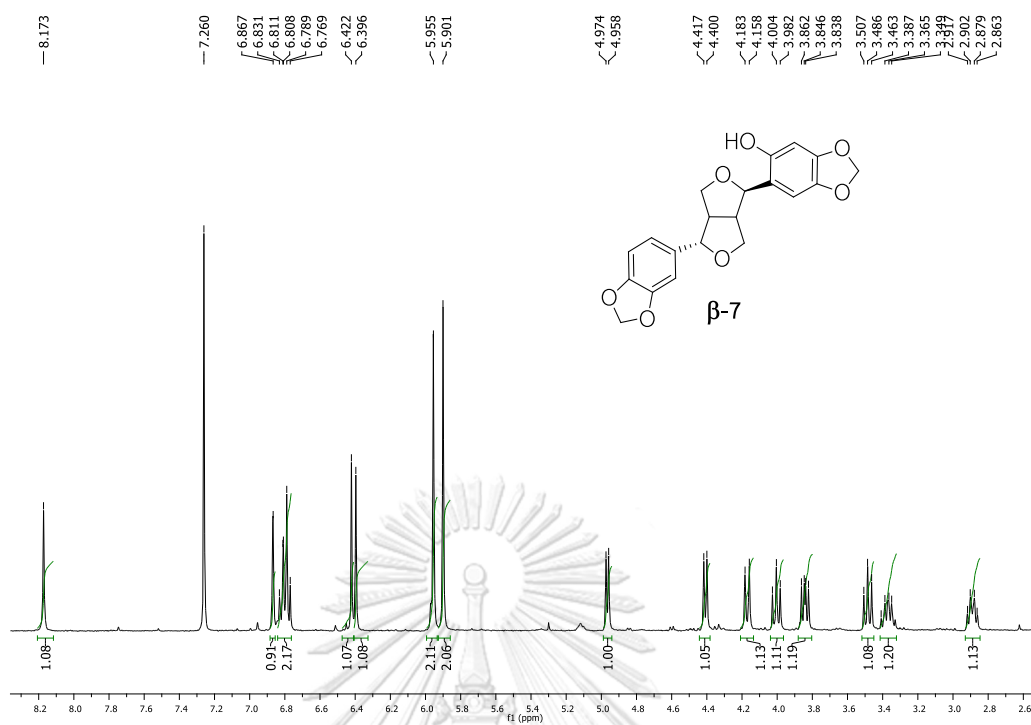


Figure S61. ^1H NMR spectrum of β -sesaminol (β -7) (CDCl_3)

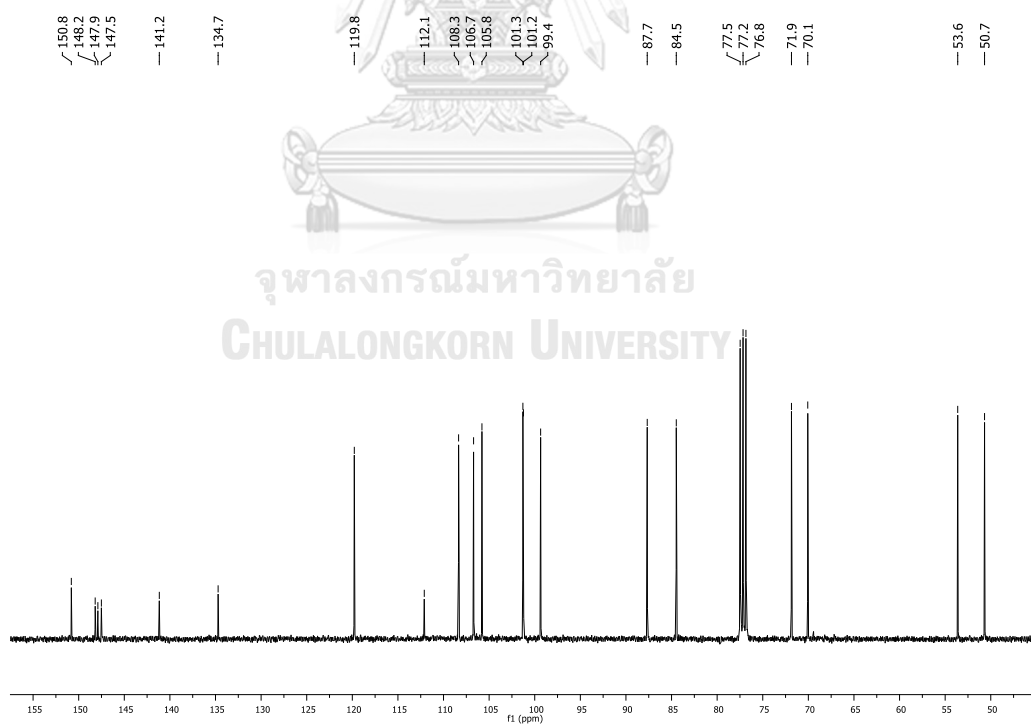
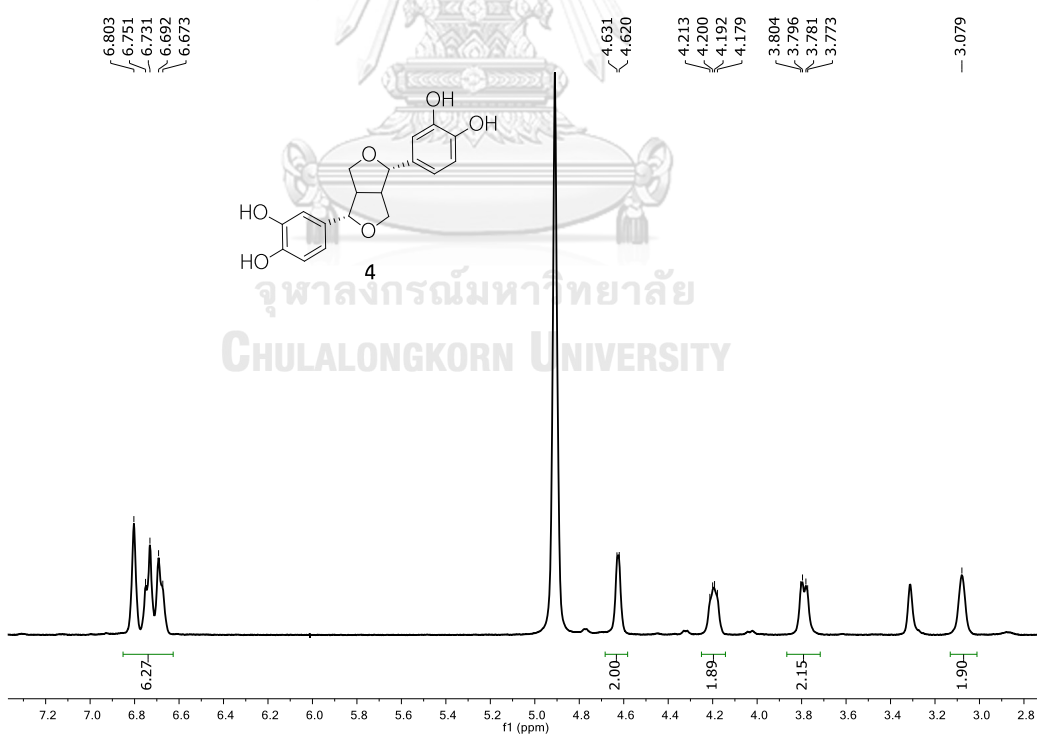
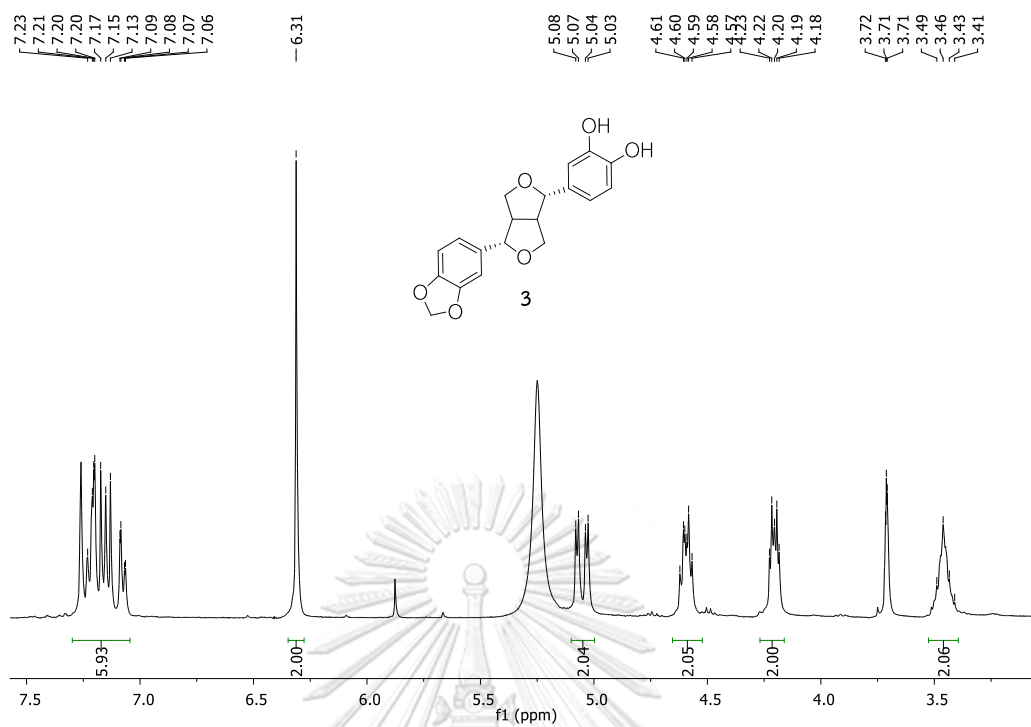
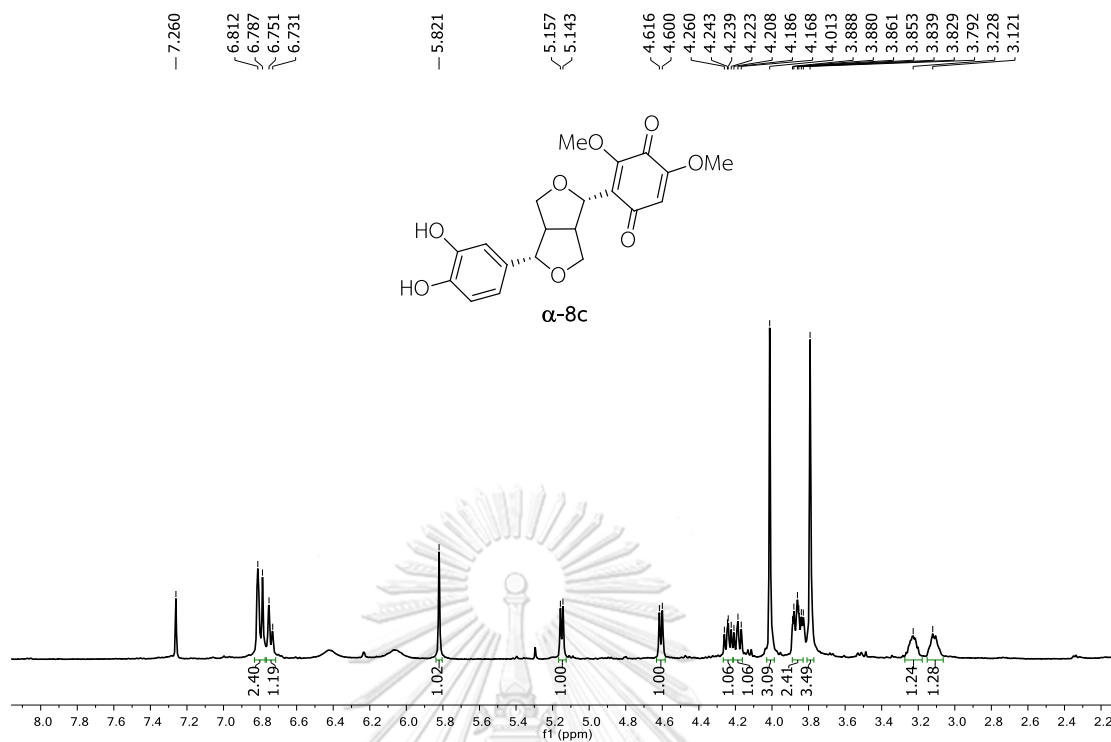
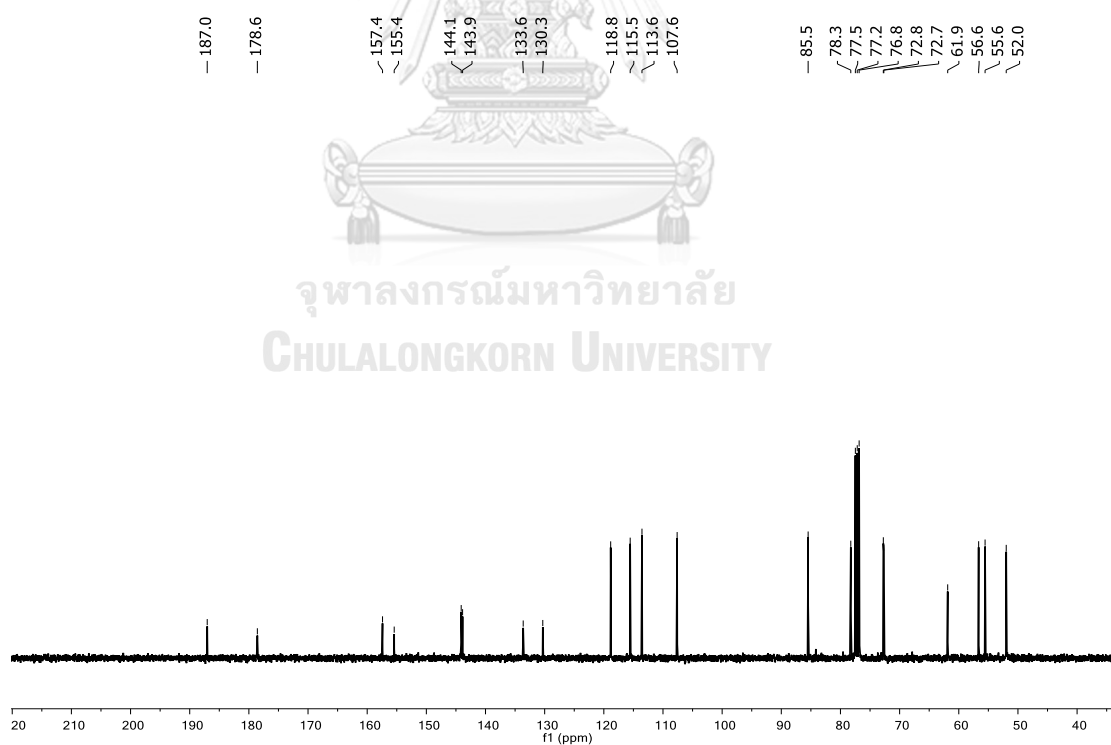


Figure S62. ^{13}C NMR spectrum of β -sesaminol (β -7) (CDCl_3)



Figure S65. ^1H NMR spectrum of α -8c (CDCl_3)Figure S66. ^{13}C NMR spectrum of α -8c (CDCl_3)

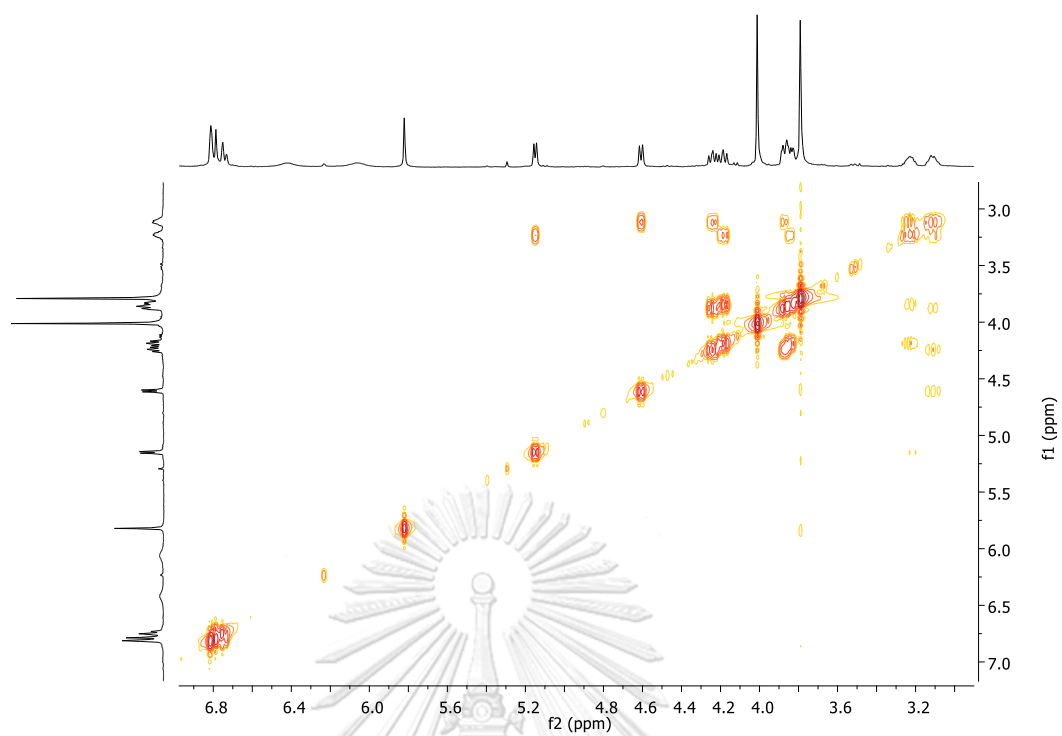


Figure S67. COSY spectrum of α -8c (CDCl_3)

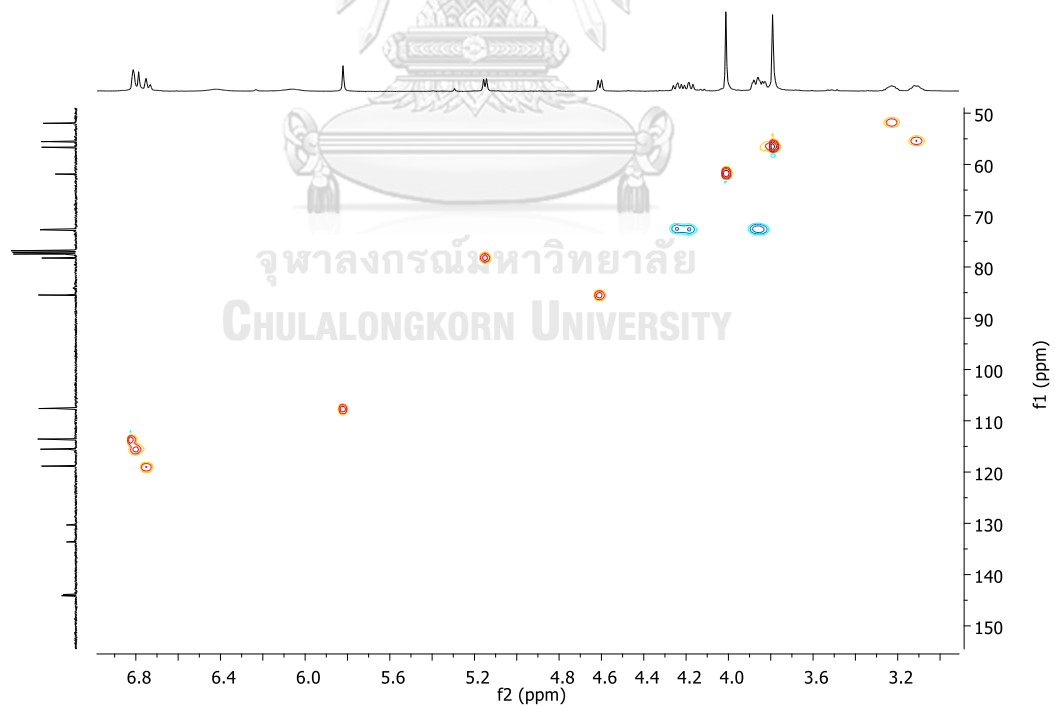


Figure S68. HSQC spectrum of α -8c (CDCl_3)

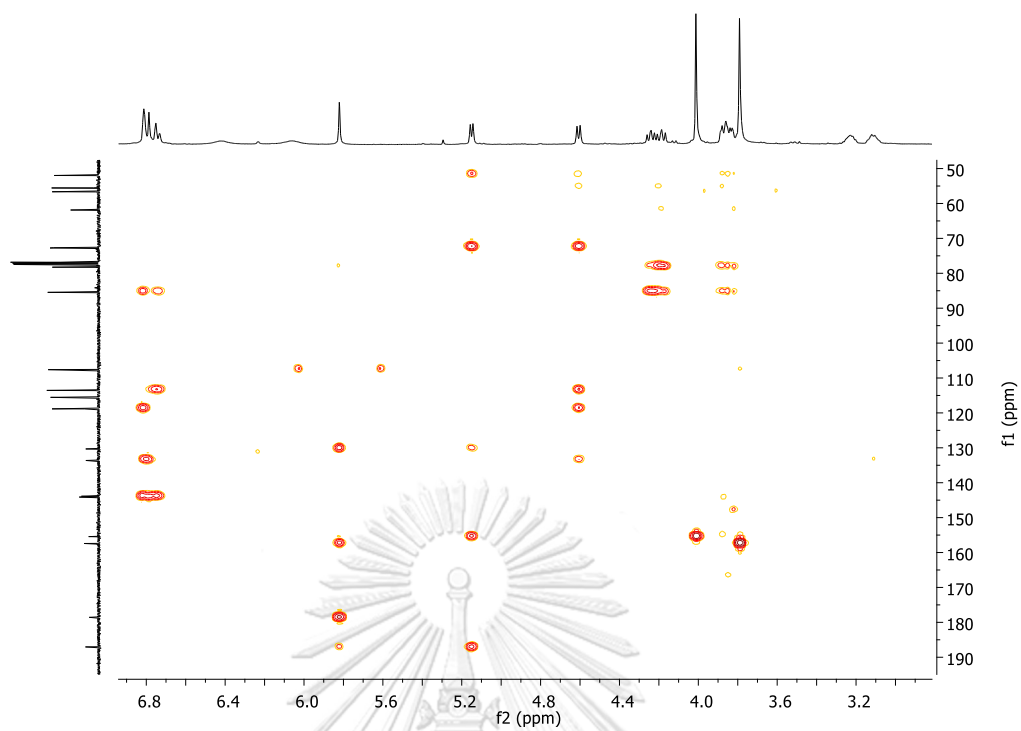


Figure S69. HMBC spectrum of α -8c (CDCl_3)

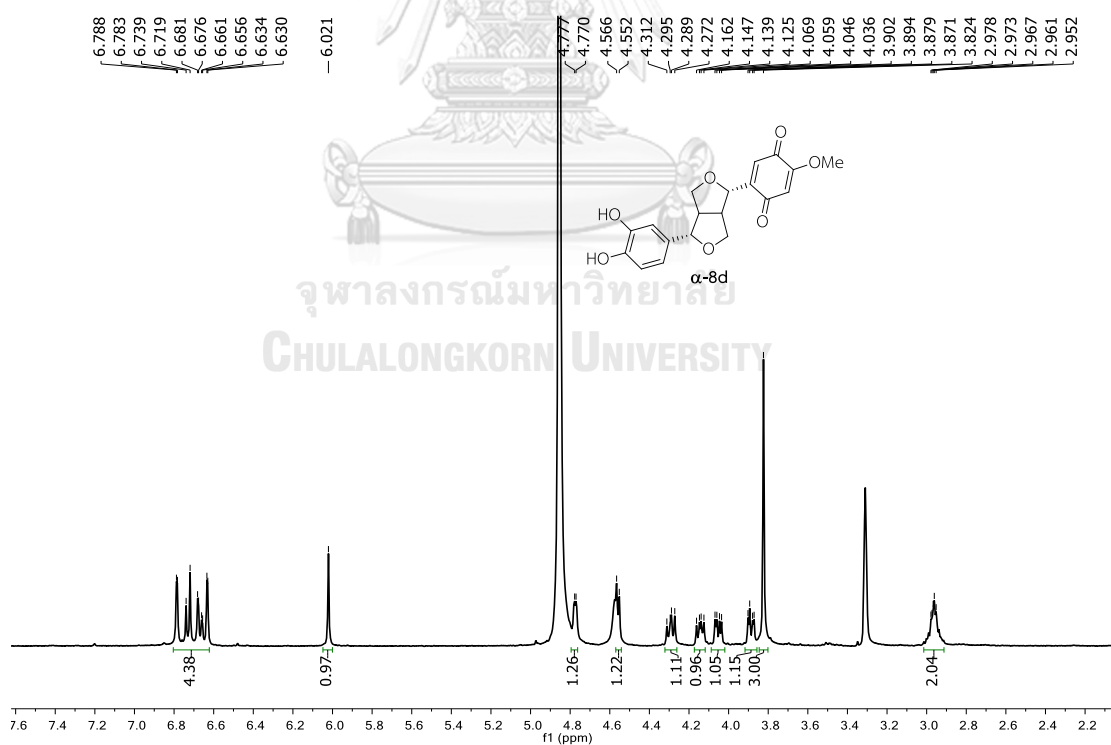
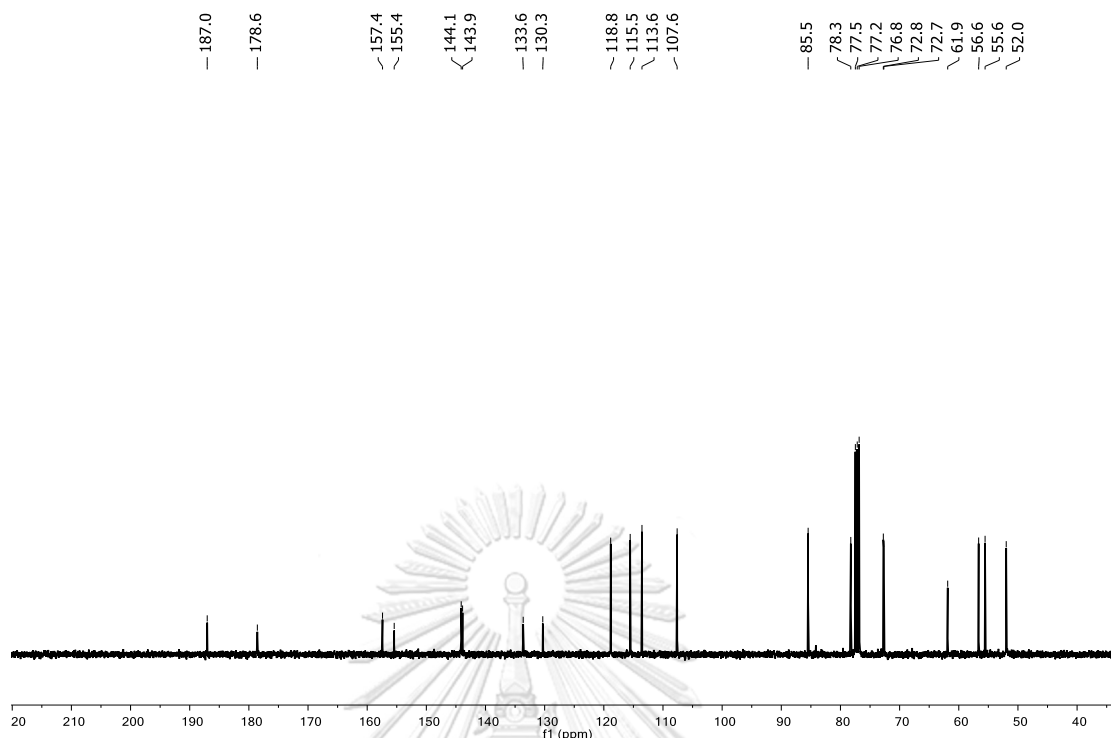
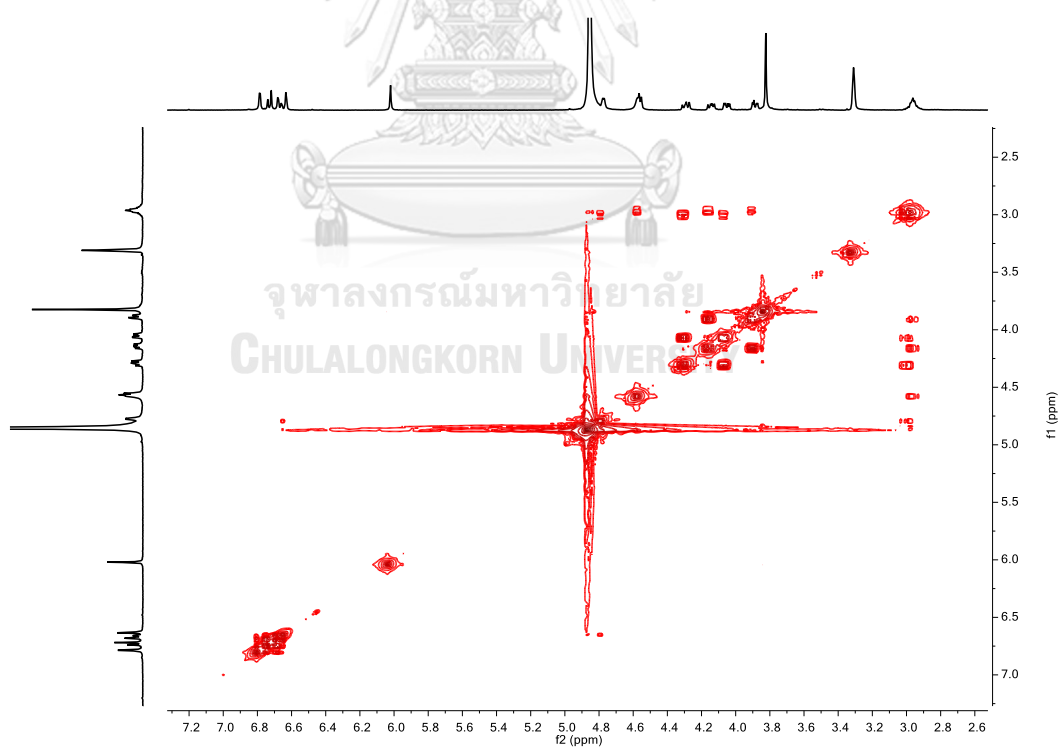


Figure S70. ^1H NMR spectrum of α -8d (CD_3OD)

Figure S71. ^{13}C NMR spectrum of α -8d (CD_3OD)Figure S72. COSY spectrum of α -8d (CD_3OD)

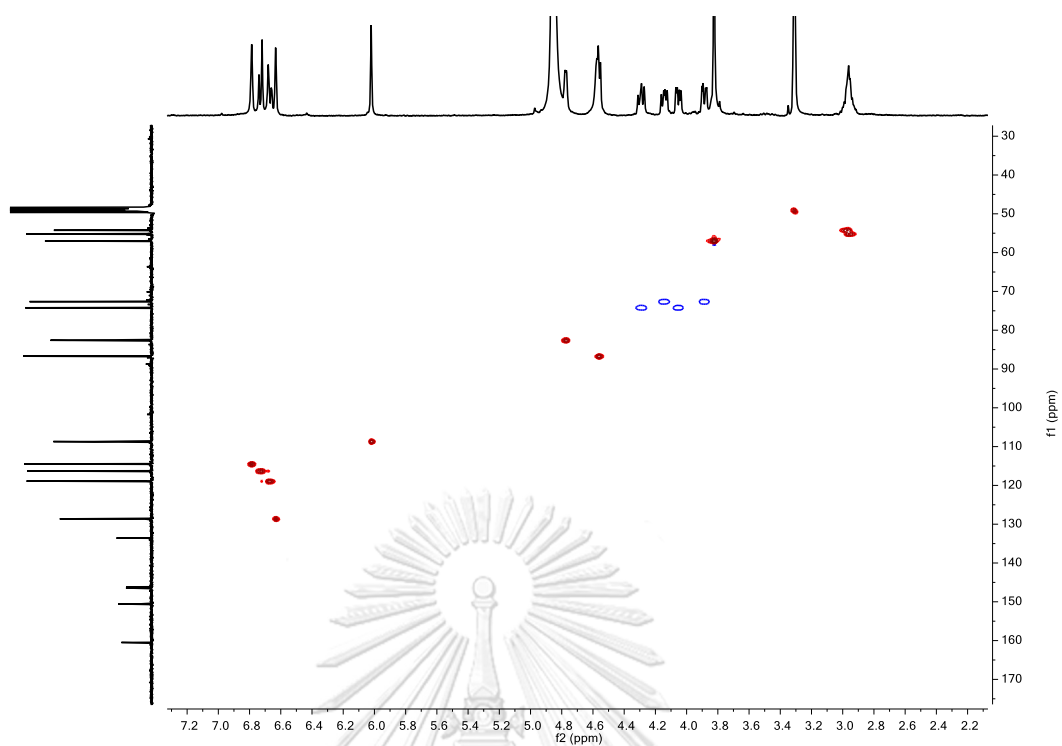


Figure S73. HSQC spectrum of α -8d (CD_3OD)

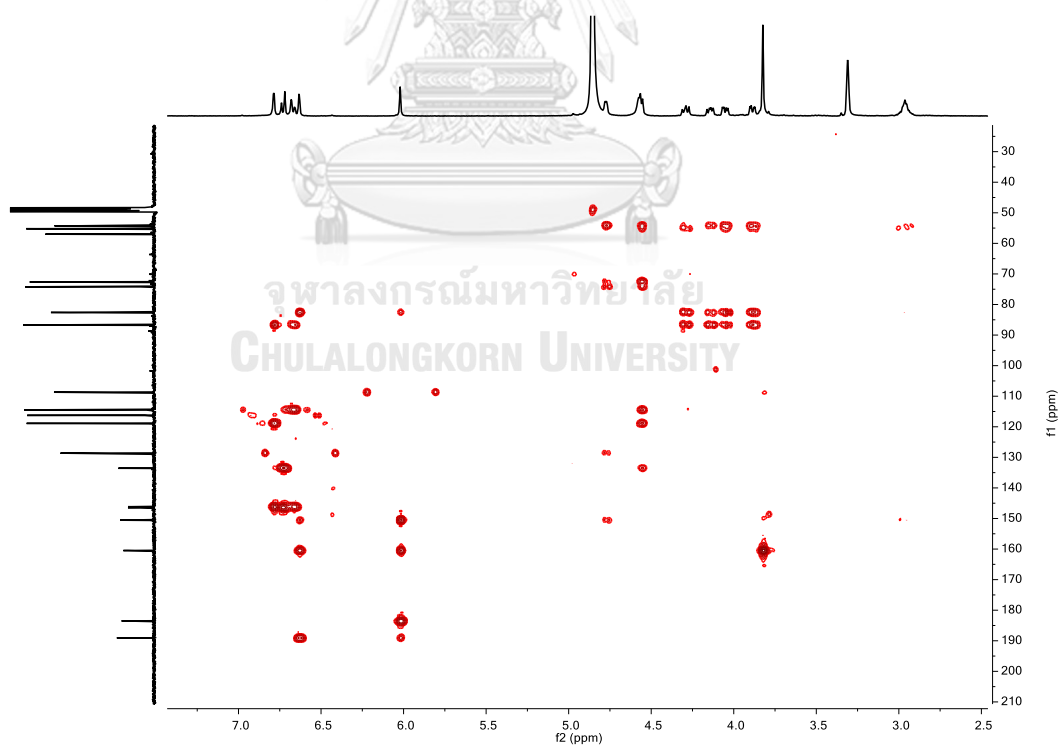


Figure S74. HMBC spectrum of α -8d (CD_3OD)

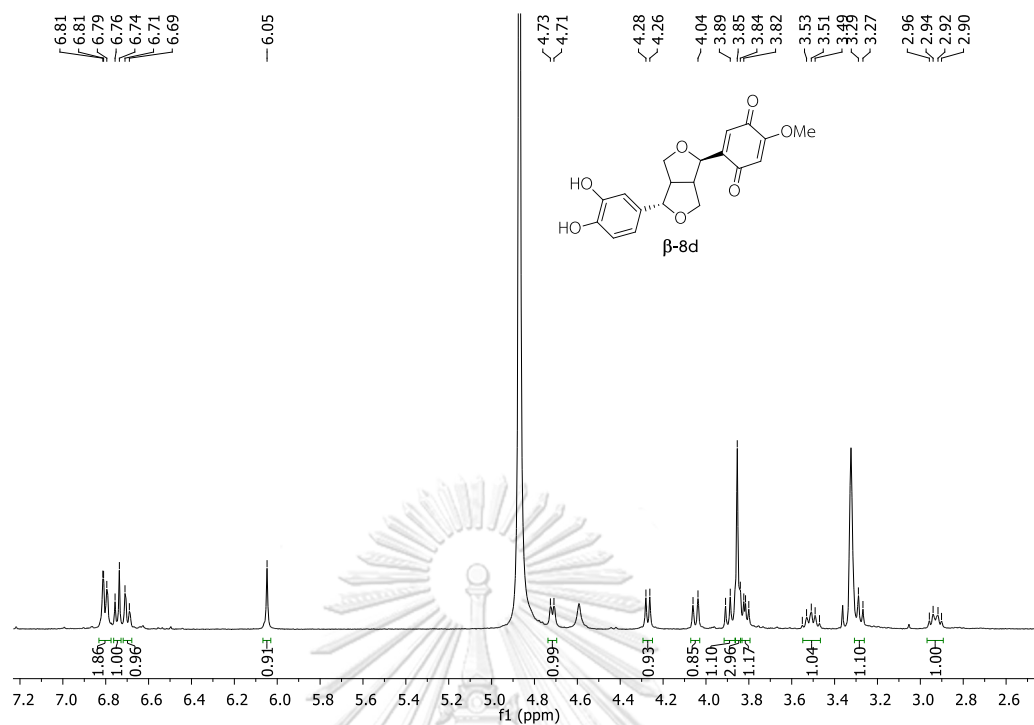


Figure S75. ^1H NMR spectrum of β -8d (CD_3OD)

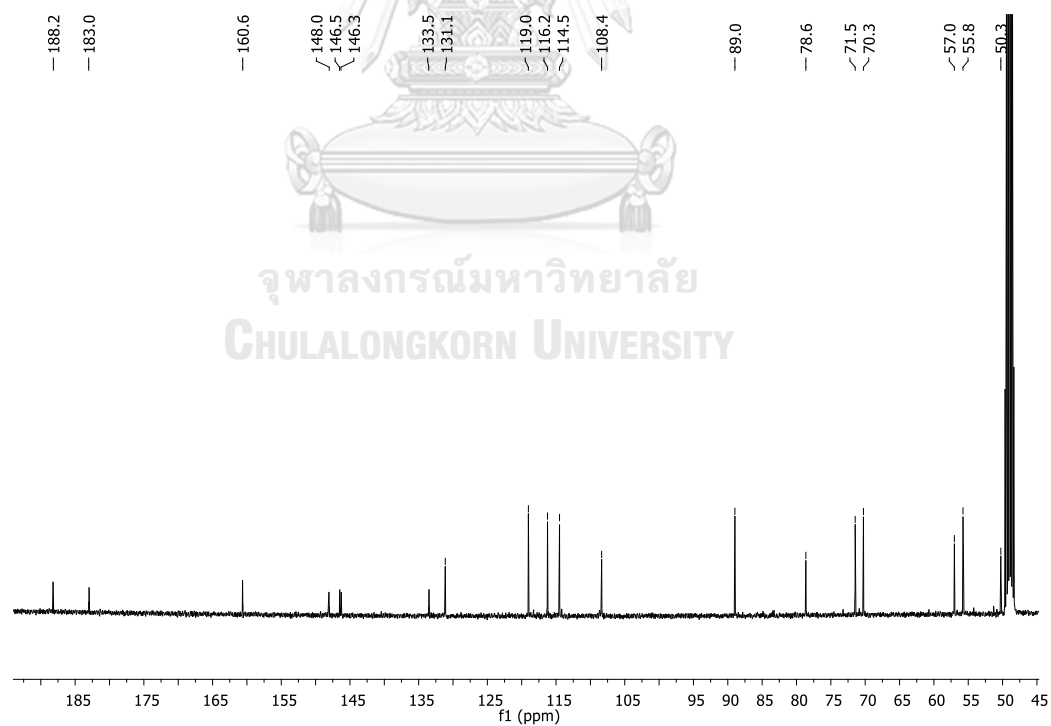


Figure S76. ^{13}C NMR spectrum of β -8d (CD_3OD)

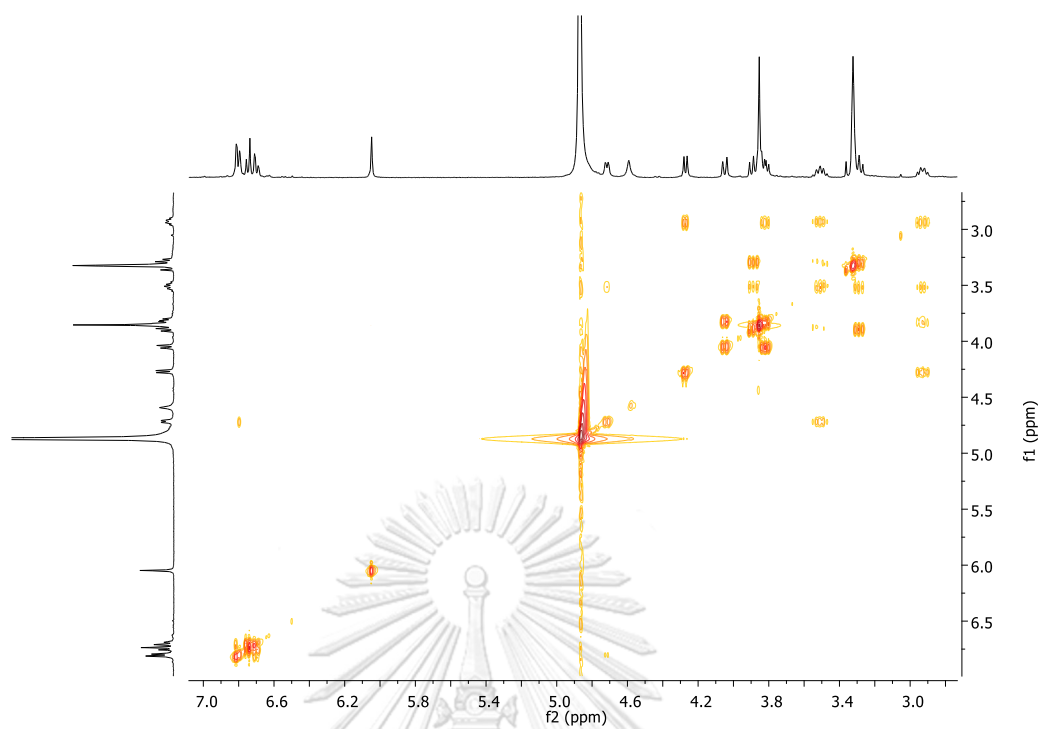


Figure S77. COSY spectrum of β -8d (CD_3OD)

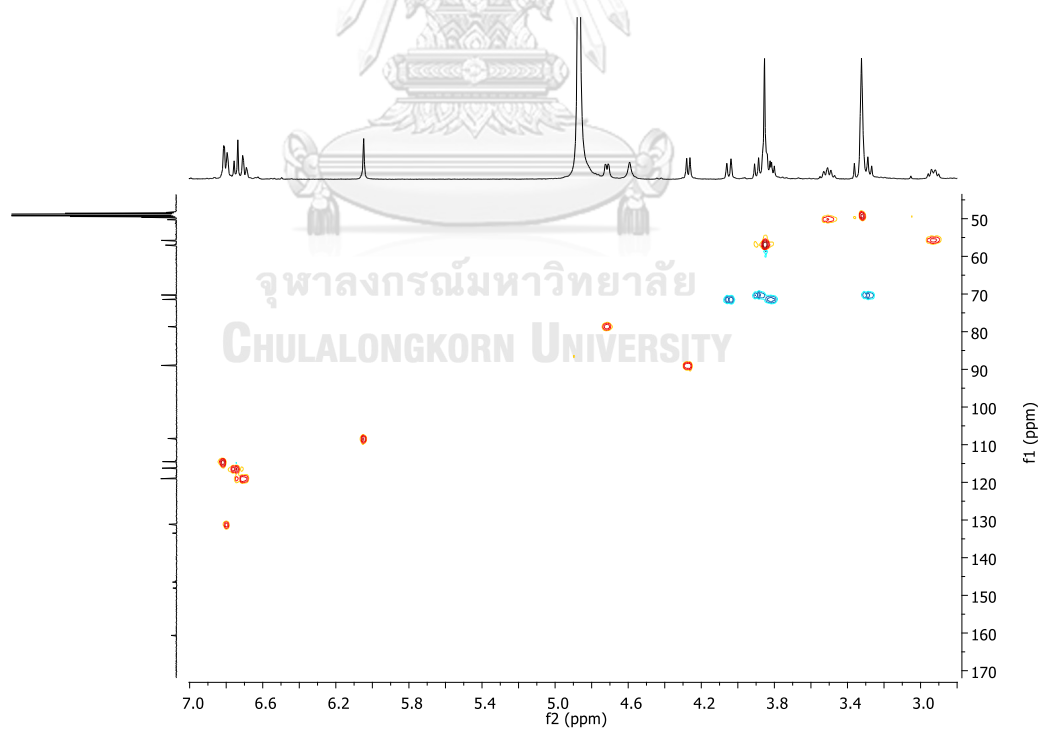


Figure S78. HSQC spectrum of β -8d (CD_3OD)

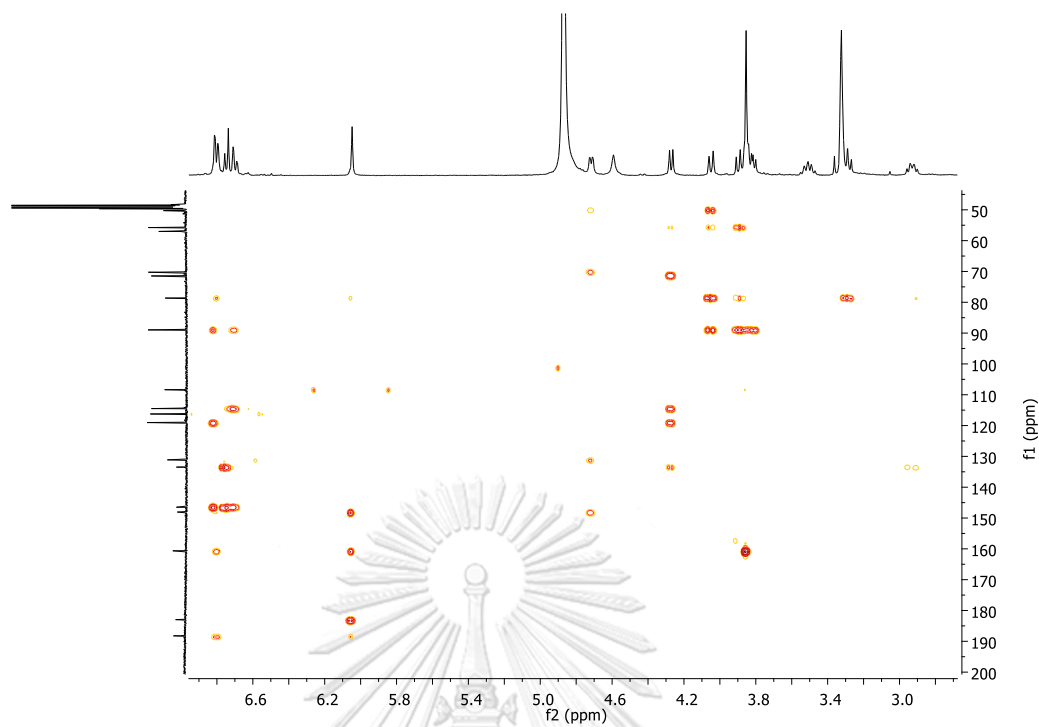


Figure S79. HMBC spectrum of β -8d (CD_3OD)

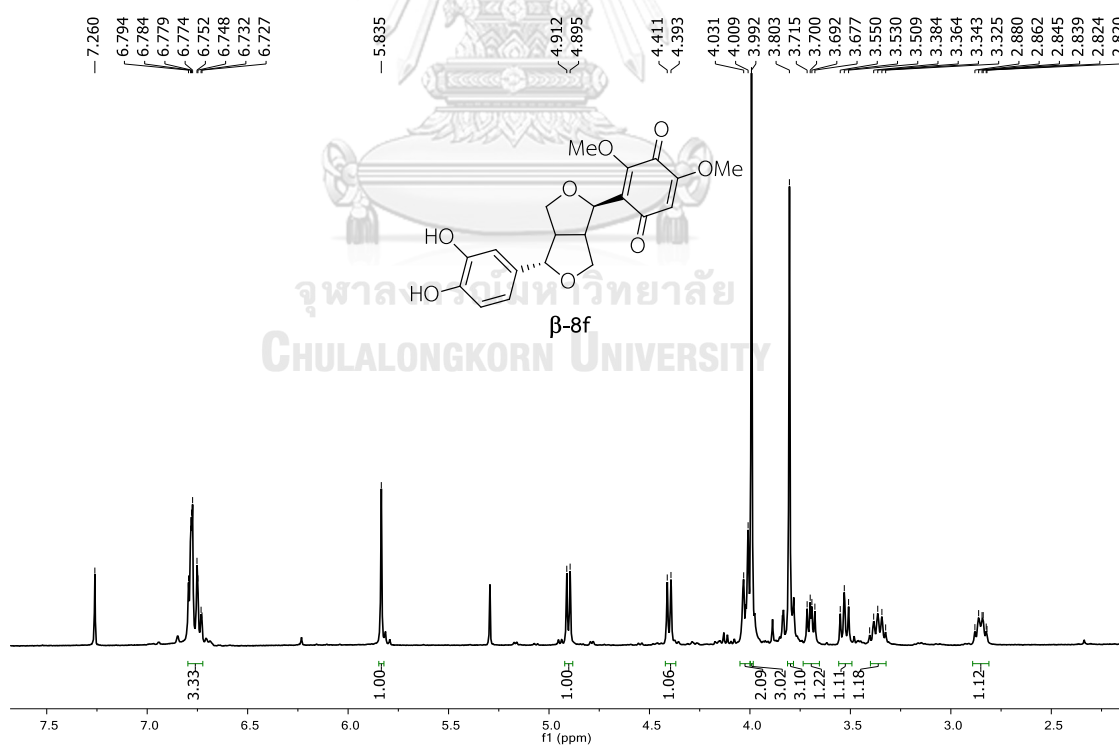


Figure S80. ^1H NMR spectrum of β -8f (CD_3OD)

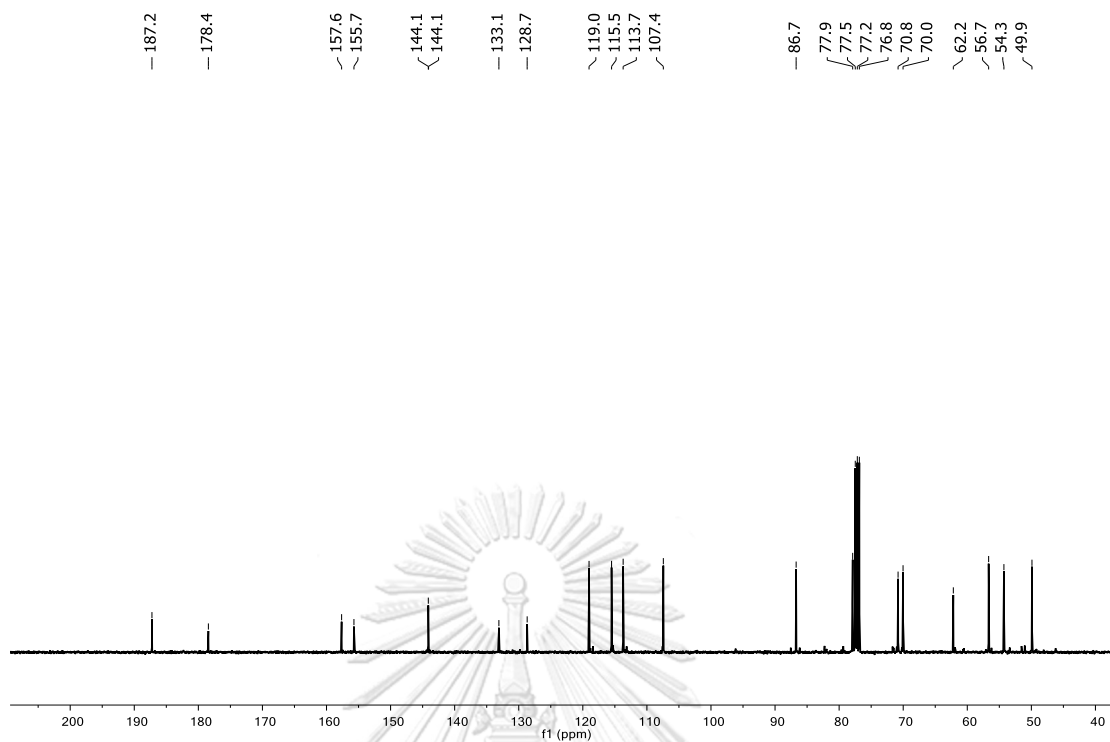


Figure S81. ^{13}C NMR spectrum of $\beta\text{-8f}$ (CD_3OD)

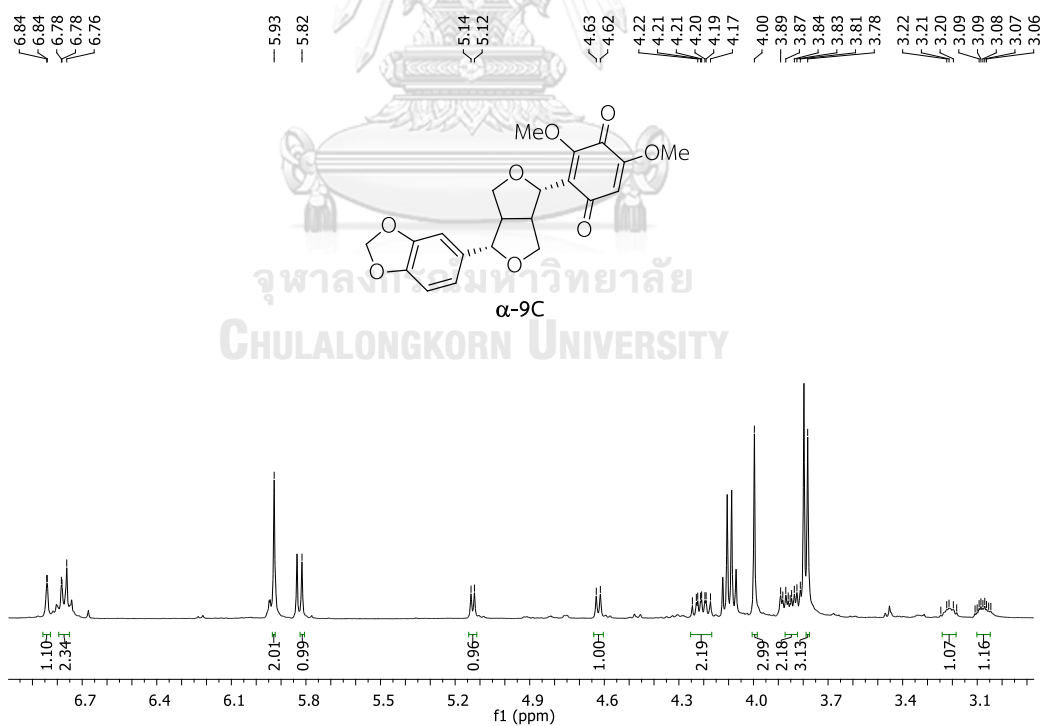


Figure S82. ^1H NMR spectrum of $\alpha\text{-9c}$ (CDCl_3)

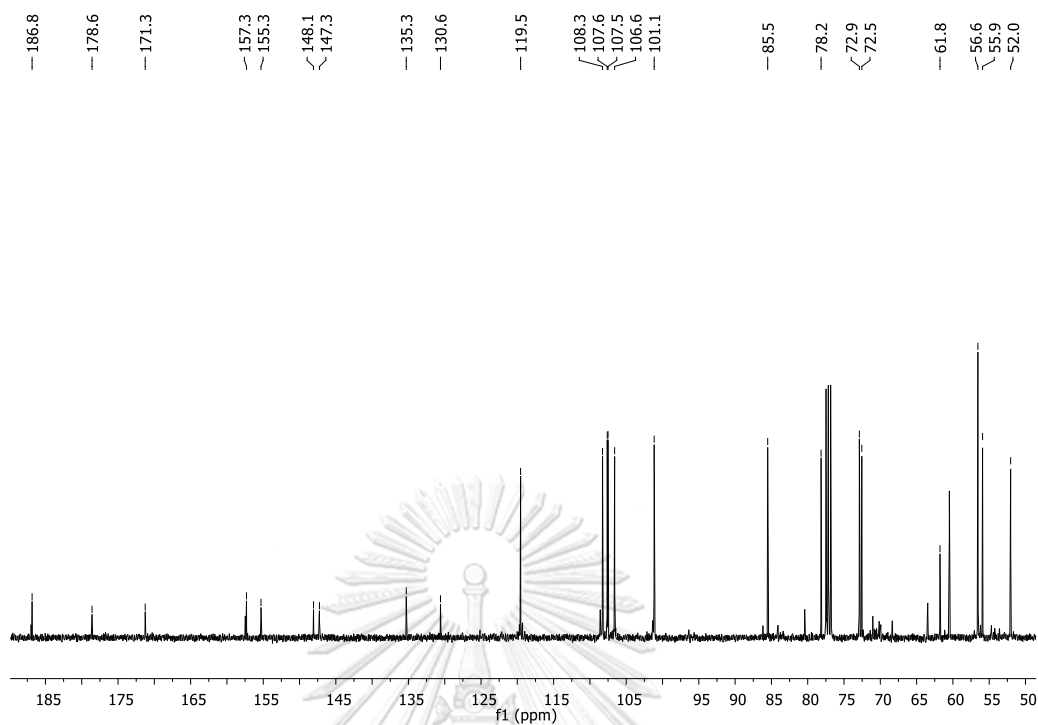


Figure S83. ^{13}C NMR spectrum of α -9c (CDCl_3)

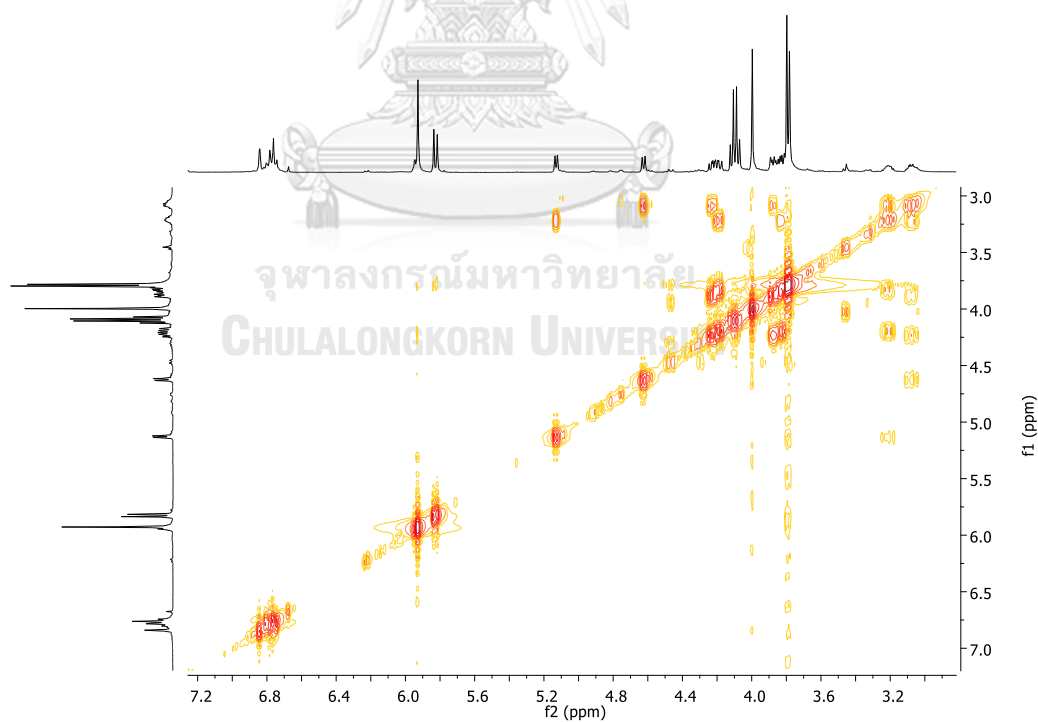


Figure S84. COSY spectrum of α -9c (CDCl_3)

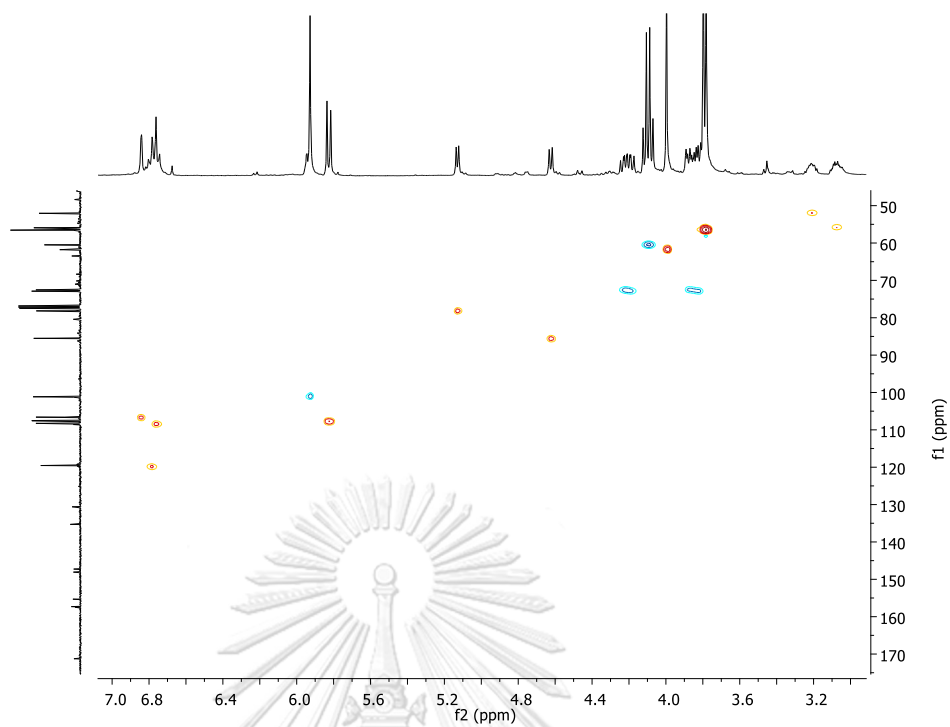


Figure S85. HSQC spectrum of α -9c (CDCl_3)

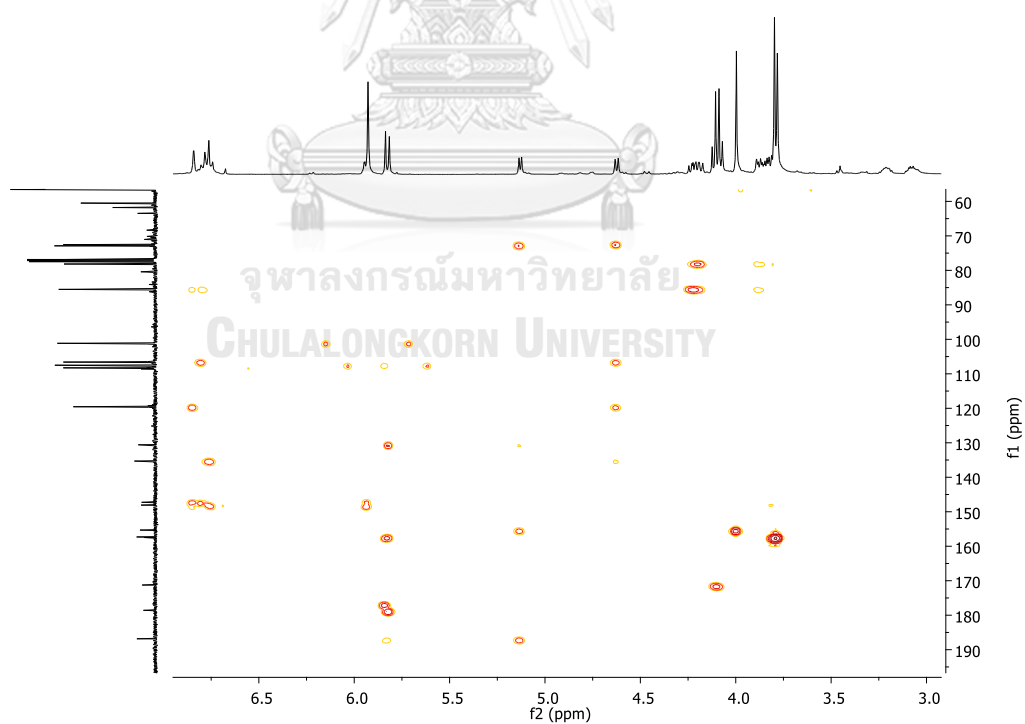


Figure S86. HMBC spectrum of α -9c (CDCl_3)

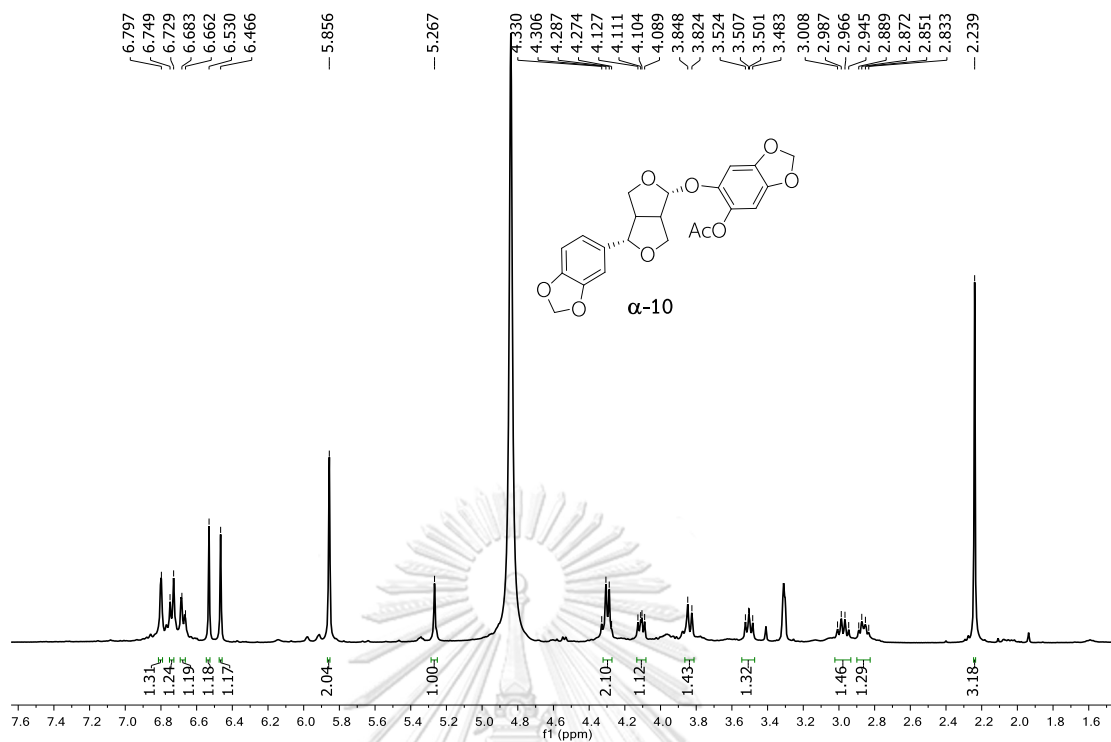


Figure S87. ^1H NMR spectrum of α -10 (CD_3OD)

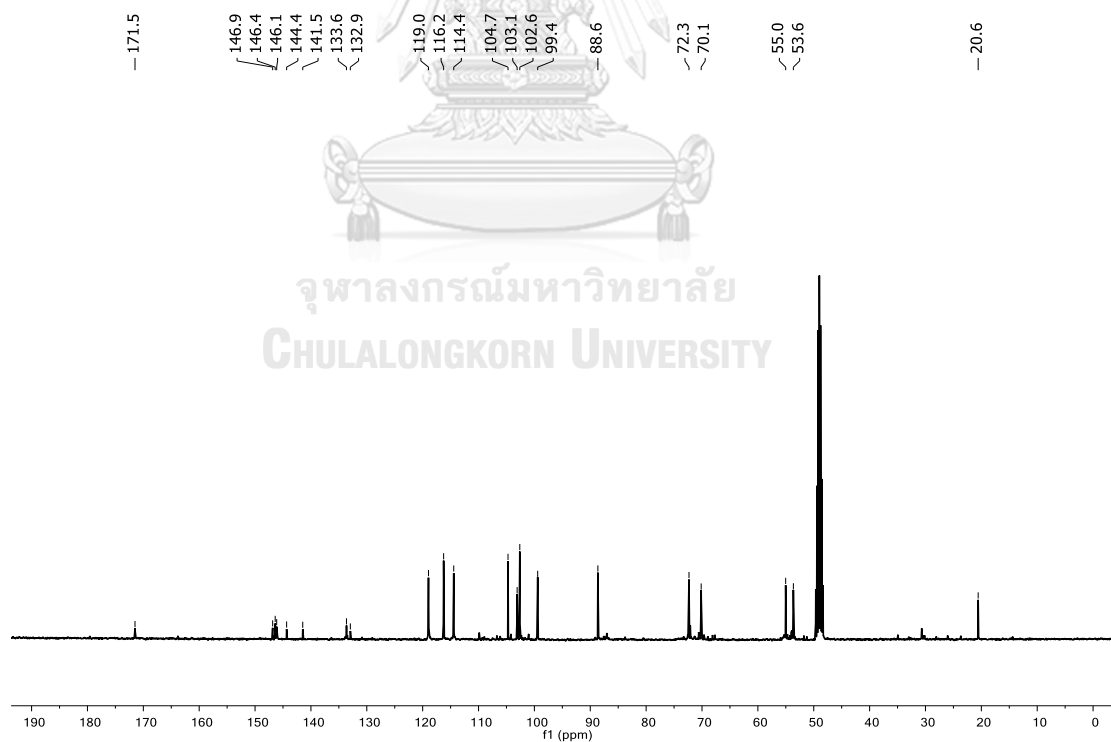


Figure S88. ^{13}C NMR spectrum of α -10 (CD_3OD)

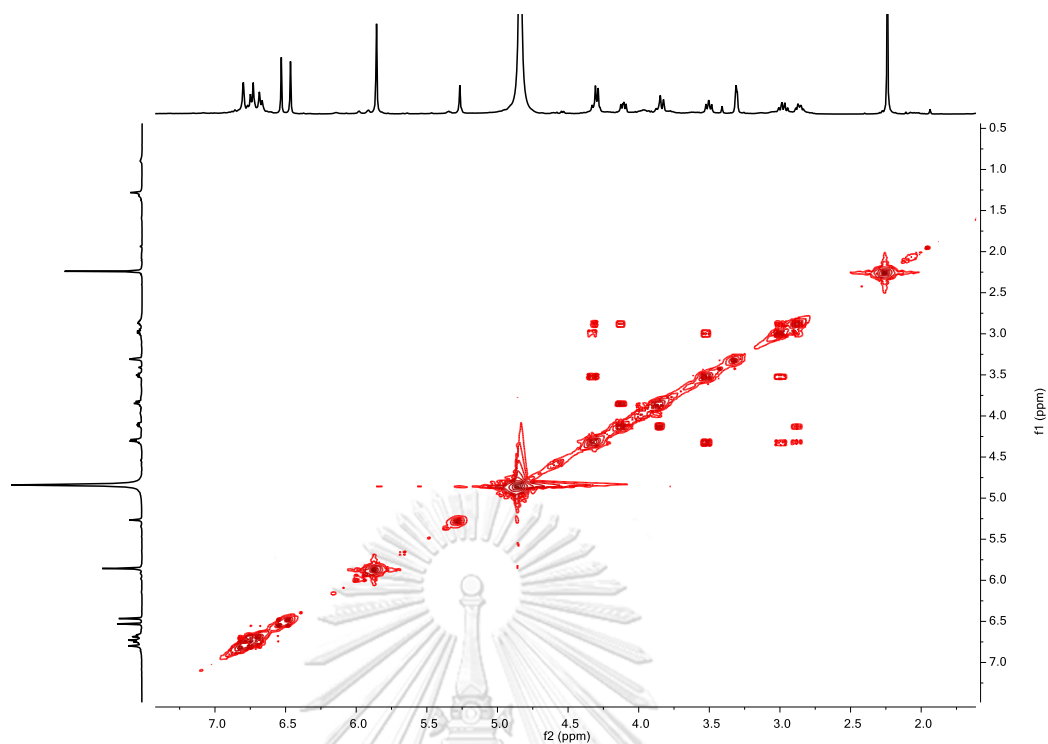


Figure S89. COSY spectrum of α -10 (CD_3OD)

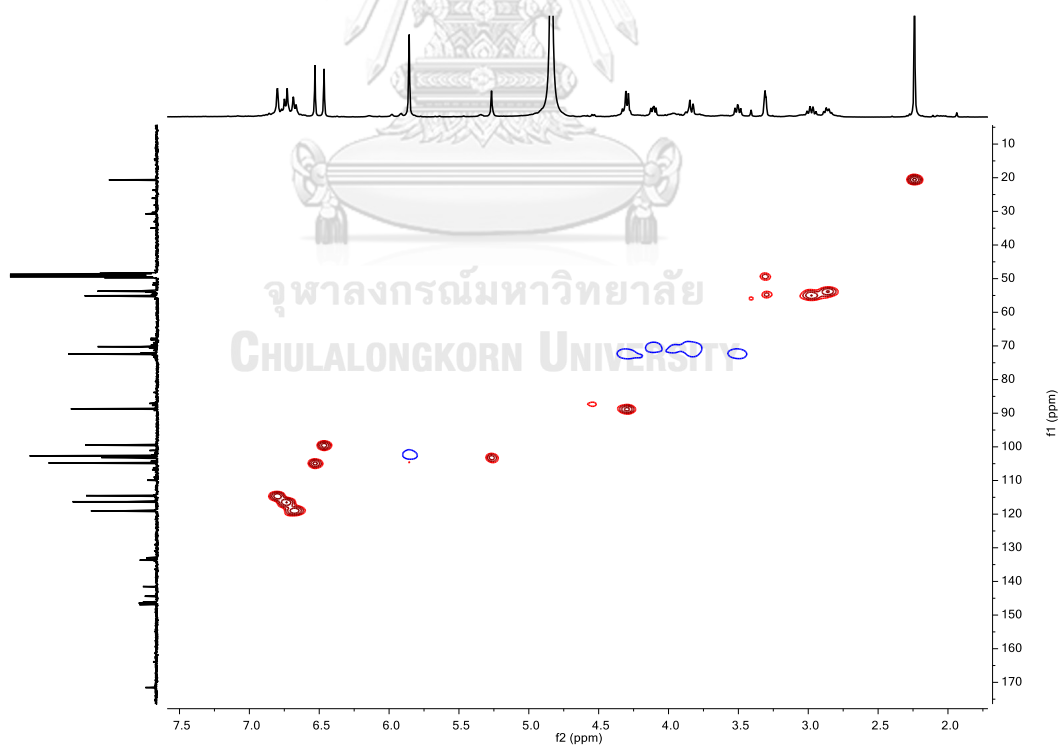


Figure S90. HSQC spectrum of α -10 (CD_3OD)

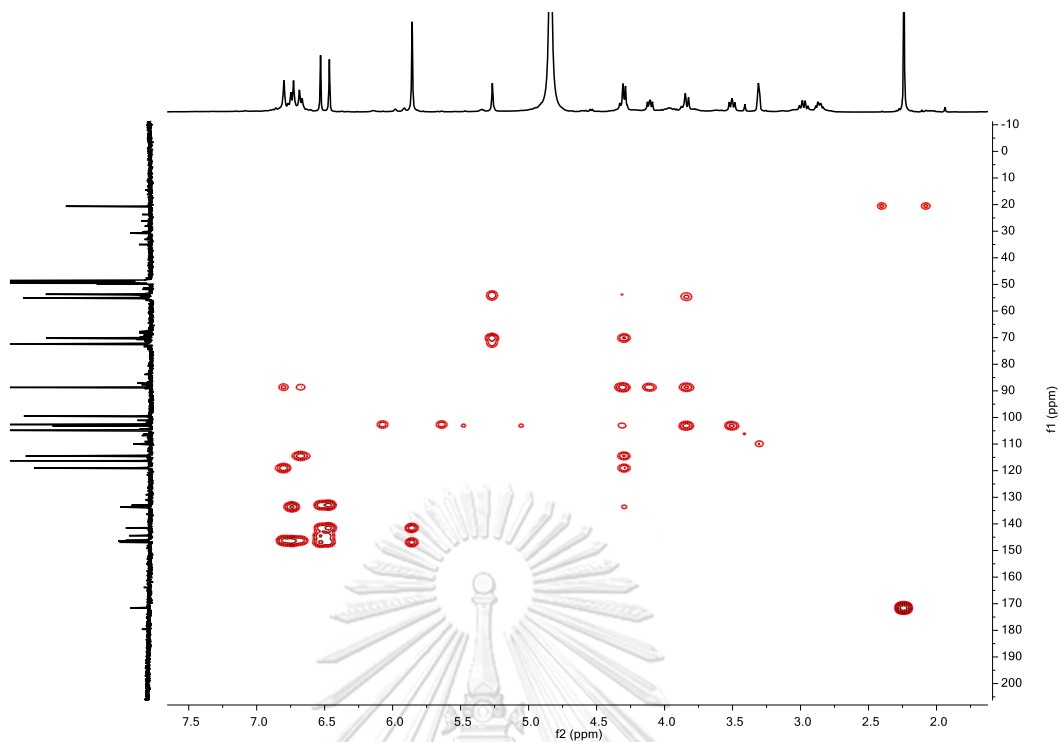


Figure S91. HMBC spectrum of α -10 (CD_3OD)

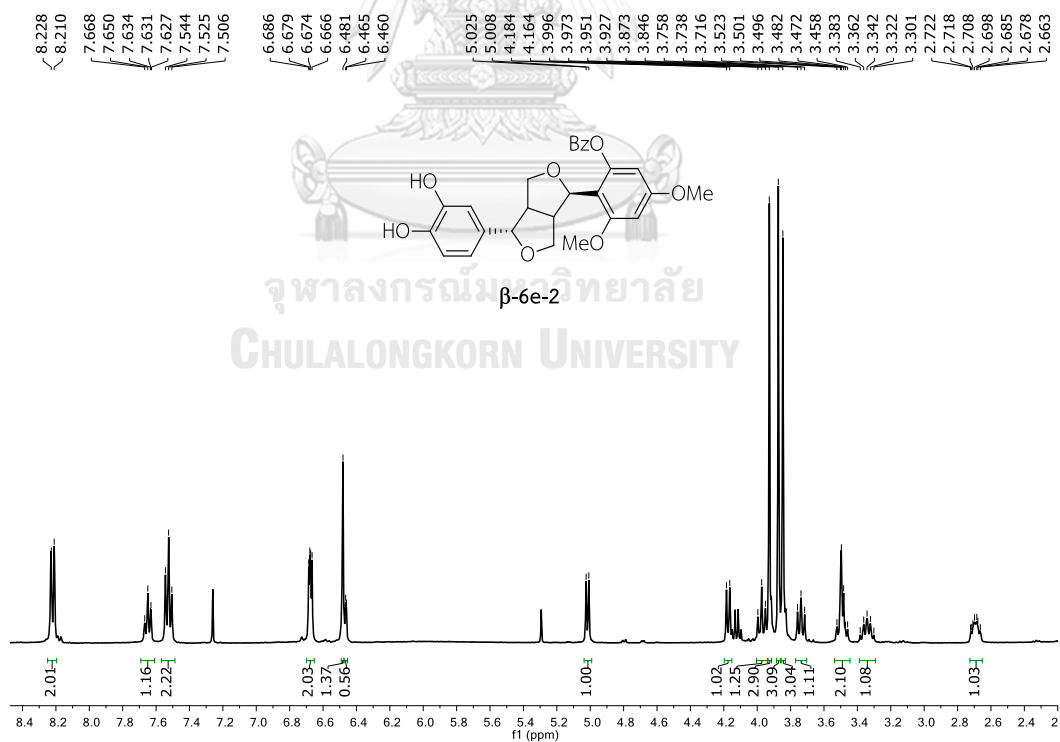


Figure S92. ^1H NMR spectrum of β -6e-2 (CDCl_3)

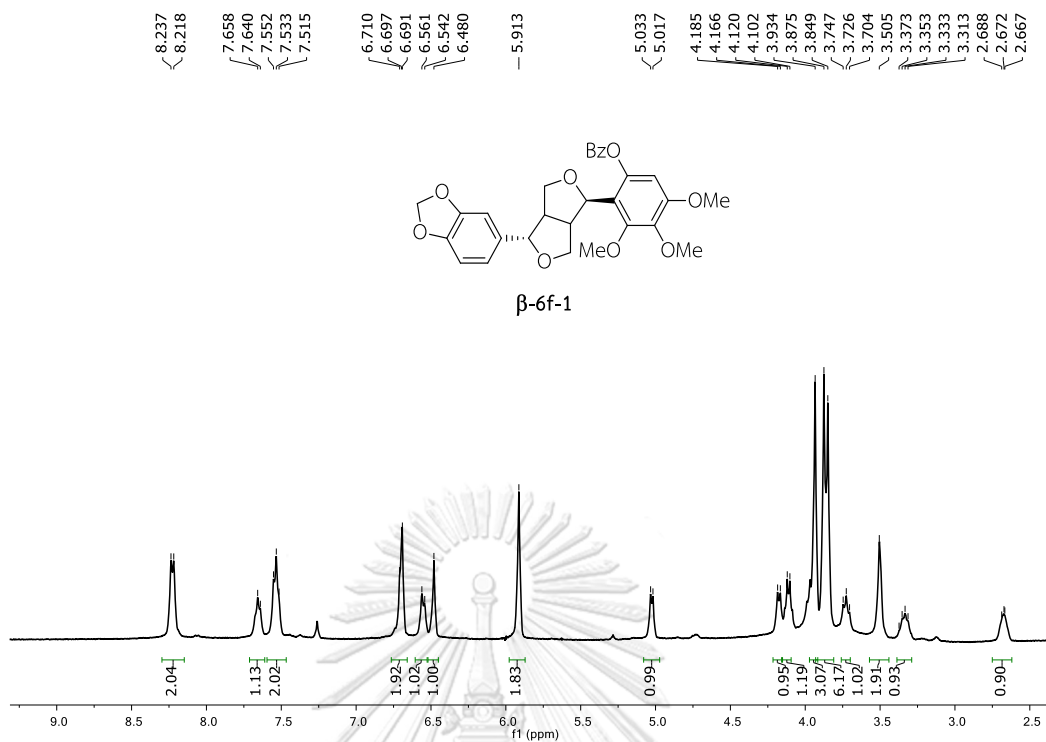


Figure S93. ^1H NMR spectrum of β -6f-1 (CDCl_3)

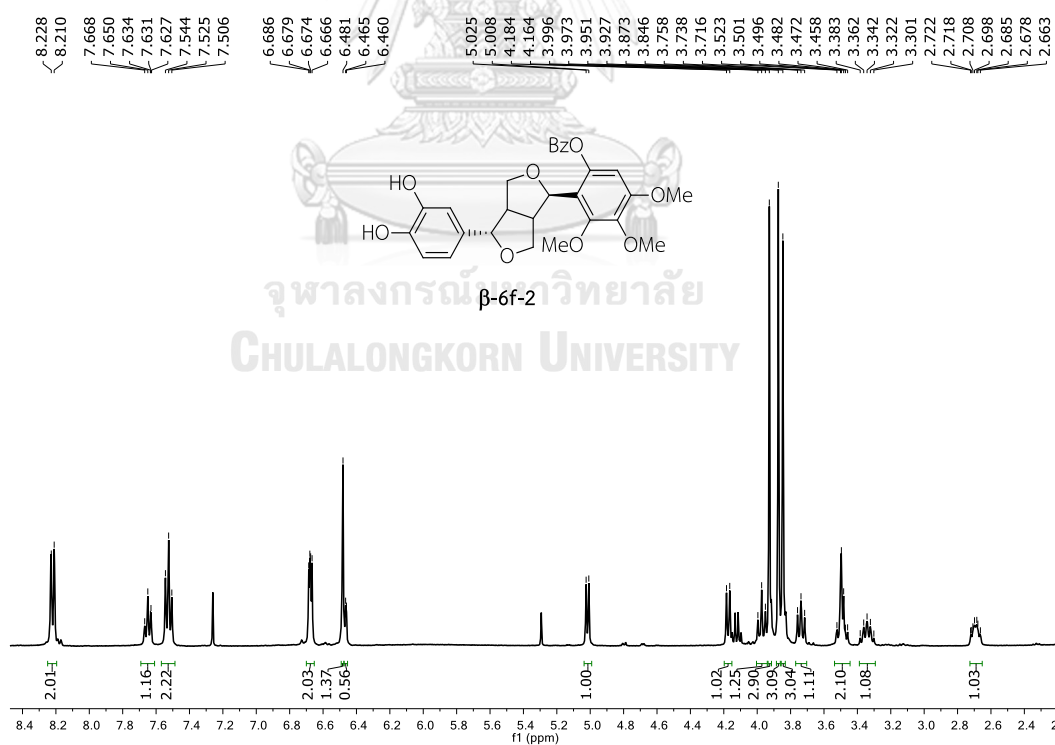


Figure S94. ^1H NMR spectrum of β -6f-2 (CDCl_3)

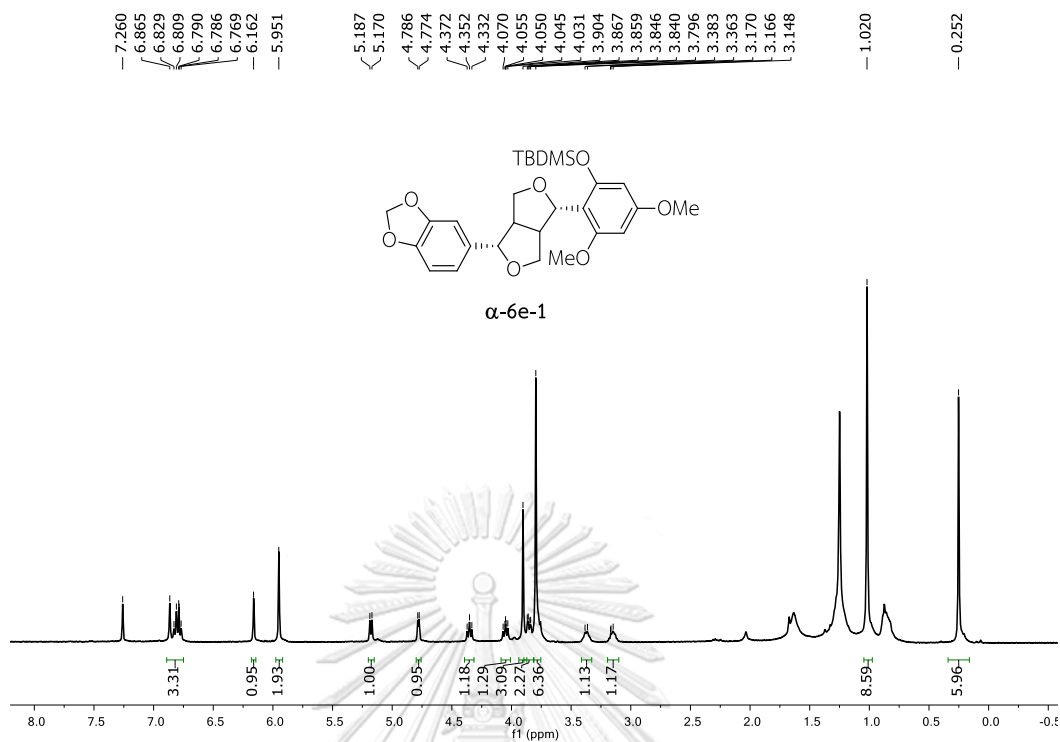


Figure S95. ^1H NMR spectrum of α -6e-1 (CDCl_3)

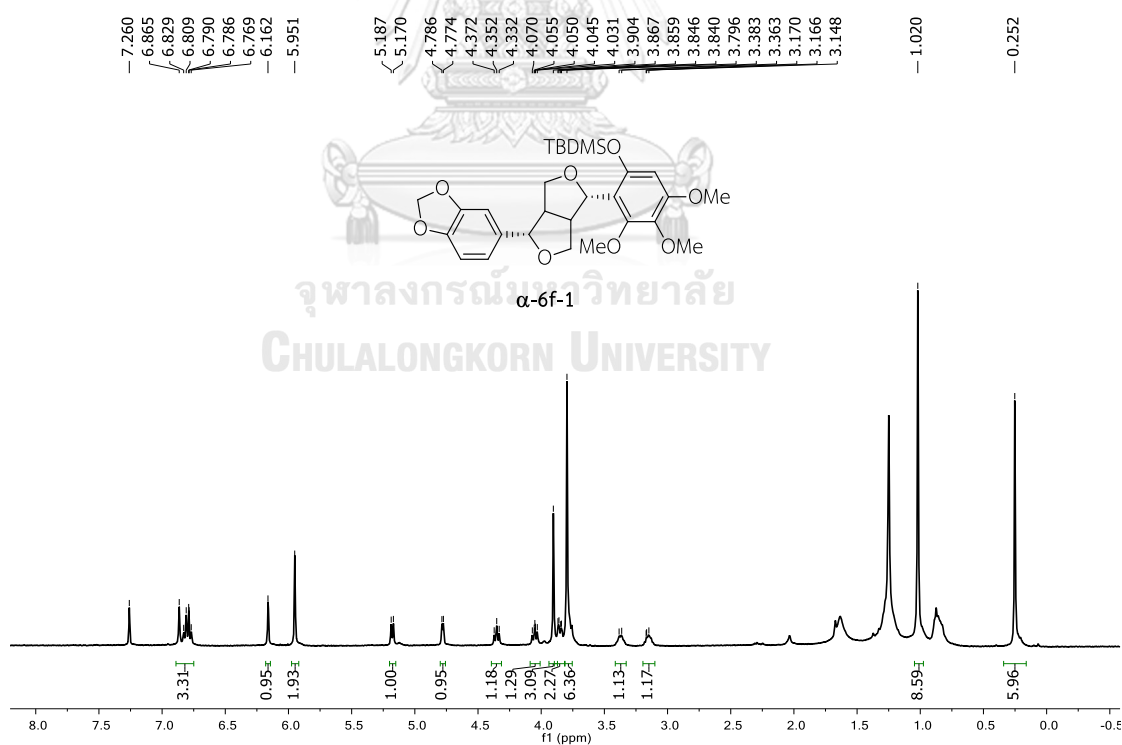
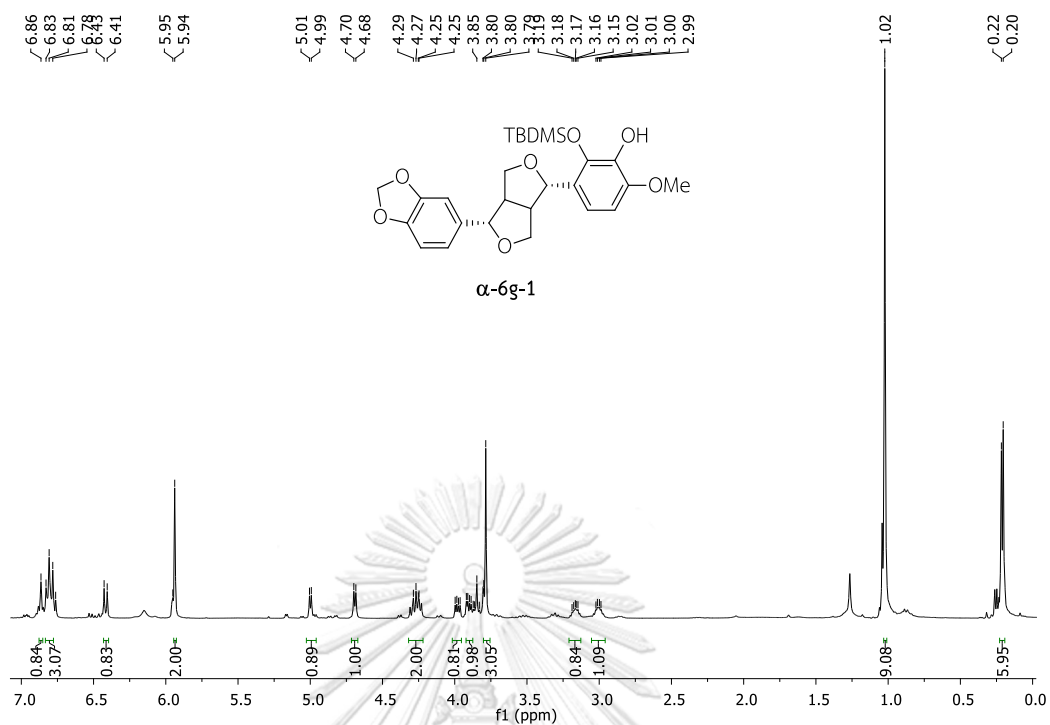
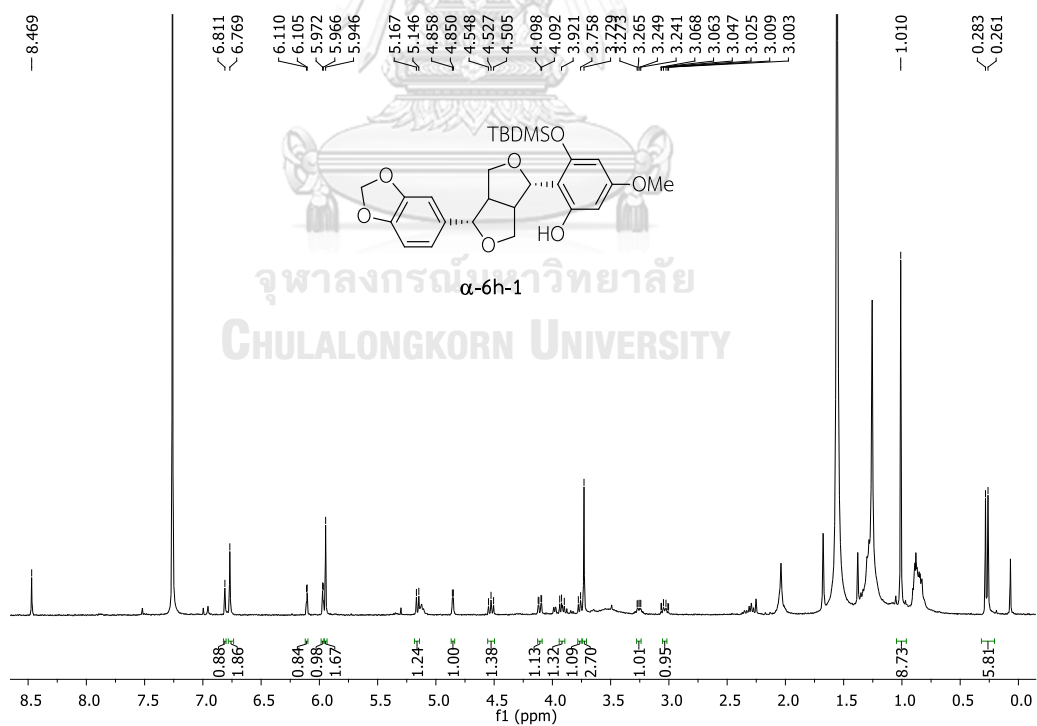


Figure S96. ^1H NMR spectrum of α -6f-1 (CDCl_3)

Figure S97. ^1H NMR spectrum of α -6g-1 (CDCl_3)Figure S98. ^1H NMR spectrum of α -6h-1 (CDCl_3)

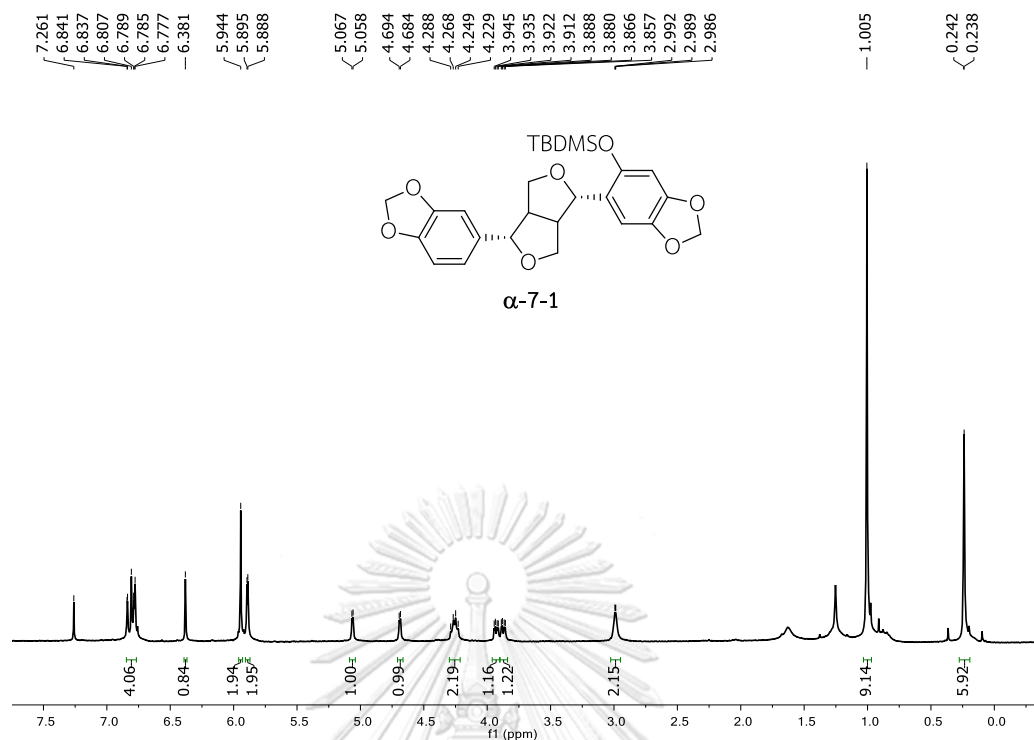


Figure S99. ^1H NMR spectrum of α -7-1 (CDCl_3)

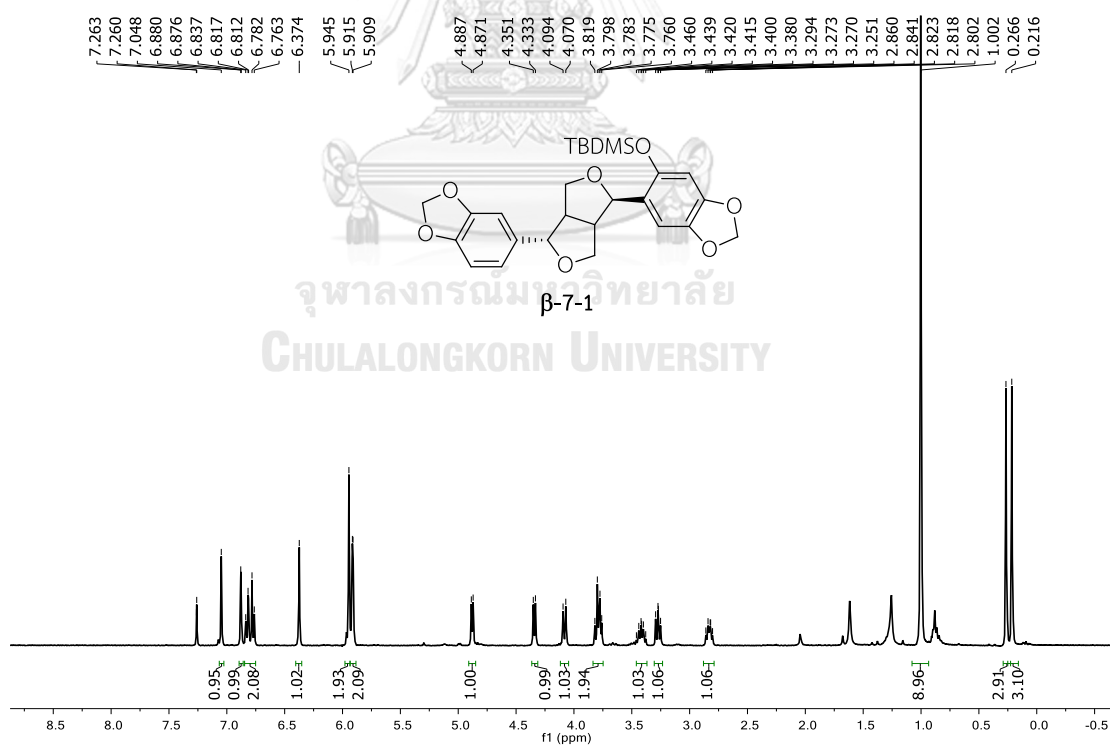
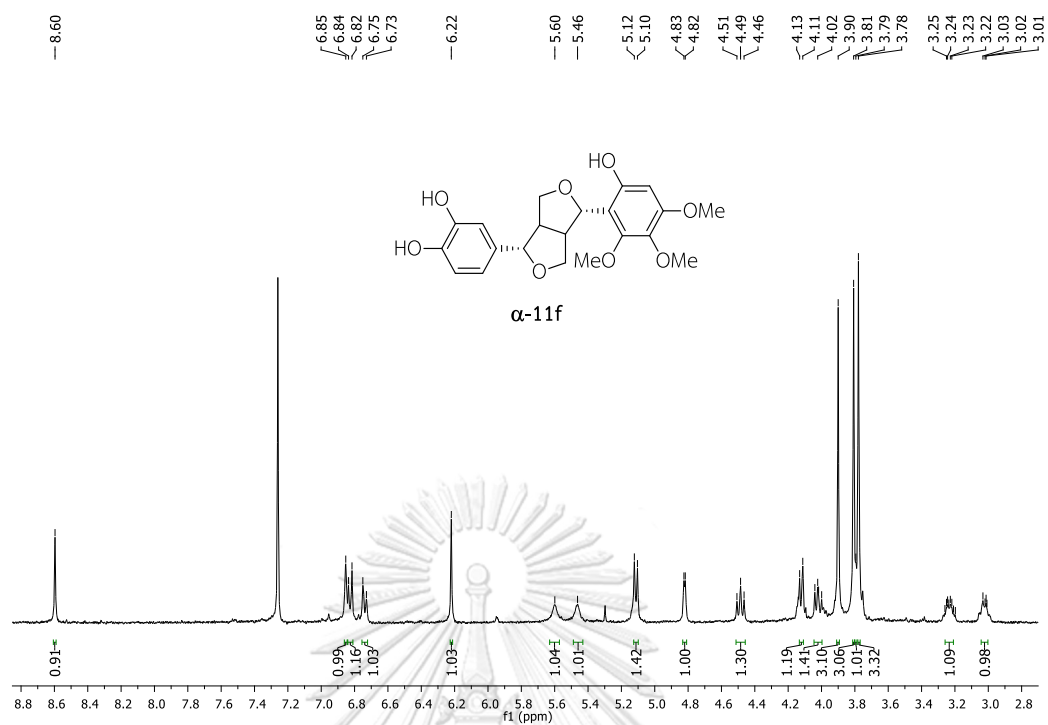
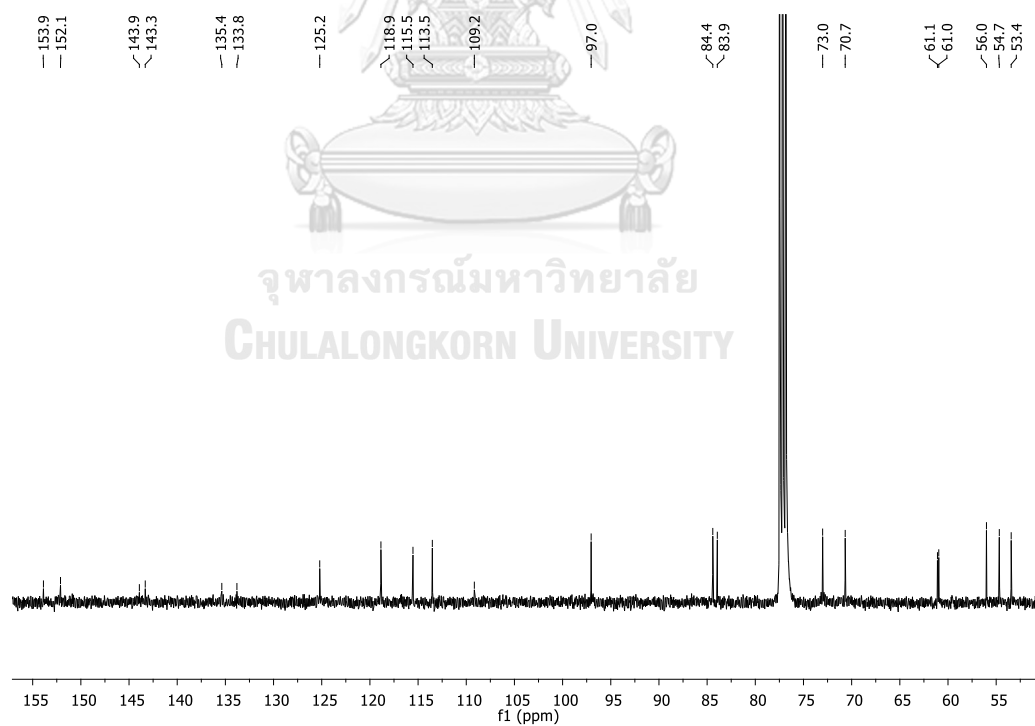


Figure S100. ^1H NMR spectrum of β -7-1 (CDCl_3)

Figure S101. ^1H NMR spectrum of α -11f (CDCl_3)Figure S102. ^{13}C NMR spectrum of α -11f (CDCl_3)

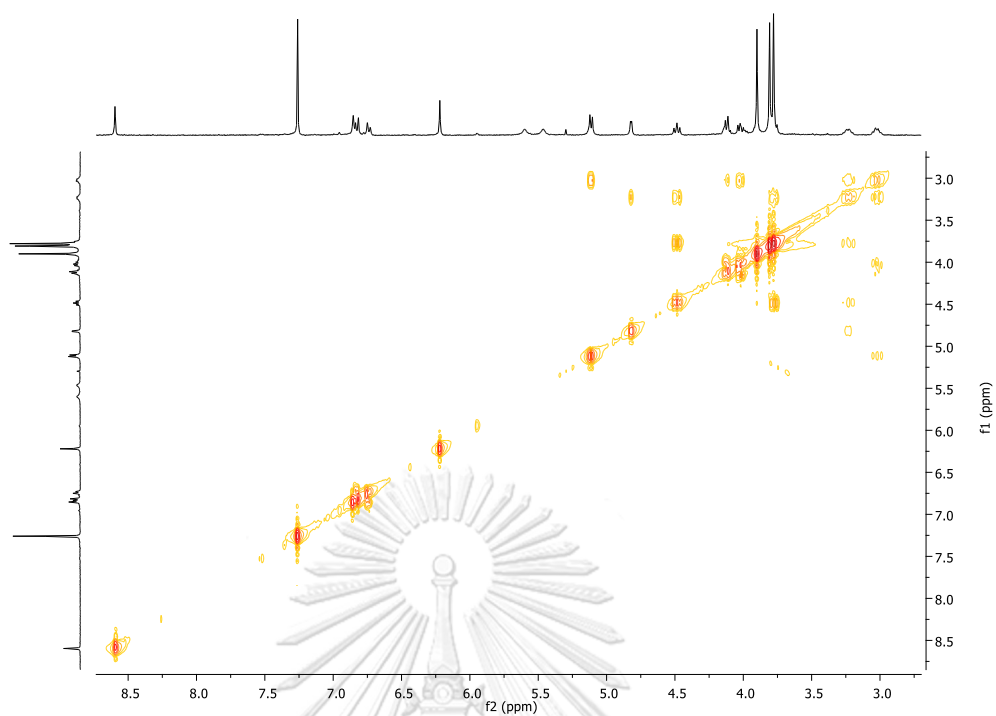


Figure S103. COSY experiment of α -11f (CDCl_3)

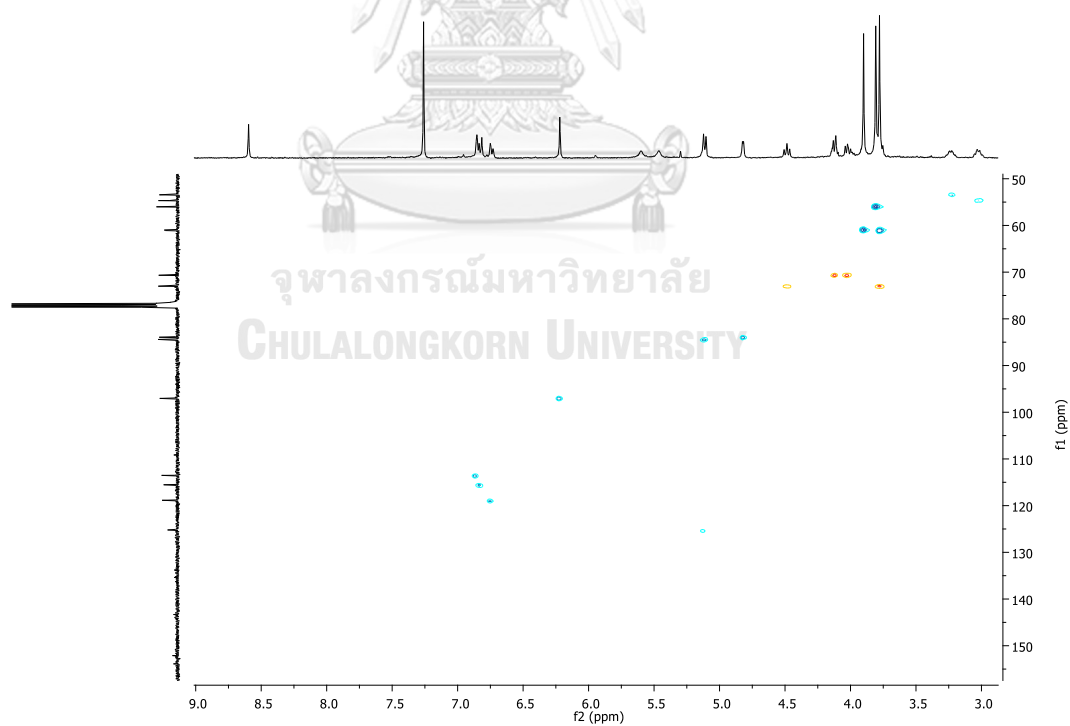
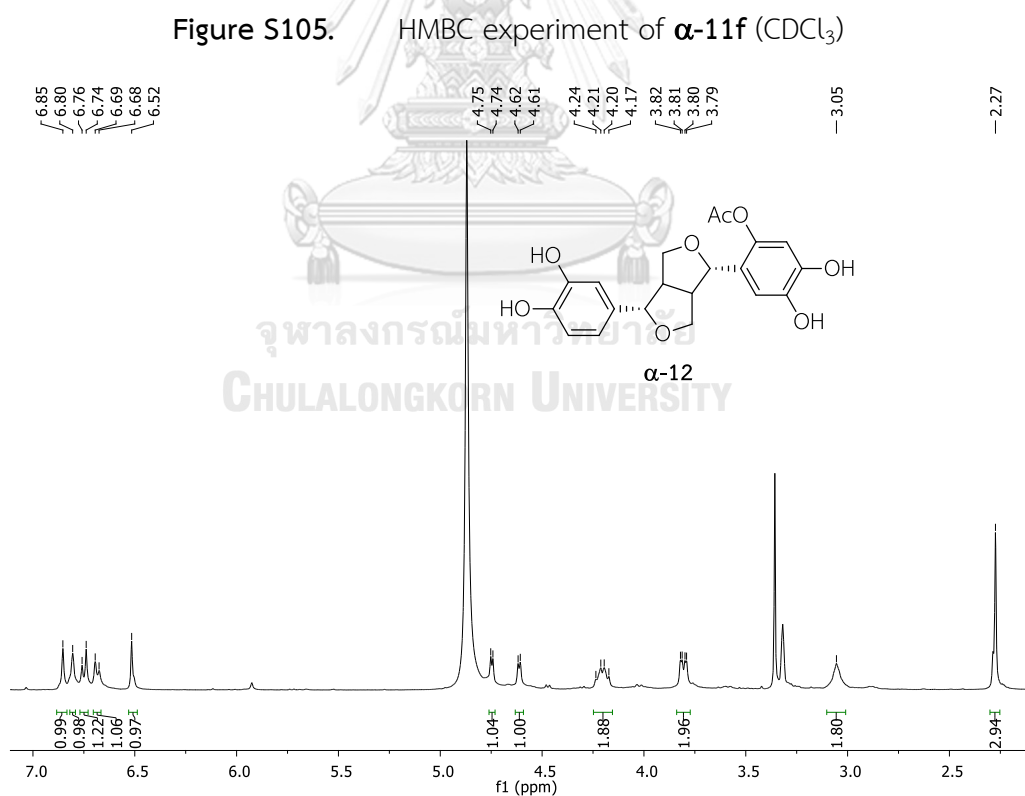
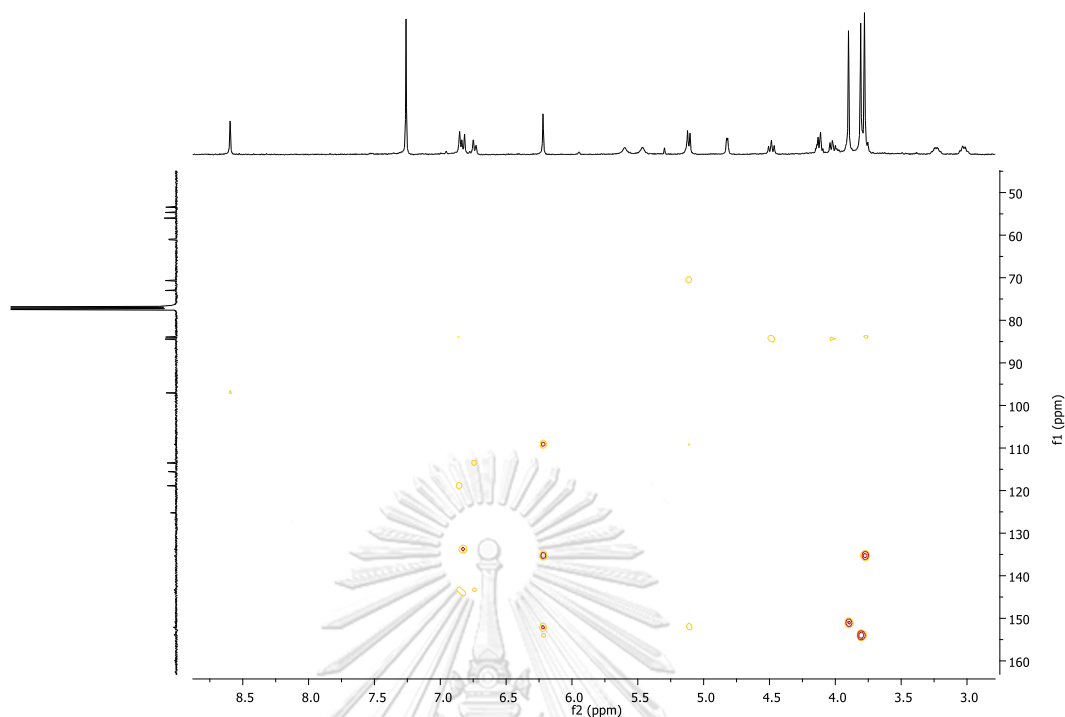


Figure S104. HSQC experiment of α -11f (CDCl_3)



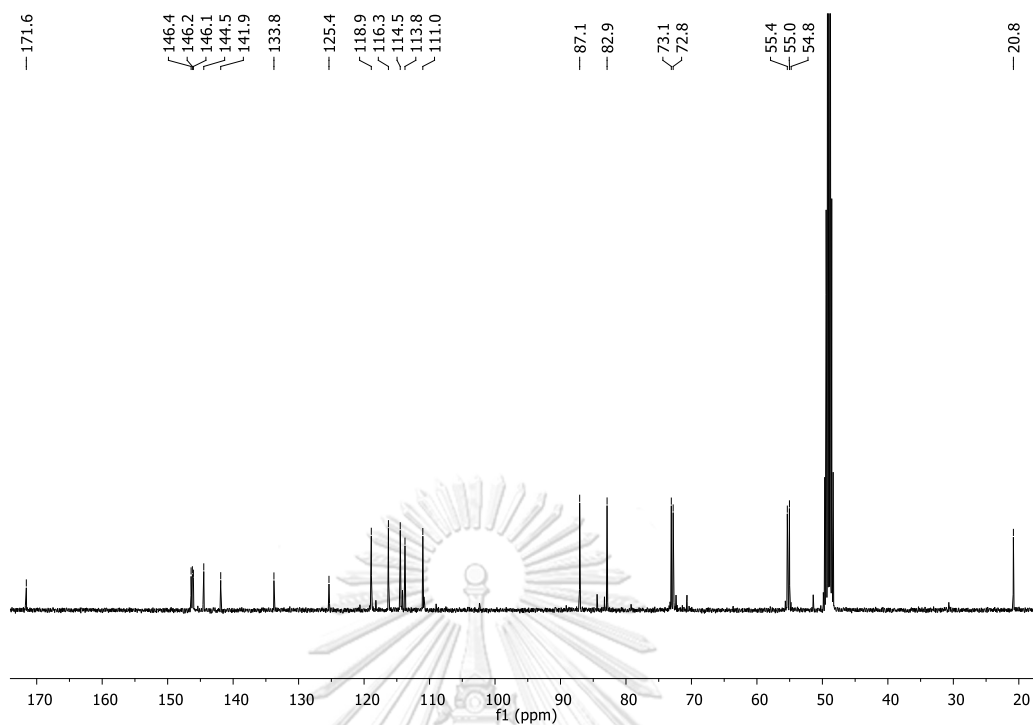


Figure S107. ^{13}C NMR spectrum of α -12 (CD_3OD)

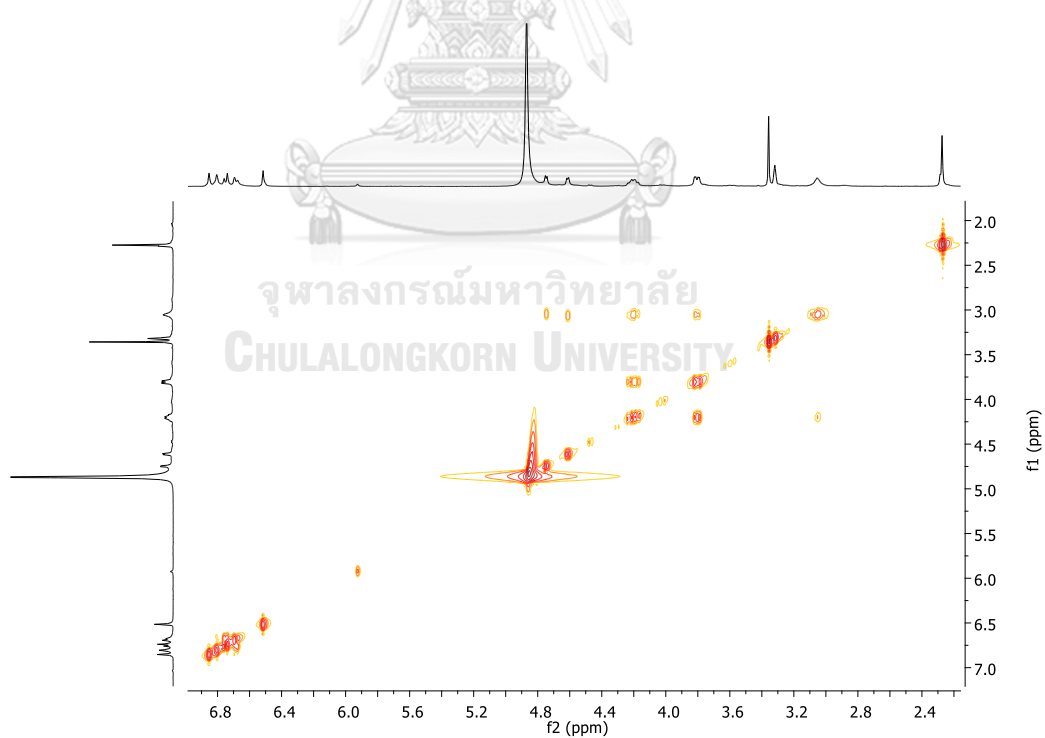


Figure S108. COSY experiment of α -12 (CD_3OD)

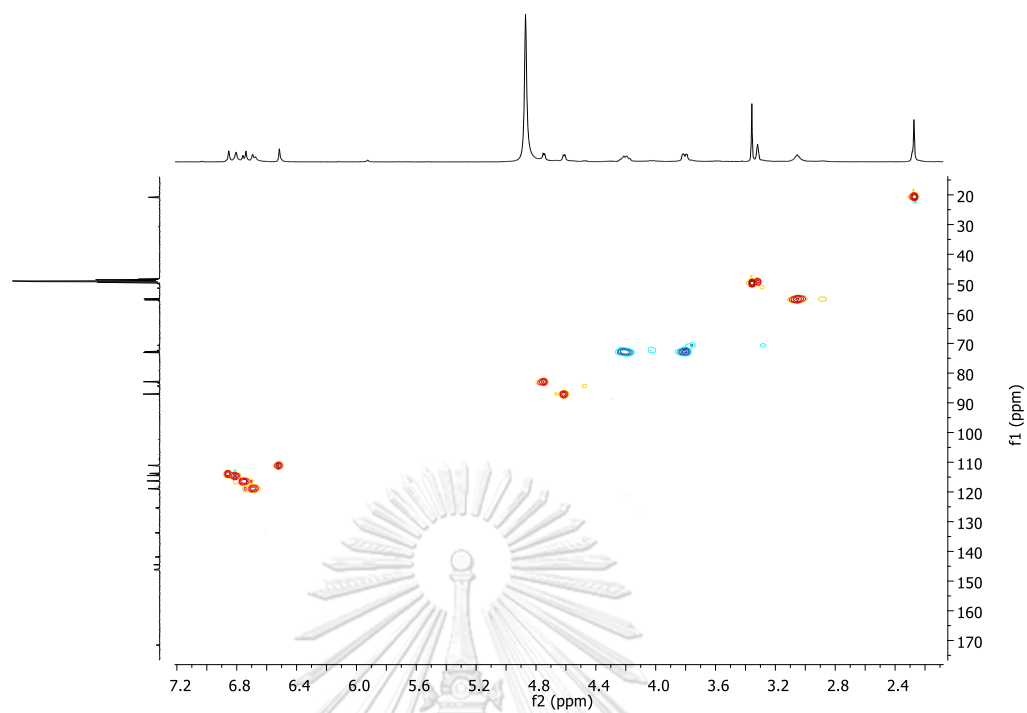


Figure S109. HSQC experiment of α -12 (CD_3OD)

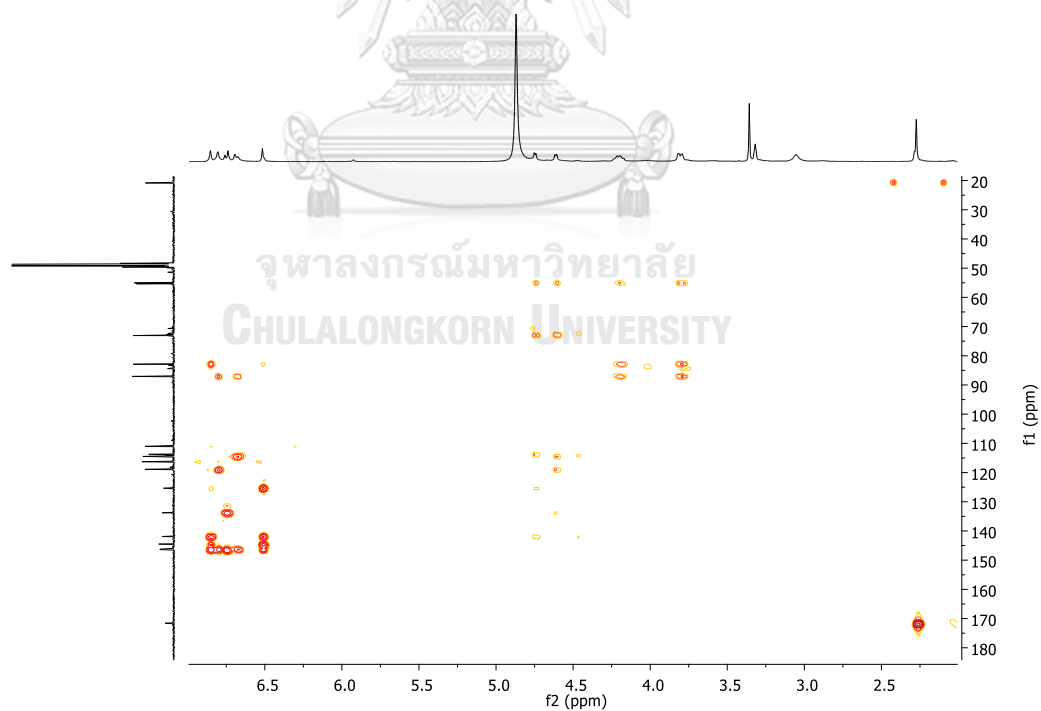


Figure S110. HMBC experiment of α -12 (CD_3OD)

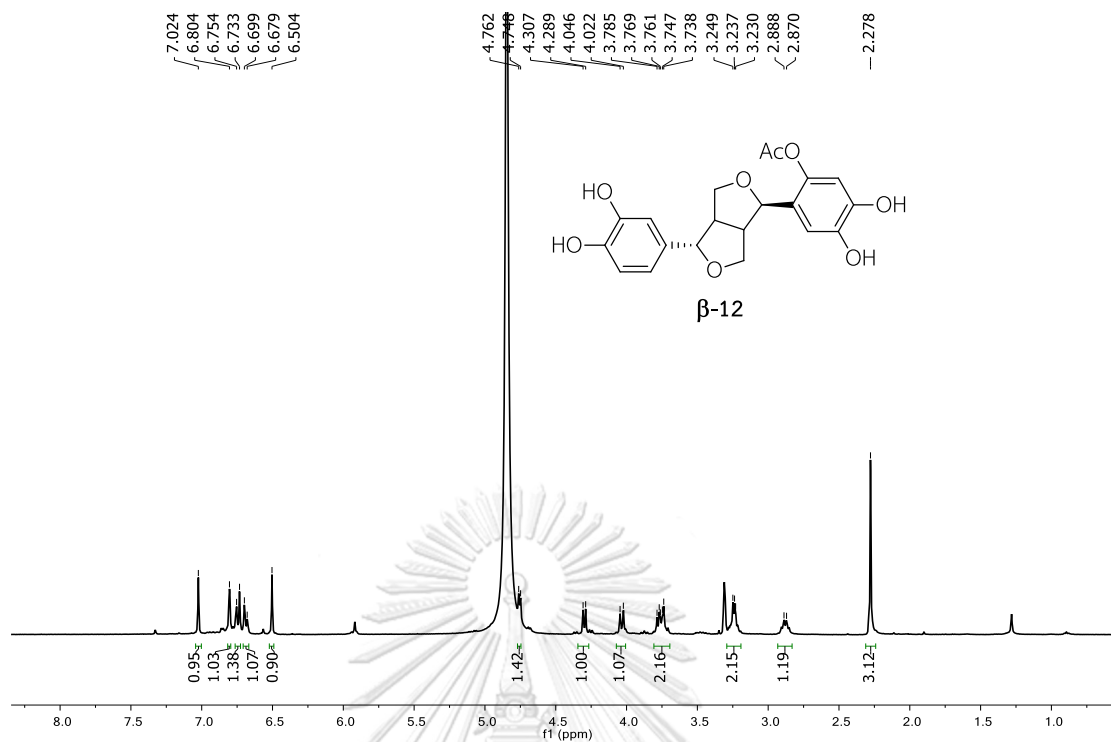


Figure S111. ^1H NMR spectrum of β -12 (CD_3OD)

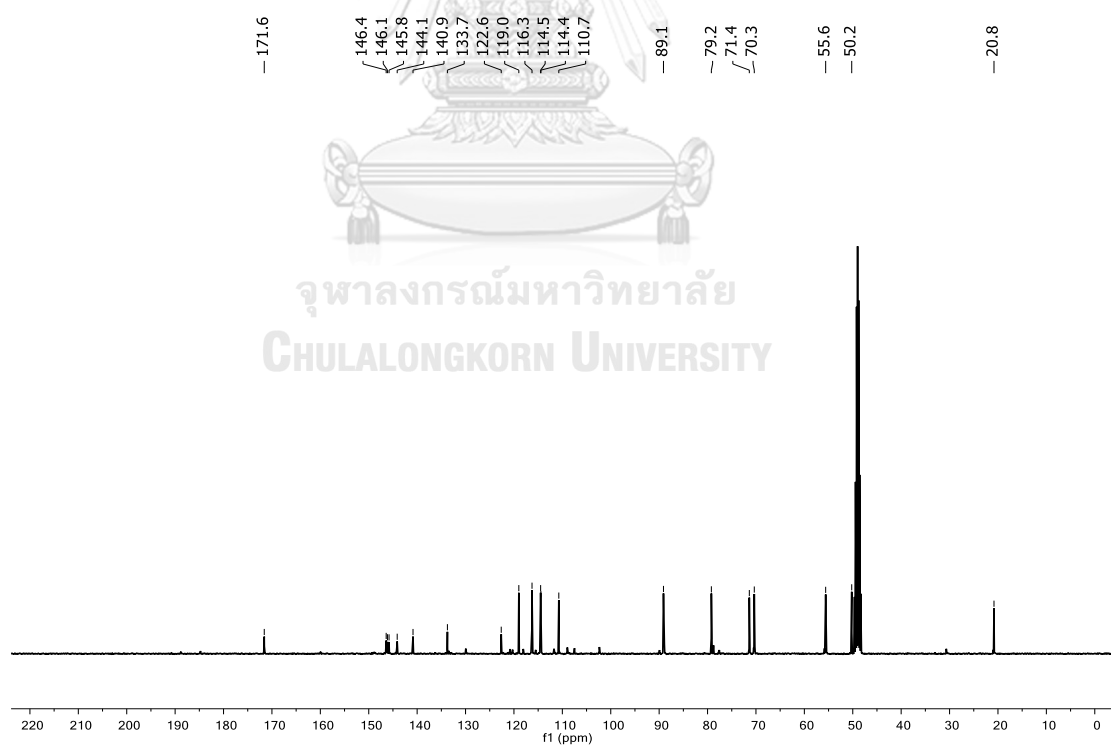


Figure S112. ^{13}C NMR spectrum of β -12 (CD_3OD)

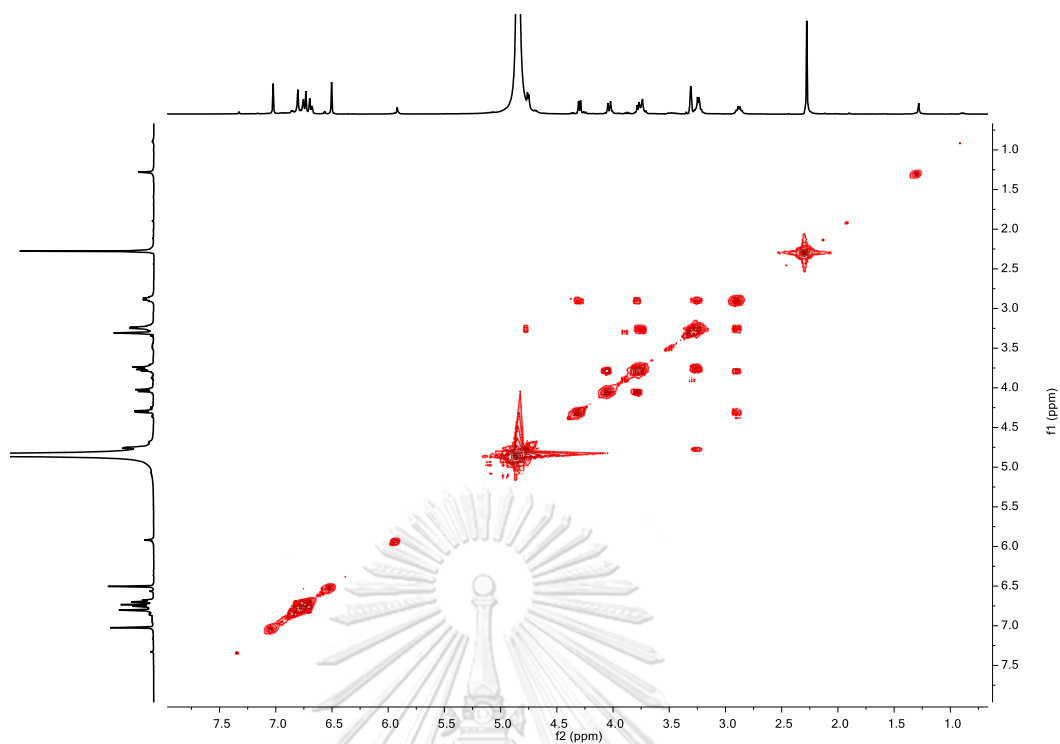


Figure S113. COSY experiment of β -12 (CD_3OD)

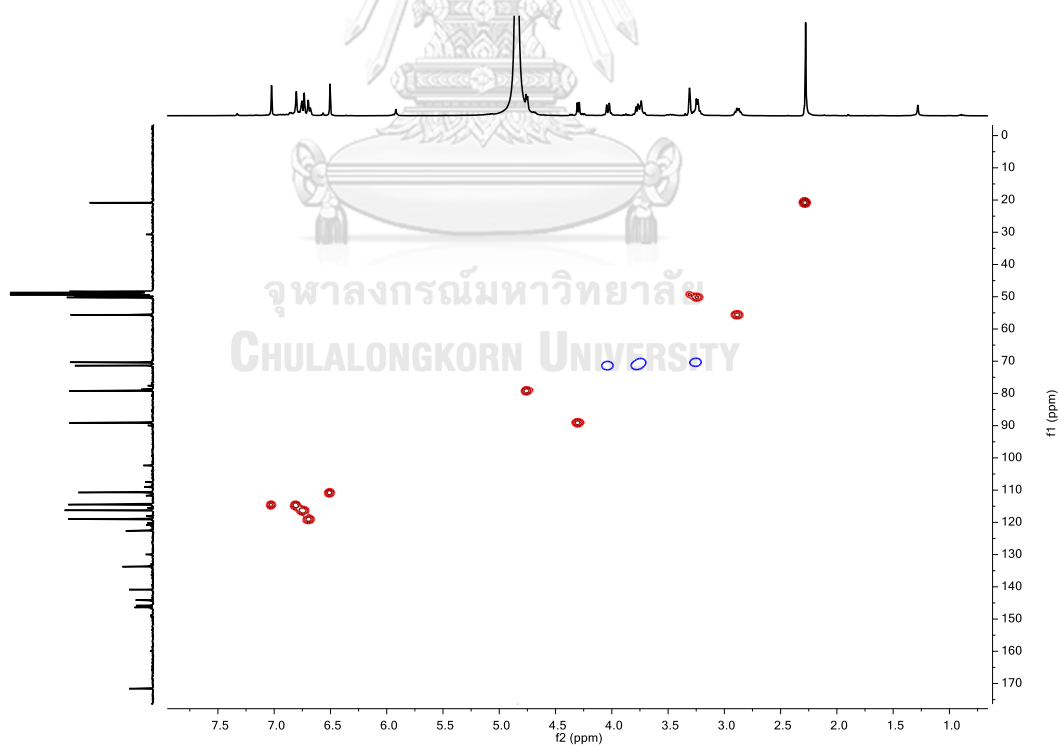
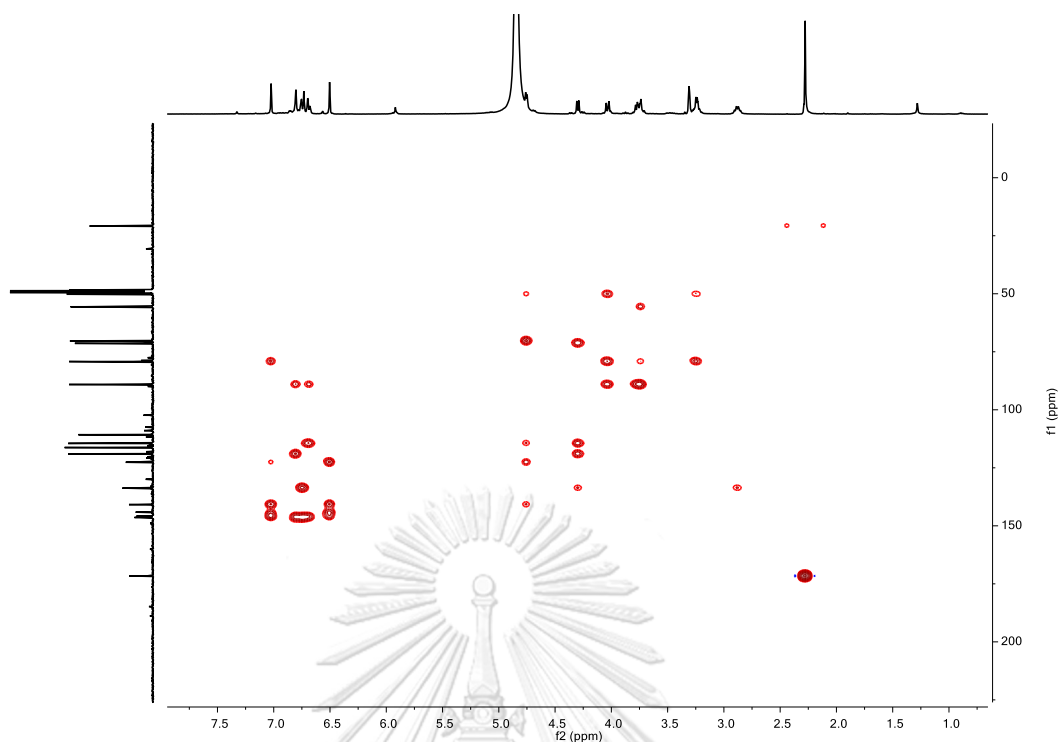
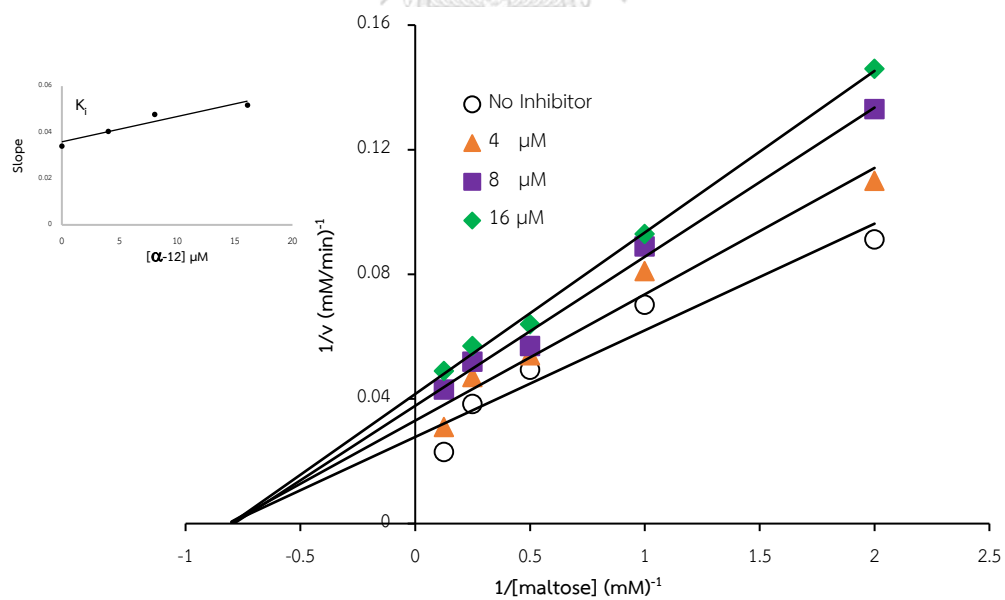


Figure S114. HSQC experiment of β -12 (CD_3OD)



A)



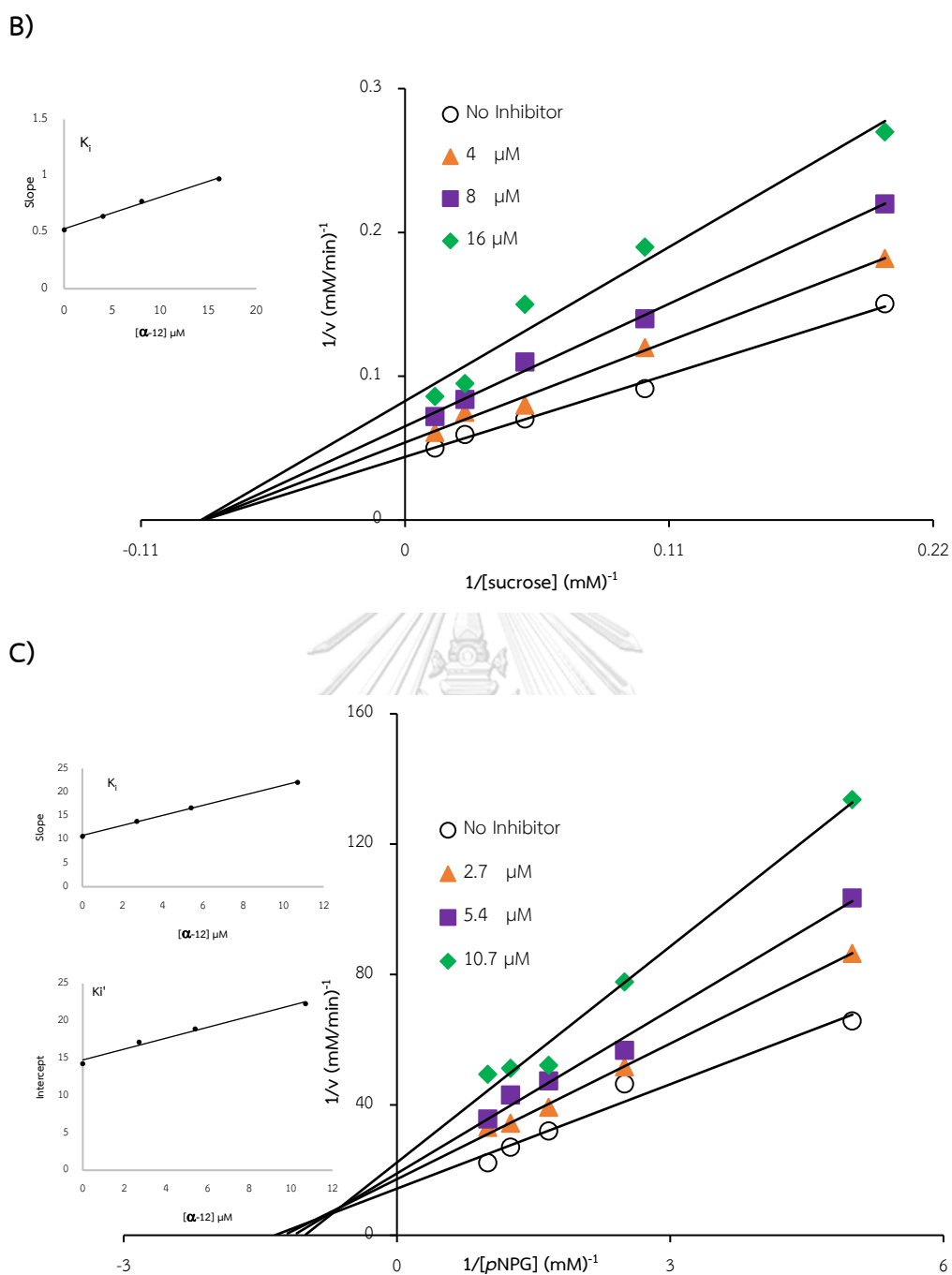
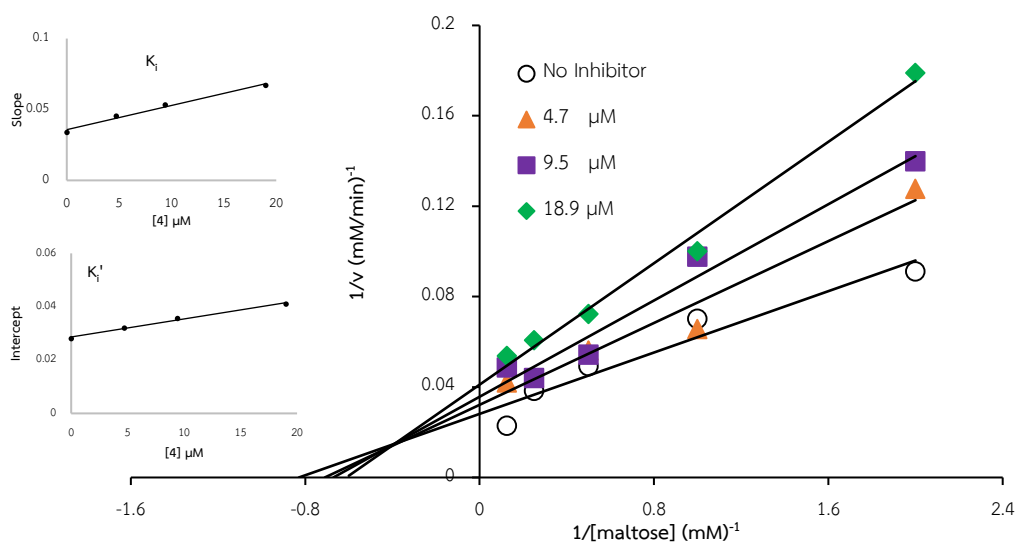
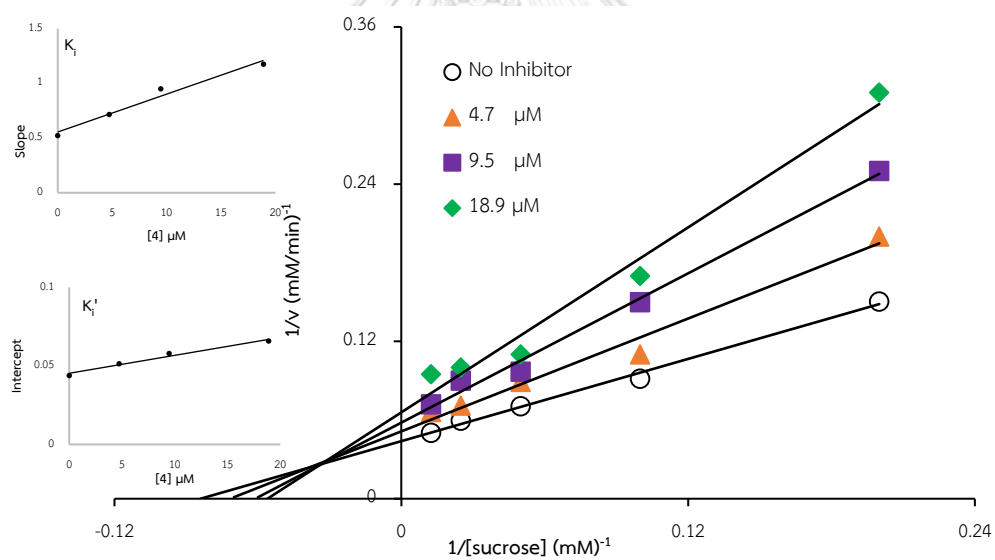


Figure S116. Lineweaver-Burk and secondary plots for inhibitory activity of α -12 against A) maltase, B) sucrose and C) baker's yeast.

A)



B)



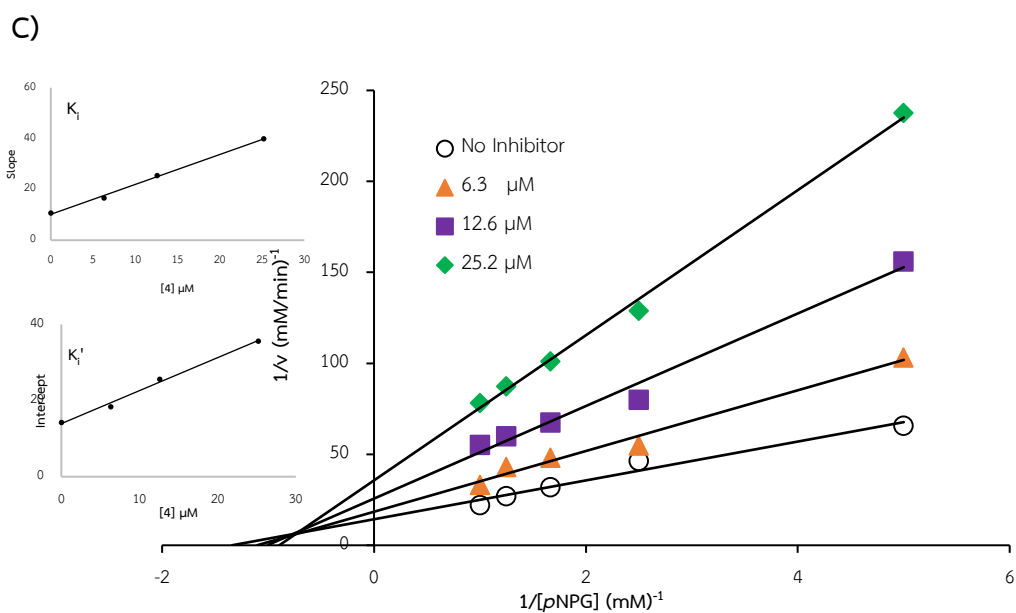
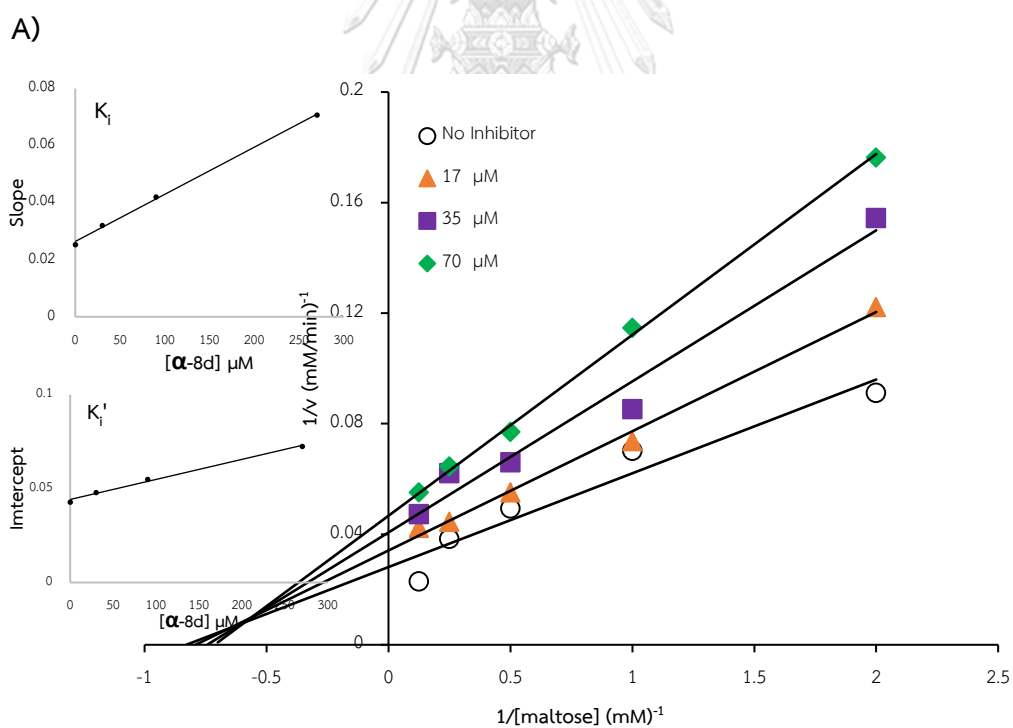


Figure S117. Lineweaver-Burk plots for inhibitory activity of **4** against A) maltase, B) sucrase and C) baker's yeast.



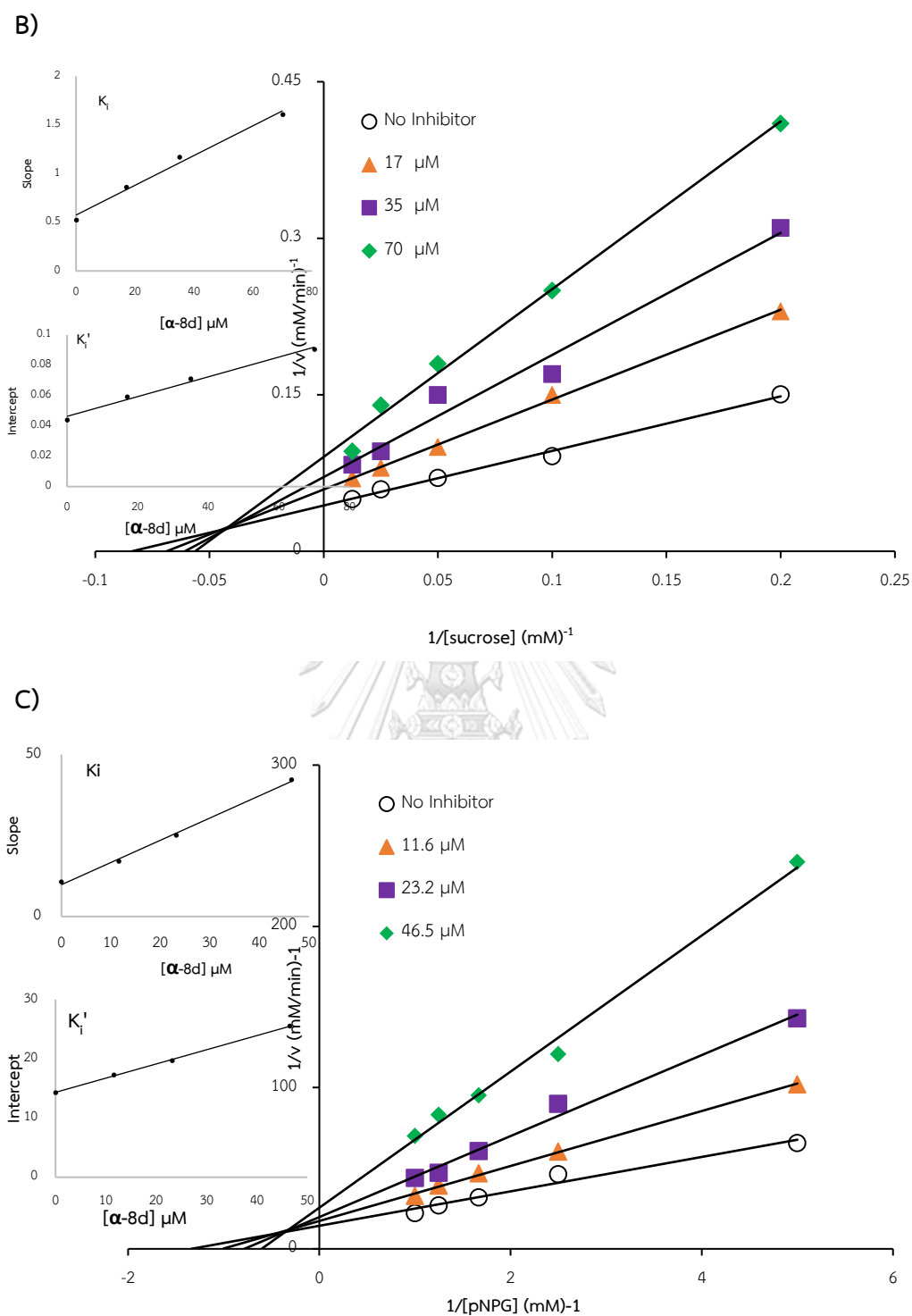


Figure S118. Lineweaver-Burk plots for inhibitory activity of α -8d against A) maltase, B) sucrase and C) baker's yeast.

VITA

NAME Titiruetai Doungwichitrkul

DATE OF BIRTH 23 June 1993

PLACE OF BIRTH Bangkok

INSTITUTIONS ATTENDED Department of Chemistry, Faculty of Science and Technology, Thammasat University

HOME ADDRESS 349/158 Bhuddhamonthonsai 2, Bangphai, Bangkok, BKK 10160

PUBLICATION Worawalai, W.; Doungwichitrkul, T.; Rangubpit, W.; Taweecat, P.; Sompornpisut, P.; Phuwapraisirisan, P., Furofuran lignans as a new series of antidiabetic agents exerting α -glucosidase inhibition and radical scavenging: Semisynthesis, kinetic study and molecular modeling. *Biorganic Chemistry* 2019, 87, 783-793.